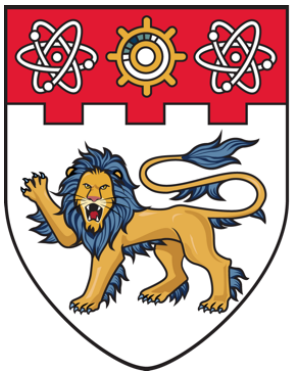

NANYANG TECHNOLOGICAL UNIVERSITY
SINGAPORE

Synthesis and Properties of Novel Polycyclic (Hetero)aromatic Systems

MD. SHAFIQUR RAHMAN

SCHOOL OF PHYSICAL AND MATHEMATICAL SCIENCES

2019

Synthesis and Properties of Novel Polycyclic (Hetero)aromatic Systems

MD. SHAFIQUR RAHMAN

SCHOOL OF PHYSICAL AND MATHEMATICAL SCIENCES

A thesis submitted to the Nanyang Technological University in partial fulfilment of the requirement for the degree of Doctor of Philosophy

2019

Statement of Originality

I hereby certify that the work embodied in this thesis is the result of original research done by me except where otherwise stated in this thesis. The thesis work has not been submitted for a degree or professional qualification to any other university or institution. I declare that this thesis is written by myself and is free of plagiarism and of sufficient grammatical clarity to be examined. I confirm that the investigations were conducted in accord with the ethics policies and integrity standards of Nanyang Technological University and that the research data are presented honestly and without prejudice.

[29 July 2019] [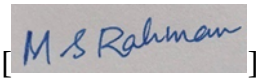]

. . . .

Date [MD. SHAFIQUR RAHMAN]

Supervisor Declaration Statement

I have reviewed the content and presentation style of this thesis and declare it of sufficient grammatical clarity to be examined. To the best of my knowledge, the thesis is free of plagiarism and the research and writing are those of the candidate's except as acknowledged in the Author Attribution Statement. I confirm that the investigations were conducted in accord with the ethics policies and integrity standards of Nanyang Technological University and that the research data are presented honestly and without prejudice.

[31 July 2019] []

. . . . . .

Date

. . . . . .

[Naohiko Yoshikai]

Authorship Attribution Statement

Please select one of the following; *delete as appropriate:

~~*(A)~~ This thesis **does not** contain any materials from papers published in peer-reviewed journals or from papers accepted at conferences in which I am listed as an author.

*(B) This thesis contains material from [3 number] paper(s) published in the following peer-reviewed journal(s) / from papers accepted at conferences in which I am listed as an author.

Please amend the typical statements below to suit your circumstances if (B) is selected.

Chapter 2 is published as M. S. Rahman, N. Yoshikai. Synthesis and properties of phospha[5]helicenes bearing an inner-rim phosphorus center. *Organic Letters* **21**, 3232-3236 (2019). DOI: 10.1021/acs.orglett.9b00955.

The contributions of the co-authors are as follows:

- Prof Yoshikai provided the initial project direction and helped me to analyze the problems encountered in the project and edited the manuscript drafts and supporting information for me.
- I performed all the laboratory work, analyzed the experimental spectroscopic data and prepared supporting information for this paper.
- All UV-vis and fluorescent spectra, (preparative) HPLC, including sample preparation, was conducted by me.
- Dr Li Yongxin assisted in the single crystal X-ray analysis.

Chapter 3 is communicated as M. S. Rahman, N. Yoshikai. Synthesis and optical properties of phosphole oxide-fused triphenylene derivatives (*Beilstein Journal of Organic Chemistry*).

The contributions of the co-authors are as follows:

- Prof Yoshikai provided the initial project direction and helped me to analyze the problems encountered in the project.
- I performed all the laboratory work, analyzed the experimental spectroscopic data and prepared supporting information for this paper.
- I performed all the compounds synthesis, collected X-ray diffraction patterns and UV-visible and fluorescent spectra.
- Dr Li Yongxin assisted in the analysis of the single crystal X-ray.

Chapter 4 is published as J. Yan, M. S. Rahman, N. Yoshikai. Pd-Catalyzed annulation of 1-halo-8-arylnaphthalenes and alkynes leading to heptagon-embedded aromatic systems. *Chemistry A European Journal* **25**, 9395-9399 (2019). DOI: 10.1002/chem.201805746.

The contributions of the co-authors are as follows:

- Prof Yoshikai provided the project direction and helped me to analyze the problems encountered in the project and edited the manuscript drafts and supporting information for me.
- I performed this project in collaboration with Dr. Jianming Yan with equal contribution. I performed half of the laboratory work, analyzed the experimental spectroscopic data and prepared supporting information for this paper.
- All UV-vis and fluorescent spectra, including sample preparation, was conducted by me.
- Dr Li Yongxin assisted in the single crystal X-ray analysis.

[29 July 2019] [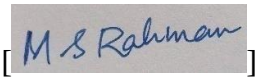]

. . . .

Date [MD. SHAFIQUR RAHMAN]

Abstract

Polycyclic aromatic hydrocarbons are ubiquitous functional molecules that have numerous applications in optoelectronic devices, molecular recognition and sensing, dye materials. Therefore, various synthetic organic chemistry and material research groups have devoted a significant effort towards these structural scaffolds. In this context, we describe the synthesis and properties of novel polycyclic (hetero)aromatic systems.

Part 1 of the thesis begins with Chapter 1, which describes the synthesis and properties of phosphole-embedded polycyclic aromatic compounds (PACs). Chapter 2 describes the synthesis and properties of phospha[5]helicenes bearing an inner-rim phosphorus center (Scheme 1). The key intermediate, 7-hydroxybenzo[*b*]phosphole oxide, was prepared in a regioselective manner from 3-(methoxymethoxy)phenylzinc reagent, 5-decyne, and $PPhCl_2$ in a one-pot protocol. By utilizing the hydroxyl group as a synthetic handle, allowing the construction of the angularly fused carbohelicene moiety bearing an inner-rim phosphorus center in a concise manner. Based on ^1H NMR and single crystal analysis, the thus-synthesized phospha[5]helicenes were demonstrated to undergo facile helicity inversion in solution, which was also corroborated by DFT calculations. Chapter 3 discusses about the synthesis and optical properties of phosphole oxide-fused triphenylene derivatives (Scheme 2). As was the case of phospha[5]helicenes synthesis, 7-hydroxybenzo[*b*]phoshole oxide was utilized as a key precursor for the extension of the π-conjugation system, and the triphenylene core was furnished through dehydrogenative C-C coupling of biaryl (Scholl reaction). The present compounds represent rare examples of phosphole-embedded triphenylenes. The thus-synthesized compounds displayed strong blue fluorescence.

Scheme 1. Synthesis of phospha[5]helicenes bearing an inner-rim P-center (**Chapter 2**)

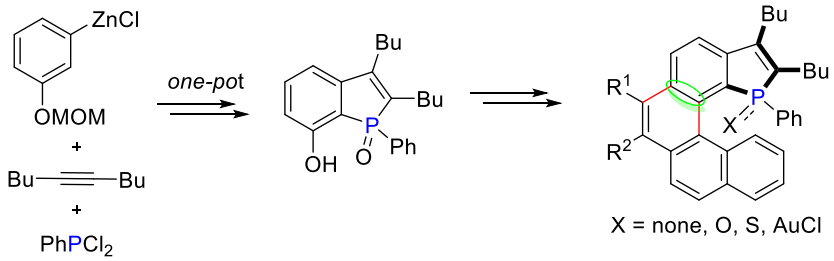

Scheme 2. Synthesis of phosphole oxide-fused triphenylene derivatives (**Chapter 3**)

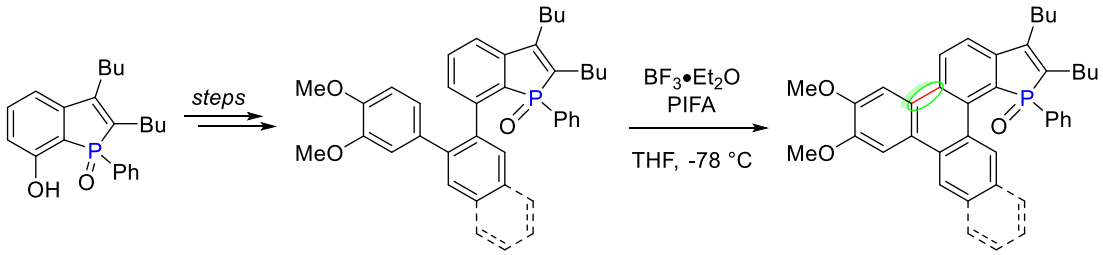

Part 2, Chapter 4 of the thesis, firstly describes a brief review on synthesis and properties of heptagon-embedded polyaromatic hydrocarbons and transition metal-catalyzed annulation reactions between alkynes and aromatic substrates. Secondly, this chapter describes the palladium-catalyzed annulation of 1-halo-8-arylnapthalenes and alkynes leading to heptagon-embedded aromatic systems with all sp^2 carbon center (Scheme 3). The reaction is promoted by the catalytic system comprised of $Pd(OAc)_2$, moderate electron-deficient triarylphosphine $P(4\text{-}ClC_6H_4)_3$ and Ag_2CO_3. Notable feature of the reaction is the broad substrate scope and variety of aryl groups on the 7- and 8-positions of the benzo[4,5]cyclohepta[1,2,3-*de*]naphthalenes and two-fold annulated heptagon containing PAHs.

Scheme 3. Pd-Catalyzed synthesis of heptagon-embedded PAHs (**Chapter 4**)

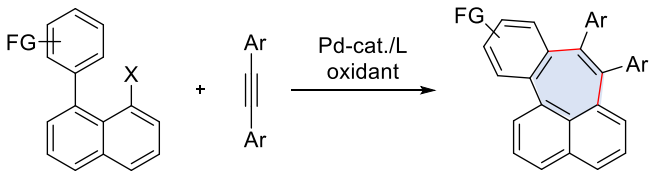

Acknowledgements

First and foremost, I would like to thank to Almighty Allah for his boundless blessings to carry out the work successfully. With immense pleasure, I would like to express my sincere gratitude and reverence to my supervisor Professor Naohiko Yoshikai for his scrupulous guidance and enthusiastic interest throughout my PhD study and research. His sincerity, positive attitudes and passion towards chemistry continues to inspire and motivate me.

I would like to thank my thesis advisor committee members, Prof. Atsushi Goto, NTU and Prof. Chi Chunyan, NUS for their valuable suggestions and encouragement.

My profound thank to my senior colleague, Dr. Bin Wu, for his kind assistance and training for Schlenk techniques and instrumentation. I also sincerely appreciate to all our group members, both past and present, for their fruitful discussion and kind assistance: Dr. Junfeng Yang, Dr. Junliang Wu, Dr. Jianming Yan, Dr. Wengang Xu, Dr. Simon Tan, Dr. Chunlin Wu, Ms. Qiao Sun, Mr. Roshayed Ali Laskar, Dr. Wei Ding, Mr. Sekiguchi Yoshiya, Dr. Wang Changsheng, Ms. Seng S. M. Caroline, and Mr. Benjamin Y. R. Peng.

I would like to thank Dr. Rakesh Ganguly and Dr. Li Yongxin for assistance in X-ray crystallographic analysis, Mdm. Zhu Wen-Wei (Low- and High-Resolution Mass Spectroscopy) for training on the use of the equipment, and Ms. Goh Ee-Ling for training on the use of the NMR spectrometers.

I would like to thank my NTU friends, Mr. Md. Arif Hussain, Dr. Khursheed Ahmad, Dr. Munir Shahzad and my CBC colleagues.

I would like to thank Nanyang Technological University (NTU) for providing me the graduate research scholarship and an opportunity to pursue my PhD in a world-renowned university. I enjoyed multiculturism of vibrant international university, NTU.

Finally, I wish to sincerely appreciate to my beloved parents, Alhaj Mr. Md. Mojibur Rahman and Mdm. Nazmun Nisa for their countless blessings and love. My deepest gratitude to my brothers and sisters for giving me long standing moral support and encouragement.

Table of Contents

List of Abbreviations

Ar	aryl (substituted aromatic ring)
a.u.	arbitrary unit
B3LYP	Becke, 3-parameter, Lee-Yang-Parr
Boc	*tert*-butyloxycarbonyl
bs	broad singlet
Bu	butyl
Calcd	calculated
cat.	catalytic
cm^{-1}	wave number
d	doublet
DCM	dichloromethane
DCE	1,2-dichloroethane
dd	doublet of doublets
DDQ	2,3-dichloro-5,6-dicyano-1,4-benzoquinone
δ	chemical shift (ppm)
°C	degree centigrade
DFT	density functional theory
DME	1,2-dimethoxyethane
DMF	*N*,*N*-dimethylformamide
DMSO	dimethylsulfoxide
DIPEA	diisopropylethylamine
dr	diastereomeric ratio
ee	enantiomeric excess
equiv	equivalent
ε	molar extinction coefficient

ESIHRMS	Electrospray Ionization High Resolution Mass Spectrometry
Et	ethyl
EWG	electron withdrawing group
g	gram
h	hour
Hz	hertz
ICl	iodine monochloride
*i*Pr	isopropyl
J	coupling constants
kcal	kilocalorie
LED	light emitting diode
LG	leaving group
M	concentration (N, mol/dm^{-3})
M^+	parent molecular ion peak (mass spectrum)
m	multiplet
Me	methyl
MeOH	methanol
mg	milligram
MHz	megahertz
min	minutes
mL	milliliters
mmol	millimole
mol%	mole percent
MOM	methoxymethyl
NMR	nuclear magnetic resonance
Nu	nucleophile
OTf	trifluoromethanesulfonate

Φ_F	quantum yield
Ph	phenyl
$PhNTf_2$	*N*-phenyl-bis(trifluoromethanesulfonimide)
PIFA	(bis(trifluoroacetoxy)iodo)benzene
ppm	parts per million
Pr	propyl
q	quartet
rt	room temperature
s	singlet
S_NAr	nucleophilic aromatic substitution
UV-vis	ultraviolet–visible spectroscopy
t	triplet
TEA	triethylamine
Tf	trifluoromethanesulfonyl
THF	tetrahydrofuran
TLC	thin layer chromatography
TMEDA	*N*,*N*,*N*',*N*'-tetramethylethylenediamine
TMDS	1,1,3,3-tetramethyldisiloxane
TS	transition state

Chapter 1. General Introduction

1.1 Importance of Phosphole-Embedded Polycyclic Aromatic Systems

Polycyclic aromatic compounds (PACs) embedded with a phosphorus-containing five-membered ring, phosphole, have attracted substantial interest from the synthetic and materials chemistry community as novel functional molecules featuring properties such as low HOMO-LUMO energy gap, electron accepting and n-type semiconducting properties. They hold promise for applications in organic field effect transistors, photovoltaics, organic light emitting diodes, sensing and fluorescent probes, and so on.[1-9] Several notable examples of phosphole-containing polycyclic aromatic systems (**1.1**-**1.9**) are shown in Figure 1.1.[10-19]

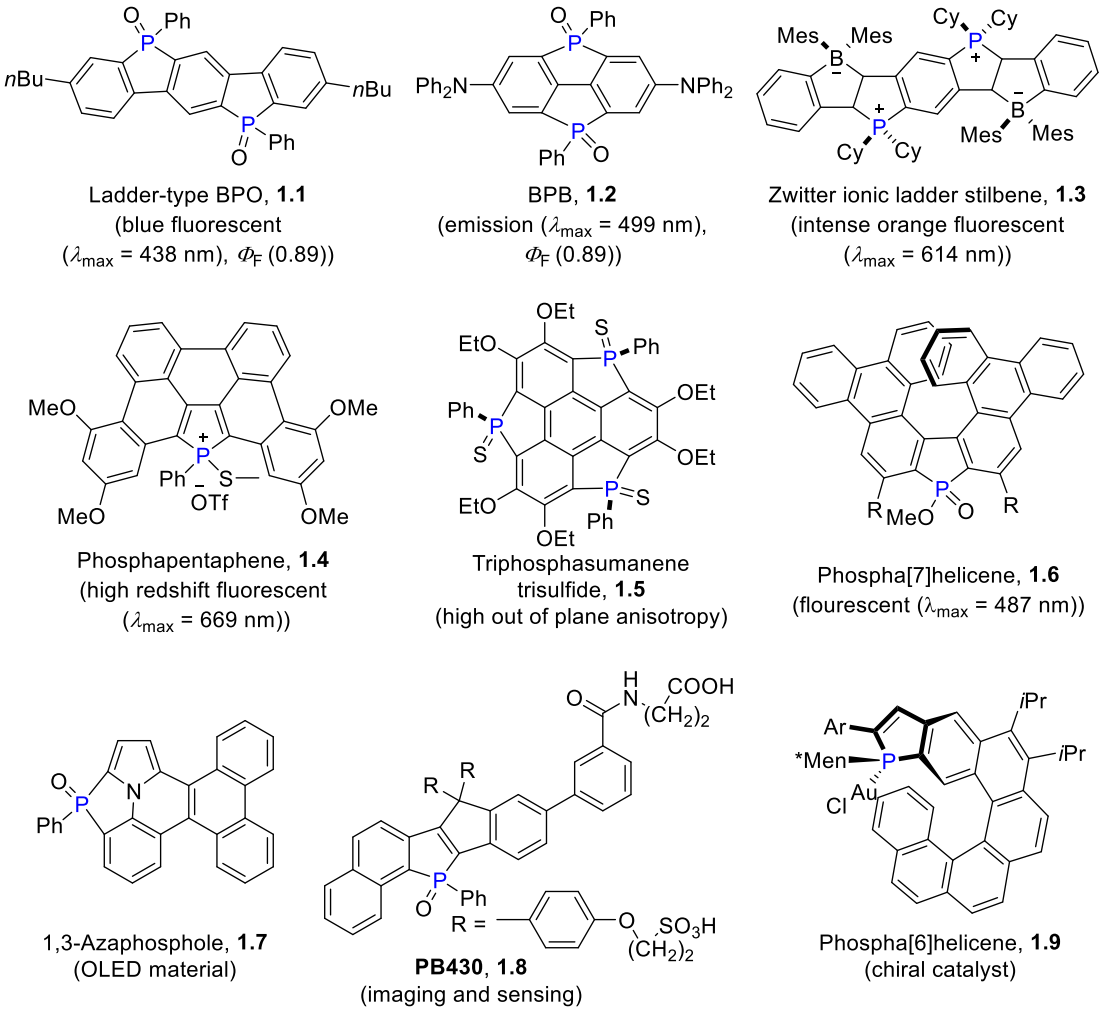

Figure 1.1. Phosphole-containing polycyclic aromatic compounds as novel functional molecules.

1.2 Synthesis of Phosphole-Embedded Polycyclic Aromatic Compounds

The synthesis of the above and other phosphorus-containing PACs requires efficient strategies and methods for the critical C–P and C–C bond formations, which allow for the installation of the phosphole unit or the closure of the ring system. In this section, representative examples of such synthetic approaches, including oxidative

photocyclization, transition metal-catalyzed P–C bond-forming cyclization, transition metal-catalyzed cyclotrimerization of alkynes, and others, are discussed.

1.2.1 Oxidative Photocyclization

The C-C bond formation reaction via oxidative photocyclization is a straightforward strategy to construct PACs.[13, 20-23] In this context, Reau,[13] Hissler,[24] and Marinetti[19] exploited the oxidative photocyclization reaction to achieve phosphole-fused PACs as summarized below. Despite the straightforwardness of the approach, dehydrogenative photocyclization reactions often suffer low efficiency and formation of side products.

1.2.1.1 Synthesis of Dibenzophosphapentaphene Derivatives

In 2012, Reau and coworkers reported the synthesis of planar dibenzophosphapentaphene derivatives via dehydrogenative photocyclization of a partially fused pentaarylphosphole sulfide **1.10** (Scheme 1.1).[13] The reaction afforded a mixture of the products **1.11** and **1.12**, and the latter, fully fused product was further subjected to modification on the phosphorus atom. The dibenzophosphapentaphene derivatives showed large bathochromic shift. Among them, σ^3,λ^3-dibenzophosphapentaphene sulfonium triflate **1.13** showed strong fluorescence (λ_{em} = 669 nm). In addition, the solid state structure of **1.13** is superimposable on that of its neutral precursor **1.12**, indicating that chemical modification of the P-moiety does not alter the planar sp^2 carbon backbone. DFT calculations revealed that the central

phosphole ring of **1.13** and **1.15** has an antiaromatic character, and the frontier orbitals are highly delocalized on the sp^2-carbon skeletons.

Scheme 1.1. Synthesis of dibenzophosphapentaphenes via dehydrogenative photocyclization

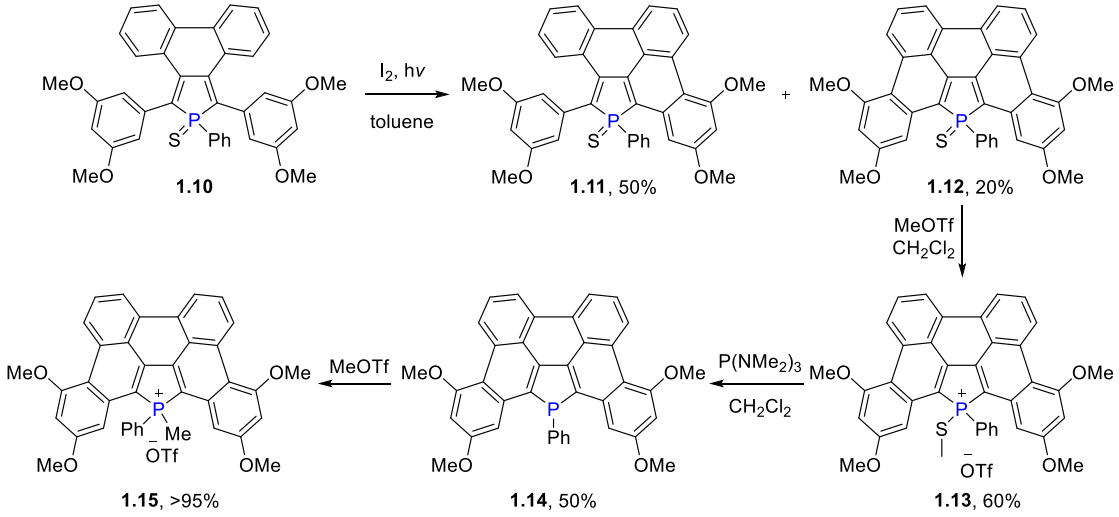

Hissler and coworkers also attempted to synthesize planar dibenzophosphapentaphene and related derivatives via photochemical oxidative cyclization (Scheme 1.2).[24-25] The reaction of pentaarylphosphole oxide **1.16** resulted in the formation of only one C–C bond to afford the product **1.17** in 5% yield (Scheme 1.2a). In contrast, phosphole **1.18** bearing thienyl and phenyl moieties underwent twofold dehydrogenative cyclization, affording **1.19** in 52% yield (Scheme 1.2b). Attempts on further dehydrogenative ring closure of **1.18** and **1.19** were unsuccessful.

Scheme 1.2. Attempts on synthesis of dibenzophosphapentaphenes via dehydrogenative photocyclization

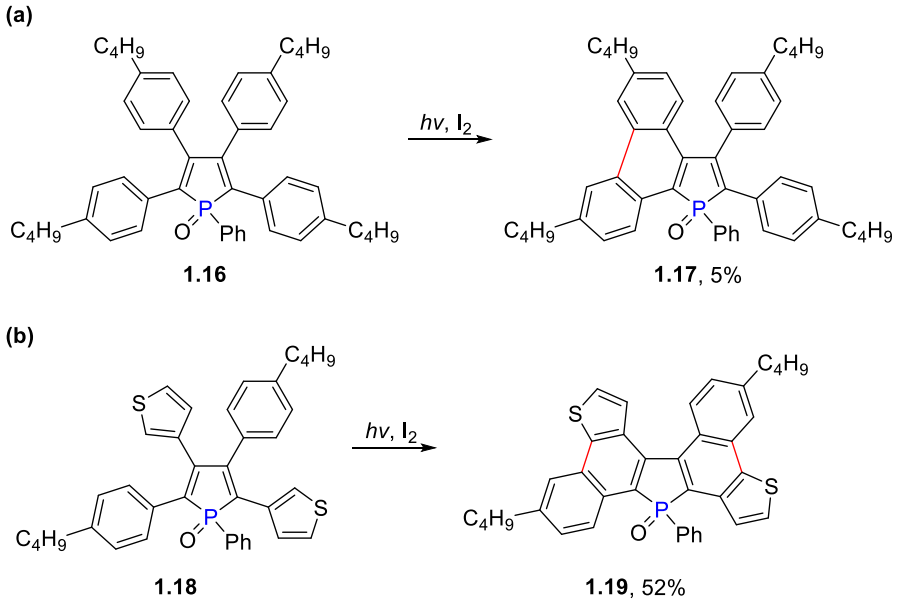

1.2.1.2 Synthesis of Phospha[6]helicenes and Related Derivatives

Over the last several years, Marinetti *et al.* have reported the synthesis of novel chiral phospha[6]helicene and related derivatives with the aid of oxidative photochemical cyclization conditions (Scheme 1.3).[19, 26] The notable feature about their synthetic design is that the helicity of phosphahelicenes and can be controlled by the central chirality of the phosphorous atom. The key starting precursor is *l*-menthyl-5-triflate-benzo[*b*]phosphole **1.20**, which is synthesized from (*Z*)-(4-bromo-3-(2-bromovinyl)phenoxy)(*tert*-butyl)dimethylsilane and *l*-menthyldichlorophosphine. The compounds **1.21** and **1.24** were irradiated in the presence of molecular iodine to afford cyclized products phospha[6]helicenes **1.22** and **1.25**, respectively, along with

phospha[8]helicenes as side products. The compounds **1.22** and **1.25** could be efficiently reduced to the corresponding free phosphines by hydrosilane, followed by complexation with gold to afford phosphine-gold complexes **1.23** and **1.26**, respectively. The chiral phospha[6]helicene gold complex **1.27** has been used as ligands for gold-catalyzed enantioselective enyne cycloisomerizations[18, 27-28] whereas phospha[6]helicene **1.28** has been used as a nucleophilic catalyst for enantioselective [3 + 2] cycloaddition of electron poor alkenes and allenes (Scheme 1.4).[29-30] Furthermore, the authors recently investigated the chiroptical and electronic properties of phosphahelicenes and tested their performance in OLED devices.[8]

Scheme 1.3. Synthesis of phosphahelicenes via photochemical oxidative C-C coupling

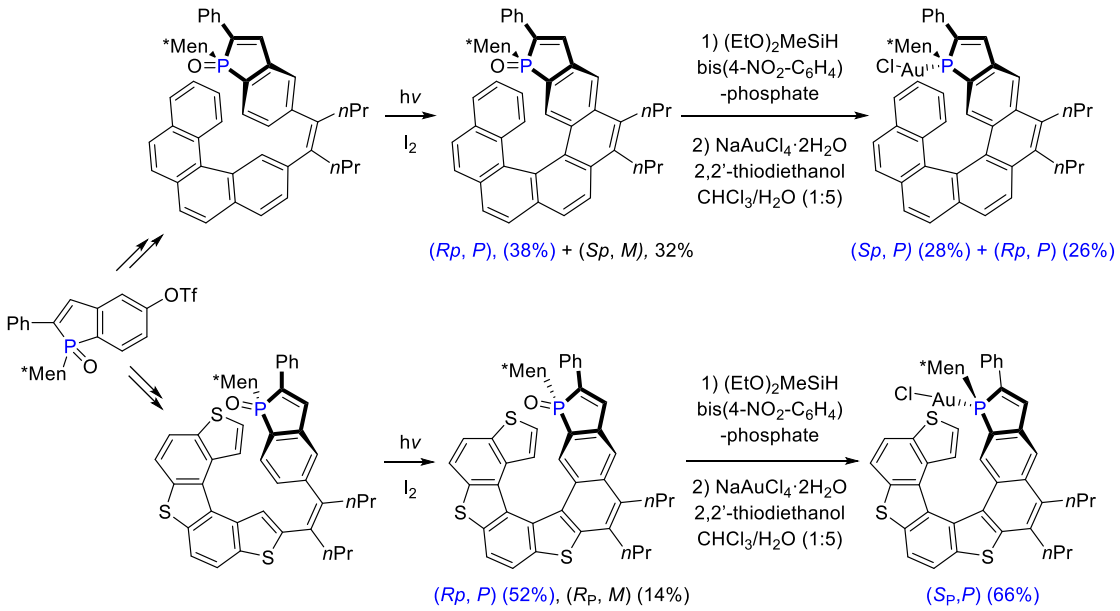

Scheme 1.4. Applications of phospha[6]helicenes in asymmetric synthesis

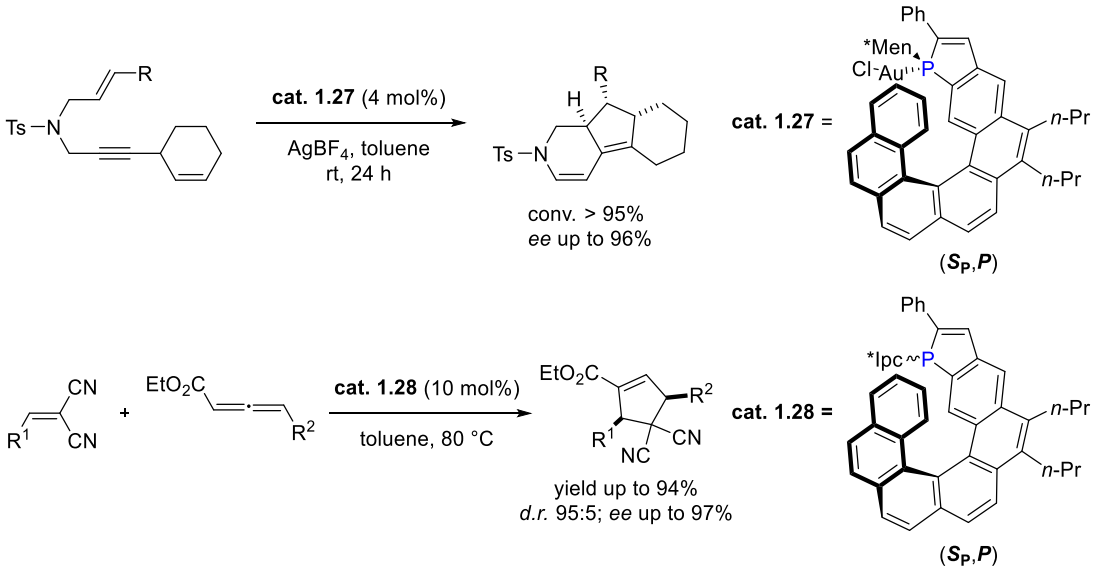

1.2.2 P–C Bond-Forming Cyclization

P–C bond-forming cyclization has been widely explored for the synthesis of phosphorus-containing PACs. The critical P–C bond formation can be achieved through several approaches, such as (1) palladium-mediated P–C coupling, (2) addition of a phosphorus-centered radical or a phosphorus nucleophile onto aromatic ring or alkyne, (3) trapping of an organometallic nucleophile by a phosphorus electrophile, and so on. Selected examples of the synthesis of phosphorus-containing PACs by different approaches are discussed below.

1.2.2.1 Palladium-Catalyzed P–C Coupling

Nozaki *et al*. achieved the synthesis of a λ^5-phospha[7]helicene via palladium-catalyzed C–P coupling as key steps (Scheme 1.5).[31] The synthesis started with the reaction of [4,4'-biphenanthrene]-3,3'-diylbis(trifluoromethanesulfonate) **1.29** and ethylphenylphosphinate **1.30** in the presence of $Pd(OAc)_2$, followed by reduction of

P=O of **1.31** with $LiAlH_4$ and TMSCl under the elevated conditions. The resulting biphenanthrene bearing phosphine and triflate groups **1.32** was directly subjected to palladium-catalyzed intramolecular P-C coupling, followed by oxidation with H_2O_2, affording the phospha[7]helicene oxide **1.34** in a decent yield. The authors studied the physico-chemical properties of the phospha[7]helicene oxide and showed its strong fluorescent and one-dimensional columnar aggregation properties.

Scheme 1.5. Palladium-Catalyzed synthesis of λ^5-phospha[7]helicene

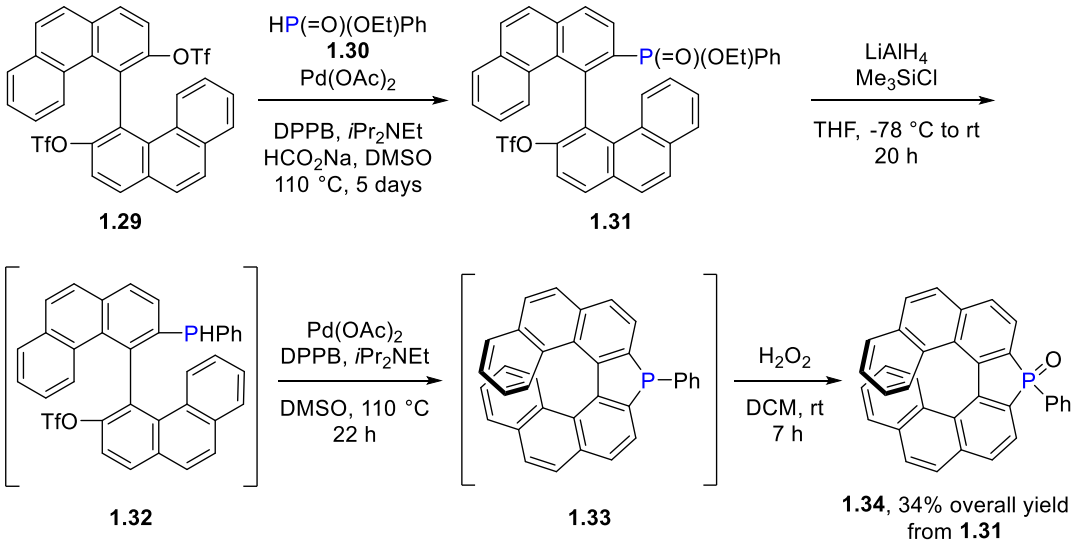

1.2.2.2 P–C Cyclization Involving P-Centered Radical or Nucleophile

Kobayashi, Kawashima and coworkers reported the synthesis of ladder-type dibenzophospholes via oxidative intramolecular radical cyclization (Scheme 1.6).[10] Bis(phenylphosphinyl)-*p*-terphenyl **1.35** was treated with an excess amount of triethylborane in the presence of oxygen, affording phosphoryl-bridged teraryl as a mixture of *syn*-**1.37** and *anti*-**1.38** (~ 1:2) diastereomers. The absorption and emission

profiles of the *syn*-**1.37** and *anti*-**1.38** diasteromers in solution were similar. On the other hand, their solid-state fluorescence behaviors were different. The emission maximum of the *syn*-**137** (λ_{em} = 476 nm) was slightly red-shifted compared with that of the *anti*-**138** (λ_{em} = 454 nm). In addition, the quantum yield of the *syn*-**137** was higher (Φ_F = 0.63) than that of the *anti*-**138** (Φ_F = 0.46).

Scheme 1.6. Synthesis of ladder-type dibenzophosphole through intramolecular radical cyclization

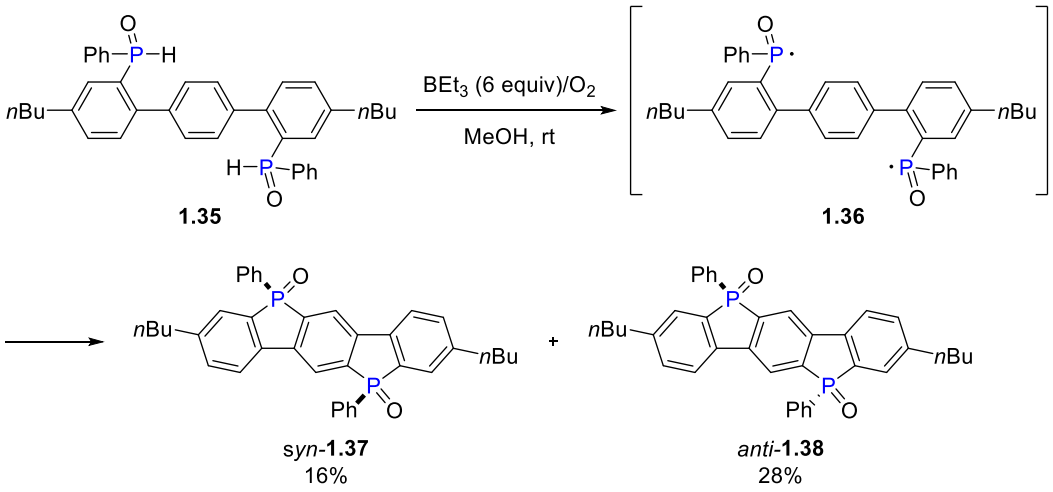

Yamaguchi and coworkers reported the synthesis of bis-phosphoryl-bridged stilbenes via two-fold P–C bond-forming cyclization (Scheme 1.7).[32] The synthesis comprised of four-steps in a sequential manner. The dilithiation of bis(2-bromophenyl)acetylene **1.39** followed by trapping with $PhP(NEt_2)Cl$ **1.40** resulted in the formation of bis(aminophosphanyl) intermediate **1.41**. Treatment of this intermediate with PCl_3 promoted cascade cyclization, and subsequent oxidation with H_2O_2, afforded the bis-phosphoryl-bridged stilbene as a mixture of *cis*-**1.42** and *trans*-

1.43 isomers (Scheme 1.7a). In another report, Yamaguchi and Studer described the preparation of bis(phosphoryl)-bridged biphenyls through radical phosphanylation of tetrabromobiphenyls in the presence of 1,1'-azobis(cyclohex-ane-1-carbonitrile) (V-40) as a radical initiator (Scheme 1.7b).[11]

Scheme 1.7. Synthesis of bis-phosphoryl-bridged stilbenes

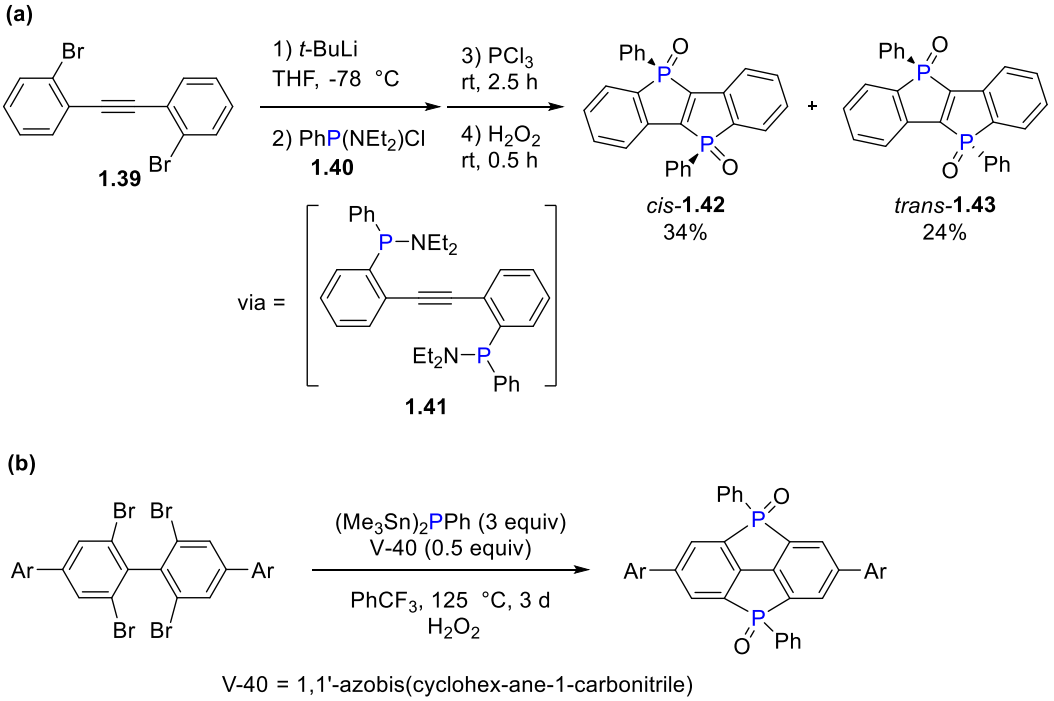

Recently, Yamaguchi explored the substrate scope and applications of bis-phosphoryl-bridged stilbenes as biological fluorescence sensing and imaging.[17, 33-35] By utilizing the PCl_3-mediated nucleophilic cascade cyclization of bis(2-bromophenyl)acetylene (Scheme 1.7a), a series of new phospholo[3,2-*b*]phosphole-based water soluble dyes were synthesized (Scheme 1.8).[33] To make phospholo[3,2-*b*]phosphole derivatives water soluble, a sulfonate-substituted aryl groups at the

bridging P=O moieties and a carbonate-substituted phenyl groups at the terminal position of benzene were introduced. The compounds *trans*-**1.44** and *trans*-**1.45** demonstrated interesting physico-chemical properties. Both the compounds were highly soluble and stable in water without forming any aggregation, and the emission behaviors were free from concentration, polarity and pH of the solutions.

Scheme 1.8. Synthesis of phospholo[3,2-*b*]phosphole-based water soluble dyes

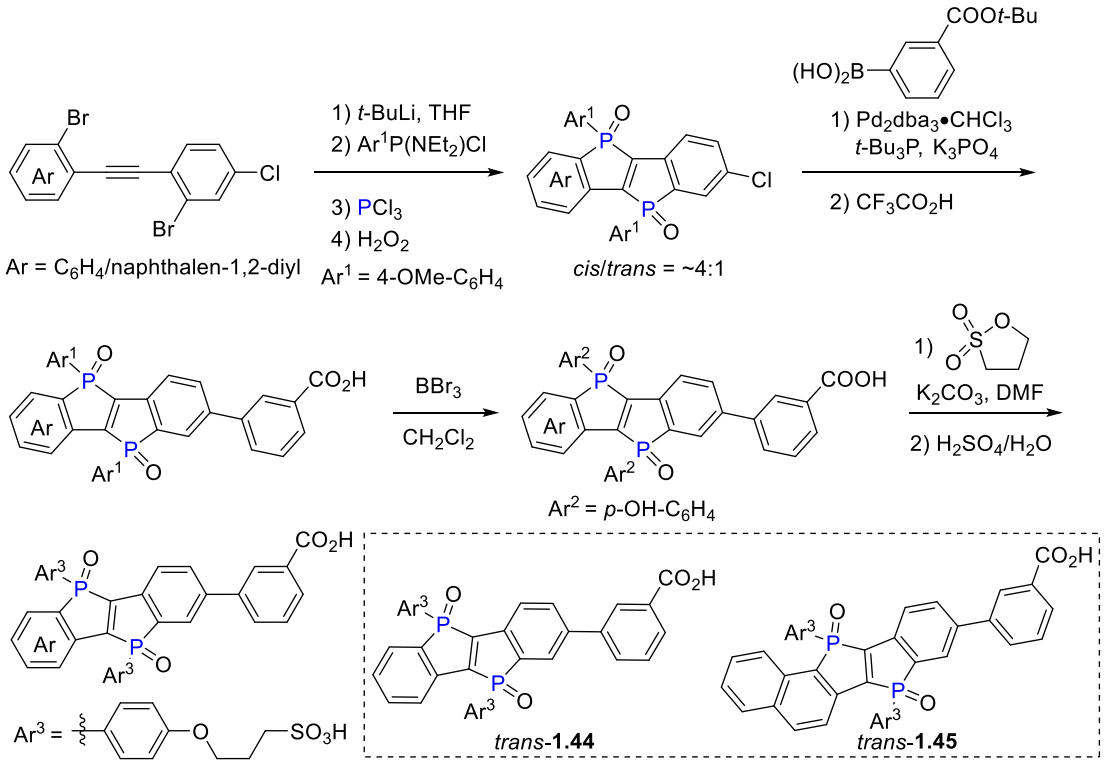

Yamaguchi *et al.* devised another elegant synthetic route to access water soluble, super photostable phosphole-embedded PACs (Scheme 1.9).[17, 35] The reaction started with the lithiation of 2-bromo-diphenylacetylene, trapping with $PhP(NEt_2)Cl$ followed by PBr_3-mediated cyclization and oxidation with H_2O_2, affording 3-bromo-

substituted benzophosphole oxide as a key precursor.[34] After several steps, a series of novel water soluble, highly photostable methylene-bridged phosphole oxide-based fluorescent dyes were synthesized (Scheme 1.9).[17, 35] C-BPhox **1.46** and C-Naphox **1.47** showed high photostability under stimulated emission depletion (STED) conditions. C-Naphox **1.47** is more potent for visualization of various biological events, presumably due to high polarity responsive fluorescence and low photobleaching.[35] On the other hand PB430 **1.8**[17] exhibited super photostability for multicolour and repeated STED imaging for 3-D-reconstruction and also was utilized as fluorescent labelling reagent for proteins.

Scheme 1.9. Synthesis of highly photostable fluorescent phosphole-based dyes

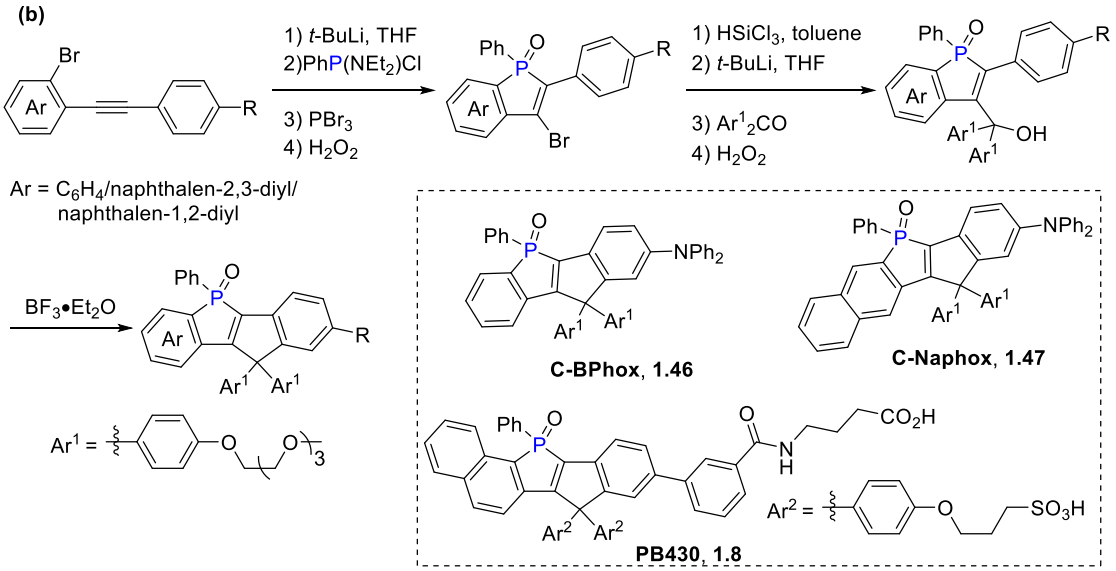

1.2.2.3 Tapping of an Organometallic Nucleophile by a Phosphorus Electrophile

Yamaguchi and coworkers described the synthesis of rigid, ladder-type, polycyclic phosphonium- and borate-bridged zwitterionic stilbenes through P-C/C-B

bond formation (Scheme 1.10).[12] The synthesis started with monolithiation of bis(2-bromophenyl)acetylene followed by trapping with Mes_2BF, which afforded (2-((2-bromophenyl)ethynyl)phenyl)dimesitylborane. Lithiation of with *t*-BuLi and subsequent treatment with dialkylchlorophosphine resulted in the formation of corresponding zwitterionic stilbenes. This methodology could be utilized to prepare more extended homologues and heteroaromatic derivatives **1.48-1.50** (Scheme 1.10). The authors revealed unique photophysical, electrochemical and highly electron accepting properties of the P,B-bridged π-systems.

Scheme 1.10. Preparation of phosphonium- and borate-bridge zwitter-ionic stilbenes

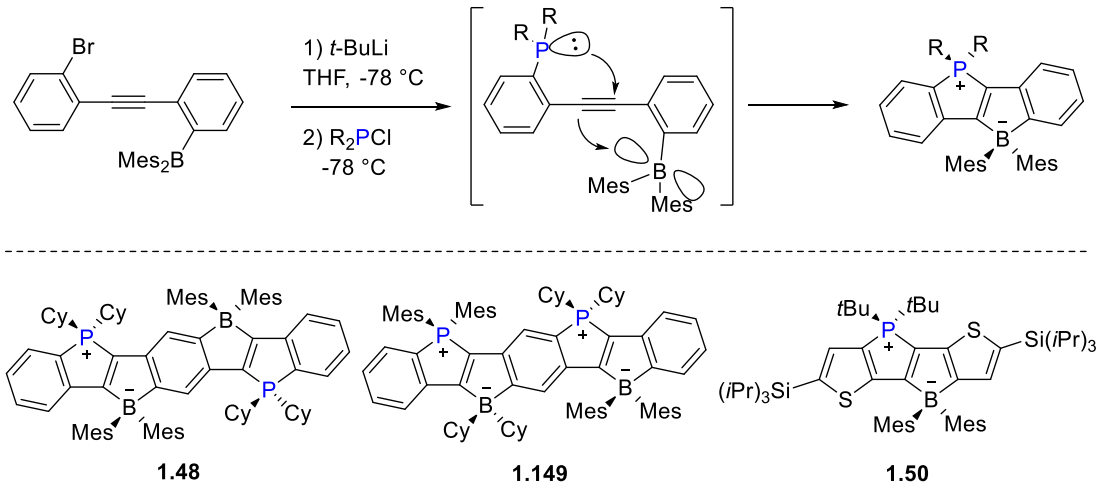

1.48 **1.149** **1.50**

Recently, Duan, Mathey and coworkers reported the synthesis of phosphindole-fused pyrroles and related derivatives via sequential P–C bond formations (Scheme 1.11).[16, 36-37] 1,3-Azaphosphole derivatives **1.53-1.54**, which were utilized in OLED devices, were synthesized by sequential treatment of pyrrolo[1,2-*a*]quinoline **1.51** with *n*-BuLi, followed by treatment with dichlorophenylphosphine

1.52, and then with H_2O_2 or S_8 (Scheme 1.11a).[16] It is likely that lithiation took place at the pyrrole C2 position, and that upon the first P–C bond formation, the second P–C bond was formed through an intramolecular electrophilic aromatic substitution (S_EAr) pathway. The organolithium trapping/intramolecular S_EAr approach was also applied to the conversion of bis(2-bromophenyl)-tertaarylpyrrolo[3,2-*b*]pyrrole into a novel phosphindole-fused pyrrolo[3,2-*b*]pyrrole derivatives **1.55-1.60** in good to moderate yield and ca. 1:1 *cis*/*trans* ratio (Scheme 1.11b).[37]

Scheme 1.11. Preparation of phosphindole-fused pyrroles

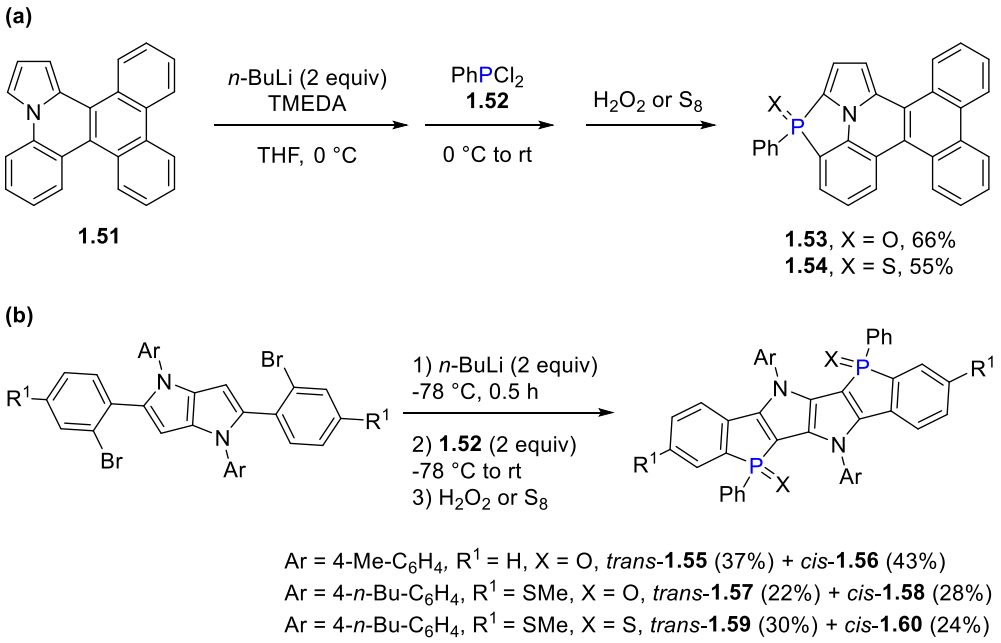

Saito and coworkers designed and synthesized a novel triphosphasumanene trisulfide **1.63-1.66** from 2,3,6,7,10,11-hexyethoxytriphenylene **1.61** (Scheme 1.12).[14] The preparation started with the lithiation of **1.61** by using excess amount of *n*-BuLi (10 equiv) in hexane under reflux conditions. This resulted in generation of a

hexalithiated intermediate **1.62**, which, upon sequential treatment with dichlorophenylphosphine **1.52** and elemental sulfur, yielded *syn* and *anti* isomers of triphosphasumanene trisulfide (**1.63-1.64**) together with the corresponding *syn* and *anti* isomers of the triphenylenodiphosphole disulfide (**1.65-1.66**). The authors disclosed the unique physicochemical properties of *syn*-**1.63** and *anti*-**1.64**. *syn*-**1.63** demonstrates a high dipole moment (12.0 D) than that of *anti*-**1.64** (3.97 D) in the perpendicular direction of the π-system. Furthermore, *syn*-**1.63** possessed a high out-of-plane anisotropy, high adsorption ability on Au(111) surface and high electronic conductivity compared to that of *anti*-**1.64**.

Scheme 1.12. Synthesis of novel triphosphasumanene trisulfide

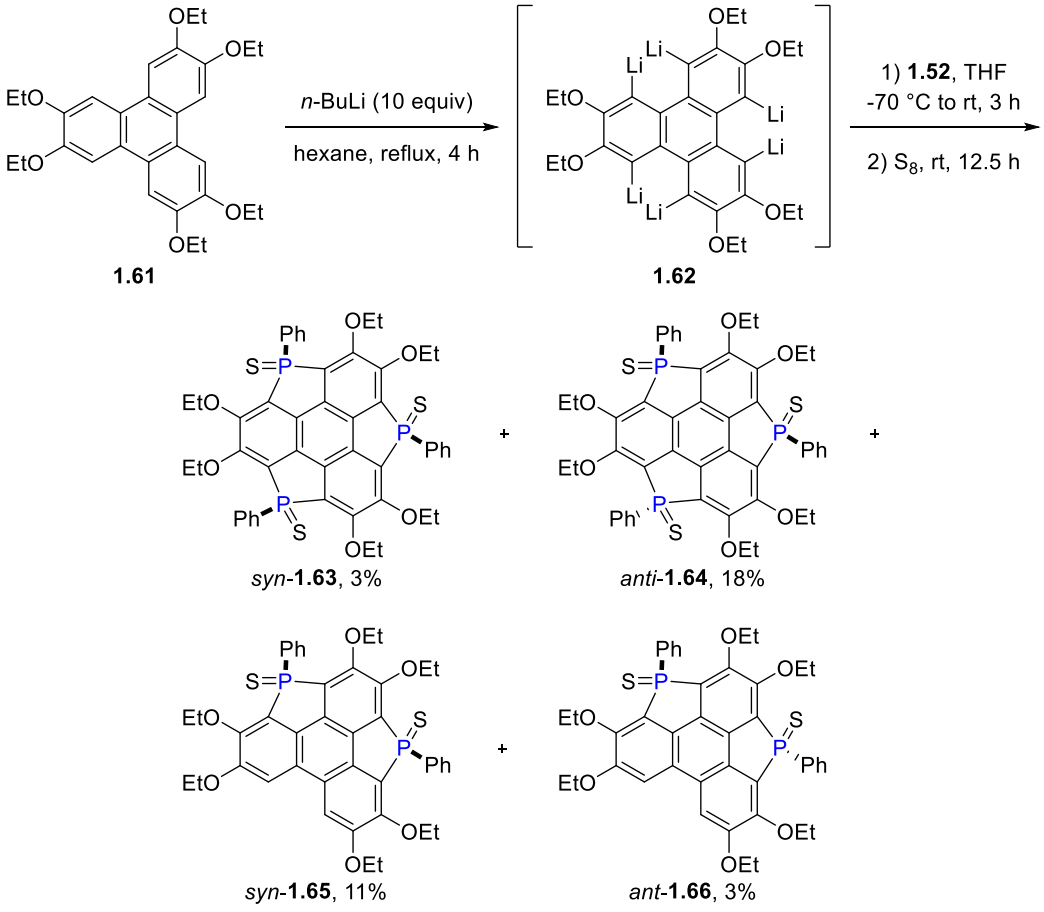

1.2.3 Transition Metal-Catalyzed [2 + 2 + 2] Cycloaddition

Transition metal-catalyzed [2 + 2 + 2] cycloaddition of alkynes to create a library of polycyclic aromatic hydrocarbons has been explored by several groups including Stara (Ni and Co),[38-43] Shibata (Ir),[44] Tanaka (Rh),[45-47] However, this methodology has been used only sporadically for the synthesis of phosphorus-containing PACs. As discussed below, Tanaka employed rhodium catalysis to synthesis phosphafluorene-based [7]helicenes and bitriphenylenes.[15, 48] On the other hand, Marinetti utilized nickel catalysis to prepare phosphorus-embedded [6]helicenes.[28, 49]

1.2.3.1 Rhodium-Catalyzed Synthesis of Phosphafluorenes and 1,1'-Bitriphenylenes

In 2010, Tanaka and coworkers reported the first enantioselective synthesis of benzopyrano- or naphthopyrano-fused, helicene-like phosphafluorene derivatives via rhodium-catalyzed [2 + 2 + 2] cycloaddition of phenol- or naphthol-linked tetraynes and dialkynyl phosphorus compounds (Scheme 1.13).[50] The phosphafluorenes showed high photoluminescence properties. However, the reaction suffered relatively modest enantioselectivity and efficiency. In 2012, the same group developed a highly enantioselective protocol to synthesize helically chiral 1,1'-bitriphenylenes featuring fluorenone- or dibenzophosphole-type bridges via rhodium-catalyzed double [2 + 2 + 2] cycloaddition (Scheme 1.14).[15] 1,1'-Bitriphenylenes featuring fluorenone were obtained in moderate to good yields and high enantiomeric excess (up to 93% *ee*),

whereas dibenzophospholes **1.67-1.68** were obtained in decent yields and moderate enantiomeric excess (up to 75%). They derivatized the fluorenone-type product to the corresponding fluorene and spirofluorene to investigate their photoluminescence properties. The spirofluorene- and dibenzophopshole-type helicenes showed particularly high circularly polarized luminescence (CPL) and high red-shift properties.

Scheme 1.13. Synthesis of phosphafluorenes via Rh-catalyzed [2 + 2 + 2] cycloaddition

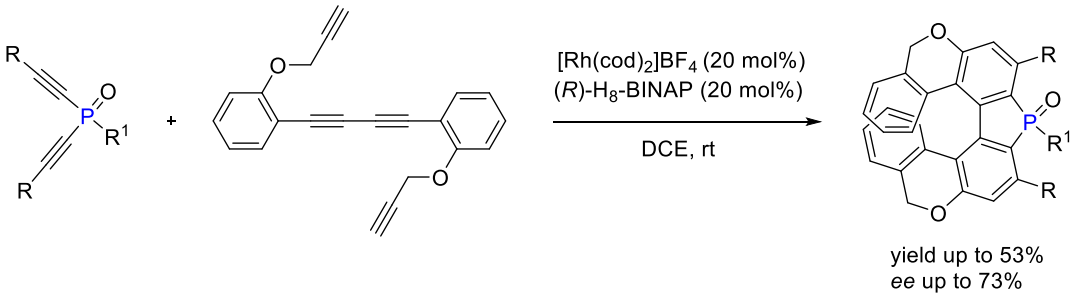

Scheme 1.14. Rh-Catalyzed enantioselective synthesis of helical 1,1'-bitriphenylenes

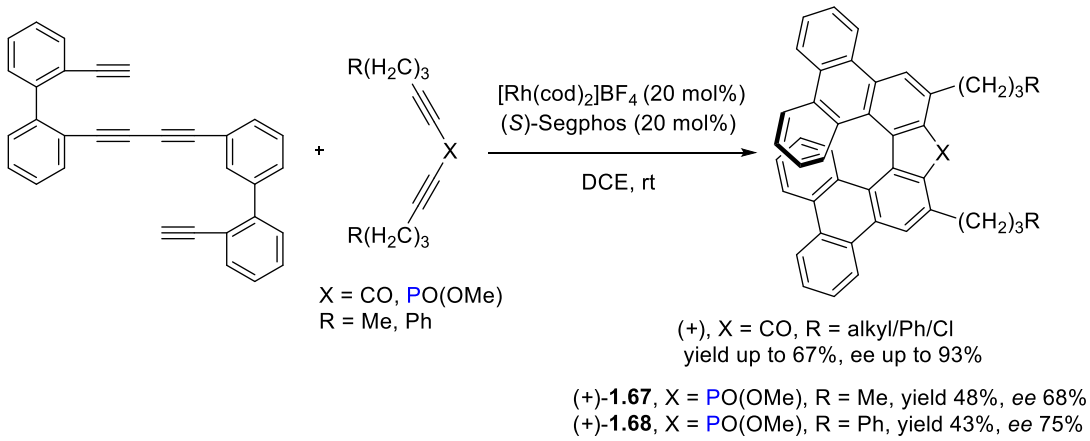

1.2.3.2 Nickel-Catalyzed Synthesis of Phosphole-Embedded Helicenes

Marinetti and coworkers achieved the synthesis of phosphorus-embedded [6]helicenes via nickel-catalyzed intramolecular [2 + 2 +2] cyclotrimerization of triynes (Scheme 1.15).[28, 49] Enantiomerically pure, P-*l*-menthyl-substituted triyne precursors such as (S_P)-**1.71**, (R_P)-**1.72** which were synthesized from *l*-menthyl-5-hydroxybenzo[*b*]phosphole derivatives (S_P)-**1.69** and (R_P)-**1.70** through several steps. (S_P)-**1.69** and (R_P)-**1.70** were subjected to $Ni(cod)_2/PPh_3$-mediated intramolecular [2 + 2 + 2] cycloaddition, thus affording phosphole-emdedded [6]helicene derivatives **1.73** and **1.74**, respectively, in good yield and ca. 2:1 to 6:1 diastereomeric ratio (Scheme 1.15a). Based on the single crystal X-ray analysis, the P=O bond of the major isomer was exposed outside the helical scaffold, while the P-menthyl group was pointed toward the internal face of the helical scaffold. The authors further extended the scope of nickel-catalyzed intramolecular [2 + 2 +2] cyclotrimerization to P-*l*-menthyl-substituted triyne (+)-**1.76**, which afforded phospha[6]helicene **1.77** in excellent yield but with poor diastereomeric ratio ((+)-*M*/(+)-*P* = 40:60) (Scheme 1.15b). The (+)-*M* and (+)-*P* isomers of **1.77** were separated and transformed into the respective gold complexes, which were tested for enantioselective gold catalysis.

Scheme 1.15. Synthesis of P-embedded [6]helicenes via Ni(0)-catalyzed [2 + 2 + 2] cycloaddition of triynes

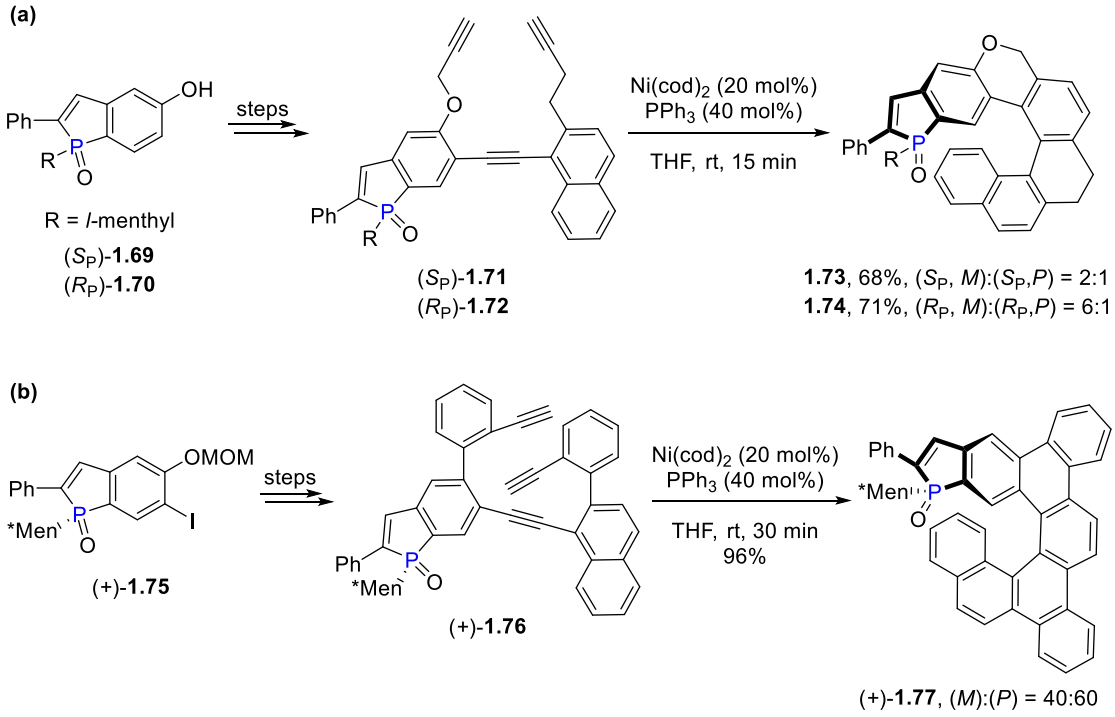

1.3 Perspective for Chapters 2 and 3

As described above, phosphole-embedded PACs have received considerable attention as organic materials for optoelectronic devices, asymmetric catalysis, biological fluorescent probes and so on. Given this growing interest, the development of a new strategy for the synthesis of phosphole and its benzo-fused derivatives is desirable, because it may open a route to novel phosphole-containing polycyclic scaffolds that are not readily accessible by existing strategies. In this context, my attention was drawn to the one-pot multicomponent synthesis of benzo[*b*]phospholes from arylzinc reagents, alkynes, and phosphorus electrophiles, which was developed by Yoshikai group (Scheme 1.16).[7, 51-52] Thus, a cobalt–Xantphos complex catalyzes the addition of an arylzinc reagent to an internal alkyne to form an *ortho*-alkenylarylzinc reagent through 1,4-cobalt migration as a key step.[53-55] This organozinc intermediate is directly subjected to copper-mediated reaction with

dichlorophenylphosphine, followed by oxidation with H_2O_2 or elemental sufur, thus affording benzophosphole oxide or sulfide, respectively. Alternatively, the use of phosphorus trichloride and a Grignard reagent in place of dichlorophenylphosphine in this synthetic sequence allows for the installation of different aryl and alkyl substituents to the P atom of the benzophosphole.

Scheme 1.16. Modular synthesis of benzo[*b*]phosphole oxides via 1,4-cobalt migration

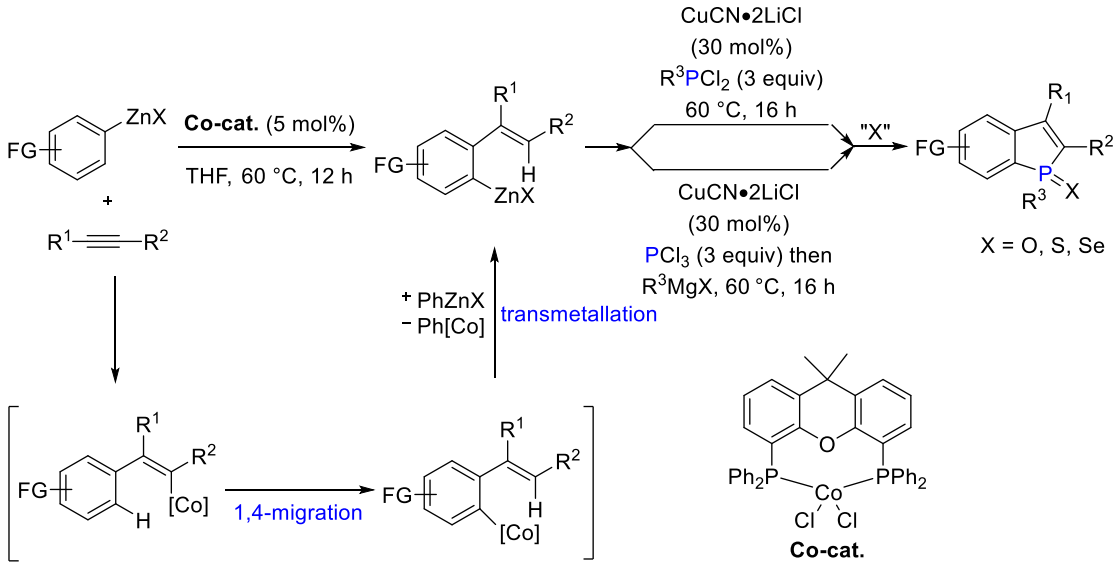

Besides the highly modular nature, this benzophopshole synthesis features unique regioselectivity. Thus, arylzinc reagents bearing alkoxy- or fluorine substituent at the 3-position regioselectively afford 7-substituted benzophosphole derivatives because of preferential 1,4-cobalt migration to the position proximal to such substituents (Scheme 1.17).[51] Despite various synthetic methods for benzophospholes developed over the last years[32, 56-69] the selective synthesis of such 7-substituted

benzophospholes is nontrivial. Given this regioselectivity, I reasoned that 7-alkoxy substituted benzophosphole derivatives would serve as useful starting materials for the synthesis of novel phosphole-embedded PACs, as the 7-alkoxy substituent could be used as a synthetic handle to extend the π-conjugated system.[70] As such, the research projects detailed in Chapters 2 and 3 were designed.

Scheme 1.17. Regioselective synthesis of 7-alkoxybenzophosphole via secondary directing effect on 1,4-cobalt migration

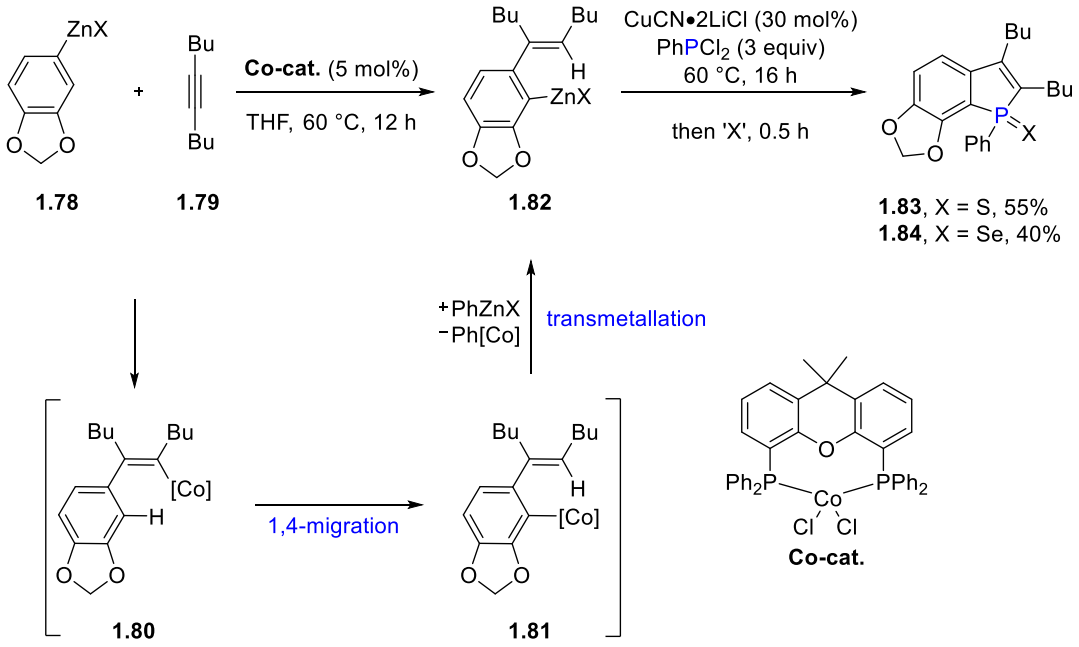

Chapter 2 describes the synthesis and properties of phospha[5]helicenes bearing an inner-rim phosphorus center (Scheme 1.18).[70] The key intermediate, 7-hydroxybenzo[*b*]phosphole oxide, was synthesized in a regioselective manner from 3-(methoxymethoxy)phenylzinc reagent, 5-decyne, and $PPhCl_2$. The hydroxy group of this intermediate was used as a synthetic handle, allowing the construction of the

carbohelicene moiety in a concise manner. The thus-synthesized phosphahelicenes are structurally distinct from previously synthesized phosphahelicenes with respect to the position of the phosphorus atom. Based on ^{1}H NMR and single crystal X-ray analysis, the present phospha[5]helicenes were demonstrated to undergo facile helicity inversion in solution, which was also supported by DFT calculations.

Scheme 1.18. Synthesis of phospha[5]helicenes bearing an inner-rim P-center

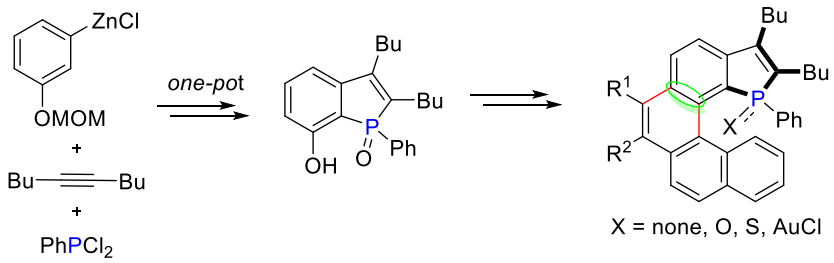

Chapter 3 describes the synthesis and properties of phosphole oxide-fused triphenylene derivatives (Scheme 1.19). As was the case for the phosphahelicene synthesis, 7-hydroxybenzophosphole was used as the key intermediate for the extension of the conjugated system, and the triphenylene core was furnished through oxidative biaryl formation (Scholl reaction). Besides triphosphasumanene trisulfide (or disulphide) by Saito *et al*. (Scheme 1.12), the present compounds represent rare examples of phosphole-embedded triphenylenes, and have been found to display strong blue fluorescence.[71]

Scheme 1.19. Synthesis of phosphole-fused triphenylene derivatives via C-C aryl coupling

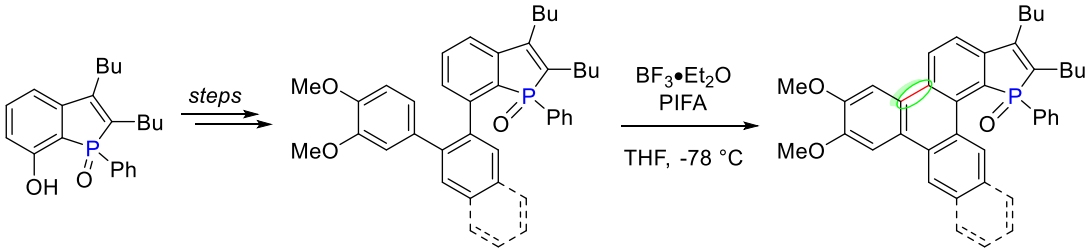

1.4 References

1. Hibner-Kulicka, P.; Joule, J. A.; Skalik, J.; Bałczewski, P. *RSC Adv.* **2017**, *7*, 9194.
2. Baumgartner, T.; Réau, R. *Chem. Rev.* **2006**, *106*, 4681.
3. Hobbs, M. G.; Baumgartner, T. *Eur. J. Inorg. Chem.* **2007**, *2007*, 3611.
4. Baumgartner, T. *Acc. Chem. Res.* **2014**, *47*, 1613.
5. Joly, D.; Bouit, P. A.; Hissler, M. *J. Mat. Chem. C* **2016**, *4*, 3686.
6. Duffy, M. P.; Delaunay, W.; Bouit, P. A.; Hissler, M. *Chem. Soc. Rev.* **2016**, *45*, 5296.
7. Wu, B.; Yoshikai, N. *Org. Biomol. Chem.* **2016**, *14*, 5402.
8. Yavari, K.; Delaunay, W.; De Rycke, N.; Reynaldo, T.; Aillard, P.; Srebro-Hooper, M.; Chang, V. Y.; Muller, G.; Tondelier, D.; Geffroy, B.; Voituriez, A.; Marinetti, A.; Hissler, M.; Crassous, J. *Chem. Eur. J.* **2019**, *25*, 5303.
9. Reus, C.; Baumgartner, T. *Dalton Trans.* **2016**, *45*, 1850.

10. Furukawa, S.; Haga, S.; Kobayashi, J.; Kawashima, T. *Org. Lett.* **2014**, *16*, 3228.

11. Bruch, A.; Fukazawa, A.; Yamaguchi, E.; Yamaguchi, S.; Studer, A. *Angew. Chem. Int. Ed.* **2011**, *50*, 12094.

12. Fukazawa, A.; Yamada, H.; Yamaguchi, S. *Angew. Chem. Int. Ed.* **2008**, *47*, 5582.

13. Bouit, P.-A.; Escande, A.; Szűcs, R.; Szieberth, D.; Lescop, C.; Nyulászi, L.; Hissler, M.; Réau, R. *J. Am. Chem. Soc.* **2012**, *134*, 6524.

14. Furukawa, S.; Suda, Y.; Kobayashi, J.; Kawashima, T.; Tada, T.; Fujii, S.; Kiguchi, M.; Saito, M. *J. Am. Chem. Soc.* **2017**, *139*, 5787.

15. Sawada, Y.; Furumi, S.; Takai, A.; Takeuchi, M.; Noguchi, K.; Tanaka, K. *J. Am. Chem. Soc.* **2012**, *134*, 4080.

16. Wu, D.; Chen, L.; Ma, S.; Luo, H.; Cao, J.; Chen, R.; Duan, Z.; Mathey, F. *Org. Lett.* **2018**, *20*, 4103.

17. Wang, C.; Taki, M.; Sato, Y.; Fukazawa, A.; Higashiyama, T.; Yamaguchi, S. *J. Am. Chem. Soc.* **2017**, *139*, 10374.

18. Yavari, K.; Aillard, P.; Zhang, Y.; Nuter, F.; Retailleau, P.; Voituriez, A.; Marinetti, A. *Angew. Chem. Int. Ed.* **2014**, *126*, 880.

19. Demmer, C. S.; Voituriez, A.; Marinetti, A. *C. R. Chim.* **2017**, *20*, 860.

20. Flammang-Barbieux, M.; Nasielski, J.; Martin, R. H. *Tet. Lett.* **1967**, *8*, 743.

21. Martin, R. H. *Angew. Chem. Int. Ed.* **1974**, *13*, 649.

22. Liu, L.; Yang, B.; Katz, T. J.; Poindexter, M. K. *J. Org. Chem.* **1991**, *56*, 3769.

23. Ravelli, D.; Protti, S.; Fagnoni, M. *Chem. Rev.* **2016**, *116*, 9850.

24. Delaunay, W.; Szűcs, R.; Pascal, S.; Mocanu, A.; Bouit, P. A.; Nyulászi, L.; Hissler, M. *Dalton Trans.* **2016**, *45*, 1896.

25. Szűcs, R.; Riobé, F.; Escande, A.; Joly, D.; Bouit, P.-A.; Nyulászi, L.; Hissler, M. *Pure Appl. Chem.* **2017**, *89*, 341.

26. Aillard, P.; Voituriez, A.; Marinetti, A. *Dalton Trans.* **2014**, *43*, 15263.

27. Aillard, P.; Voituriez, A.; Dova, D.; Cauteruccio, S.; Licandro, E.; Marinetti, A. *Chem. Eur. J.* **2014**, *20*, 12373.

28. Aillard, P.; Retailleau, P.; Voituriez, A.; Marinetti, A. *Chem. Eur. J.* **2015**, *21*, 11989.

29. Gicquel, M.; Zhang, Y.; Aillard, P.; Retailleau, P.; Voituriez, A.; Marinetti, A. *Angew. Chem. Int. Ed.* **2015**, *54*, 5470.

30. Aillard, P.; Gicquel, M.; Yavari, K.; Retailleau, P.; Voituriez, A.; Marinetti, A. *Eur. J. Org. Chem.* **2018**, *2018*, 5853.

31. Nakano, K.; Oyama, H.; Nishimura, Y.; Nakasako, S.; Nozaki, K. *Angew. Chem. Int. Ed.* **2012**, *51*, 695.

32. Fukazawa, A.; Hara, M.; Okamoto, T.; Son, E.-C.; Xu, C.; Tamao, K.; Yamaguchi, S. *Org. Lett.* **2008**, *10*, 913.

33. Wang, C.; Fukazawa, A.; Tanabe, Y.; Inai, N.; Yokogawa, D.; Yamaguchi, S. *Chem. Asian J.* **2018**, *13*, 1616.

34. Yamaguchi, E.; Wang, C.; Fukazawa, A.; Taki, M.; Sato, Y.; Sasaki, T.; Ueda, M.; Sasaki, N.; Higashiyama, T.; Yamaguchi, S. *Angew. Chem. Int. Ed.* **2015**, *54*, 4539.

35. Wang, C.; Fukazawa, A.; Taki, M.; Sato, Y.; Higashiyama, T.; Yamaguchi, S. *Angew. Chem. Int. Ed.* **2015**, *54*, 15213.

36. Zhou, Y.; Yang, S.; Li, J.; He, G.; Duan, Z.; Mathey, F. *Dalton Trans.* **2016**, *45*, 18308.

37. Wu, D.; Zheng, J.; Xu, C.; Kang, D.; Hong, W.; Duan, Z.; Mathey, F. *Dalton Trans.* **2019**, *48*, 6347.

38. Míšek, J.; Teplý, F.; Stará, I. G.; Tichý, M.; Šaman, D.; Císařová, I.; Vojtíšek, P.; Starý, I. *Angew. Chem. Int. Ed.* **2008**, *47*, 3188.

39. Sehnal, P.; Krausová, Z.; Teplý, F.; Stará, I. G.; Starý, I.; Rulíšek, L.; Šaman, D.; Císařová, I. *J. Org. Chem.* **2008**, *73*, 2074.

40. Stará, I. G.; Starý, I.; Kollárovič, A.; Teplý, F.; Šaman, D.; Tichý, M. *J. Org. Chem.* **1998**, *63*, 4046.

41. Jančařík, A.; Rybáček, J.; Cocq, K.; Vacek Chocholoušová, J.; Vacek, J.; Pohl, R.; Bednárová, L.; Fiedler, P.; Císařová, I.; Stará, I. G.; Starý, I. *Angew. Chem. Int. Ed.* **2013**, *52*, 9970.

42. Heller, B.; Hapke, M.; Fischer, C.; Andronova, A.; Starý, I.; Stará, I. G. *J. Organomet. Chem.* **2013**, *723*, 98.

43. Stará, I. G.; Starý, I.; Kollárovič, A.; Teplý, F.; Vyskočil, Š.; Šaman, D. *Tet. Lett.* **1999**, *40*, 1993.

44. Shibata, T.; Uchiyama, T.; Yoshinami, Y.; Takayasu, S.; Tsuchikama, K.; Endo, K. *Chem. Commun.* **2012**, *48*, 1311.

45. Tanaka, K.; Kamisawa, A.; Suda, T.; Noguchi, K.; Hirano, M. *J. Am. Chem. Soc.* **2007**, *129*, 12078.

46. Tanaka, K.; Fukawa, N.; Suda, T.; Noguchi, K. *Angew. Chem. Int. Ed.* **2009**, *48*, 5470.

47. Yamano, R.; Hara, J.; Murayama, K.; Sugiyama, H.; Teraoka, K.; Uekusa, H.; Kawauchi, S.; Shibata, Y.; Tanaka, K. *Org. Lett.* **2017**, *19*, 42.

48. Uto, T.; Shimizu, M.; Ueura, K.; Tsurugi, H.; Satoh, T.; Miura, M. *J. Org. Chem.* **2008**, *73*, 298.

49. Aillard, P.; Retailleau, P.; Voituriez, A.; Marinetti, A. *Chem. Commun.* **2014**, *50*, 2199.

50. Fukawa, N.; Osaka, T.; Noguchi, K.; Tanaka, K. *Org. Lett.* **2010**, *12*, 1324.

51. Wu, B.; Santra, M.; Yoshikai, N. *Angew. Chem. Int. Ed.* **2014**, *53*, 7543.

52. Yoshikai, N.; Santra, M.; Wu, B. *Organometallics* **2017**, *36*, 2637.

53. Tan, B.-H.; Dong, J.; Yoshikai, N. *Angew. Chem. Int. Ed.* **2012**, *51*, 9610.

54. Tan, B.-H.; Yoshikai, N. *Org. Lett.* **2014**, *16*, 3392.

55. Yan, J.; Yoshikai, N. *ACS Catal.* **2016**, *6*, 3738.

56. Tsuji, H.; Sato, K.; Ilies, L.; Itoh, Y.; Sato, Y.; Nakamura, E. *Org. Lett.* **2008**, *10*, 2263.

57. Sanji, T.; Shiraishi, K.; Kashiwabara, T.; Tanaka, M. *Org. Lett.* **2008**, *10*, 2689.

58. Fukazawa, A.; Ichihashi, Y.; Kosaka, Y.; Yamaguchi, S. *Chem. Asian J.* **2009**, *4*, 1729.

59. Fukazawa, A.; Yamada, H.; Yamaguchi, S. *Angew. Chem. Int. Ed.* **2008**, *120*, 5664.

60. Unoh, Y.; Hirano, K.; Satoh, T.; Miura, M. *Angew. Chem. Int. Ed.* **2013**, *52*, 12975.

61. Chen, Y.-R.; Duan, W.-L. *J. Am. Chem. Soc.* **2013**, *135*, 16754.

62. Baba, K.; Tobisu, M.; Chatani, N. *Angew. Chem. Int. Ed.* **2013**, *52*, 11892.

63. Nishimura, K.; Unoh, Y.; Hirano, K.; Miura, M. *Chem. Eur. J.* **2018**, *24*, 13089.

64. Ma, W.; Ackermann, L. *Synthesis* **2014**, *46*, 2297.

65. Zhang, P.; Gao, Y.; Zhang, L.; Li, Z.; Liu, Y.; Tang, G.; Zhao, Y. *Adv. Syn. Catal.* **2016**, *358*, 138.

66. Zhang, Y.; Hu, G.; Ma, D.; Xu, P.; Gao, Y.; Zhao, Y. *Chem. Commun.* **2016**, *52*, 2815.

67. Quint, V.; Morlet-Savary, F.; Lohier, J.-F.; Lalevée, J.; Gaumont, A.-C.; Lakhdar, S. *J. Am. Chem. Soc.* **2016**, *138*, 7436.

68. Zhou, Y.; Gan, Z.; Su, B.; Li, J.; Duan, Z.; Mathey, F. *Org. Lett.* **2015**, *17*, 5722.

69. Kuninobu, Y.; Yoshida, T.; Takai, K. *J. Org. Chem.* **2011**, *76*, 7370.

70. Rahman, M. S.; Yoshikai, N. *Org. Lett.* **2019**, *21*, 3232.

71. Wu, B.; Chopra, R.; Yoshikai, N. *Org. Lett.* **2015**, *17*, 5666.

Chapter 2. Synthesis and Properties of Phospha[5]helicenes Bearing an Inner-Rim Phosphorus Center

Adapted with permission from (Rahman, M. S.; Yoshikai, N. *Org. Lett.* **2019**, *21*, 3232). Copyright (2019) American Chemistry Society

2.1 Introduction

Helicenes are screw-shaped, non-planar, *ortho*-fuzed polycyclic aromatic systems, which shows intriguing physicochemical properties owing to their inherent helical chirality and the extended π-conjugation and thus, have attracted significant attention as constitutional units for chiroptical devices, chiral recognition and sensing, self-assembly, molecular machines, polymers, and dye materials.[1-6,7] Helicenes containing heteroatom in their helical framework offers an attractive method to modulate electronic and structural properties. Some of the representative examples of such heterohelicenes are shown in Figure 2.1 (**2.1-2.4**).[8-19] The heteroatom of the helical moiety could also be utilized in coordination chemistry[20-23] as well as in asymmetric catalysis.[24-26] Representative examples of heterohelicenes that have found applications in asymmetric synthesis are shown in Figure 2.2 (**2.5-2.8**).[26-29]

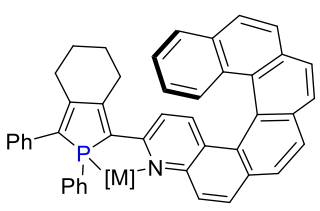

Phosphole-1-azahelicene, **2.1**
Reau 2009

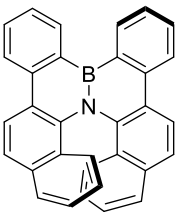

Azaboradibenzo[6]helicene, **2.2**
Nakamura 2012

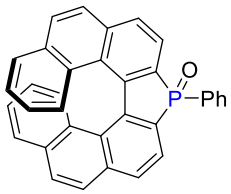

Phospha[7]helicenes, **2.3**
Nozaki 2012

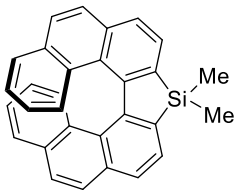

Sila[7]lehelicene, **2.4**
Nozaki 2013

Figure 2.1. Representative example of functional heterohelicenes.

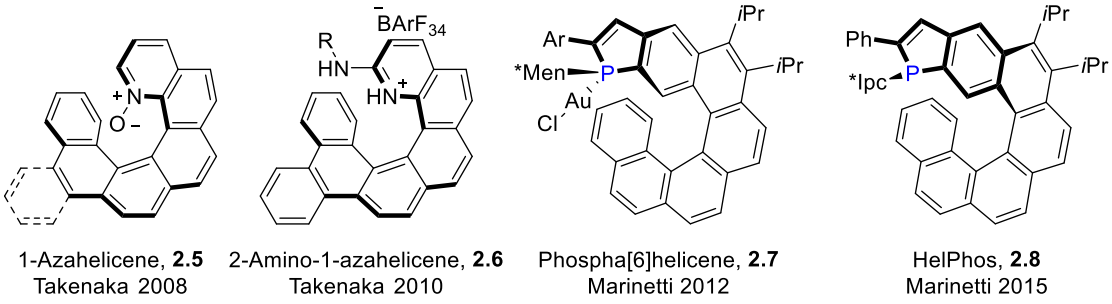

1-Azahelicene, **2.5** Takenaka 2008 | 2-Amino-1-azahelicene, **2.6** Takenaka 2010 | Phospha[6]helicene, **2.7** Marinetti 2012 | HelPhos, **2.8** Marinetti 2015

Figure 2.2. Heterohelicenes utilized in asymmetric synthesis.

In the above context, phosphahelicenes, which feature a phosphorus atom containing five-membered ring, phosphole, embedded in the helicene framework, have attracted significant attention among the synthetic community. Tanaka and coworkers reported the first enantioselective synthesis of phosphorus-embedded helicene derivatives via cationic rhodium-catalyzed [2 + 2 + 2] cycloaddition reaction of tetraynes and dialkynyl phosphorus compounds (*cf.* Chapter 1).[30-31] Apart from synthesis, they discussed about the photoluminescence properties and high helical stability of chiral phosphahelicene and related derivatives in both the solid and solution states. On the other hand, Nozaki group achieved the synthesis of a λ^5-phospha[7]helicene via palladium-catalyzed C–P coupling as key step (*cf.* Chapter1).[32] The λ^5-phospha[7]helicene showed one-dimensional columnar aggregation in crystal packing structure and strong luminescence properties. Over the last several years, Marinetti and co-workers communicated several reports on the synthesis of novel chiral phospha[6]helicene and related derivatives by capitalizing the oxidative

photochemical cyclization (*cf.* Chapter 1).[29, 33-38] They also described the nickel-catalyzed [2 + 2 + 2] cyclotrimerization of benzo[*b*]phosphole containing triynes to construct phosphole-embedded [6]helicenes.[37, 39-40] Noteworthy, the helicity of the final products could be controlled by utilizing a chiral benzo[*b*]phosphole as the starting precursor. Later, they used chiral phospha[6]helicenes as efficient ligands for enantioselective gold catalysis[35-36, 40] and as nucleophilic organocatalysts for [4 + 2] cycloaddition of electron-poor alkenes and allenes.[29, 37] Although not defined as phosphahelicenes, phosphole-substituted azahelicene derivatives and their metal complexes reported by Reau also represent examples of phosphole-containing helical systems that display interesting chiroptical properties.[21]

In Tanaka's and Nozaki's phospha[7]helicenes, the phosphorous atom is embedded in the middle of the outer-rim of helical framework which is shown in the Figure 2.3 (**2.9**-**2.10**). On the other hand, in the Marinetti's phosphahelicenes, the helical structures are linearly fused with the terminal position of benzo[*b*]phosphole, i.e., C5 and C6 positions of the benzo[*b*]phosphole (Figure 2.3) (**2.11**). Though the phosphorus atom is on the inner edge of the helical framework, it is away from the helical axis. To the best of our knowledge, phosphahelicenes comprised of angularly fused phosphole and carbohelicene moieties with an inner-rim phosphorus center have not been explored. Such phosphahelicenes are expected to have a close interaction between the helical axis and the P-centered chirality and, thus, would serve as attractive scaffolds as chiral ligands and catalysts. In addition, Yamaguchi and coworkers have disclosed the applications of phosphorus embedded PAHs as biological fluorescent probes for sensing and imaging of cellular processes (*cf.* Chapter 1).[41-42] Furthermore, phosphahelicenes bearing long alkyl side chain showed high luminescence properties as outlined by Tanaka. Therefore, by clubbing the

properties of benzophosphole and helicene, we envisioned that the phosphole-fused helicene might influence the luminescent properties.

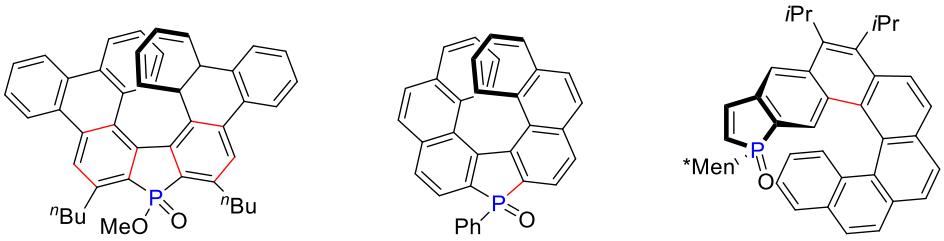

Tanaka, **2.9**
Rh-catalyzed [2 + 2 + 2]

Nozaki, **2.10**
Pd-catalyzed P-C coupling

Marinetti, **2.11**
oxidative photocyclization

Figure 2.3. Previous examples of phosphahelicenes

Recently, we have developed a versatile cobalt-catalyzed one-pot procedure for the synthesis of highly functionalized benzo[*b*]phosphole and naphtho[*b*]phosphole oxides from arylzinc reagents (generated from 1:1 mixture of the corresponding aryl Grignard reagent and $ZnCl_2$•TMEDA), internal alkynes, and dichloroaryl phosphines (or PCl_3 and another Grignard reagents) (*cf.* Chapter 1).[43-44] This synthetic protocol involves arylzincation of the alkyne via 1,4-cobalt migration, which displays unique regioselectivity for arylzinc reagents bearing 3-alkoxy substituents and allows regioselective access to 7-alkoxybenzo[*b*]phospholes. This feature prompted us to design the synthesis of novel phosphahelicenes featuring angular fusion of phosphole and carbohelicene units, as detailed below.

2.2 Results and Discussion

The present synthetic study commenced with a one-pot preparation of 7-hydroxy-benzo[*b*]phosphole oxide **2.14** as a key precursor via sequential treatment of

3-(methoxymethoxy)phenylzinc reagent (**2.12**), 5-decyne (**2.13**) and $PhPCl_2$.[43-44] The cobalt-catalyzed migratory arylzincation reaction[45] of **2.12** (prepared from an equal ratio of the corresponding Grignard reagent and $ZnCl_2$•TMEDA) with **2.12** was followed by treatment of the *ortho*-alkenylarylzinc intermediate with CuCN•2LiCl and $PhPCl_2$, and then with H_2O_2, thus affording the desired product 7-hydroxybenzo[*b*]phosphole oxide **2.14** in 33% yield on 5 mmol scale (Scheme 2.1). We observed formation of **2.14** preferentially over the other isomer **2.15** (ratio = ca 3:1), which could be ascribed due to secondary effect of the alkoxy group on the 1,4-cobalt migration step (*cf.* Chapter 1).[45-46]

Scheme 2.1. One-pot preparation of 7-hydroxy-benzo[*b*]phosphole oxide

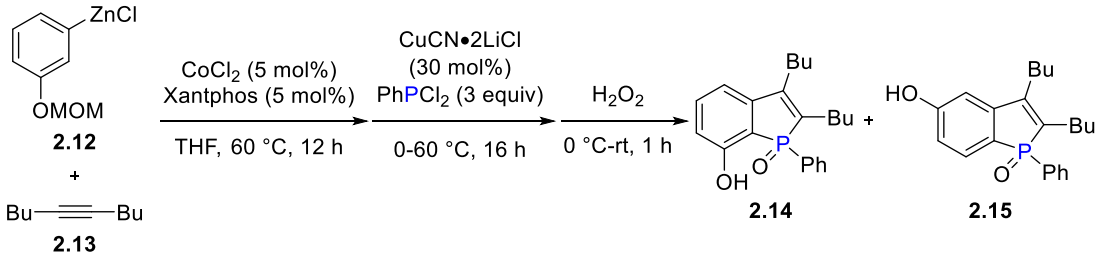

The hydroxyl group of **2.14** was subjected to triflation by using *N*-phenyl-bis(trifluoromethanesulfonimide), which afforded **2.16** in 90% yield. Suzuki Miyaura coupling of **2.16** with 2-alkynyl-1-naphthylboronic acid **2.17** produced an alkynylbiaryl derivative **2.18** in a moderate yield. Next, the iodocyclization of **2.18**, which is a helicene-building step, by using ICl[47] afforded an iodinated phospha[5]helicene **2.19** in 56% yield (Scheme 2.1). The compound **2.19** is a gummy like material and while dissolved in $CDCl_3$ showed two ^{31}P NMR signals (δ ppm 40.2

and 46.3) at room temperature in a ratio of 5:1, which indicates the presence of two diastereomers. Furthermore, compound **2.19** was subjected to Suzuki-Miyuara coupling with phenylboronic acid and 4-(hydroxymethyl)phenylboronic acid, affording phospha[5]helicenes **2.20** and **2.21** with 89% and 65% yield respectively, with similar diastereomeric ratios to that of **2.19**. However, treatment of compound **2.21** with Lawesson's reagent afforded phosphine sulfide analogue **2.22** as a single diastereomer (dr < 1:20) with 64% yield and showed single ^{31}P NMR signal (δ ppm 55.0).

Scheme 2.2. Synthesis of phospha[5]helicene derivatives

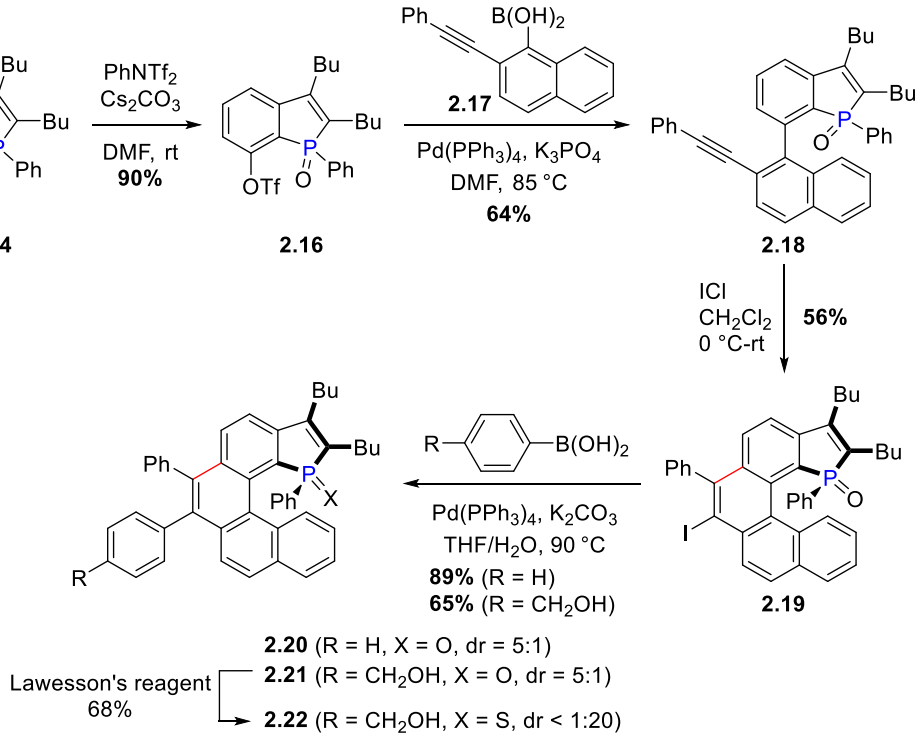

The aromatic region of the ^{1}H NMR spectra of **2.19**, **2.20** and **2.21** showed a major doublet signal at the highest chemical shift of ~ 9 ppm and a minor doublet signal ~ 7.8 ppm and major doublet of doublet ca 6.4 ppm and minor apparent triplet

signal at the lowest chemical shift ca. 6 ppm (Figure 2.4). In comparison, the ^{1}H NMR spectrum of **2.22** showed virtually no signal above 8 ppm and while showing a major apparent triplet at 5.9 ppm (Figure 2.5). These spectral behaviors indicate that the major diastereomers of **2.19-2.21** and **2.22** have different relative configurations. The doublet signal at ca. 9 ppm can be assigned to the inner-rim proton (H^{13}) of (R_P,*P*)/(S_P,*M*) diastereomers, which is strongly deshielded by the nearby aromatic rings (Figure 2.4). The minor doublet at ca. 8.2 ppm is attributed to H^{13} proton of the (S_P,*P*)/(R_P,*M*) isomer, which is shielded to some extent by the phenyl group on phosphorus center. On the other hand, the apparent triplet signal at ~6 ppm could be assigned to the H^{12} proton of the (R_P,*P*)/(S_P,*M*) diastereomers, which would be under the strong shielding effect of the P-Ph group as supported by single crystal X-ray analysis and DFT calculations (vide infra).

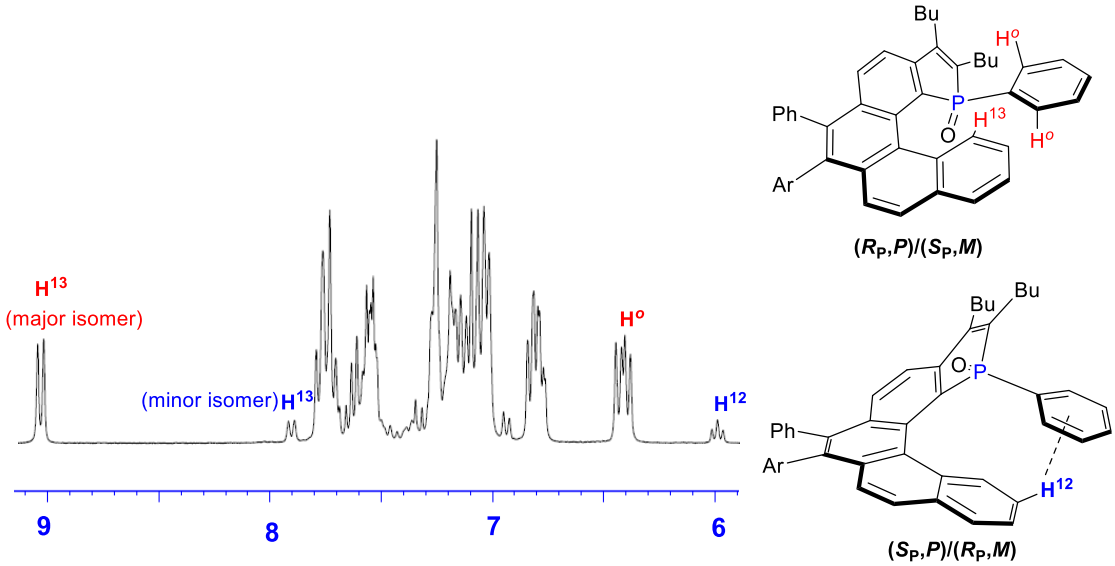

Figure 2.4. Structures of phospha[5]helicene oxide in $CDCl_3$

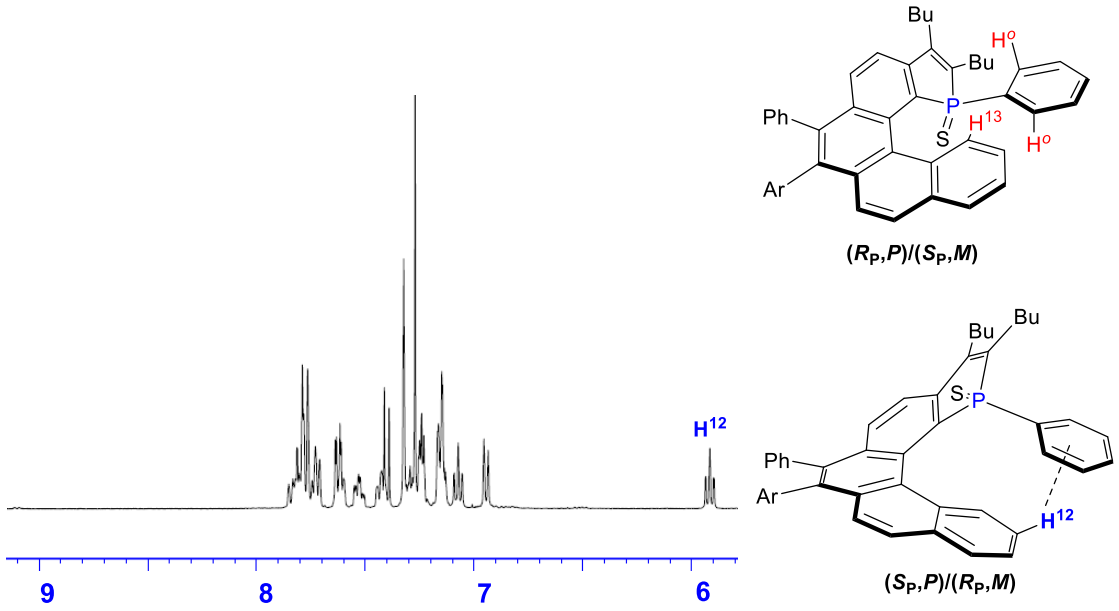

Figure 2.5. Structures of phospha[5]helicene sulfide in $CDCl_3$

Although the compound **2.20** was a gummy material, the compounds **2.21** and **2.22** were obtained as light yellow solids and could be recrystallized from CH_2Cl_2. Both of the thus-obtained single crystals proved to consist of a racemic mixture of the (*S*P,*P*) and (*R*P,*M*) enantiomers by X-ray diffraction analysis (Figure 2.6a). The P-Ph group is pointed toward the helicene edge, indicating that the H^{12} atom is positioned just below the benzene ring. Presumably due to this structural arrangement, the interplanar angles formed by the phosphole ring and terminal benzene ring (72.4° and 71.6° for **2.21** and **2.22**, respectively) are substantially larger than the corresponding angle of carbo[5]helicene (51.2°).[48] In the crystal packing, the (*S*P,*P*) and (*R*P,*M*) enantiomers of compound **2.21** are paired by mutual hydrogen bonding between the P=O and OH groups, with a relatively short distance (2.720 Å) between the two oxygen atoms (Figure 2.6b). However, redissolution of the crystals of **2.21** in $CDCl_3$ reproduced the ^{31}P NMR spectra of the as-synthesized **2.21**, which indicates facile helicity inversion in solution at room temperature.

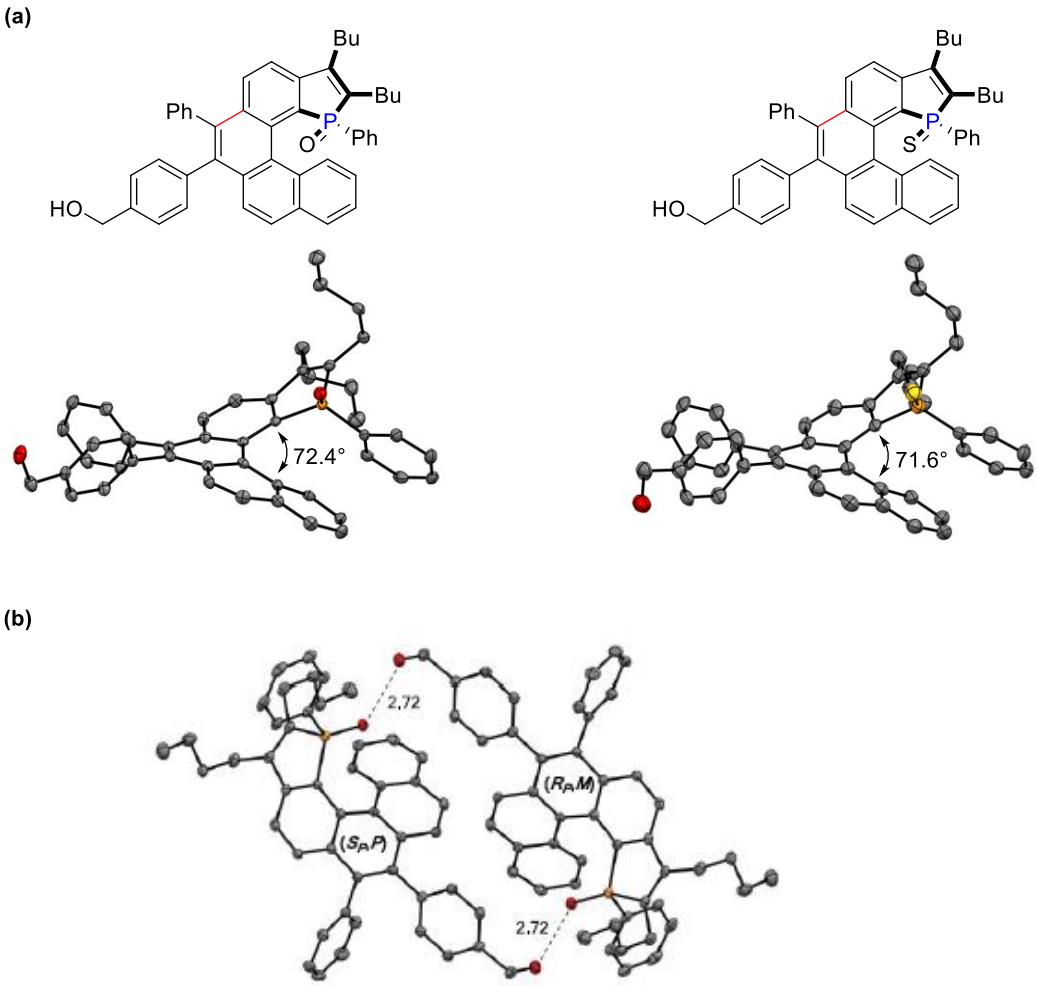

Figure 2.6. (a) ORTEP diagrams of (R_P,*M*)-**2.21** and (R_P,*M*)-**2.22** in their racemic single-crystals and (b) a hydrogen-bonded pair of (S_P,*P*)-**2.21** and (R_P,*M*)-**2.21**. Thermal ellipsoids are shown at 50% probability.

Next we focused on the synthesis of a phospha[5]helicene-gold complex (Scheme 2.3). The phosphine oxide **2.20** was reduced to free phosphine derivative, **2.23** in 74% yield by employing 1,1,3,3-tetramethyldisiloxane (TMDS) and copper triflate, $Cu(OTf)_2$ as catalyst.[49] Note that the compound **2.23** existed as a single diastereomer with the (R_P,*M*)/(S_P,*P*) configuration, as assigned by ^{1}H NMR (Figure 2.7). A multiplet signal at the highest chemical shift of ~9.1 ppm could be attributable

to H^{13} proton of (R_P,*M*)/(S_P,*P*) isomer, presumably due to deshielding effect of proximal aromatic rings. The apparent triplet signal at ca. 6.2 ppm was attributable to the *ortho* protons of phenyl group attached to phosphorus. The free phosphine **2.23** was treated with $AuCl(SMe_2)$, which upon recrystallization from CH_2Cl_2, afforded the phosphine-gold complex **2.24** in 70% yield. Unlike the configuration of **2.21** and **2.22**, the single crystals of **2.24** were found to have the (R_P,*P*)/(S_P,*P*) configuration. The interplanar angle of the helix was determined to be 61.1°, which was narrower than that of **2.21** and **2.22**. Upon redissolution in $CDCl_3$, **2.24** exhibited two ^{31}P NMR signals (δ 45.5 and 41.9 ppm) in a 1.4:1 ratio. The relative configurations of the major and minor diastereomers were assigned as (R_P,*P*)/(S_P,*M*) and (S_P,*P*)/(R_P,*M*) (Figure 2.8), respectively, on the basis of ^1H NMR spectrum in comparison with that of analogous compounds **2.19–2.23**. This again suggested helicity inversion in solution.

Scheme 2.3. Synthesis and X-ray structure of phospha[5]helicene-gold complex[a]

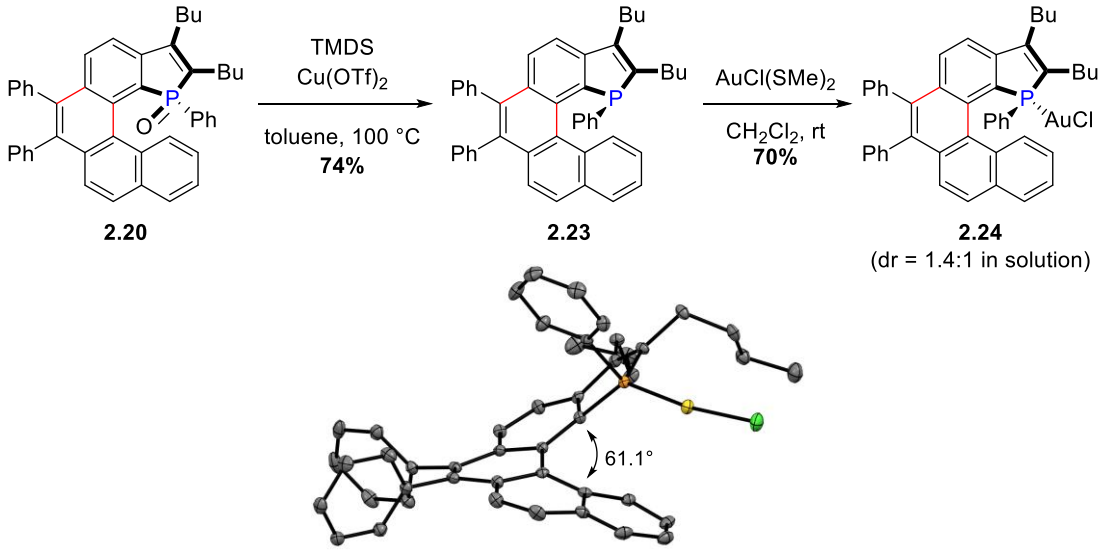

[a]Thermal ellipsoids are shown at 50% probability.

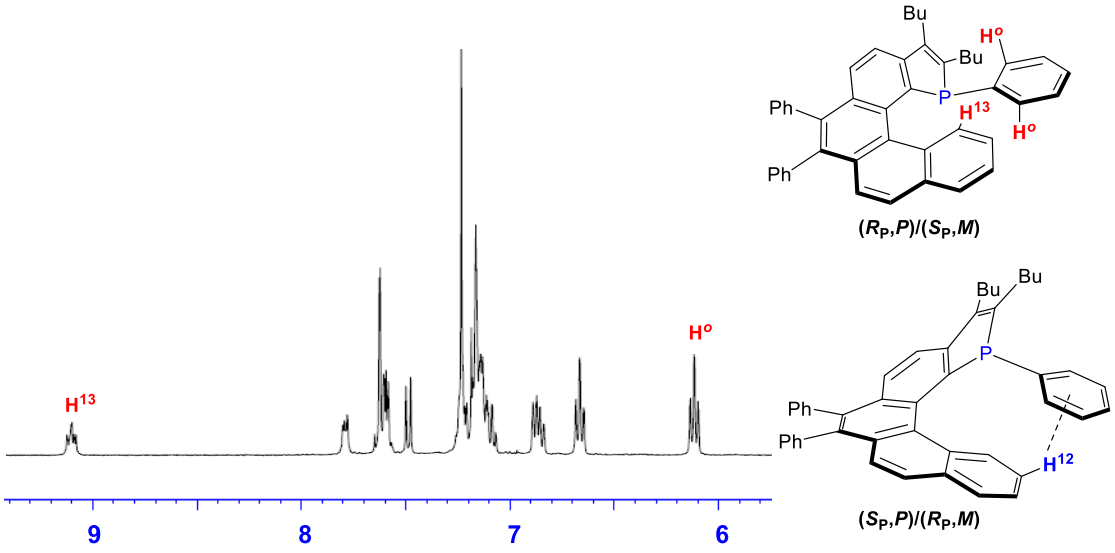

Figure 2.7. Structures of free phospha[5]helicene in $CDCl_3$.

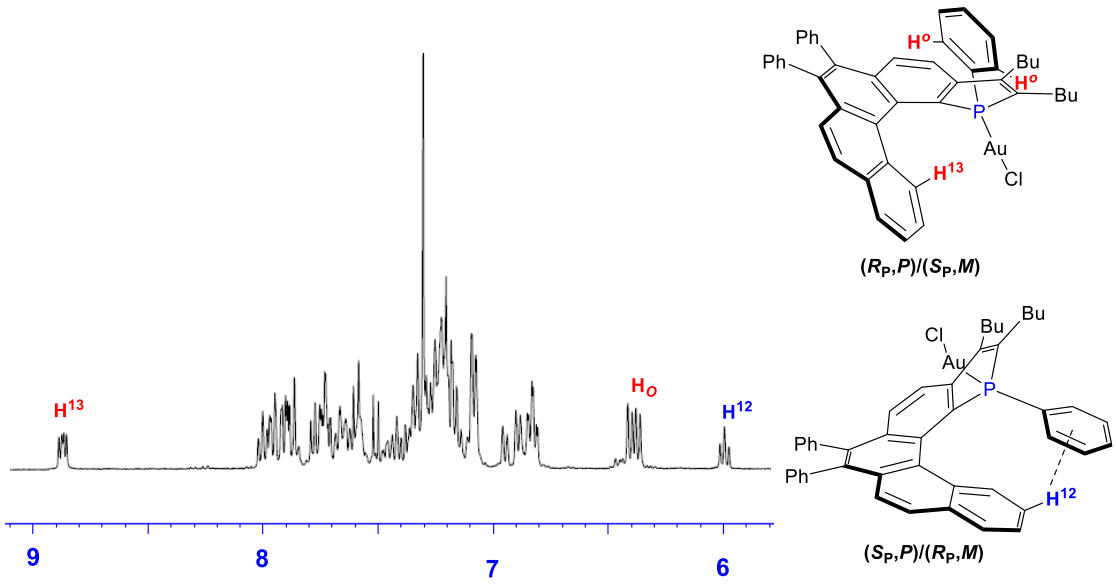

Figure 2.8. Structures of phospha[5]helicene-gold complex in $CDCl_3$.

Next, we performed DFT calculations (B3LYP/6-31G(d)) to gain insight into the structural behaviors of the model compound phospha[5]helicene oxide **Ao**, which was generated by replacing the peripheral Ph and Bu groups of **2.20** with H and Me groups, respectively (Figure 2.9). From the calculations, (R_P,P)-A_O is more stable than

(R_P,*M*)-A_O by 4.1 kcal/mol. This is presumably because of steric repulsion between the helicene edge and the P-Ph group, which is qualitatively (though not quantitatively) in line with the relative configuration of the major diastereomers of **2.19-2.21** assigned by ^{1}H NMR. Moreover, the H^{12} atom of (R_P,*M*)-**A**$_O$ is positioned right below the benzene ring of the P-Ph group, with distances between H^{12} and the phenyl carbons of 3.21-3.41 Å. These diastereomers are connected by the transition state of helix inversion (TS-**A**$_O$), with low activation energy of 16.9 kcal/mol from (R_P,*P*)-**A**$_O$. Given this energy profile, selective crystallization of (R_P,*M*)/(S_P,*P*) isomers of **2.21** may be attributed to facile interconversion between diastereomers and favorable intermolecular interactions, including hydrogen bonding, in the crystal packing. By replacing the oxygen atom of **A**$_O$ with a sulfur atom, **A**$_S$ was found to affect the relative energies of the diastereomers, favoring (R_P,*M*)-**A**$_S$ over (R_P,*P*)-**A**$_S$ by 0.6 kcal/mol (Figure 2.10). The activation energy barrier of transition state of helix inversion, TS-**A**$_S$ ($\Delta G^{\ddagger}$ = 16.0 kcal/mol) is slightly lower than that of TS-**A**$_O$. This energy trend, which is qualitatively consistent with the relative configuration of **2.22**, may be ascribed to greater steric clash between S and the helicene terminal in (R_P,*P*)-**A**$_S$. We also performed the DFT calculations on a free phospha[5]helicene **A** to study its structural behavior. The energy diagram indicates that the (R_P,*M*)/(S_P,*P*) isomers are more stable than the (R_P,*P*)/(S_P,*M*) isomers by 5.4 kcal/mol and isomerization between these isomers can take place through either helix inversion ($\Delta G^{\ddagger}$ = 17.3 kcal/mol) or phosphorus inversion ($\Delta G^{\ddagger}$ = 23.0 kcal/mol) (Figure 2.11).[50] Thus, this would suggests that the optical resolution of free phospha[5]helicene, **2.23** is quite difficult.

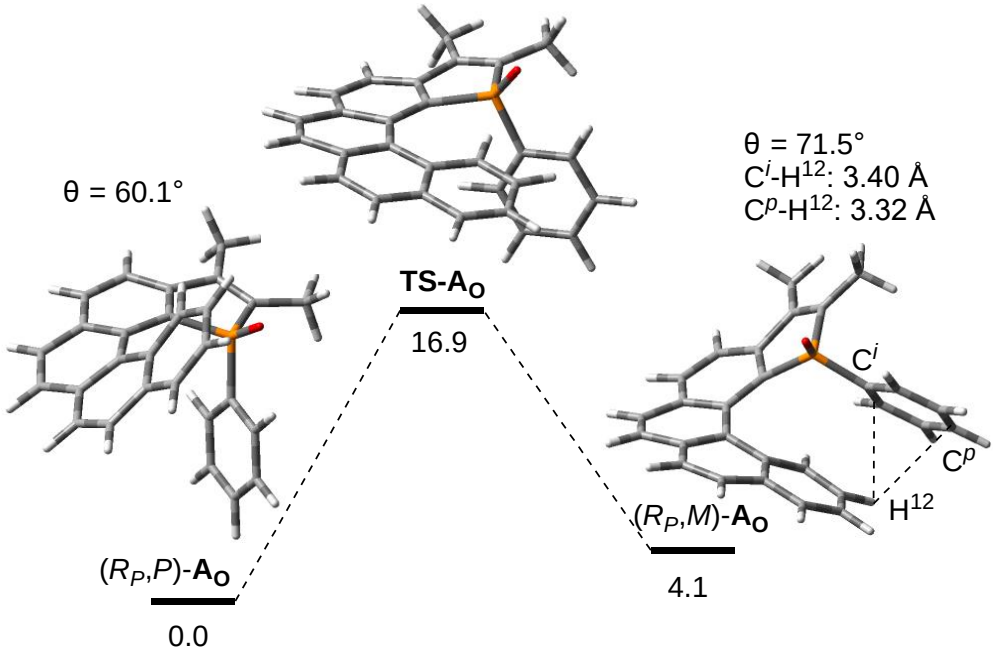

Figure 2.9. Free energy diagram (kcal/mol) for the isomerization of model phospha[5]helicene oxide $\mathbf{A_O}$ and phospha[5]helicene sulfide $\mathbf{A_S}$ (B3LYP/6-31G(d)).

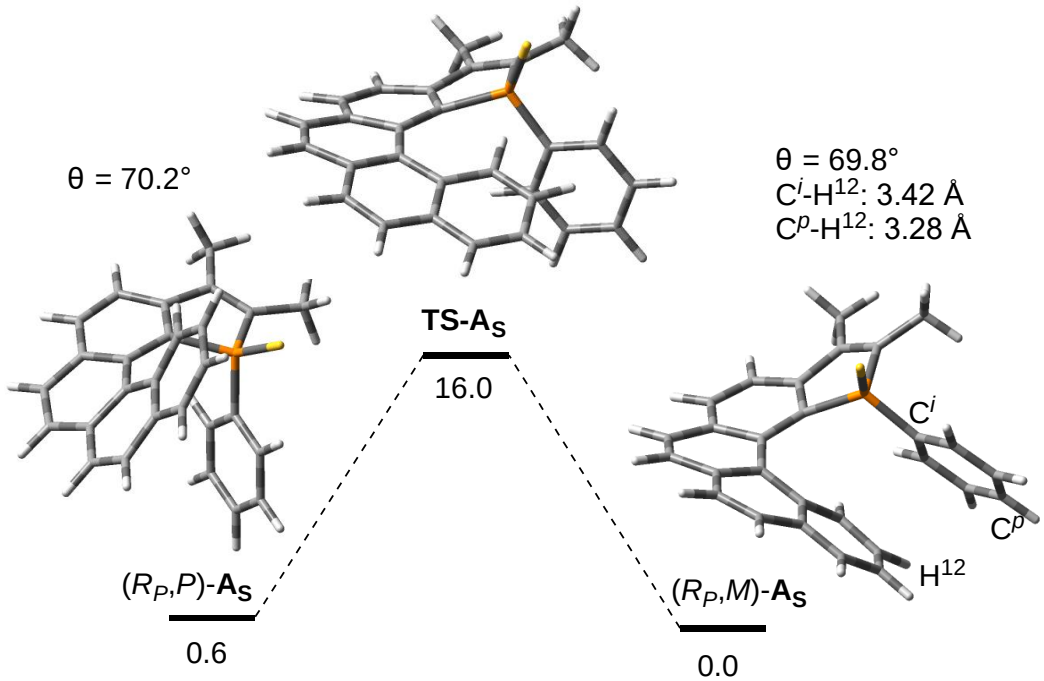

Figure 2.10. Free energy diagram (kcal/mol) for the isomerization of model phospha[5]helicene oxide $\mathbf{A_O}$ and phospha[5]helicene sulfide $\mathbf{A_S}$ (B3LYP/6-31G(d)).

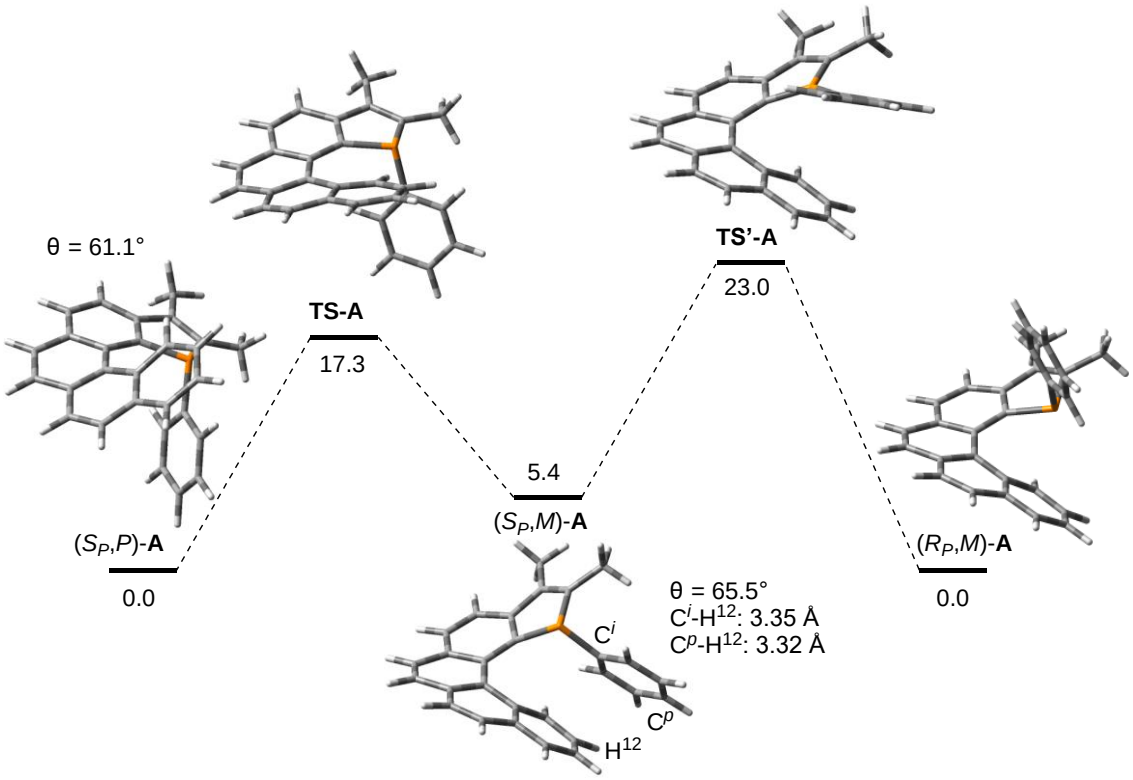

Figure 2.11. Free energy diagram (kcal/mol) for the isomerization of model phospha[5]helicene **A** (B3LYP/6-31G(d)). The angle θ refers to the interplanar angle between the phosphole ring and the terminal benzene ring.

Next, we studied the absorption and emission behavior of the compounds **2.20**, **2.21**, and **2.22**. The absorption and emission spectra of **2.20**, **2.21**, and **2.22** are shown in Figure 2.12 and Figure 2.13, respectively. The absorption profile of **2.21** was quite broad and tailing with absorption maxima at 322, 338, and 390 nm (shoulder), which might be ascribed to the presence of two diastereomers and also to the contribution

from vibronic progression. The compounds **2.20** and **2.22** also showed similar complex absorption patterns. The emission color of compound **2.21** was light-blue, with a broad peak at 454 nm and a quantum yield of 0.42 (reference with quinine sulfate). The compound **2.20** also showed light-blue emission with somewhat lower emission wavelength i.e., 431 nm with a similar quantum yield (0.44). However, the phospha[5]helicene sulfide **2.22** and the phospha[5]helicene-gold complex **2.24** were virtually nonemissive, presumably due to the heavy atom effect.

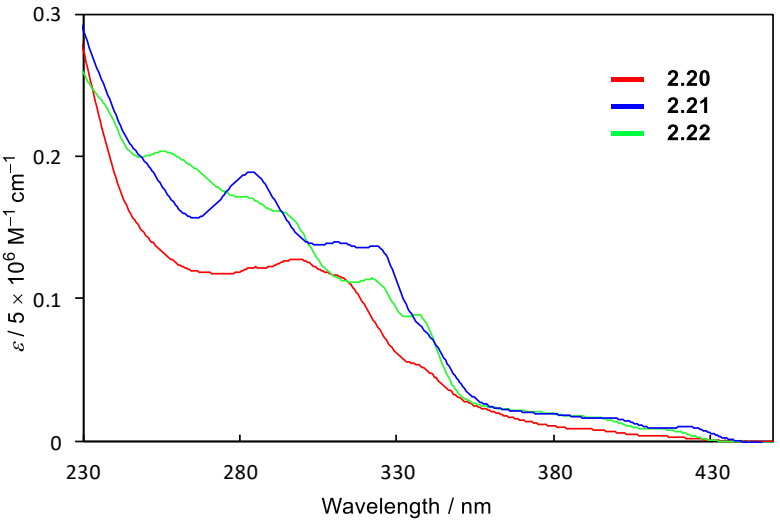

Figure 2.12. Absorption spectra of **2.20**, **2.21**, and **2.22** in CH_2Cl_2 (5×10^{-6} M).

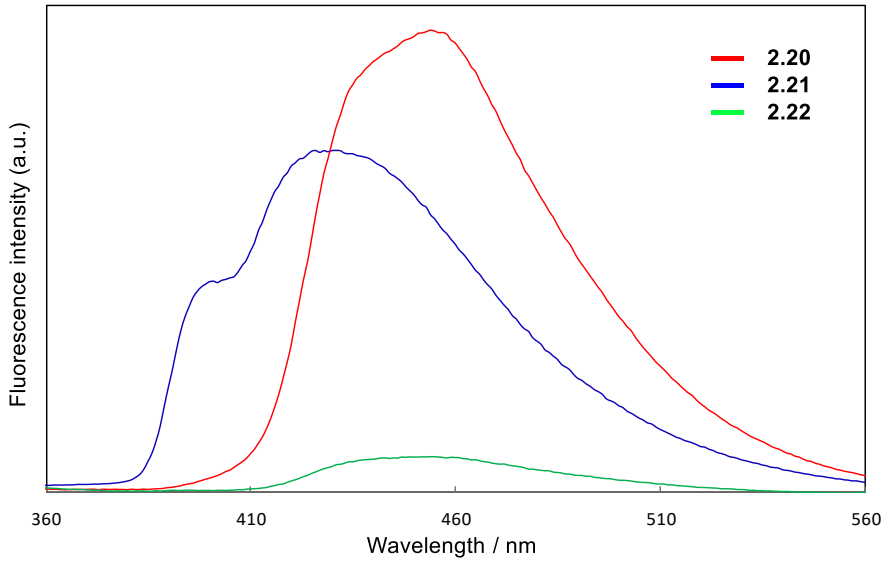

Figure 2.13. Emission spectra of **2.20**, **2.21**, and **2.22** in CH_2Cl_2 (5×10^{-6} M).

We also performed optical resolution of diastereomeric mixtures (R_P,*P*)/(R_P,*M*) and (S_P,*M*)/(S_P,*P*) isomers) of the compound **2.20** by using preparative chiral HPLC. The enantiomerically pure samples with respect to phosphorus center showed optical rotations of $[\alpha]^{23}_D$ = –759.6° (*c* = 0.61 in $CHCl_3$) (Fraction 1) and +689.7° (*c* = 0.57 in $CHCl_3$) (Fraction 2), respectively. The circular dichroism (CD) spectra of enantiomerically pure samples of compound **2.20** with respect to phosphorus center have been measured in $CHCl_3$ (2×10^{-5} M) at 20 °C. The enantiomeric pure fraction **1** of compound of **2.20** showed intense negative dichroic signal at 336 nm, an intense positive signal at around 293 nm, and relatively intense negative signal around 257 nm (Figure 2.14, dashed line). On the other hand, the dichroic signals of enantiomeric pure fraction **2** of compound **2.20** showed opposite CD behavior to that of fraction **1** (Figure 2.14, solid line).

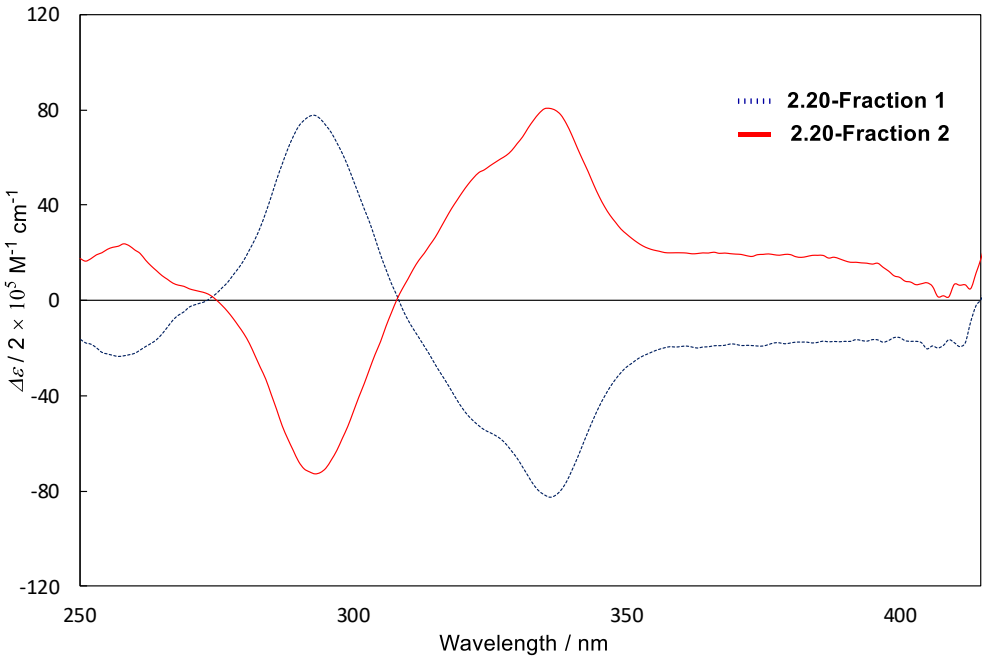

Figure 2.14. CD spectra of compound **2.20** (2×10^{-5} M in $CHCl_3$, for both enantiomers).

2.3 Conclusion

In summary, we have synthesized phospha[5]helicene derivatives that feature angularly fused phosphole and cabrohelicene moieties and an inner-rim phosphorus center capitalizing 7-hydroxybenzo[b]phosphole as the key precursor, which is typically accessed by our previous report on benzo[*b*]phosphole synthesis. The X-ray crystallographic structures of phospha[5]helicene oxide, sulfide, and gold complex demonstrated their inherent helical and P-centered chirality. Their behavior in solution and DFT calculations suggest the significant impact of phosphorus center on the diastereomer ratio as well as facile equilibration between the diastereomers through helix inversion.

2.4 Experimental Section

Materials and Methods

General. All reactions dealing with air- or moisture-sensitive compounds were performed by standard Schlenk techniques in oven-dried reaction vessels under nitrogen atmosphere or in the argon-filled glove box. Analytical thin-layer chromatography (TLC) was performed on Merck 60 F254 silica gel plates. Flash chromatography was performed as described by Still et al., using 40–63 μm silica gel (Si 60, Merck). Preparative HPLC was performed on a Japan Analytical Industry LC-9110NEXT system equipped with GPC columns JAIGEL-1H and JAIGEL-2H and a UV detector using chloroform as an eluent. ^{1}H, ^{13}C, and ^{31}P nuclear magnetic resonance (NMR) spectra were recorded on Bruker AV-300 (300MHz), AV-500 (500 MHz), BBF 02 (400 MHz), JEOL ECA 400SL (400 MHz) NMR spectrometers. ^{1}H and ^{13}C NMR spectra are reported in parts per million (ppm) downfield from an internal standard, tetramethylsilane (0 ppm) and $CHCl_3$ (77.0 ppm), respectively. ^{31}P NMR spectra are referenced to an external reference (85% H_3PO_4, 0 ppm). High-resolution mass spectra (HRMS)/Liquid chromatography mass spectra (LCMS) were obtained with a Q-Tof Premier LC HR mass spectrometer. UV-vis and fluorescence spectra were recorded on Shimadzu UV-1800 spectrophotometer and Shimadzu RF-5301PC spectrofluorophotometer respectively. The spectra were recorded on JASCO J-815 CD Spectrometer.

Materials. Unless otherwise noted, commercial reagents were purchased from Aldrich, Alfa Aesar, TCI and other commercial suppliers and were used as received.

Anhydrous $CoCl_2$ (97%) was purchased from Alfa Aesar and was used as received. $ZnCl_2$•TMEDA was prepared according to the literature procedures. Tetrahydrofuran (THF) and 1,4-dioxane was distilled over Na/benzophenone. Dichloromethane (DCM) was distilled over calcium hydride. Anhydrous dimethylformamide (DMF) was purchased from Sigma-Aldrich and used as it is. Grignard reagents were prepared from the corresponding bromide and magnesium turnings in anhydrous THF and titrated before use.

Synthesis of phospha[5]helicenes

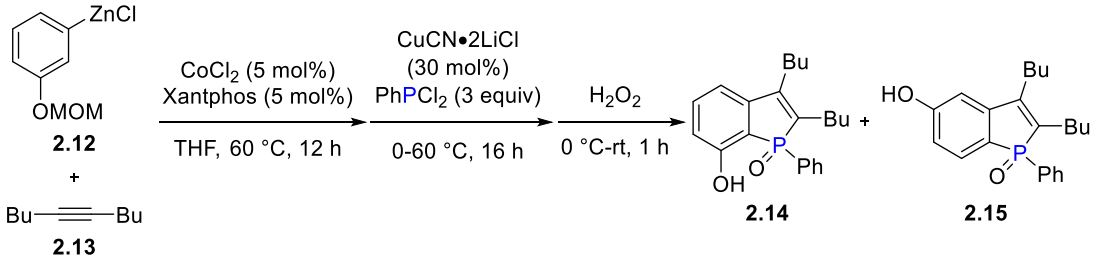

2,3-Dibutyl-7-hydroxy-1-phenylphosphindole 1-oxide (2.14): The title compound was prepared based on our previous report.[43] An oven-dried 50 mL Schlenk tube charged with TMEDA•$ZnCl_2$ (1.39 g, 5.5 mmol) was evacuated and backfilled with nitrogen three times. The Schlenk tube was then submerged in an ice bath for 15 min, followed by dropwise addition of (3-(methoxymethoxy)phenyl)magnesium bromide (1.11 M in THF, 4.95 mL, 5.5 mmol). The resulting mixture was stirred for 1 h at 0 °C and then allowed to room temperature. To the arylzinc reagent were added Xantphos (145 mg, 0.25 mmol) and $CoCl_2$ (32 mg, 0.25 mmol). After stirring for 5 min, 5-decyne (0.90 mL, 5.0 mmol) was added. The reaction mixture was stirred at 60 °C for 12 h and allowed to cool to room temperature. The Schlenk tube was submerged in an ice bath, followed by the addition of CuCN•2LiCl (1.0 M in THF, 1.5

mL, 1.5 mmol) in one portion and $PhPCl_2$ (2.0 mL, 15 mmol) in dropwise manner. The resulting reaction mixture was stirred at 60 °C for 16 h and then allowed to cool to room temperature. Then 30% H_2O_2 (0.5 mL) was carefully added in dropwise manner at 0 °C and kept stirring at room temperature for 1 h. The reaction mixture was extracted with ethyl acetate (50 mL × 3). The combined organic layer was dried over $MgSO_4$ and concentrated under reduced pressure. The residue was purified by silica gel column chromatography (eluent: hexane/ethyl acetate = 4/6) to afford the title compound **2.14** as an off-white solid (0.58 g, 33%). m.p. 178.6-179.8 °C; ^{1}H NMR (400 MHz, $CDCl_3$, 298 K): δ 9.13 (bs, 1H), 7.69-7.63 (m, 2H) 7.48-7.44 (m, 1H), 7.38-7.34 (m, 2H), 7.25 (t, *J* = 7.9 Hz, 1H), 6.83 (dd, *J* = 8.2, 2.4 Hz, 2H), 2.54 (t, *J* = 7.5 Hz, 2H), 2.46-2.39 (m, 1H), 2.26-2.20 (m, 1H), 1.59-1.51 (m, 2H), 1.48-1.43 (m, 2H), 1.42-1.29 (m, 2H), 1.27-1.20 (m, 2H), 0.98 (t, *J* = 7.2 Hz, 3H), 0.78 (t, *J* = 7.2 Hz, 3H); ^{13}C NMR (100 MHz, $CDCl_3$): δ 158.8 (d, J_{PC} = 4.5 Hz), 151.9 (d, J_{PC} = 20.3 Hz), 144.9 (d, J_{PC} = 26.8 Hz), 134.8, 134.5 (d, J_{PC} = 97.6 Hz), 131.8 (d, J_{PC} = 3.1 Hz), 131.0, 130.9, 129.7 (J_{PC} = 100.8 Hz), 128.7, 128.6, 118.5 (d, J_{PC} = 6.1 Hz), 115.0 (J_{PC} = 105.4 Hz), 113.43 (d, J_{PC} = 10.9 Hz), 31.1 (d, J_{PC} = 1.5 Hz), 31.0 (d, J_{PC} = 1.7 Hz), 26.5 (d, J_{PC} = 13.8 Hz), 25.7 (d, J_{PC} = 10.9 Hz), 23.1, 22.8, 13.9, 13.7; ^{31}P NMR (161 MHz, $CDCl_3$, 298 K): δ 41.9; HRMS (ESI) Calcd for $C_{22}H_{27}O_2P$ $[M + H]^+$ 355.1827, found 355.1825.

Note that **2.14** was accompanied by 2,3-dibutyl-5-hydroxy-1-phenylphosphindole 1-oxide (**2.15**) as the minor isomer (ratio = ca. 3:1) as judged from ^{31}P NMR and thus, difficult to separate completely from **2.14**. The characterization data were collected for partially separated sample of **2.15**, as follows. ^{1}H NMR (400 MHz, $CDCl_3$, 298 K): δ 10.40 (s, 1H), 7.62- 7.57 (m, 2H) 7.47 (t, *J* = 7.5 Hz, 1H), 7.40-7.35 (m, 2H), 7.16 (t, *J* = 8.5 Hz, 1H), 6.89 (t, *J* = 1.8 Hz, 1H), 6.72-6.69 (m, 1H), 2.55-2.35 (m, 3H), 2.23-

2.14 (m, 1H), 1.53-1.43 (m, 2H), 1.41-1.31 (m, 3H), 1.28-1.14 (m, 3H), 0.89 (t, J = 7.2 Hz, 3H), 0.74 (t, J = 7.2 Hz, 3H); ^{13}C NMR (100 MHz, $CDCl_3$, 298 K), δ 162.9 (d, J_{PC} = 1.9 Hz), 151.0 (d, J_{PC} = 20.0 Hz), 146.2 (d, J_{PC} = 31.1 Hz), 135.0, 134.4 (d, J_{PC} = 96.4 Hz), 131.9 (d, J_{PC} = 2.6 Hz), 131.1, 130.9, 130.3 (d, J_{PC} = 98.8 Hz), 130.0, 129.9, 128.8, 128.6, 119.4 (d, J_{PC} = 112.9 Hz), 115.0 (d, J_{PC} = 11.8 Hz), 110.6 (d, J_{PC} = 12.7 Hz), 30.9 (d, J_{PC} = 1.2 Hz), 30.7 (d, J_{PC} = 1.3 Hz), 26.3 (d, J_{PC} = 13.2 Hz), 25.8 (d, J_{PC} = 10.7 Hz), 23.0, 22.8, 13.9, 13.6; ^{31}P NMR (161 MHz, $CDCl_3$, 298 K), δ 41.1; HRMS (ESI) Calcd for $C_{22}H_{27}O_2P$ $[M + H]^+$ 355.1827, found 355.1844.

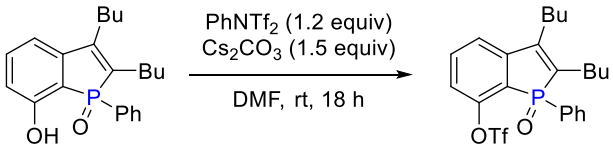

2.14 **2.16**

2,3-Dibutyl-1-oxido-1-phenylphosphindol-7-yl trifluoromethanesulfonate (2.16): The reaction was performed according to the literature procedure.[51] To a solution of 7-hydroxybenzo[*b*]phosphole, **2.14** (0.71 g, 2.0 mmol) in anhydrous DMF (10 mL) was added sequentially Cs_2CO_3 (0.98 g, 3.0 mmol) and $PhNTf_2$ (0.86 g, 2.4 mmol). The reaction mixture was stirred at room temperature for 18 h under N_2, followed by quenching with saturated aqueous solution of NH_4Cl (3 mL). The resulting crude mixture was extracted twice with ethyl acetate (20 mL). The combined organic layer was dried over $MgSO_4$ and concentrated under reduced pressure. The crude reaction mixture was purified by silica gel column chromatography (eluent: hexane/EA = 3/1) to afford the title compound as a colorless oil (0.87 g, 90%). ^{1}H NMR (400 MHz, $CDCl_3$, 298 K): δ 7.71-7.66 (m, 2H), 7.58-7.52 (m, 2H), 7.46-7.42 (m, 2H), 7.34 (dd, *J*

= 7.6, 1.7 Hz, 1H), 7.18 (dd, *J* = 8.4, 4.8 Hz, 1H), 2.62 (t, *J* = 7.4 Hz, 2H), 2.57-2.45 (m, 1H), 2.32-2.20 (m, 1H), 1.62-1.53 (m, 2H), 1.51-1.36 (m, 4H), 1.30-1.20 (m, 2H), 0.99 (t, *J* = 7.2 Hz, 3H), 0.79 (t, *J* = 7.3 Hz, 3H); ^{13}C NMR (100 MHz, $CDCl_3$, 298 K): δ 149.6 (d, J_{PC} = 17.6 Hz), 149.4 (d, J_{PC} = 2.3 Hz), 146.6 (d, J_{PC} = 25.3 Hz), 136.2 (d, J_{PC} = 97.0 Hz), 135.4 (d, J_{PC} = 1.5 Hz), 132.5 (d, J_{PC} = 3.0 Hz), 131.0 (d, J_{PC} = 11.1 Hz), 128.9, 128.81, 127.5 (d, J_{PC} = 100.4 Hz), 125.3 (d, J_{PC} = 98.8 Hz), 120.9 (d, J_{PC} = 9.7 Hz), 119.9 (d, J_{PC} = 4.2 Hz), 118.3 (q, J_{CF} = 318.6 Hz), 30.7 (d, J_{PC} = 1.9 Hz), 30.5 (d, J_{PC} = 1.8 Hz), 26.6 (d, J_{PC} = 13.5 Hz), 26.0 (d, J_{PC} = 11.4 Hz), 23.0, 22.9, 13.9, 13.6; ^{31}P NMR (161 MHz, $CDCl_3$, 298 K): δ 36.9; HRMS (ESI) Calcd for $C_{23}H_{26}FO_4P$ $[M + H]^+$ 487.1320, found 487.1315.

Preparation of (2-(phenylethynyl)naphthalen-1-yl)boronic acid

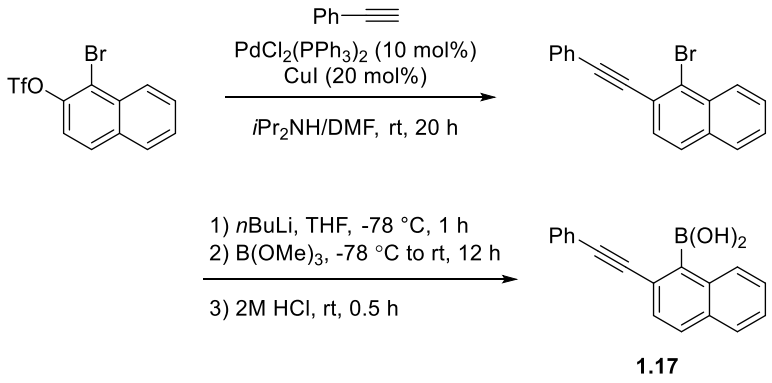

1.17

1-Bromo-2-(phenylethynyl)naphthalene: The Sonogashira coupling reaction was performed according to the literature procedure.[52] An oven-dried 100 mL two-neck round bottom flask equipped with a magnetic stir bar, under N_2, was charged with 1-bromonaphthalen-2-yl trifluoromethanesulfonate (1.58 g, 5.0 mmol)[53], DMF (19 mL) and diisopropylamine (19 mL). Then $PdCl_2(PPh_3)_2$ (351 mg, 0.50 mmol), CuI (190 mg, 1.0 mmol) and phenylacetylene (0.55 mL, 5.0 mmol) were sequentially added.

The resulting mixture was stirred at room temperature for 20 h under N_2 atmosphere. The volatiles were removed under vacuum, and the residue was partitioned in ethyl acetate and water. The organic layer was washed with water, dried over $MgSO_4$ and concentrated under reduced pressure. The crude product was purified by flash chromatography on silica gel (eluent: hexane/CH_2Cl_2 = 80:20) to afford product 1-bromo-2- (phenylethynyl)naphthalene as a white solid (1.05 g, 68% yield). m.p. 73.5-75.1 °C; ^{1}H NMR (400 MHz, $CDCl_3$, 298 K): δ 8.32 (d, *J* = 8.5 Hz, 1H), 7.82 (d, *J* = 8.1 Hz, 1H), 7.78 (d, *J* = 8.5 Hz, 1H), 7.66-7.58 (m, 4H), 7.56-7.52 (m, 1H), 7.41-7.38 (m, 3H); ^{13}C NMR (100 MHz, $CDCl_3$, 298 K): δ 133.7, 132.3, 131.8, 129.0, 128.7, 128.4, 128.2, 127.9, 127.8, 127.5, 127.2, 126.5, 123.5, 123.1, 94.7, 89.4; HRMS (ESI) Calcd for $C_{18}H_{12}Br$ $[M + H]^+$ 307.0122, found 307.0125.

(2-(Phenylethynyl)naphthalen-1-yl)boronic acid (2.17): To a stirred solution of 1-bromo-2- (phenylethynyl)naphthalene (1.00 g, 3.26 mmol) in anhydrous diethyl ether (10 mL) was added *n*-BuLi (2.0 M in cyclohexane, 1.96 mL, 3.91 mmol) in dropwise manner at –78 °C. The reaction mixture was stirred for 1 h followed by the addition of trimethyl borate (0.73 mL, 6.5 mmol) in a dropwise manner. The reaction mixture was kept stirring at –78 °C for 2 h and slowly warmed up to room temperature and stirred 12 h. Then 2 M HCl (8 mL) was added, and the resulting mixture was stirred for another 30 min. The reaction mixture was partitioned in diethyl ether and water. The aqueous layer was neutralized with 3 M NaOH and extracted three times with diethyl ether (30 mL). The combined organic layer was dried over $MgSO_4$, concentrated under reduced pressure, purified by flash chromatography on a short silica gel bed (eluent: hexane/ethyl acetate = 6/4) to afford the title compound as a white solid (0.51 g, 58% yield). m.p. 167.9-170.0 °C; ^{1}H NMR (400 MHz, acetone-d_6, 298 K): δ 8.02 (d, *J* = 7.3 Hz, 1H), 7.94-7.89 (m, 2H), 7.70 (s, 2H), 7.63-7.60 (m, 3H), 7.59-7.53 (m, 2H),

7.49-7.43 (m, 3H); ^{13}C NMR (100 MHz, acetone-d_6, 298 K): δ 134.8, 132.4, 131.3, 128.7, 128.5, 128.3, 128.1, 128.0, 127.8, 126.30 (d, 2C), 123.6, 122.5, 91.1, 90.3, carbon adjacent to boron not observed; HRMS (ESI) Calcd for $C_{18}H_{14}BO_2$ $[M + H]^+$ 273.1087, found 273.1092.

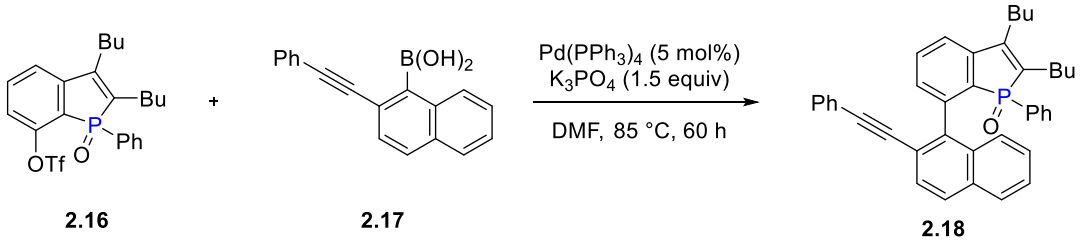

2.16 **2.17** **2.18**

2,3-Dibutyl-1-phenyl-7-(2-(phenylethynyl)naphthalen-1-yl)phosphindole 1-oxide (2.18): A 25 mL Schenk tube charged with **2.16** (487 mg, 1.00 mmol) and DMF (4 mL) was degassed twice by freeze-pump-thaw cycle. To this solution were added $Pd(PPh_3)_4$ (57.8 mg, 0.050 mmol), K_3PO_4 (318 mg, 1.50 mmol), and (2-(phenylethynyl)naphthalen-1-yl)boronic acid **2.17**, (327 mg, 1.20 mmol) sequentially. The reaction mixture was stirred at room temperature for 0.5 h and then at 85 °C for 60 h. The reaction was cooled to room temperature and quenched with saturated aqueous solution of NH_4Cl. The aqueous layer was extracted twice with ethyl acetate (10 mL). The combined organic layer was washed with water, dried over $MgSO_4$, and concentrated under reduce pressure. The crude product was purified by column chromatography on silica gel (eluent: hexane/ethyl acetate = 7/3) to afford the title compound as a light yellow oil (361 mg, 64%). ^{1}H NMR (400 MHz, $CDCl_3$, 298 K): δ 7.84-7.82 (m, 1H), 7.75 (d, *J* = 8.5 Hz, 1H), 7.66-7.62 (m, 2H), 7.51-7.48 (m, 3H), 7.29-7.19 (m, 5H), 7.16 (d, *J* = 8.5 Hz, 1H), 7.02-6.93 (m, 4H), 6.91-6.88 (m, 2H), 2.72 (t, *J* = 7.8 Hz, 2H), 2.50-2.38 (m, 1H), 2.24-2.14 (m, 1H), 1.74-1.61 (m, 2H),

1.61-152 (m, 2H), 1.35-1.25 (m, 2H), 1.20-1.14 (m, 2H), 1.07 (t, J = 7.3 Hz, 3H), 0.71 (t, J = 7.2 Hz, 3H); ^{13}C NMR (100 MHz, $CDCl_3$, 298 K): δ 150.5 (d, J_{PC} = 19.0 Hz), 143.8, 143.5, 141.5 (d, J_{PC} = 8.5 Hz), 139.7 (d, J_{PC} = 3.1 Hz), 134.2 (d, J_{PC} = 95.8 Hz), 132.6, 132.5 (d, J_{PC} = 5.9 Hz), 132.3 (d, J_{PC} = 102.8 Hz), 131.3 (d, J_{PC} = 3.0 Hz), 131.2, 130.77, 130.66, 130.6 (d, J_{PC} = 8.5 Hz), 128.8 (d, J_{PC} = 97.9 Hz), 128.06, 128.04, 127.99, 127.8, 127.77, 127.71, 127.4, 126.97, 126.81, 126.64, 123.6, 120.5 (d, J_{PC} = 10.9 Hz), 120.2, 93.3, 89.5, 30.8 (d, J_{PC} = 1.3 Hz), 30.6 (d, J_{PC} = 1.9 Hz), 26.5 (d, J_{PC} = 13.0 Hz), 26.1 (d, J_{PC} = 10.8 Hz), 20.2, 20.0, 14.1, 13.6; ^{31}P NMR (161 MHz, $CDCl_3$, 298 K): δ 38.3; HRMS (ESI) Calcd for $C_{40}H_{37}OP$ $[M + H]^+$ 565.2660, found 565.2665.

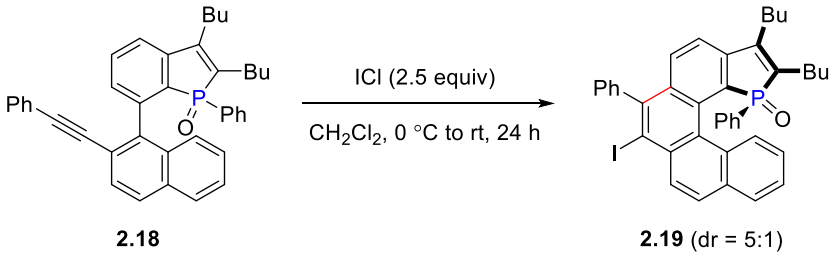

2.18 **2.19** (dr = 5:1)

2,3-Dibutyl-7-iodo-1,6-diphenylphenanthro[3,4-*g*]phosphindole 1-oxide (2.19): A 25 mL Schlenk tube was charged with **2.18** (282 mg, 0.50 mmol) and CH_2Cl_2 (9 mL) under N_2. The Schlenk tube was submerged in an ice-water bath, and iodine monochloride (1.0 M in CH_2Cl_2, 1.25 mL, 1.25 mmol) was added dropwise. The reaction mixture was stirred at room temperature for 24 h, and then quenched with saturated aqueous solution of $Na_2S_2O_3$. The aqueous layer was extracted twice with CH_2Cl_2 (30 mL). The combined organic layer was dried over $MgSO_4$ and concentrated under reduced pressure. The crude product was purified by silica gel column chromatography (eluent: hexane/ethyl acetate = 3/1) to afford the title compound as a

yellow oil (194 mg, 56%). The ^{31}P NMR and ^{1}H NMR analysis indicated the presence of two diastereomers in a ratio of 5:1. The relative configurations of the major and minor diastereomers were assigned as (R_P,*P*)/(S_P,*M*) and (S_P,*P*)/(R_P,*M*), respectively on the basis of the following ^{1}H NMR characteristics (Figure 2.15): (1) The major doublet at the highest chemical shift (8.96 ppm) is attributable to H^{13} of the (R_P,*P*)/(S_P,*M*) isomer, which should be under strong deshielding effect of the peripheral aromatic rings. The minor doublet at a lower chemical shift (8.2 ppm) is attributable to H^{13} of the (S_P,*P*)/(R_P,*M*) isomer, which should be shielded to some extent by the phenyl group on phosphorus. (2) The minor apparent triplet at an unusually low chemical shift of 5.98 ppm is attributable to H^{12} of the (S_P,*P*)/(R_P,*M*) isomer, which should be under strong shielding effect of the phenyl group on phosphorus. (3) The multiplet (2H) at relatively low chemical shift of ~ 6.4 ppm is attributable to the *ortho* protons of the P-Ph group, which should be under shielding effect of the helicene moiety. ^{1}H NMR (400 MHz, $CDCl_3$, 298 K, major isomer): δ 8.96 (d, *J* = 8.2 Hz, 1H), 7.93 (d, *J* = 8.8 Hz, 1H), 7.87 (d, *J* = 8.1 Hz, 1H), 7.78 (d, *J* = 8.9 Hz, 1H), 7.74 (dd, *J* = 8.0, 1.1 Hz, 1H), 7.69-7.63 (m, 2H), 7.59-7.55 (m, 1H), 7.54-7.49 (m, 3H), 7.37 (dd, *J* = 8.2, 0.8 Hz, 1H), 7.15-7.13 (m, 1H), 7.06-7.02 (m, 1H), 6.82-6.78 (m, 2H), 6.40-6.35 (m, 2H), 2.74-2.62 (m, 2H), 2.58-2.46 (m, 1H), 2.41-2.26 (m, 1H), 1.73-1.66 (m, 2H), 1.56-1.51 (m, 3H), 1.18-1.06 (m, 4H), 1.02 (t, *J* = 7.3 Hz, 3H), 0.90-0.83 (m, 3H), 0.63 (t, *J* = 7.1 Hz, 3H); ^{13}C NMR (400 MHz, $CDCl_3$, 298 K, major isomer): δ 149.2 (d, J_{PC} = 19.9 Hz), 144.5, 144.3, 143.9 (d, J_{PC} = 29.2 Hz), 135.6 (d, J_{PC} = 100.5 Hz), 133.6 (d, J_{PC} = 7.8 Hz), 132.7, 132.6, 132.4 (d, J_{PC} = 2.2 Hz), 131.9, 131.1, 131.0, 130.9 (d, J_{PC} = 2.3 Hz), 130.2, 129.9, 129.8 (d, J_{PC} = 96.6 Hz), 129.6, 129.5, 129.3, 129.1, 128.8, 128.7, 128.2, 127.6, 127.5 (d, J_{PC} = 103.8 Hz), 127.4 (d, J_{PC} = 4.5 Hz), 125.2, 120.1 (d, J_{PC} = 12.9 Hz), 105.5, 31.0 (d, J_{PC}

= 1.3 Hz), 30.7 (d, J_{PC} = 1.5 Hz), 26.4 (d, J_{PC} = 13.7 Hz), 26.1 (d, J_{PC} = 11.2 Hz), 23.2, 22.8, 14.0, 13.5; ^{31}P NMR (161 MHz, $CDCl_3$, 298 K): δ 46.3 (minor), 40.2 (major); HRMS (ESI) Calcd for $C_{40}H_{36}IOP$ $[M + H]^+$ 691.1627, found 691.1625.

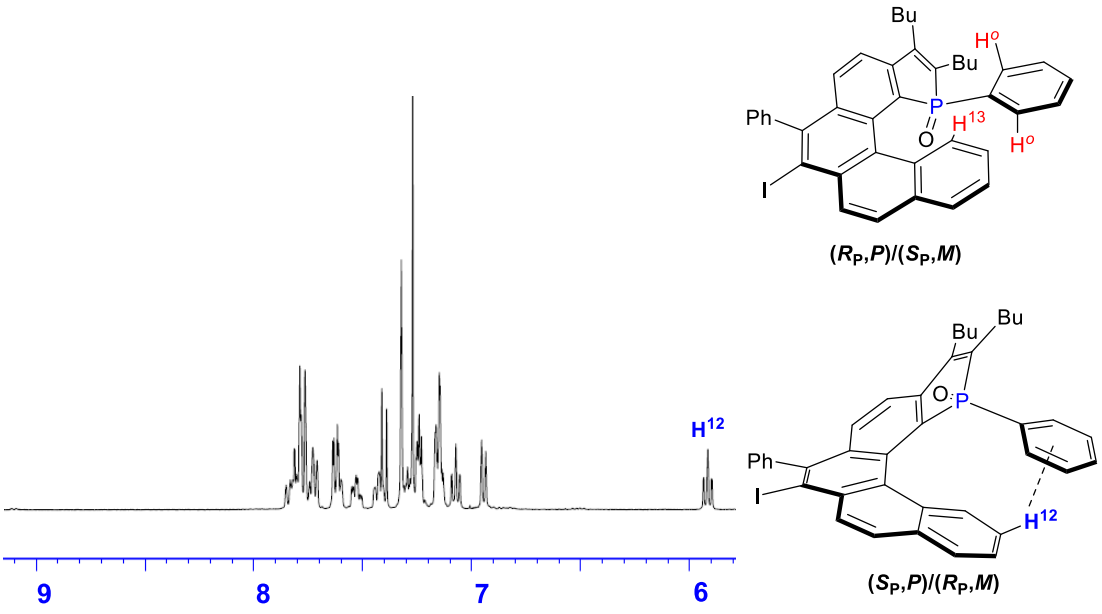

Figure 2.15. Aromatic region of ^{1}H NMR spectrum of compound **2.19**.

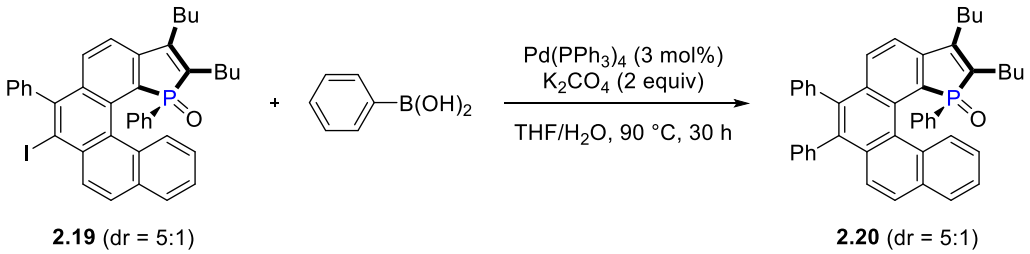

2,3-Dibutyl-1,6,7-triphenylphenanthro[3,4-*g*]phosphindole 1-oxide (2.20): A mixture of **2.19** (160 mg, 0.23 mmol), $Pd(PPh_3)_4$ (8.1 mg, 0.007 mmol), and THF (4 mL) in a 25 mL Schlenk tube was degassed through freeze-pump-thaw cycle under N_2. To the mixture was added phenylboronic acid (34 mg, 0.28 mmol), K_2CO_3 (64 mg,

0.46 mmol), and deionised water (0.68 mL). The reaction mixture was stirred at 90 °C for 30 h. The reaction mixture was cooled to room temperature and filtered through a pad of celite while washing with ethyl acetate. The filtrate was extracted twice with ethyl acetate (10 mL). The combined organic layer was dried over $MgSO_4$ and concentrated under reduced pressure. The residue was purified by silica gel column chromatography (eluent: hexane/ethyl acetate = 2/1), and the collected sample was subjected to further purification by recycling preparative HPLC to afford the title compound as a yellow oil (160 mg, 89%). The ^{31}P NMR analysis indicated the presence of two diastereomers in a ratio of 5:1. The relative configurations of the major and minor diastereomers were assigned as (R_P,*P*)/(S_P,*M*) and (S_P,*P*)/(R_P,*M*), respectively on the basis of similar ^{1}H NMR characteristics compared with that of the compound **2.19** (Figure 2.16). ^{1}H NMR (400 MHz, $CDCl_3$, 298 K, major isomer): δ 9.07 (d, *J* = 8.2 Hz, 1H), 7.82-7.72 (m, 4H), 7.66-7.58 (m, 2H), 7.55 (dd, *J* = 8.7, 2.3 Hz, 1H), 7.29 (dd, *J* = 7.3, 1.7 Hz, 1H), 7.257.14 (m, 5H), 7.12-7.08 (m, 2H), 7.05-7.01 (m, 2H), 6.85 (d, *J* = 7.5 Hz, 1H), 6.82-6.78 (m, 2H), 6.41 (m, 2H), 2.74-2.66 (m, 2H), 2.60-2.52 (m, 1H), 2.44-2.31 (m, 1H), 1.77-1.69 (m, 2H), 1.60-1.51 (m, 2H), 1.22-1.09 (m, 4H), 1.03 (t, *J* = 7.3 Hz, 3H), 0.65 (t, *J* = 7.2 Hz, 3H); ^{13}C NMR (100 MHz, $CDCl_3$, 298 K, major isomer): δ 149.5 (d, J_{PC} = 19.9 Hz), 143.5 (d, J_{PC} = 29.1 Hz), 138.9 (d, J_{PC} = 17.8 Hz), 136.9, 136.8, 135.0 (d, J_{PC} = 100.6 Hz), 133.5 (d, J_{PC} = 7.6 Hz), 132.6, 132.1, 131.7, 131.4, 131.3, 131.2, 130.77, 130.7 (d, J_{PC} = 3.3 Hz), 130.6, 130.4 (d, J_{PC} = 87.6 Hz), 130.0, 129.9, 129.7, 129.6, 128.2, 127.7 (d, J_{PC} = 3.3 Hz), 127.6, 127.5, 127.33 (d, J_{PC} = 99.6 Hz), 127.31 (d, J_{PC} = 5.6 Hz), 127.2, 126.8, 126.6 (d, J_{PC} = 6.7 Hz), 125.3, 123.3, 119.7 (d, J_{PC} = 13.2 Hz), 31.1 (d, J_{PC} = 1.7 Hz), 30.7 (d, J_{PC} = 1.7 Hz), 26.4 (d, J_{PC} = 13.4 Hz), 26.1 (d, J_{PC} = 11.0 Hz), 23.2, 22.8,

14.0, 13.5; ^{31}P NMR (161 MHz, $CDCl_3$, 298 K): δ 46.6 (minor), 40.5 (major); HRMS (ESI) Calcd for $C_{46}H_{41}OP$ [M + H]+ 641.2973, found 641.2972.

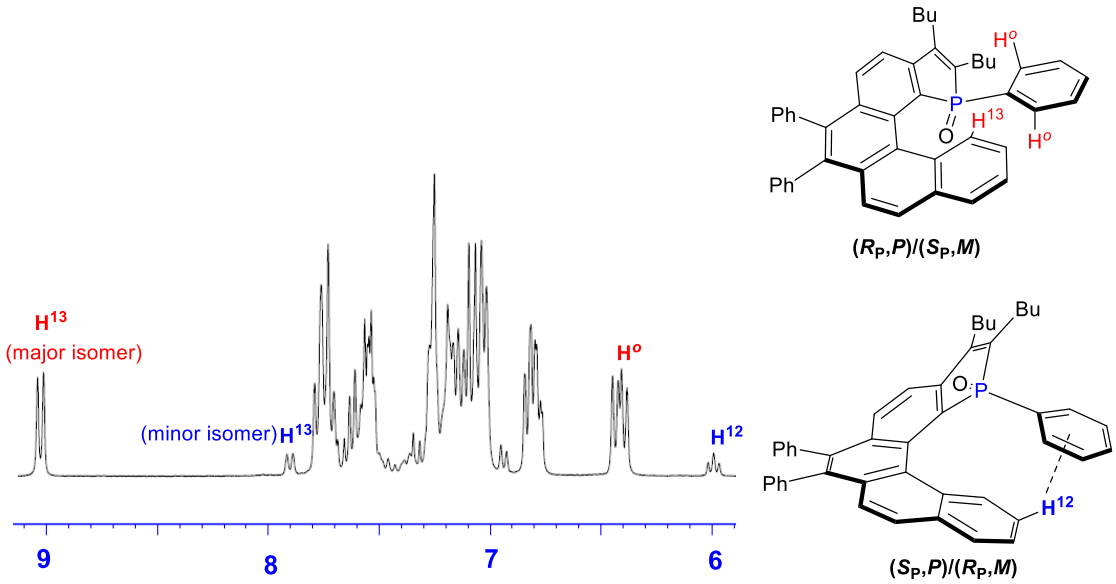

Figure 2.16. Aromatic region of ^{1}H NMR spectrum of compound **2.20**.

Optical resolution of 2.20: The enantiomeric pair of diastereomeric mixtures (i.e., (R_P,*P*)/(R_P,*M*) and (S_P,*M*)/(S_P,*P*) isomers) of the compound **2.20** could be separated by chiral HPLC (Figure 2.17a) according to the following conditions: Chiralpak ID, hexane/isopropanol (95/5), isocratic, 1 mL/min, 25 °C, 15.2 min and 18.5 min. Having established the analytical HPLC result, preparative HPLC was performed under the following conditions: Chiralpak ID, hexane/isopropanol (95/5), isocratic, 12 mL/min, 25 °C, 43.0 min and 55.0 min. Thus, two enantiomerically pure fractions (11.2 mg and 10.9 mg) (Figure 2.17b and 2.17c) with respect to phosphorus center, were separated from ca. 30 mg of compound **2.20**. These samples showed specific optical rotations of $[\alpha]^{23}_D$ = –759.6° (*c* = 0.61 in $CHCl_3$) and +689.7° (*c* = 0.57 in $CHCl_3$), respectively.

C:\LabSolutions\Data\SHAFIQ\SR-03-516-Racemic-30min.lcd

Acquired by	: Admin
Sample Name	:
Sample ID	:
Tray#	: 1
Vail #	: 1
Injection Volume	: 2 uL
Data File Name	: SR-03-516-Racemic-30min.lcd
Method File Name	: Method ID 95% 1.0ml 30min.lcm
Batch File Name	: YS-20190227-3.lcb
Report File Name	: Default.lcr
Data Acquired	: 15/Mar/19 12:47:03 PM
Data Processed	: 15/Mar/19 1:17:12 PM

<Chromatogram>

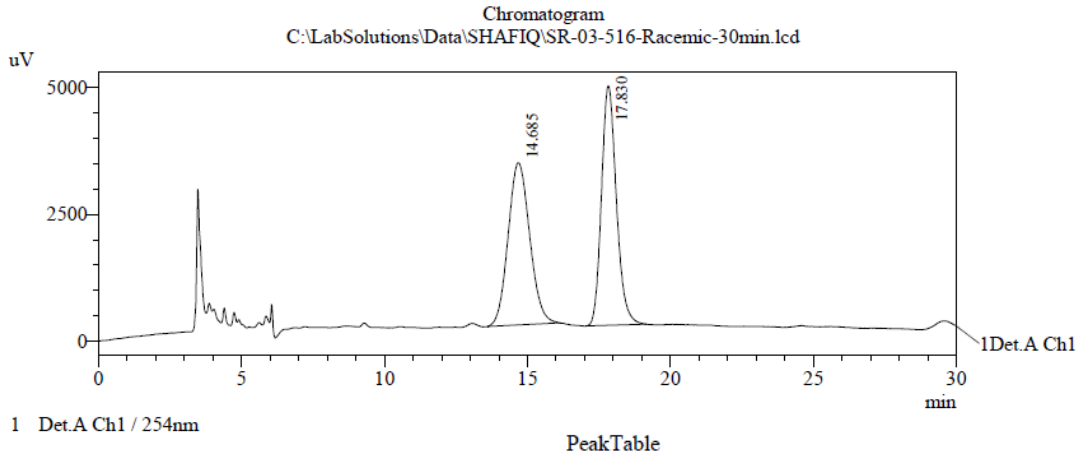

1 Det.A Ch1 / 254nm

PeakTable

Detector A Ch1 254nm

Peak#	Ret. Time	Area %
1	14.685	49.516
2	17.830	50.484
Total		100.000

Figure 2.17a. HPLC analysis of racemic sample **2.20.**

C:\LabSolutions\Data\SHAFIQ\SR-03-516-2nd-FractionPHPLC20Feb2019-redo.lcd

Acquired by	: Admin
Sample Name	:
Sample ID	:
Tray#	: 1
Vail #	: 62
Injection Volume	: 1 uL
Data File Name	: SR-03-516-2nd-FractionPHPLC20Feb2019-redo.lcd
Method File Name	: Method ID 95% 1.0ml 45min.lcm
Batch File Name	: YS-20190219.lcb
Report File Name	: Default.lcr
Data Acquired	: 20/Feb/19 6:25:41 PM
Data Processed	: 20/Feb/19 7:10:45 PM

<Chromatogram>

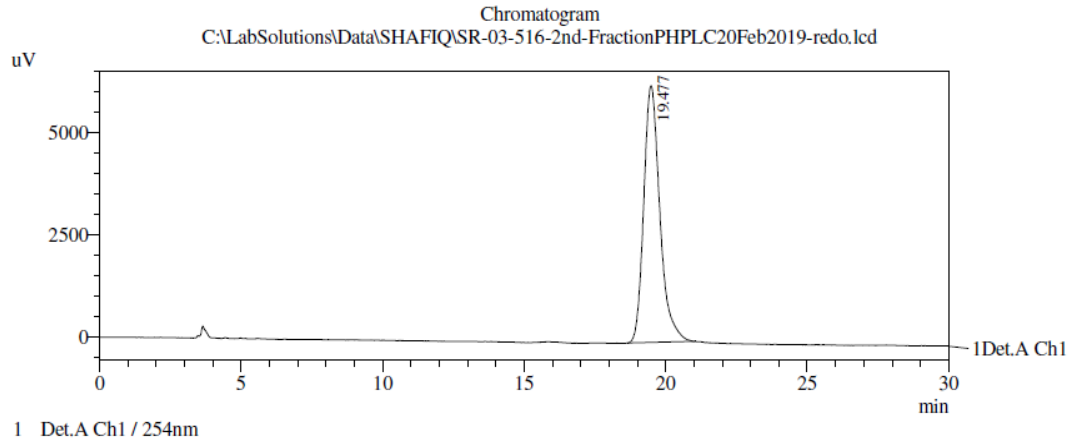

PeakTable

Detector A Ch1 254nm

Peak#	Ret. Time	Area %
1	19.477	100.000
Total		100.000

Figure 2.17b. HPLC analysis of enantiopure fraction 1 separated from racemic sample **2.20.**

C:\LabSolutions\Data\SHAFIQ\SR-03-516-1st-FractionPHPLC20Feb2019-redo.lcd

Acquired by	: Admin
Sample Name	:
Sample ID	:
Tray#	: 1
Vail #	: 61
Injection Volume	: 1 uL
Data File Name	: SR-03-516-1st-FractionPHPLC20Feb2019-redo.lcd
Method File Name	: Method ID 95% 1.0ml 45min.lcm
Batch File Name	: YS-20190219.lcb
Report File Name	: Default.lcr
Data Acquired	: 20/Feb/19 5:40:15 PM
Data Processed	: 20/Feb/19 6:25:17 PM

<Chromatogram>

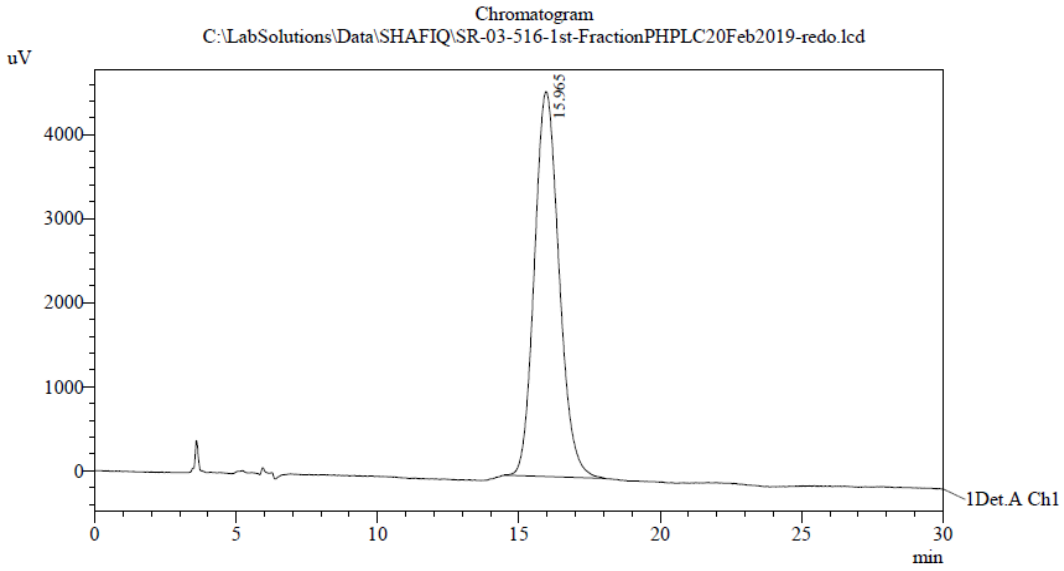

1 Det.A Ch1 / 254nm

PeakTable

Detector A Ch1 254nm

Peak#	Ret. Time	Area %
1	15.965	100.000
Total		100.000

Figure 2.17c. HPLC analysis of enantiopure fraction 2 separated from racemic sample **2.20.**

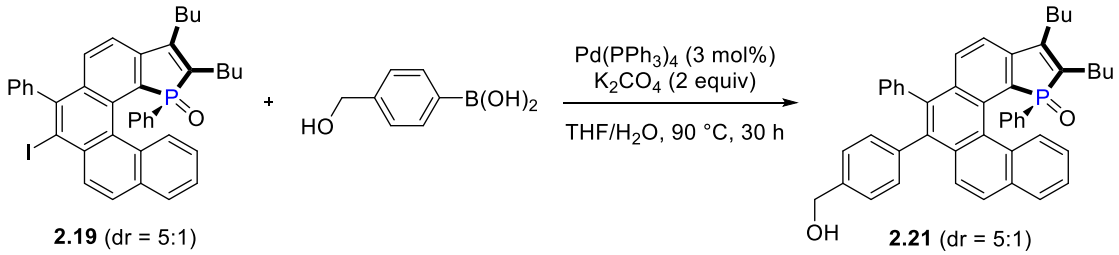

2.19 (dr = 5:1) **2.21** (dr = 5:1)

2,3-Dibutyl-7-(4-(hydroxymethyl)phenyl)-1,6-diphenylphenanthro[3,4-*g*]phosphindole 1oxide (2.21): The reaction was performed on a 0.20 mmol scale according the same procedure as described for **2.20**. Purification by silica gel column chromatography (eluent: hexane/ethyl acetate = 3/2) afford the title compound as a light yellow solid (87.2 mg, 65%). The ^{31}P NMR analysis indicated the presence of two diastereomers in a ratio of 5:1. The relative configurations of the major and minor diastereomers were assigned as (R_P,*P*)/(S_P,*M*) and (S_P,*P*)/(R_P,*M*), respectively on the basis of similar ^{1}H NMR characteristics compared with that of the compound **2.19** (Figure 2.18). ^{1}H NMR (300 MHz, $CDCl_3$, 298 K): δ 9.05 (d, *J* = 8.2 Hz, 1H), 7.81-7.72 (m, 3H), 7.67-7.53 (m, 4H), 7.33 (app. t, *J* = 8.8 Hz, 1H), 7.20-7.13 (m, 3H), 7.10-7.02 (m, 5H), 6.86-6.78 (m, 3H), 6.43 (d, *J* = 7.7 Hz, 1H), 6.39 (d, *J* = 7.6 Hz, 1H), 4.61 (s, 2H), 2.72-2.67 (m, 2H), 2.56-2.52 (m, 1H), 2.40-2.35 (m, 1H), 1.76-1.69 (m, 2H), 1.54-1.51 (m, 2H), 1.25-1.07 (m, 4H), 1.03 (t, *J* = 8.2 Hz, 1H), 0.64 (t, J = 7.2 Hz, 3H); ^{13}C NMR (100 MHz, $CDCl_3$, 298 K): δ 149.6 (d, J_{PC} = 20.0 Hz), 143.7, 143.4, 139.3 (d, J_{PC} = 1.0 Hz), 139.0, 138.1, 137.0 (d, J_{PC} = 2.0 Hz), 136.6, 135.5, 134.5, 133.7, 133.6, 133.1 (d, J_{PC} = 102.0 Hz), 132.6, 132.2, 131.9 (d, J_{PC} = 2.0 Hz), 131.8, 131.5, 131.4, 131.2 (d, J_{PC} = 1.0 Hz), 130.8, 130.7, 130.5 (d, J_{PC} = 95.0 Hz), 130.3, 129.8, 129.7, 128.3 (d, J_{PC} = 3.0 Hz), 127.9, 127.8, 127.7, 127.5, 126.9, 126.8, 126.7, 126.5, 126.0, 125.9 (d, J_{PC} = 102.0 Hz), 123.4, 119.8 (d, J_{PC} = 14.0 Hz), 65.0, 31.2 (d, J_{PC} = 1.0 Hz), 30.8 (d, J_{PC} = 2.0 Hz), 26.5 (d, J_{PC} = 14.0 Hz), 26.2 (d, J_{PC} = 12.0 Hz), 23.3, 22.8, 14.1, 13.6; ^{31}P NMR (161 MHz, $CDCl_3$, 298 K): δ 46.5 (minor), 40.5 (major); HRMS (ESI) Calcd for $C_{47}H_{43}O_2P$ $[M + H]^+$ 671.3079, found 671.3085. Recrystallization from CH_2Cl_2 afforded single crystals suitable for X-ray diffraction analysis, which confirmed the molecular structure and revealed (S_P,*P*)/(R_P,*M*) configuration (Figure 2.6).

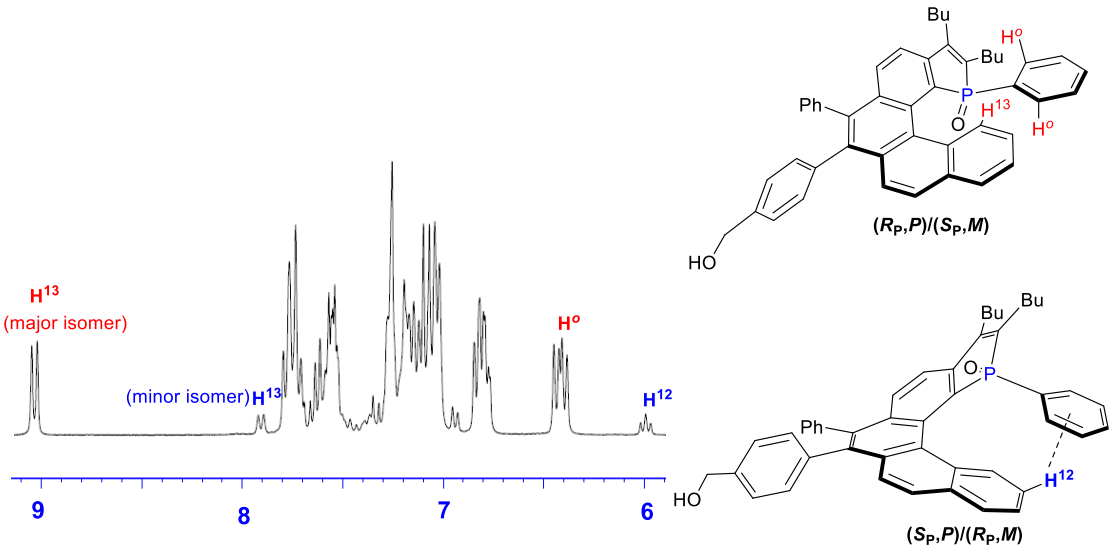

Figure 2.18. Aromatic region of ^{1}H NMR spectrum of compound **2.21**.

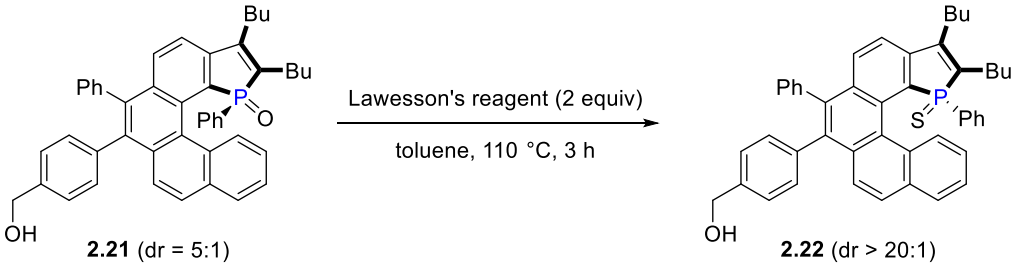

2,3-Dibutyl-7-(4-(hydroxymethyl)phenyl)-1,6-diphenylphenanthro[3,4-g]phosphindole 1sulfide (2.22): In a sealed 25 mL Schlenk tube, a solution of **2.21** (42 mg, 0.060 mmol) and Lawesson's reagent (51 mg, 0.12 mmol) in toluene (3 mL) was stirred at 110 °C under N_2 for 3 h. The reaction mixture was concentrated under reduced pressure, and the residue was purified firstly by a short silica gel column chromatography (eluent: hexane/ethyl acetate = 4/1) and then by recycling preparative HPLC to afford the title compound as a yellow solid (29.6 mg, 68%). The ^{31}P NMR analysis indicated that the compound was diastereomerically pure (dr > 20:1). The

relative configuration of the major diastereomer was assigned as (S_P,*P*)/(R_P,*M*) on the basis of the following ^{1}H NMR characteristics (Figure 2.19): (1) Unlike the analogous compounds **2.19–2.21**, no significant signal was observed beyond 8 ppm, which indicated the absence of a highly deshielded proton like H^{13} of the (R_P,*P*)/(S_P,*M*) isomer. (2) The major apparent triplet at an unusually low chemical shift of 5.90 ppm is attributable to H^{12} of the (S_P,*P*)/(R_P,*M*) isomer, which should be under strong shielding effect of the phenyl group on phosphorus. (3) Unlike the analogous compounds **2.19–2.21**, ortho protons of the P-Ph group were not observed in the region below 7 ppm. ^{1}H NMR (400 MHz, $CDCl_3$, 298 K): δ 7.84-7.70 (m, 6H), 7.62-7.59 (m, 2H), 7.54-7.50 (m, 1H), 7.43-7.38 (m, 2H), 7.31-7.27 (m, 3H), 7.24-7.22 (m, 2H), 7.15-7.12 (m, 3H), 7.08-7.04 (m, 1H), 6.93 (d, *J* = 7.84 Hz, 1H), 5.92-5.88 (m, 1H), 4.66 (s, 2H), 2.67-2.63 (t, *J* = 6.8 Hz, 2H), 2.29-2.17 (m, 1H), 1.85-1.78 (m, 2H), 1.61-1.55 (m, 3H), 1.43-1.26 (m, 2H), 1.15-1.07 (m, 2H), 1.05 (t, *J* = 7.3 Hz, 3H), 0.70 (t, *J* = 7.1 Hz, 3H); ^{13}C NMR (100 MHz, $CDCl_3$, 298 K): δ 146.4 (d, J_{PC} = 5.5 Hz), 146.2 (d, J_{PC} = 15.1 Hz), 140.5, 139.7, 139.1, 138.2, 137.3, 136.8, 134.4, 133.1, 132.5 (d, J_{PC} = 101.5 Hz), 132.48, 131.7, 131.6 (d, J_{PC} = 2.3 Hz), 131.5, 131.2 (d, J_{PC} = 95.3 Hz), 131.1 (d, J_{PC} = 3.2 Hz), 131.0, 130.5, 130.4, 129.7 (d, J_{PC} = 8.5 Hz), 129.1 (d, J_{PC} = 1.7 Hz), 129.0 (d, J_{PC} = 13.1 Hz), 128.5 (d, J_{PC} = 9.9 Hz), 128.1, 128.0, 127.9, 127.8, 127.7 (d, J_{PC} = 2.8 Hz), 127.6, 126.7, 126.5, 126.2 (d, J_{PC} = 6.7 Hz), 124.8 (d, J_{PC} = 103.7 Hz), 123.8, 120.5 (d, J_{PC} = 12.2 Hz), 65.2, 31.9, 30.7, 26.7 (d, J_{PC} = 13.0 Hz), 25.3 (d, J_{PC} = 13.1 Hz), 23.2, 22.9, 14.0, 13.6; ^{31}P NMR (161 MHz, $CDCl_3$, 298 K): δ 55.0; HRMS (ESI) Calcd for C47H43OPS $[M + H]^+$ 687.2851, found 687.2850. Recrystallization from CH_2Cl_2 afforded single crystals suitable for X-ray diffraction analysis, which confirmed the molecular structure and revealed (S_P,*P*)/(R_P,*M*) configuration.

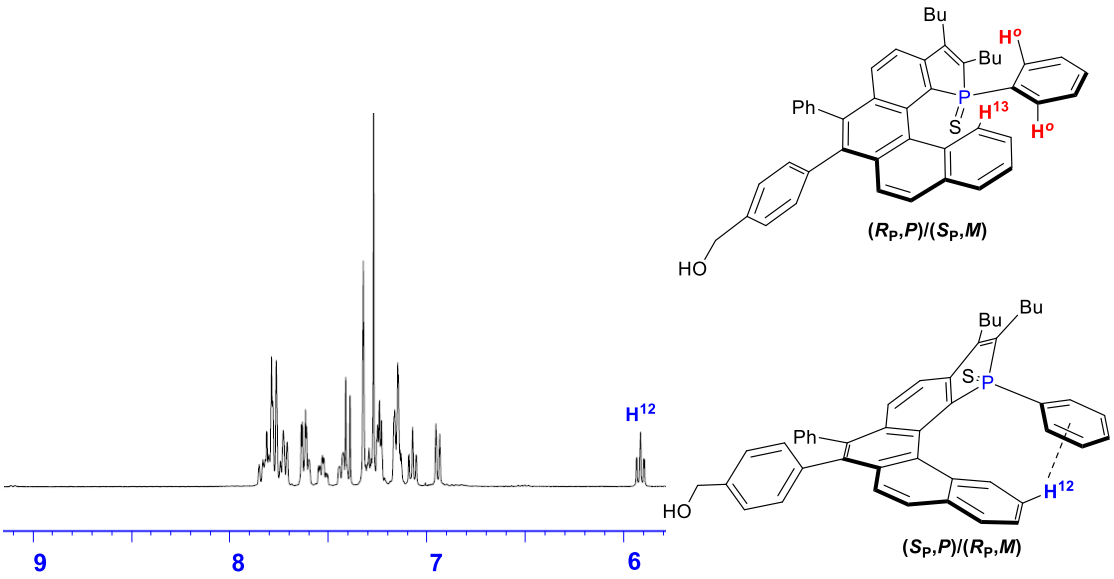

Figure 2.19. Aromatic region of ^{1}H NMR spectrum of compound **2.22**.

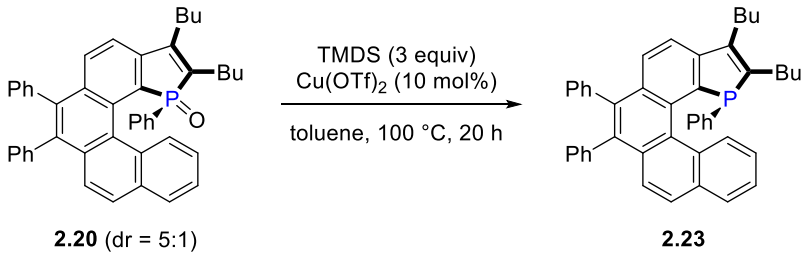

2,3-Dibutyl-1,6,7-triphenyl-1H-phenanthro[3,4-*g*]phosphindole (2.23): The compound was prepared according to the literature procedure with slight modification.[49] A 10 mL Schlenk tube charged with $Cu(OTf)_2$ (5.1 mg, 0.014 mmol) was dried under vacuum at 130 °C for 1 h. Upon cooling under N_2, **2.20** (89.7 mg, 0.14 mmol), toluene (1 mL) and tetramethyl disiloxane (75 µL, 0.42 mmol) were added. The Schlenk tube was sealed and the reaction mixture was stirred at 100 °C for 20 h. The reaction mixture was cooled to room temperature and concentrated under reduced pressure. The residue was purified by preparative thin layer chromatography

(eluent: hexane) to afford the title compound as a light yellow oil (64.3 mg, 74%). The ^{31}P NMR analysis indicated that the compound was diastereomerically pure (dr > 20:1). The relative configuration was assigned as (R_P,*M*)/(S_P,*P*) on the basis of the following ^{1}H NMR characteristics (Figure 2.20): (1) A multiplet (1H) at the highest chemical shift of ~9.1 ppm is attributable to H^{13} of the (R_P,*M*)/(S_P,*P*) isomer, which should be deshielded by the proximal aromatic rings. (2) The apparent triplet (2H) at a low chemical shift of ~6.2 ppm is attributable to the ortho protons of the P-Ph group, which should be under shielding effect of the helicene moiety. ^{1}H NMR (400 MHz, $CDCl_3$, 298 K): δ 9.12-9.08 (m, 1H), 7.81 (dd, *J* = 6.4, 2.2 Hz, 1H), 7.67-7.59 (m, 4H), 7.51 (d, *J* = 8.7 Hz, 1H), 7.28-7.23 (m, 2H), 7.21-7.10 (m, 8H), 6.92-6.87 (m, 2H), 6.72-6.68 (m, 2H), 6.18-6.14 (m, 2H), 2.79-2.69 (m, 2H), 2.62-2.52 (m, 1H), 2.27-2.17 (m, 1H), 1.69-1.63 (m, 2H), 1.52-1.38 (m, 4H), 1.32-1.23 (m, 2H), 1.00 (t, *J* = 7.3 H, 3H), 0.82 (t, *J* = 7.3 Hz, 3H); ^{13}C NMR (100 MHz, $CDCl_3$, 298 K): δ 146.8 (d, J_{PC} = 8.0 Hz), 144.2 (d, J_{PC} = 10.4 Hz), 143.1 (d, J_{PC} = 8.8 Hz), 141.5 (d, J_{PC} = 6.7 Hz), 139.8, 139.4, 137.8, 135.3, 133.5, 133.3, 132.6, 132.4, 132.2, 131.7, 131.5, 131.4, 131.3 (d, J_{PC} = 97.7 Hz), 131.0, 130.5, 130.4, 129.9, 129.8, 128.2 (d, J_{PC} = 2.4 Hz), 128.0 (d, J_{PC} = 104.5 Hz), 127.6, 127.4, 127.3, 127.2, 127.1 (d, J_{PC} = 2.6 Hz), 126.8, 126.4 (d, J_{PC} = 2.3 Hz), 126.3 (d, J_{PC} = 2.6 Hz), 124.4 (d, J_{PC} = 2.3 Hz), 124.1, 120.8, 33.4 (d, J_{PC} = 5.6 Hz), 31.9 (d, J_{PC} = 4.2 Hz), 28.1 (d, J_{PC} = 20.5 Hz), 27.0, 23.2, 22.9, 14.1, 13.8; ^{31}P NMR (161 MHz, $CDCl_3$, 298 K): δ 10.8; HRMS (ESI) Calcd for $C_{46}H_{41}P$ $[M + H]^+$ 625.3024, found 625.3052.

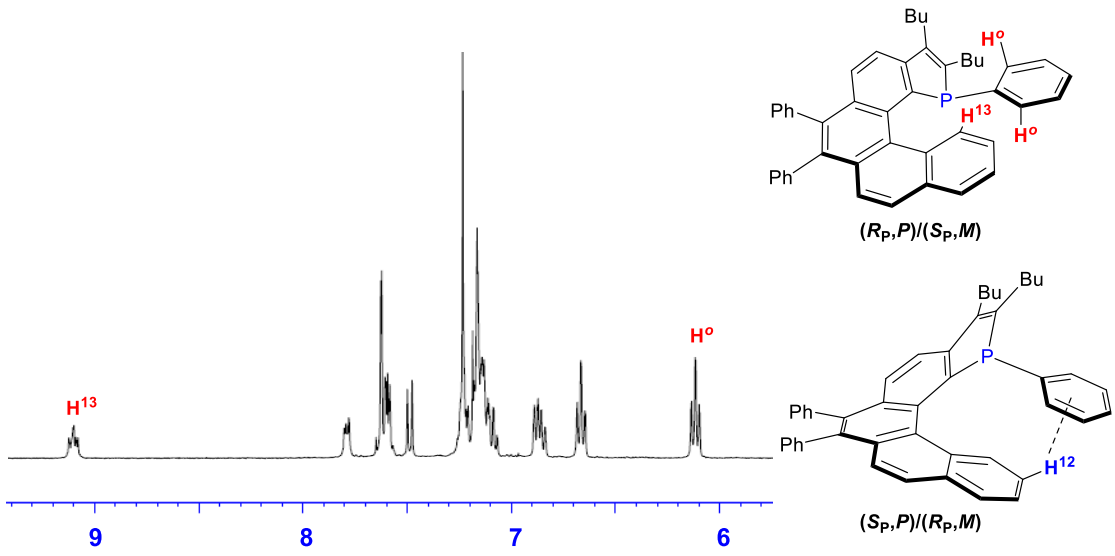

Figure 2.20. Aromatic region of ^{1}H NMR spectrum of compound **2.23**.

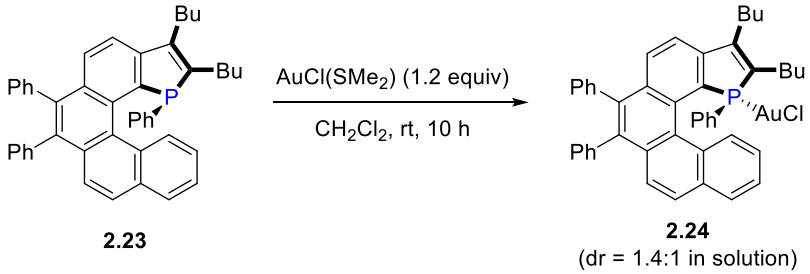

(2,3-Dibutyl-1,6,7-triphenyl-1H-phenanthro[3,4-*g*]phosphindol-1-yl)gold(I) chloride (2.24): This reaction was performed according to the literature procedure with slight modification.[54] A CH_2Cl_2 solution (0.5 mL) of chloro(dimethylsulfide)gold(I) (24.3 mg, 0.082 mmol) was added to a solution of **2.23** (43 mg, 0.070 mmol) in CH_2Cl_2 (1.5 mL) under N_2 atmosphere. The resulting mixture was stirred at room temperature for 10 h. The reaction mixture was concentrated to half under reduced pressure and transferred to an 8 mL vial, which was kept standing for 24 h. The solution was decanted off to another 8 mL vial. The vial was placed in a hexane-containing 60 mL glass bottle, which was capped for recrystallization at room temperature. A yellow crystalline solid precipitated out after 48 h, which was filtered

and dried to afford the title compound (41.2 mg, 70%). X-ray diffraction analysis of the crystalline sample confirmed the molecular structure and revealed (S_P,*P*)/(R_P,*M*) configuration. Meanwhile, ^{31}P NMR analysis of the sample in $CDCl_3$ indicated the presence of two diastereomers in a ratio of 1.4:1. The relative configurations of the major and minor diastereomers were assigned as (R_P,*P*)/(S_P,*M*) and (S_P,*P*)/(R_P,*M*), respectively on the basis of ^{1}H NMR spectrum in comparison with that of analogous compounds **2.19**–**2.23** (Figure 2.21). ^{1}H NMR (400 MHz, $CDCl_3$, 298 K, except for some cases indicated, peaks of the diastereomers are heavily overlapped and clear assignment was difficult due to the poor ratio): δ 8.80 (dd, *J* = 8.1, 3.1 Hz, 1H, major isomer), 7.96-7.79 (m, 6H), 7.74-7.65 (m, 4H), 7.63-7.54 (m, 5H), 7.47-7.28 (m, 6H), 7.24-7.10 (m, 13H), 7.05 (d, *J* = 7.9 Hz, 3H), 6.91 (d, *J* = 7.6 Hz, 1H, minor isomer), 6.86-6.77 (m, 4H), 6.37 (d, *J* = 7.2 Hz, 1H, major isomer), 6.34 (d, *J* = 7.2 Hz, 1H, major isomer), 5.97 (t, *J* = 7.2 Hz, 1H, minor isomer), 2.75-2.64 (m, 4H), 2.42-2.31 (m, 2H), 1.74-1.48 (m, 12H), 1.28-1.22 (m, 3H), 1.17-1.07 (m, 3H), 1.04 (t, *J* = 7.2 Hz, 6H), 0.74 (t, *J* = 7.3 Hz, 3H, minor isomer), 0.65 (t, *J* = 7.3 Hz, 3H, major isomer); ^{13}C NMR (100 MHz, $CDCl_3$, 298 K, both isomers; complete peak picking was difficult due to the poor diastereomer ratio, extensive peak overlaps, and ^{31}P-^{13}C couplings): δ 149.1 (d, J_{PC} = 12.3 Hz), 148.8 (d, J_{PC} = 18.2 Hz), 147.2, 147.0 (d, J_{PC} = 18.9 Hz), 139.1, 138.8 (d, J_{PC} = 10.7 Hz), 138.5 (d, J_{PC} = 4.3 Hz), 138.3 (d, J_{PC} = 2.8 Hz), 137.4, 137.3, 136.8 (d, J_{PC} = 90.5 Hz), 136.7, 135.8, 133.2, 133.16, 133.10, 132.5, 132.1, 132.0, 131.8, 131.7, 131.53, 131.51 (d, J_{PC} = 97.9 Hz) 131.49, 131.46, 131.3, 131.2, 131.1, 131.0 (d, J_{PC} = 95.3 Hz), 130.0, 129.9, 129.8, 129.6, 129.4 (d, J_{PC} = 89.6 Hz), 129.4, 129.3, 129.2 (d, J_{PC} = 3.6 Hz), 129.1, 129.9, 128.5 (d, J_{PC} = 4.7 Hz), 127.95, 127.86, 127.83, 127.75, 127.66, 127.59, 127.4, 126.8 (d, J_{PC} = 3.1 Hz), 126.7, 126.66, 126.58, 126.44, 126.3, 126.0, 125.7, 125.1, 124.3, 123.6, 121.1 (d, J_{PC}

= 9.2 Hz), 120.8 (d, J_{PC} = 9.6 Hz), 32.8 (d, J_{PC} = 3.0 Hz), 32.3 (d, J_{PC} = 2.1 Hz), 31.1, 31.0, 27.7 (d, J_{PC} = 18.6 Hz), 27.0 (d, J_{PC} = 9.7 Hz), 26.6 (d, J_{PC} = 9.2 Hz), 26.2 (d, J_{PC} = 14.6 Hz), 23.2, 23.0, 22.62, 22.59, 14.0, 13.9, 13.6, 13.5; ^{31}P NMR (161 MHz, $CDCl_3$, 298 K), δ 45.5 (major), 41.9 (minor); HRMS (ESI) Calcd for $C_{46}H_{41}PAuCl$ [M + H]$^+$ 857.2378, found 857.2383.

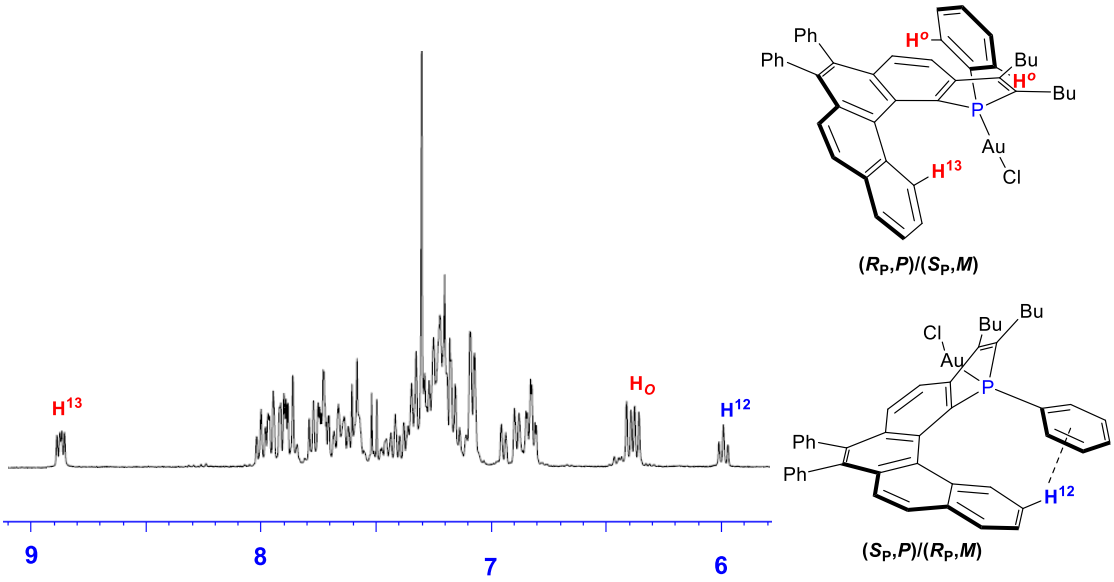

Figure 2.21. Aromatic region of ^{1}H NMR spectrum of compound **2.24**.

DFT Calculations

All density functional theory (DFT) calculations employed the B3LYP functional and 6-31G(d) basis set and were performed using Gaussian 09 program. Harmonic frequency calculation was performed to verify each optimized structure and to calculate the Gibbs free energy (298.15 K, 1 atm).

2.5 References

1. Shen, Y.; Chen, C.-F. *Chem. Rev.* **2012**, *112*, 1463.
2. Gingras, M. *Chem. Soc. Rev.* **2013**, *42*, 968.
3. Gingras, M.; Félix, G.; Peresutti, R. *Chem. Soc. Rev.* **2013**, *42*, 1007.
4. Gingras, M. *Chem. Soc. Rev.* **2013**, *42*, 1051.
5. Botek, E.; André, J.-M.; Champagne, B.; Verbiest, T.; Persoons, A. *J. Chem. Phys.* **2005**, *122*, 234713.
6. Isla, H.; Crassous, J. *C. R. Chem.* **2016**, *19*, 39.
7. Chen, C. -F.; Shen, Y. Helicene Chemistry; Springer-Verlag: Berlin, Heidelberg, **2017**.
8. Goto, K.; Yamaguchi, R.; Hiroto, S.; Ueno, H.; Kawai, T.; Shinokubo, H. *Angew. Chem. Int. Ed.* **2012**, *51*, 10333.
9. Ueda, A.; Wasa, H.; Suzuki, S.; Okada, K.; Sato, K.; Takui, T.; Morita, Y. *Angew. Chem. Int. Ed.* **2012**, *51*, 6691.
10. Hatakeyama, T.; Hashimoto, S.; Oba, T.; Nakamura, M. *J. Am. Chem. Soc.* **2012**, *134*, 19600.
11. Kaneko, E.; Matsumoto, Y.; Kamikawa, K. *Chem. Eur. J.* **2013**, *19*, 11837.
12. Nakamura, K.; Furumi, S.; Takeuchi, M.; Shibuya, T.; Tanaka, K. *J. Am. Chem. Soc.* **2014**, *136*, 5555.
13. Hirai, H.; Nakajima, K.; Nakatsuka, S.; Shiren, K.; Ni, J.; Nomura, S.; Ikuta, T.; Hatakeyama, T. *Angew. Chem. Int. Ed.* **2015**, *54*, 13581.
14. Wang, X.-Y.; Wang, X.-C.; Narita, A.; Wagner, M.; Cao, X.-Y.; Feng, X.; Müllen, K. *J. Am. Chem. Soc.* **2016**, *138*, 12783.

15. Wang, Y.; Zhang, H.; Pink, M.; Olankitwanit, A.; Rajca, S.; Rajca, A. *J. Am. Chem. Soc.* **2016**, *138*, 7298.

16. Xu, K.; Fu, Y.; Zhou, Y.; Hennersdorf, F.; Machata, P.; Vincon, I.; Weigand, J. J.; Popov, A. A.; Berger, R.; Feng, X. *Angew. Chem. Int. Ed.* **2017**, *56*, 15876.

17. Otani, T.; Tsuyuki, A.; Iwachi, T.; Someya, S.; Tateno, K.; Kawai, H.; Saito, T.; Kanyiva, K. S.; Shibata, T. *Angew. Chem. Int. Ed.* **2017**, *56*, 3906.

18. Field, J. E.; Muller, G.; Riehl, J. P.; Venkataraman, D. *J. Am. Chem. Soc.* **2003**, *125*, 11808.

19. Hassey, R.; Swain, E. J.; Hammer, N. I.; Venkataraman, D.; Barnes, M. D. *Science* **2006**, *314*, 1437.

20. Vreshch, V.; El Sayed Moussa, M.; Nohra, B.; Srebro, M.; Vanthuyne, N.; Roussel, C.; Autschbach, J.; Crassous, J.; Lescop, C.; Réau, R. *Angew. Chem. Int. Ed.* **2013**, *52*, 1968.

21. Graule, S.; Rudolph, M.; Vanthuyne, N.; Autschbach, J.; Roussel, C.; Crassous, J.; Réau, R. *J. Am. Chem. Soc.* **2009**, *131*, 3183.

22. Mendola, D.; Saleh, N.; Vanthuyne, N.; Roussel, C.; Toupet, L.; Castiglione, F.; Caronna, T.; Mele, A.; Crassous, J. *Angew. Chem. Int. Ed.* **2014**, *53*, 5786.

23. Hellou, N.; Srebro-Hooper, M.; Favereau, L.; Zinna, F.; Caytan, E.; Toupet, L.; Dorcet, V.; Jean, M.; Vanthuyne, N.; Williams, J. A. G.; Di Bari, L.; Autschbach, J.; Crassous, J. *Angew. Chem. Int. Ed.* **2017**, *56*, 8236.

24. Peng, Z.; Takenaka, N. *Chem. Rec.* **2013**, *13*, 28.

25. Narcis, M. J.; Takenaka, N. *Eur. J. Org. Chem.* **2014**, *2014*, 21.

26. Aillard, P.; Voituriez, A.; Marinetti, A. *Dalton Trans.* **2014**, *43*, 15263.

27. Takenaka, N.; Sarangthem, R. S.; Captain, B. *Angew. Chem. Int. Ed.* **2008**, *120*, 9854.

28. Takenaka, N.; Chen, J.; Captain, B.; Sarangthem, R. S.; Chandrakumar, A. *J. Am. Chem. Soc.* **2010**, *132*, 4536.

29. Gicquel, M.; Zhang, Y.; Aillard, P.; Retailleau, P.; Voituriez, A.; Marinetti, A. *Angew. Chem. Int. Ed.* **2015**, *54*, 5470.

30. Fukawa, N.; Osaka, T.; Noguchi, K.; Tanaka, K. *Org. Lett.* **2010**, *12*, 1324.

31. Sawada, Y.; Furumi, S.; Takai, A.; Takeuchi, M.; Noguchi, K.; Tanaka, K. *J. Am. Chem. Soc.* **2012**, *134*, 4080.

32. Nakano, K.; Oyama, H.; Nishimura, Y.; Nakasako, S.; Nozaki, K. *Angew. Chem. Int. Ed.* **2012**, *51*, 695.

33. Yavari, K.; Moussa, S.; Ben Hassine, B.; Retailleau, P.; Voituriez, A.; Marinetti, A. *Angew. Chem. Int. Ed.* **2012**, *51*, 6748.

34. Yavari, K.; Retailleau, P.; Voituriez, A.; Marinetti, A. *Chem. Eur. J.* **2013**, *19*, 9939.

35. Aillard, P.; Voituriez, A.; Dova, D.; Cauteruccio, S.; Licandro, E.; Marinetti, A. *Chem. Eur. J.* **2014**, *20*, 12373.

36. Yavari, K.; Aillard, P.; Zhang, Y.; Nuter, F.; Retailleau, P.; Voituriez, A.; Marinetti, A. *Angew. Chem. Int. Ed.* **2014**, *126*, 880.

37. Aillard, P.; Gicquel, M.; Yavari, K.; Retailleau, P.; Voituriez, A.; Marinetti, A. *Eur. J. Org. Chem.* **2018**, *2018*, 5853.

38. Aillard, P.; Dova, D.; Magné, V.; Retailleau, P.; Cauteruccio, S.; Licandro, E.; Voituriez, A.; Marinetti, A. *Chem. Commun.* **2016**, *52*, 10984.

39. Aillard, P.; Retailleau, P.; Voituriez, A.; Marinetti, A. *Chem. Commun.* **2014**, *50*, 2199.

40. Aillard, P.; Retailleau, P.; Voituriez, A.; Marinetti, A. *Chem. Eur. J.* **2015**, *21*, 11989.

41. Yamaguchi, E.; Wang, C.; Fukazawa, A.; Taki, M.; Sato, Y.; Sasaki, T.; Ueda, M.; Sasaki, N.; Higashiyama, T.; Yamaguchi, S. *Angew. Chem. Int. Ed.* **2015**, *54*, 4539.

42. Wang, C.; Taki, M.; Sato, Y.; Fukazawa, A.; Higashiyama, T.; Yamaguchi, S. *J. Am. Chem. Soc.* **2017**, *139*, 10374.

43. Wu, B.; Santra, M.; Yoshikai, N. *Angew. Chem. Int. Ed.* **2014**, *53*, 7543.

44. Yoshikai, N.; Santra, M.; Wu, B. *Organometallics* **2017**, *36*, 2637.

45. Tan, B.-H.; Dong, J.; Yoshikai, N. *Angew. Chem. Int. Ed.* **2012**, *51*, 9610.

46. Tan, B.-H.; Yoshikai, N. *Org. Lett.* **2014**, *16*, 3392.

47. Yao, T.; Campo, M. A.; Larock, R. C. *Org. Lett.* **2004**, *6*, 2677.

48. Bédard, A.-C.; Vlassova, A.; Hernandez-Perez, A. C.; Bessette, A.; Hanan, G. S.; Heuft, M. A.; Collins, S. K. *Chem. Eur. J.* **2013**, *19*, 16295.

49. Li, Y.; Das, S.; Zhou, S.; Junge, K.; Beller, M. *J. Am. Chem. Soc.* **2012**, *134*, 9727.

50. Egan, W.; Tang, R.; Zon, G.; Mislow, K. *J. Am. Chem. Soc.* **1971**, *93*, 6205.

51. Wu, B.; Chopra, R.; Yoshikai, N. *Org. Lett.* **2015**, *17*, 5666.

52. Frigoli, M.; Marrot, J.; Gentili, P. L.; Jacquemin, D.; Vagnini, M.; Pannacci, D.; Ortica, F. *ChemPhysChem* **2015**, *16*, 2447.

53. Weimar, M.; Correa da Costa, R.; Lee, F.-H.; Fuchter, M. J. *Org. Lett.* **2013**, *15*, 1706.

54. Fourmy, K.; Mallet-Ladeira, S.; Dechy-Cabaret, O.; Gouygou, M. *Organometallics* **2013**, *32*, 1571.

Chapter 3. Synthesis and Optical Properties of Phosphole Oxide-Fused Triphenylene Derivatives

3.1 Introduction

Phosphorus-embedded five-membered ring, phosphole, recently has achieved significant attention as an important structural motif in material chemistry, because its molecular and electronic properties can be modulated via functionalization of phosphorus center and thus, leads to the development of novel extended π-conjugation materials for organic field effect transistors, photovoltaics, organic light emitting diodes.[1-12] In addition, phosphole-containing PAHs showed promising applications in asymmetric synthesis, sensor and imaging.[13-15] Yamaguchi *et al.* demonstrated that phosphole-embedded PAHs,[14-15] could be utilized in biological fluorescent probe. Representative examples of functional phosphorus containing PAHs are shown in Figure 3.1 (**3.1-3.3**). On the other hand, triphenylenes and related derivatives have gained significant attention in material science due to π-conjugation, rigid, planar, and semiconducting properties.[16-20] Triphenylenes containing long aliphatic side chains form discotic liquid crystals because of self-assembling in one-dimensional columnar aggregation and solution-processable character.[18, 21-23] For example, triphenylenes such as alkoxytriphenylene,[24-25] hexaazatriphenylene HAT[26] and related derivatives, imidazolium ion-appended triphenylene[27] (Figure 3.1) (**3.4-3.6**) applied as organic materials in optoelectronic devices and sensors.

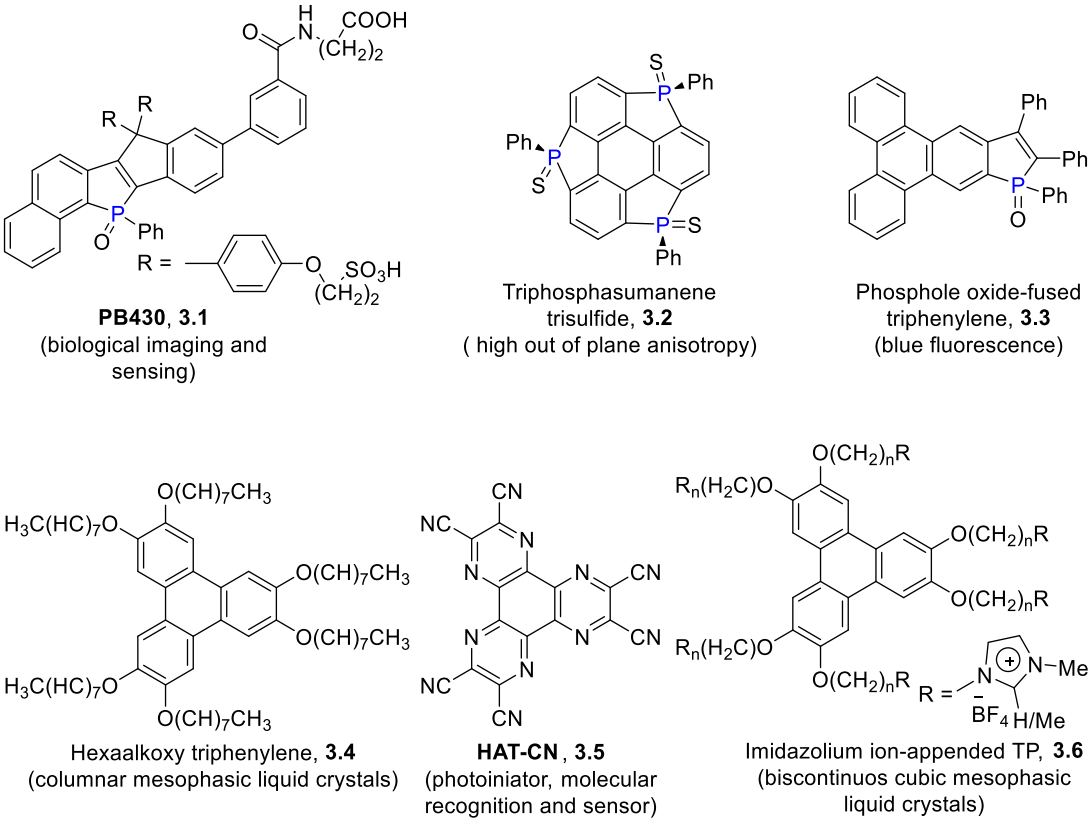

Figure 3.1. Functional molecules of phosphole oxide-fused PAHs and triphenylene derivatives.

Over the last several years, a significant attention was devoted towards the synthesis of phosphole-embedded PAHs. Saito and coworkers recently described a synthesis of novel phosphorus containing triphenylenes, such as triphosphasumanene trisulfide (diphosphasumanene disulfide) from 2,3,6,7,10,11-hexyethoxytriphenylene (*cf.* Chapter 1). The authors revealed the unique electronic properties of triphosphasumanene trisulfide and out of plane anisotropy.[28] In contrast, our group reported a synthesis of planar phosphole oxide-fused triphenylene **3.14** from 5-(trimethylsilyl)-6-triflate benzo[*b*]phosphole oxide **3.12** and 2-iodobiphenyl via 5,6-benzophospholyne **3.13** as a key intermediated (Scheme 3.1).[29] Note that, phosphole

moiety was linearly fused with triphenylene. The key precursor, 5-silyl-6-triflate benzo[*b*]phosphole oxide **3.12** was achieved through a sequence of steps. 5-Silyl-6-alkoxybenzo[*b*]phosphole oxide **3.11** was prepared through an assembly of 5-silyl-6-alkoxyphenyl Grignard **3.7** and diphenylacetylene **3.8**, followed by electrophilic trapping of styrylmagnesiation with a dichlorophenylphosphine, **3.10** and then phospha-Friedel-Crafts intramolecular cyclization, then with H_2O_2, affording a corresponding benzo[*b*]phosphole oxide **3.11**. Deprotection of 6-alkoxy-benzo[*b*]phosphole followed by triflation, produced the desired precursor, benzo[*b*]phosphole oxide 5-silyl-6-triflate **3.13**. Besides these reports, synthesis of phosphole-embedded triphenylenes remains elusive.

Scheme 3.1. Synthesis of phosphole oxide-fused triphenylene via Pd-catalyzed [4 + 2] cycloaddition of benzophospholyne and 2-iodobiphenyl

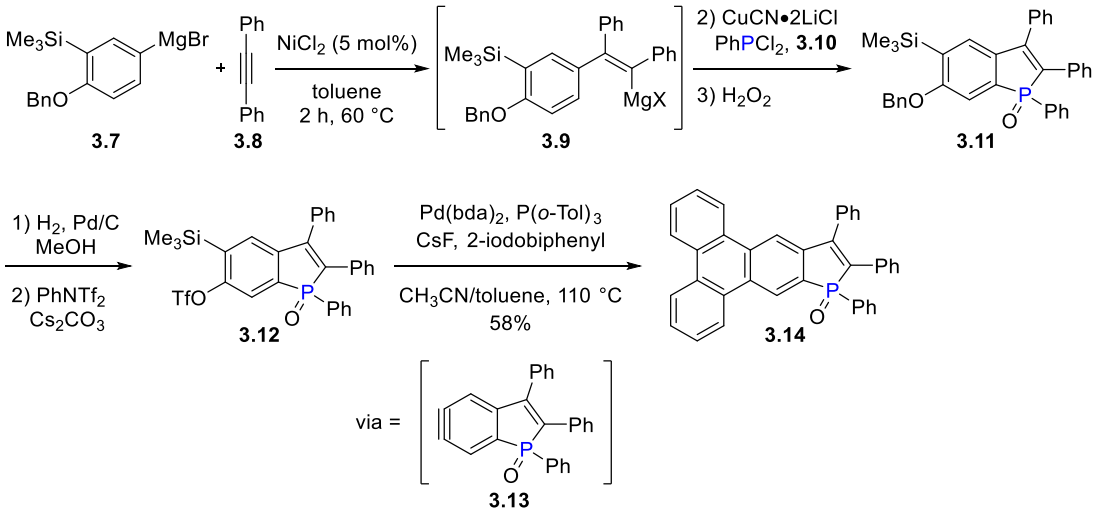

The Scholl reaction in PAHs synthesis

The Scholl reaction, developed by Roland Scholl in 1910, is a classical example to construct triphenylenes, hexa-*peri*-hexabenzocoronenes, graphenes, nanographenes, carbon nano-tubes.[19,30,31-32] The first report of dehydrogenative cyclization by using Lewis acid appeared in 1910, while heating binaphthyl and related derivatives in the presence of $AlCl_3$, thus, affording the intramolecular dehydrogenative C-C coupled product (Scheme 3.2).[33] Since then notable progress have been made and several oxidants such as $AlCl_3$, $FeCl_3$, $MoCl_5$, $SnCl_4$, PIFA/$BF_3{\cdot}Et_2O$, DDQ etc., were proved to be efficient for Scholl reaction.[31, 34] Amongst various oxidants, $FeCl_3$ in nitromethane is well explored for the synthesis of new PAHs.[35-36] However, the Scholl reaction suffers several disadvantages such as generation of unwanted products and oligomerization of starting materials, poor tolerance of functional groups.

Scheme 3.2. $AlCl_3$ mediated oxidative cyclization

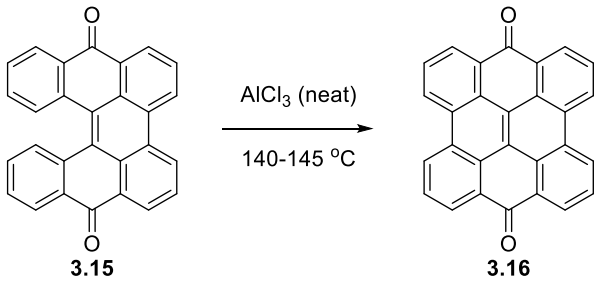

3.15 **3.16**

King and coworkers reported the synthesis of triphenylene derivatives from *ortho*-terphenyls by using PIFA/$BF_3{\cdot}Et_2O$ (Scheme 3.3).[37] Notably, the substrate scope is narrow, and the oligomerization of the starting material is a problematic. Later, a soft oxidant, $MoCl_5$ was employed to suppress the oligomerization of *ortho*-terphenyls

and to improve the substrate scope and yield.[37] However, *ortho*-terphenyls containing strong electron withdrawing groups such as nitrogen dioxide, proved to be inefficient for cyclization either by PIFA/BF_3·Et_2O or $MoCl_5$. The author reasoned that the strong electron withdrawing groups might inhibit the generation of arenium cation intermediate or intramolecular attack on the adjacent aryl ring. Furthermore, they investigated the mechanism of the Scholl reactions.[37-38]

Scheme 3.3. Oxidative cyclodehydrogenation of *ortho*-terphenyl

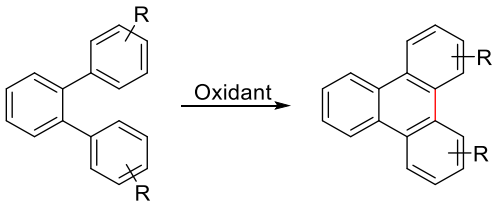

The mechanism of the Scholl reaction is still not well established and could occur either via cation radical (electron transfer) (Scheme 3.4) or arenium ion (proton transfer) pathways (Scheme 3.5).[37-39] Parker and coworkers presented a mechanistic study on oxidative C-C coupling between two aryls via cationic radical (electron transfer) pathway.[40-42] Rathore and coworkers in 2010, demonstrated that the Scholl reaction may proceeds through cationic radical pathway however, they could not rule out the possibility of arenium ion pathway.[39]

Scheme 3.4. Scholl reaction mechanism via cation radical (electron transfer) pathway

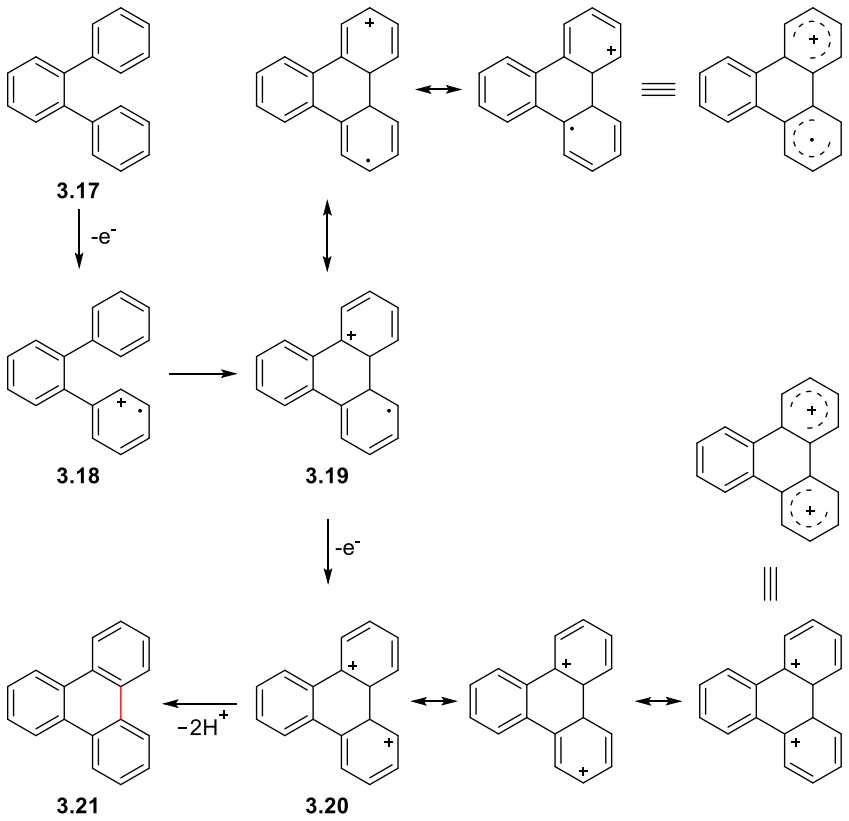

King *et al.* investigated the mechanism of intramolecular Scholl reactions involving *ortho*-terphenyl derivatives, hexaphenylbenzene. Based on DFT calculations, the author proposed that the dehydrogenative C-C coupling proceeds through a cationic arenium intermediates (Scheme 3.5) and can be accelerated with the formation of acids. The protonation occurs at *meta*-position of the electron releasing phenyl moiety and affording cyclohexadiene, which upon aromatization produced triphenylene. The arenium cation pathway requires low activation energy barrier for C-C bond formation than that of cationic radical pathway by 7 kcal mol^{-1}.

Scheme 3.5. Scholl reaction mechanism via arenium ion (proton transfer) pathway

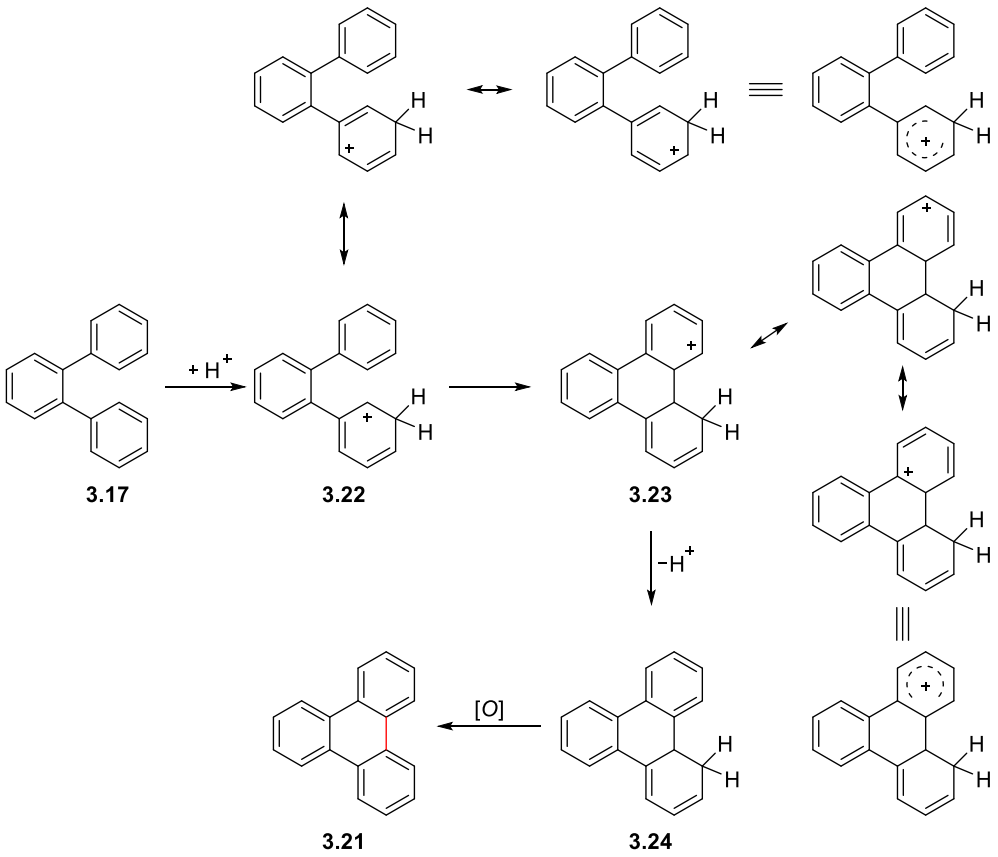

Hissler and coworkers, recently, attempted the synthesis of P-containing PAHs by utilizing the Scholl reaction conditions. They demonstrated that the substrates bearing P=O are not suitable for dehydrogenative C-C coupling between arenes (Scheme 3.6a).[43] The author examined DDQ, $FeCl_3$ as oxidants for the synthesis of phosphorus embedded PAHs but instead of desired cyclized product, they observed over oxidation of the phosphole ring. Interestingly, the substrate bearing P=S, underwent partial dehydrogenative C-C coupling between a thiophene and phenyl ring in the presence of either $FeCl_3$ or $MoCl_5$ and thus, afforded mono-cyclized analogue of phosphine sulfide (Scheme 3.6b).[44] The starting material was remain unreacted and upon elongation of reaction time, decomposition of the starting precursor was

observed. Although the fully cyclized product was observed in the crude mass spectroscopy analysis, it could not be isolated.

Scheme 3.6. Attempts on synthesis of phosphorus embedded PAHs

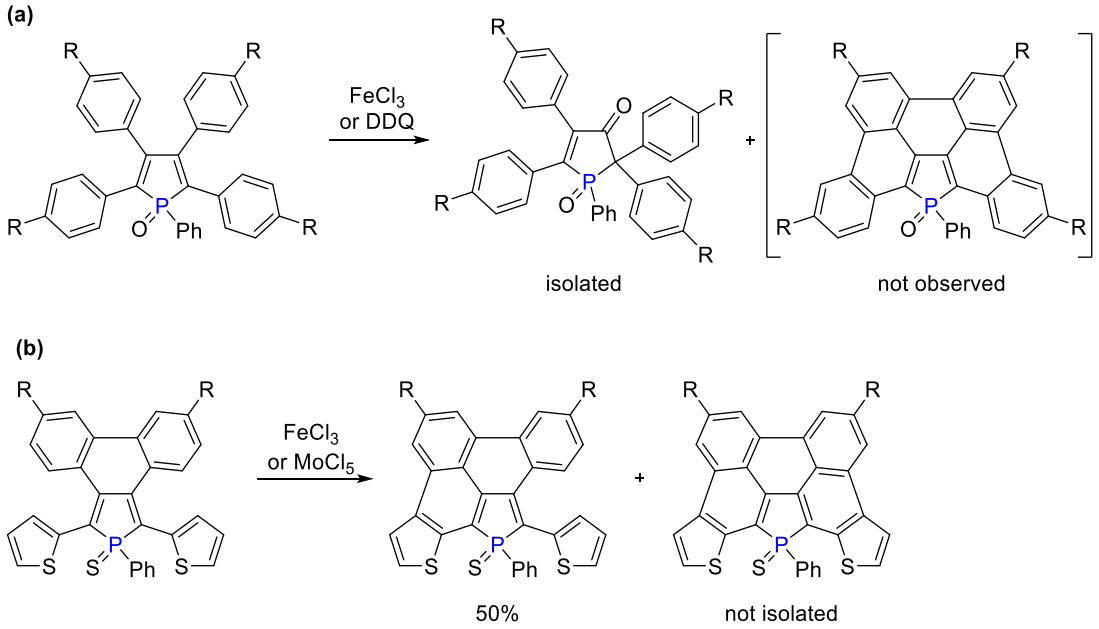

The phosphorus atom is itself versatile and highly reactive towards transition metals, chalcogenides, and other organic reagents and thus, provides an opportunity to tune the physico-chemical properties of phosphole containing conjugated π-systems. Over the last several years, a significant amount of work is dedicated towards phosphole containing π-systems because of its intriguing physical and chemical properties and promising applications in optical and electronic devices, sensing and imaging, asymmetric synthesis (*cf.* Chapter 1). In this context, our group reported a versatile synthesis of benzo- and naphtho[*b*]phosphole oxide derivatives by capitalizing on cobalt catalyzed, one-pot assembling of Grignard reagent, internal

alkyne and diorganophosphine chloride (*cf.* Chapter 1). Most of the thus-synthesized benzo- and naphtho[*b*]phosphole oxides showed strong luminescent properties and blue color emission. In contrast to phospholes with extended π-conjugation, triphenylene and related derivatives also find applications in organic field-effect transistors, solar cells, organic light emitting diodes, discotic liquid crystals, photo initiator, dye materials, molecular recognition and sensing. Thus, by clubbing the properties of phosphole oxide and triphenylene, we envisioned that phosphole oxide-fused triphenylenes would show unique optical and electronic properties. In addition, our continued interest to functionalize the benzo[*b*]phosphole oxide scaffolds prompted us to develop new molecules containing phosphorus atom in its polycyclic frame work. To synthesis phosphole-fused triphenylene derivatives, we envisaged that the Scholl reaction could be feasible for intramolecular dehydrogenative C-C coupling between arenes.[31, 36]

3.2 Results and Discussion

The present synthetic study of phosphole oxide-fused triphenylene derivatives commenced with the regioselective, one-pot preparation of 7-hydroxybenzo[*b*]phosphole oxide through sequential treatment of 3-(methoxymethoxy)phenylzinc reagent (**1**), 5-decyne (**2**) and $PhPCl_2$ (*cf.* Chapter 1).[45-46] The interception of intermediate *o*-alkenylarylzinc halide, which is generated via cobalt-catalyzed 1,4-migratory[47-49] reaction of 3-(methoxymethoxy)phenylzinc reagent (prepared from a 1:1 mixture of corresponding Grignard reagent and $ZnCl_2$•TMEDA) with $PhPCl_2$ in presence of CuCN•2LiCl, and then with H_2O_2, which resulted the desired compound **2.14** in 33% yield on a 5 mmol scale (*cf.* Chapter 2).[50] The triflation

of compound **2.14** worked smoothly and affording benzo[*b*]phosphole oxide 7-triflate **2.16** in 90% yield (*cf.* Chapter 2). The Suzuki-Miyaura coupling reaction of **2.16** with *o*-bromo-arylboronic acids, afforded 7-(2-bromophenyl)-benzo[*b*]phosphole oxide **3.26a** and 7-(3-bromonaphthalen-2-yl)-benzo[*b*]phosphole oxide **3.26b** in 73% and 65% yield respectively (Scheme 3.7)**.** The compound **3.26a** and **3.26b** were further subjected to Suzuki-Miyaura cross-coupling with arylboronic acid and thus, affording **3.27a**, **3.27b**, **3.27c**, and **3.27d** in 93%, 89%, 90% and 64% yields respectively (Scheme 3.7).

Scheme 3.7. Preparation of starting materials

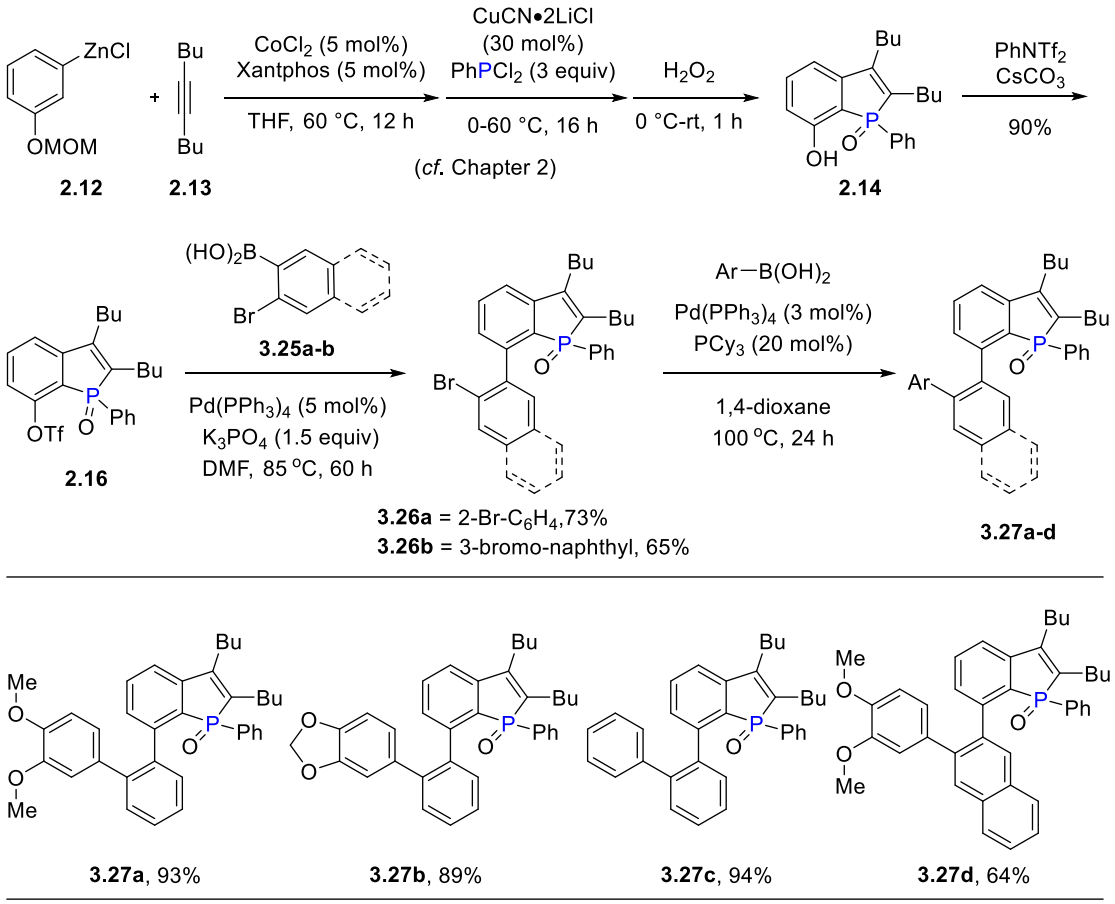

Next, we examined several oxidants for dehydrogenative cyclization of model compound **3.27a**. The reaction of **3.27a** in the presence of PIFA/BF_3•Et_2O in dichloromethane at -78 °C, afforded, after 12 h, the desired cyclized product **3.28a** in 59% yield (table 3.1, entry 1). The compound **3.28a** was crystallized from CH_2Cl_2 and the planar structure was unambiguously confirmed by single crystal X-ray analysis (Figure 3.2). Other oxidants such as $FeCl_3$, $SnCl_4$, $Cu(OTf)_2$, CuCN•2LiCl failed to promote the reaction and no product was observed. On the other hand, $AlCl_3$ at room temperature in dichloromethane, after 1 h, afforded the cyclized product in < 1% yield with low conversion of starting material and upon elongation of reaction time, the starting material was degraded and no improvement in yield was observed.

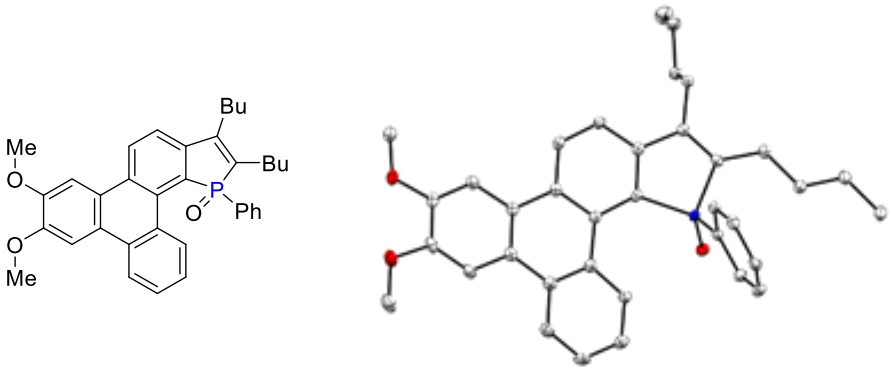

Figure 3.2. X-Ray analysis of **3.28a**. Thermal ellipsoids are shown at 50% probability.

Next, we explored substrate scope of phosphole oxide-fused triphenylenes. The oxidative cyclization of 7-(2-(benzo[*d*][1,3]dioxol-5-yl)phenyl)benzo[*b*]phosphole oxide **3.27b** in the presence of PIFA/BF_3•Et_2O at -78 °C, afforded in 58% yield (table

3.1, entry 2). Whereas, the unsubstituted biphenyl derivative, **3.27c** could not participated in the reaction (table 3.1, entry 3). This implies that the strong electron donating group favors dehydrogenative cyclization. (3-(3,4-Dimethoxyphenyl)naphthalen-2-yl)benzo[*b*]phosphole oxide **3.27d** took part in the cyclization reaction and thus, afforded the corresponding product **3.28d**, albeit with acceptable yield (table 3.1, entry 4).

Table 3.1. Synthesis of phosphole-embedded triphenylene derivatives[a]

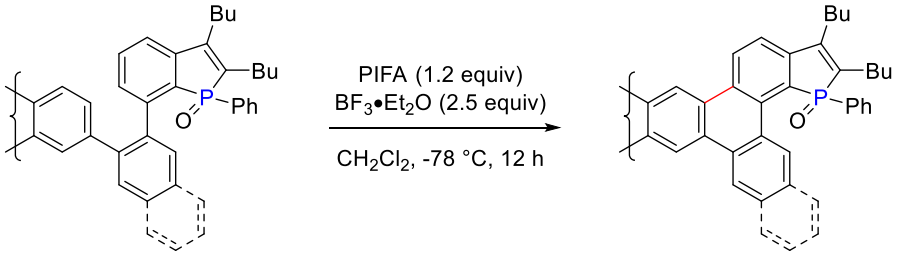

3.27a-d **3.28a-d**

Entry	Substrate	Product	Yield (%)[b]
1	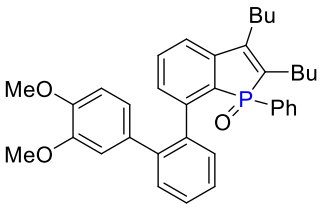 **3.27a**	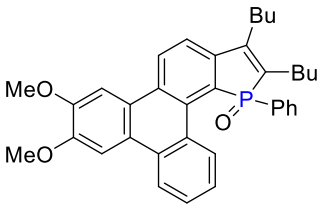 **3.28a**	59 (58)
2	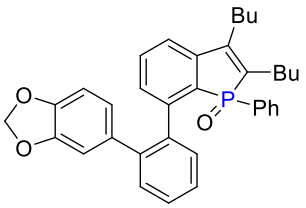 **3.27b**	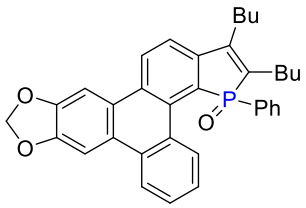 **3.28b**	56
3	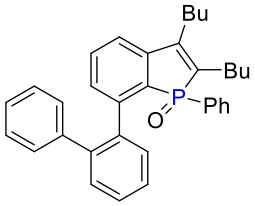 **3.27c**	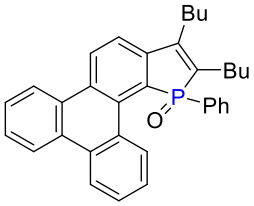 **3.28c**	0
4	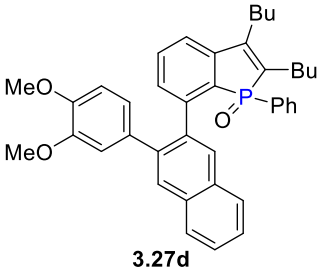 **3.27d**	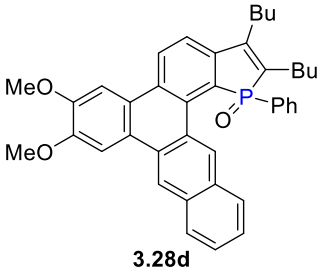 **3.28d**	40

[a] The reaction was performed on 0.1 mmol scale of **3.27a-d**. [b] Isolated yield and yield in parentheses on 0.5 mmol scale.

Having access of several phosphole oxide-fused triphenylene derivatives, next, we studied absorption and emission of the intermediates and final products. The UV-vis and fluorescent spectra of **2.14, 2.16, 3.26a**, and **3.27a** are shown in Figures 3.3 and 3.4 respectively. The absorption profile of 7-hydroxybenzo[*b*]phosphole oxide **2.14** was rather simple and showed maximum absorption wavelength (λ_{max}) 228 nm and 326 nm (shoulder). In contrast, the **2.14** is nonradiative in solution as well as under 365 nm UV-lamp. This is presumably due to close proximity of hydroxyl group and P=O that leads to intramolecular hydrogen bonding and weakly interaction of **2.14** with non-coordinating solvent, CH_2Cl_2.[51] On the other hand, benzo[*b*]phosphole oxide 7-triflate **2.16** showed absorption maxima λ_{max} at 229 nm and 327 nm (shoulder) and compound **3.26a** showed λ_{max} at 230 nm and 326 nm (shoulder). 7-(3',4'-Dimethoxy-[1,1'-biphenyl]-2-yl)benzo[*b*]phosphole oxide **3.27a** showed λ_{max} at 250 nm and 330 nm. However, 7-(2-bromophenyl)-benzo[*b*]phosphole oxide **3.26a** is nonradiative and presumably due to heavy atom effect. The maximum emission wavelength (λ_{em}) of compound **2.16** and **3.27a** is 388 nm and 390 nm respectively (Figure 3.4).

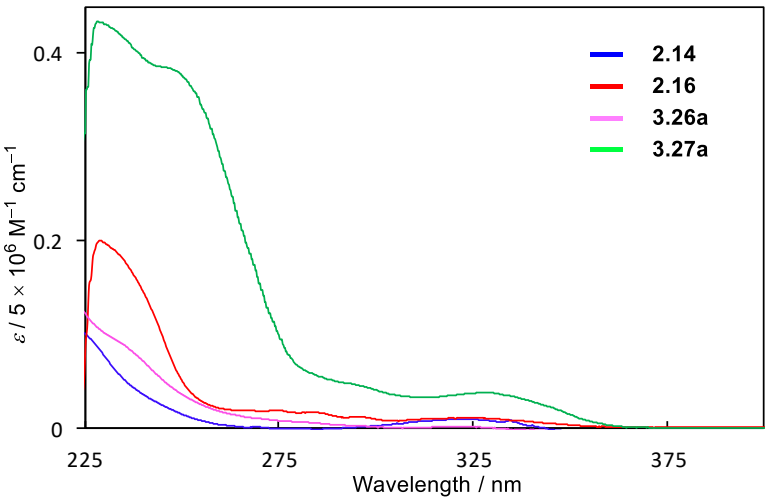

Figure 3.3. Absorption spectra of compound **2.14**, **2.16**, **3.26a**, and **3.27a** in CH_2Cl_2 (5×10^{-6} M)

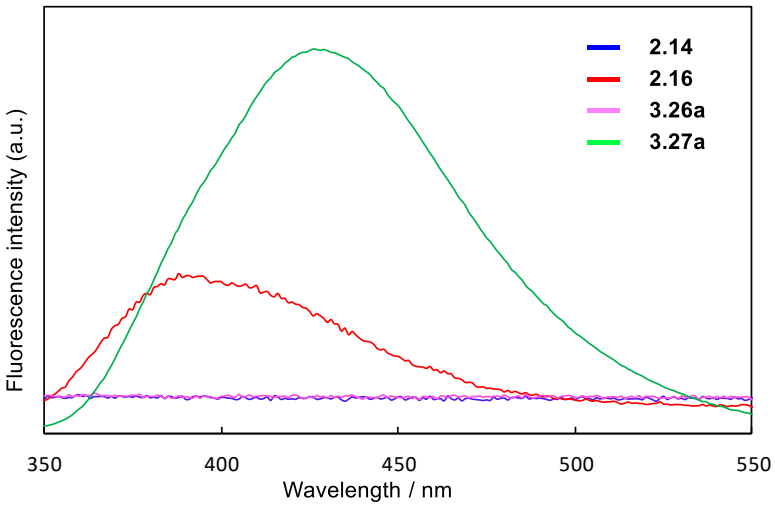

Figure 3.4. Fluorescence spectra of compound **2.14**, **2.16**, **3.26a, and 3.27a** in CH_2Cl_2 (5×10^{-6} M).

The absorption and emission spectra of the cyclized products **3.28a**, **3.28b**, and **3.28d** are shown in Figures 3.5, 3.6, and 3.7 respectively. The absorption profile **3.28a**, **3.28b**, and **3.28d** rather complex and showed λ_{max} at 330 nm, 323 nm, and 376 nm respectively in CH_2Cl_2. The absorption profile of compound **3.28a** in CH_2Cl_2 is broad and tailing with absorption maxima at 262 nm, 317 nm, and 330 nm. The absorption behavior of compound **3.28b** in CH_2Cl_2 is similar to that of compound **3.28a**. On the other hand, the absorption maxima of compound **3.28d** in CH_2Cl_2 appeared at 301 nm, 367 nm, and 377 nm. However, the phosphole-fused triphenylenes **3.28a**, **3.28b**, and **3.28d** are distinctively emissive in solution and

showed λ_{em} at 454 nm, 452 nm, and 480 nm respectively in CH_2Cl_2. The fluorescent quantum yield (Φ_F) of compounds **3.28a** and **3.28b** is 0.63 and 0.34 (reference with quinine sulfate) respectively. All the phosphole-fused triphenylene derivatives are emissive in solid state, with λ_{em} of 521 nm, 478 nm and 496 nm for compounds **3.28a**, **3.28b**, and **3.28d** respectively (Figure 3.8).

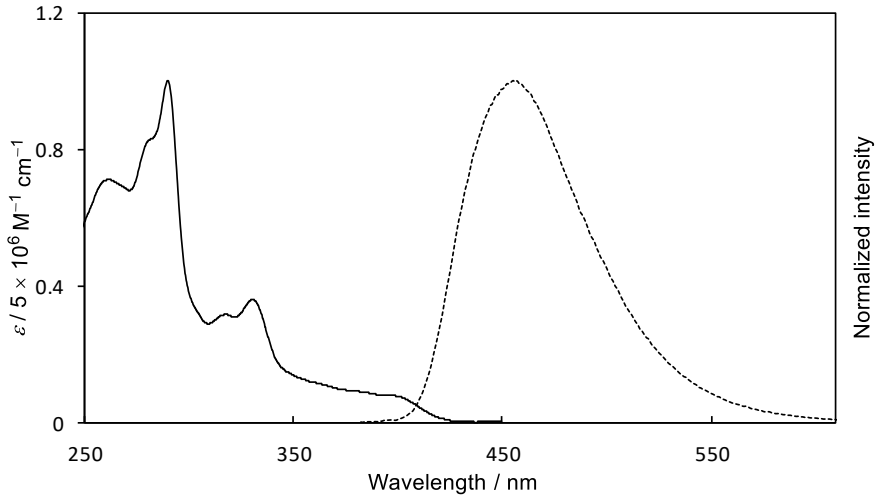

Figure 3.5. Absorption (solid line) and fluorescence (dashed line) spectra of compound **3.28a** in CH_2Cl_2 (5×10^{-6} M).

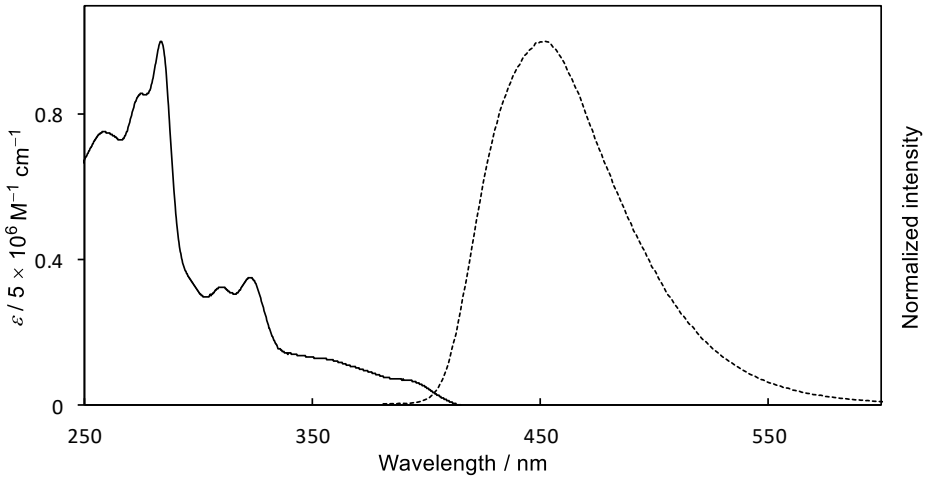

Figure 3.6. Absorption (solid line) and fluorescence (dashed line) spectra of compound **3.28b** in CH_2Cl_2 (5×10^{-6} M).

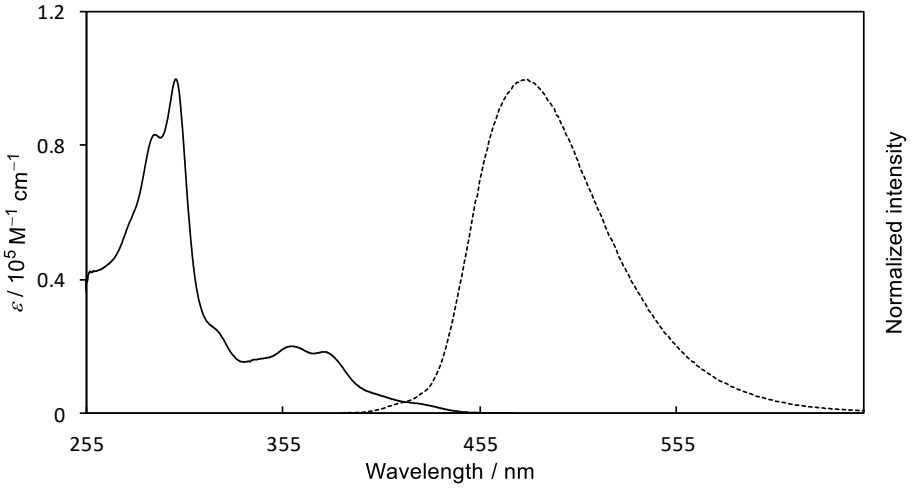

Figure 3.7. Absorption (solid line) and fluorescence (dashed line) spectra of compound **3.28d** in CH_2Cl_2 (1×10^{-5} M).

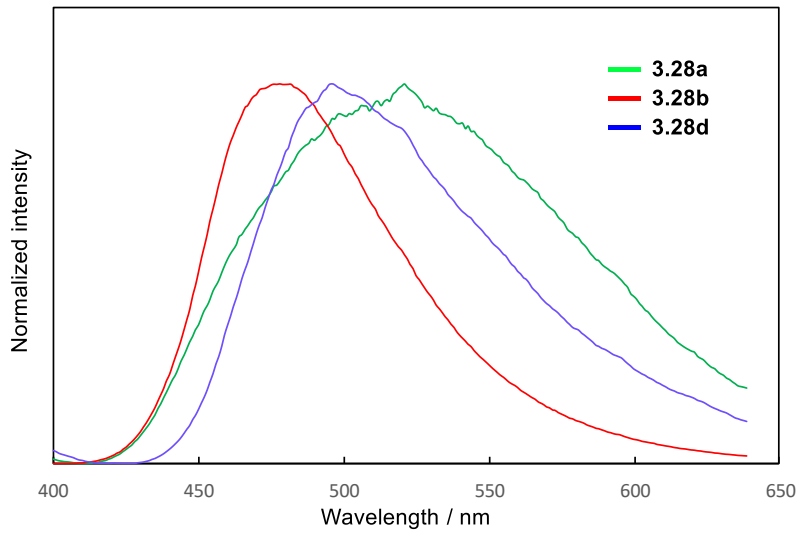

Figure 3.8. Fluorescence spectra of compound **3.28a**, **3.28b**, and **3.28d** in the thin film state.

We also studied the solvatochromism of compound **3.28d** in different solvents. The UV-vis absorption and fluorescent spectra of **3.28d** in different solvents are shown in Figures 3.9 and 3.10 respectively. The absorption profile of **3.28d** in CH_2Cl_2, $CHCl_3$, DMSO, and methanol is broad and tailing. The absorption maxima λ_{max} in $CHCl_3$ showed at 292 nm, 349 nm, and 368 nm. On the other hand, the absorption maxima λ_{max} in DMSO showed at 281 nm, 350 nm, and 367 nm and in MeOH, it showed at 279 nm, 350 nm, and 364 nm (shoulder). The emission wavelength of **3.28d** in $CHCl_3$ is comparable with that of DMSO (table 3.2, entries 2 and 3) and with fluorescent quantum yields (Φ_F) is 0.68 and 0.56 respectively. On the other hand, it showed highest absorption in CH_2Cl_2 (λ_{max} = 376 nm) (table 3.2, entry 1) and highest emission in highly polar solvent, methanol (λ_{em} = 490 nm) (table 3.2, entry 4). The Φ_F of **3.28d** in CH_2Cl_2 is 0.63 while in methanol is 0.34. The highest Stoke shifts were observed in polar protic solvent (table 3.2, entry 4).

Table 3.2. UV/Vis Absorption and Fluorescence of Compound **3.28d** in Different Solvents[a]

Entry	Solvent	λ_{abs} / nm[b]	ε / 10^4 M^{-1} cm^{-1}	λ_{em}[c] / nm	Φ_F[d]	$\Delta\nu$ / (cm^{-1})[e]
1	CH_2Cl_2	376	1.22	480	0.63	5762
2	$CHCl_3$	368	1.13	462	0.68	5529
3	DMSO	367	1.15	467	0.56	5835
4	MeOH	350	1.04	490	0.34	8162

[a] Absorption and emission spectra of **3.28d** in solvent (1×10^{-5} M). [b] Maximum absorption wavelength. [c] Excited at maximum λ_{abs}. [d] Fluorescence quantum yields determined using quinine sulfate as standard (0.1 M H_2SO_4). [e] Stokes shift ($1/\lambda_{abs} - 1/\lambda_{em}$).

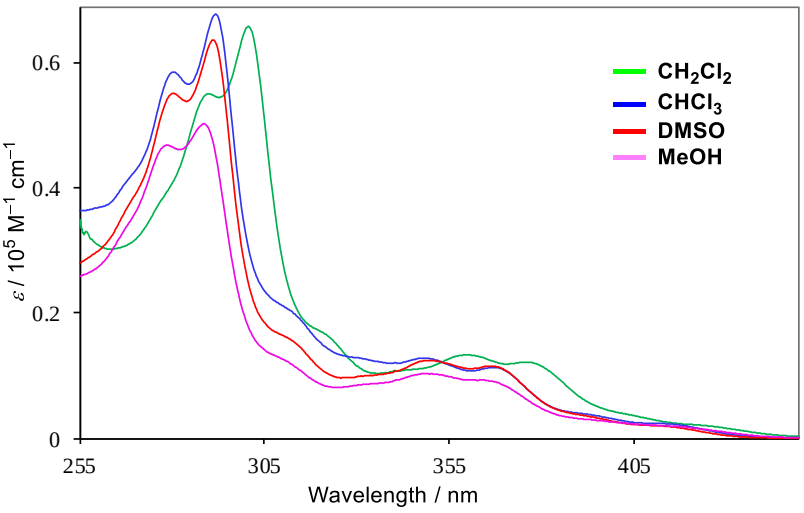

Figure 3.9. Absorption spectra of **3.28d** in different solvents (1×10^{-5} M).

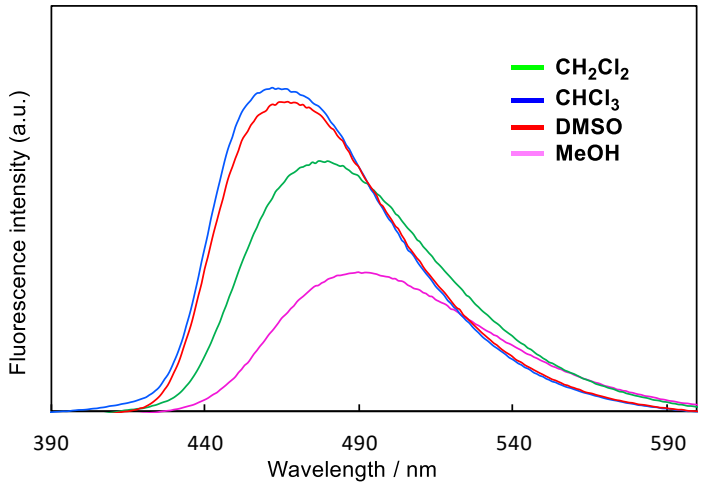

Figure 3.10. Emission spectra of **3.28d** in different solvents (1×10^{-5} M).

Next, the time-dependent density functional theory (TD-DFT) calculations were performed of compound **3.28d** with Gaussian 09 packages using the wB97XD density functional and the 6-311G* basis set on all other atoms in dichloromethane with the polarizable continuum model (PCM) (Figure 3.11). The S0-S1 transition of **3.28d** was appeared at 269 nm which is deviated from the experimental value.

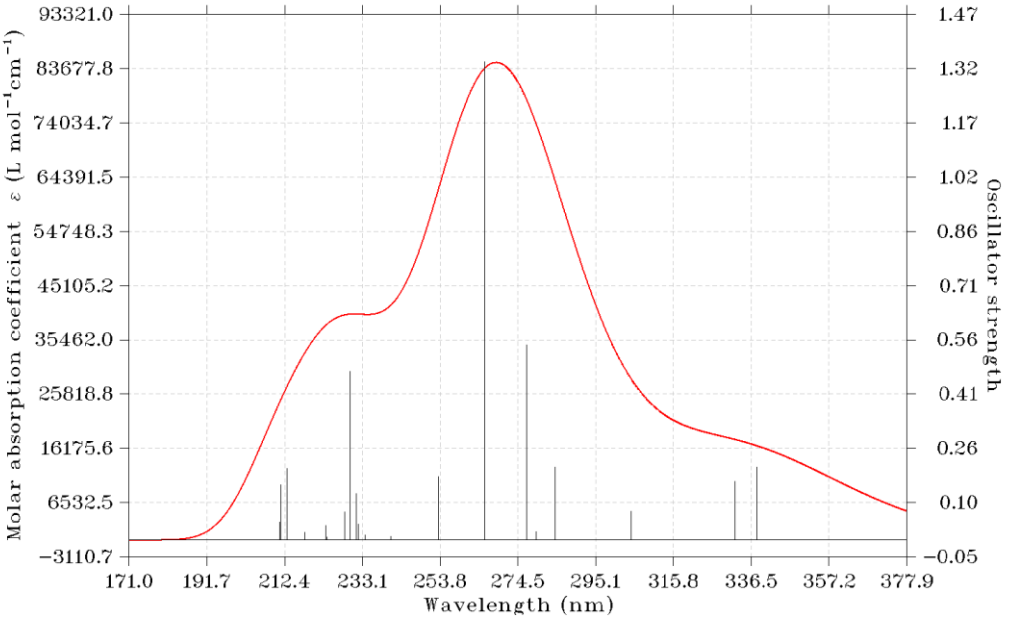

Figure 3.11. DT-DFT calculations spectra of **3.28d** in CH_2Cl_2.

3.3 Conclusion

In summary, we have synthesized new phosphole oxide-fuzed triphenylene derivatives by utilizing 7-hydroxybenzo[*b*]phosphole as key precursor, which can be accessed via low valent cobalt-catalyzed multi-component reaction of 3-(methoxymethoxy)phenylzinc reagent, 5-decyne and $PhPCl_2$. The X-ray analysis revealed planar structure of phosphole oxide-fused triphenylene. The precursor, 7-hydroxybenzo[*b*]phosphole showed weak emission presumably due to intramolecular hydrogen bonding between P=O and OH group. The final products showed strong emission compared to that of their corresponding intermediates, which suggests the influence of extended π-conjugations. Solvatochromism fluorescence demonstrated that phosphole-fused triphenylene molecules could be a potential candidate for

environment-sensitive fluorescent bioimaging probes. However, the substrate scope is narrow, and it requires electron donating substituents on benzene ring.

3.4 Experimental Section

Materials and Methods

General. All reactions dealing with air- or moisture-sensitive compound were performed by standard Schlenk techniques in oven-dried reaction vessels under nitrogen and argon atmosphere. Analytical thin-layer chromatography (TLC) was performed on Merck 60 F254 silica gel plates. Flash column chromatography was performed using 40-63 μm silica gel (Si 60, Merck). ^{1}H, ^{13}C and ^{31}P nuclear magnetic resonance (NMR) spectra were recorded on JEOL ECA-400 (400 MHz) or Bruker AV-400 (400 MHz) and AV-300 (300 MHz) NMR spectrometers. ^{1}H and ^{13}C NMR spectra are reported in parts per million (ppm) downfield from an internal standard, tetramethylsilane (0 ppm) and $CHCl_3$ (77.0 ppm), respectively. ^{31}P NMR spectra are referenced to an external reference (85% H_3PO_4, 0 ppm). High-resolution mass spectra (HRMS) were obtained with a Q-Tof Premier LC HR mass spectrometer. Melting points were determined using a capillary melting point apparatus and are uncorrected. UV-vis and fluorescence spectra were recorded on Shimadzu UV-1800 spectrophotometer and Shimadzu RF-5301PC spectrofluorophotometer, respectively.

Materials. Unless otherwise noted, commercial reagents were purchased from Alfa Aesar, Sigma Aldrich, TCI and other commercial suppliers and were used as received. Xantphos and $CoCl_2$ (anhydrous, 97%) were purchased from Alfa Aesar and was used

as received. $ZnCl_2$•TMEDA was prepared according to the literature procedures. Tetrahydrofuran (THF) and 1,4-dioxane was distilled over Na/benzophenone. Dichloromethane (DCM) was distilled over calcium hydride. Anhydrous dimethylformamide (DMF) was purchased from Sigma-Aldrich. 3-(Methoxymethoxy)phenylmagnesium bromide was prepared from the corresponding 3-(methoxymethoxy)phenyl bromide and magnesium turnings in anhydrous THF and titrated before use.

Preparation of bromo derivative of benzo[*b*]phosphole oxide

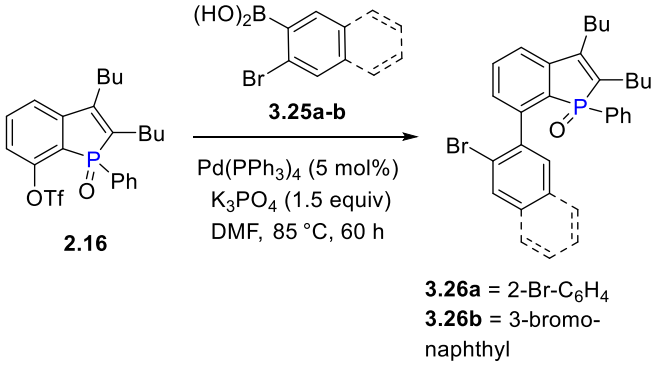

Typical procedure for the synthesis of bromo-derivatives: A 25 mL oven-dried Schlenk tube was charged with benzo[*b*]phosphole oxide 7-triflate **2.16** (0.97 g, 2.0 mmol), followed by DMF (6 mL) and then degassed through freeze-pump-thaw cycle. To this stirring solution, $Pd(PPh_3)_4$ (115.6 mg, 0.1 mmol), K_3PO_4 (0.64 g, 3.0 mmol), and 2-bromobenzene boronic acid (0.48 g, 2.4 mmol) were added sequentially. The resulting reaction mixture was kept stirring at 85 °C for 60 h and then allowed to cool down to ambient temperature. The reaction mixture was extracted with ethyl acetate (3 x 30 mL) and the combined organic layer was dried over $MgSO_4$, concentrated under

reduced pressure. The crude product was purified by silica gel chromatography (eluent: ethyl acetate/hexane = 1:2) to afford title compound.

7-(2-Bromophenyl)-2,3-dibutyl-1-phenylphosphindole 1-oxide (3.26a): The reaction was performed on 2.0 mmol scale and the title compound was afforded as colorless oil (0.72 g, 73%). ^{1}H NMR (400 MHz, $CDCl_3$, 298K): δ 7.68 (d, *J* = 7.7 Hz, 1H), 7.49 (t, *J* = 7.7 Hz, 1H), 7.42-7.35 (m, 3H), 7.28 (d, *J* = 8.2 Hz, 1H), 7.19-7.11 (m, 6H), 2.66 (t, *J* = 8.0 Hz, 2H), 2.56-2.44 (m, 1H), 2.32-2.21 (m, 1H), 1.67-1.60 (m, 2H), 1.57-1.48 (m, 2H), 1.45-1.36 (m, 2H), 1.31-1.25 (m, 2H), 1.02 (t, *J* = 7.2 Hz, 3H), 0.79 (t, *J* = 7.6 Hz, 3H); ^{13}C NMR (75 MHz, $CDCl_3$, 298 K): δ 150.8 (d, J_{PC} = 19.5 Hz), 143.6 (d, J_{PC} = 28.4 Hz), 143.2 (d, J_{PC} = 7.9 Hz), 138.2, 133.2, 132.2 (d, J_{PC} = 98.6 Hz), 131.8, 131.5, 131.0 (d, J_{PC} = 95.1 Hz), 130.5, 130.2, 128.7 (d, J_{PC} = 92.5 Hz), 128.3, 127.9, 126.7, 122.6, 120.6 (d, J_{PC} = 10.7 Hz), 30.8 (d, J_{PC} = 1.6 Hz), 30.7 (d, J_{PC} = 1.1 Hz), 26.4 (d, J_{PC} = 12.9 Hz), 26.1 (d, J_{PC} = 11.0 Hz), 23.2, 22.9, 14.0, 13.7; ^{31}P NMR (161 MHz, $CDCl_3$, 298 K): δ 39.5; HRMS (ESI) Calcd for $C_{28}H_{31}BrOP$ $[M + H]^+$ 493.1296, found 493.1286.

7-(3-Bromonaphthalen-2-yl)-2,3-dibutyl-1-phenylphosphindole 1-oxide (3.26b): The reaction was performed on 0.5 mmol scale and the title was afforded as colorless oil (182.6 mg, 65%). ^{1}H NMR (400 MHz, $CDCl_3$, 298K): δ 8.22 (s, 1H), 7.98 (app. doublet, *J* = 7.5 Hz, 1H), 7.80 (s, 1H), 7.69 (app. doublet, *J* = 7.2 Hz, 1H), 7.52 (t, *J* = 6.6 Hz, 3H), 7.40 (dd, *J* = 7.6, 2.3 Hz, 1H), 7.31 (app. d, *J* = 6.9 Hz, 1H), 7.05-6.98 (m, 4H), 2.68 (t, *J* = 7.8 Hz, 2H), 2.54-2.45 (m, 1H), 2.30-2.17 (m, 1H), 1.70-1.66 (m, 2H), 1.58-1.49 (m, 2H), 1.44-1.38 (m, 2H), 1.29-1.19 (m, 2H), 1.03 (t, *J* = 7.3 Hz, 3H), 0.78 (t, *J* = 7.2 Hz, 3H); ^{13}C NMR (100 MHz, $CDCl_3$, 298K): δ 150.8 (d, J_{PC} =

18.0 Hz), 143.7 (d, J_{PC} = 28.8 Hz), 143.1 (d, J_{PC} = 7.9 Hz), 135.0, 134.8 (d, J_{PC} = 115.0 Hz), 133.8, 133.3, 132.7, 131.7 (d, J_{PC} = 102.1 Hz),131.6, 131.5, 131.0 (d, J_{PC} = 11.1 Hz), 130.7, 130.4, 130.3, 128.9, 128.8, 128.1, 127.7 (d, J_{PC} = 102.5 Hz), 126.4 (d, J_{PC} = 35.6 Hz), 120.6 (d, J_{PC} = 10.9 Hz), 120.1, 30.9, 30.7, 26.5 (d, J_{PC} = 13.0 Hz), 26.1 (d, J_{PC} = 10.6 Hz), 23.2, 23.0, 14.0, 13.7; ^{31}P NMR (161 MHz, $CDCl_3$, 298 K): δ 39.8; HRMS (ESI) Calcd for $C_{32}H_{33}BrOP$ $[M + H]^+$ 543.1452, found 543.1463.

Preparation of (1,1'-biphenyl]-2-yl)-benzo[*b*]phosphole oxide

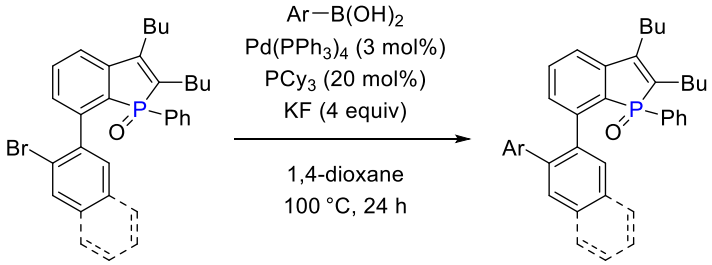

3.26a-b **3.27a-d**

Typical Procedure: In a 25 mL Schlenk tube, 7-(2-bromoaryl)-benzo[*b*]phosphole oxide, (0.3 mmol) was dissolved in 1,4-dioxane (2.0 mL) under N_2 atmosphere. Then $Pd_2(dba)_3$ (8.3 mg, 0.009 mmol), PCy_3 (16.9 mg, 0.06 mmol), KF (69.7 mg, 1.2 mmol), and arylboronic acid (0.36 mmol) were added sequentially. The resulting reaction mixture was kept stirring at 100 °C for 24 h. The reaction mixture was allowed to cool down to room temperature, extracted with ethyl acetate (3 x 20 mL). The combined organic layers were dried over $MgSO_4$, concentrated under reduced pressure, purified by silica gel chromatography (eluent: ethyl acetate/hexane = 1:2) to afford corresponding compounds. The ^{1}H NMR spectrum of the compounds **3.27a-d** showed no splitting in $CDCl_3$ at room temperature and appeared as singlets (broad singlets). This is presumably due to the C-C free rotation between aryl groups. The ^{1}H

NMR spectra of **3.27a**, **3.27b**, and **3.27d** are shown in Figure **3.12**, **3.13**, and **3.14** respectively.

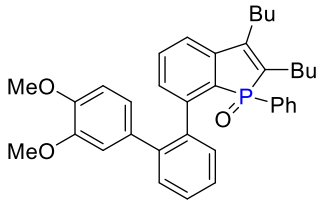

2,3-Dibutyl-7-(3',4'-dimethoxy-[1,1'-biphenyl]-2-yl)-1-phenylphosphindole 1-oxide (3.27a): The reaction was performed on 1.0 mmol scale and title compound was afforded as a colorless oil (0.51 g, 93%). ^{1}H NMR (400 MHz, $CDCl_3$, 298K): δ 8.04 (bs, 1H), 7.52-7.36 (m, 5H), 7.19-7.12 (m, 5H), 6.73-6.57 (m, 2H), 5.96 (bs, 1H), 5.66 (bs, 1H), 3.79 (s, 3H), 3.35 (s, 3H), 2.67 (app. bs, 3H), 2.33-2.31 (m, 1H), 1.77-1.59 (m, 3H), 1.56-1.47 (m, 3H), 1.42-1.25 (m, 2H), 1.02 (t, J = 7.2 Hz, 3H), 0.83 (app. triplet, J = 7.2 Hz, 3H); ^{13}C NMR (100 MHz, $CDCl_3$, 298K): δ 147.7 (d, J_{PC} = 30.3 Hz), 144.5 (d, J_{PC} = 8.1 Hz), 133.7, 133.4, 131.8, 131.3, 131.0 (d, J_{PC} = 107.3 Hz), 130.5, 129.0 (d, J_{PC} = 124.3 Hz), 128.5, 121.7, 119.7 (d, J_{PC} = 11.1 Hz), 112.8, 110.3, 55.8, 55.7, 31.0, 30.9 (d, J_{PC} = 1.5 Hz), 26.5, 26.4, 23.2, 23.1, 14.0, 13.7; ^{31}P NMR (161 MHz, $CDCl_3$, 298 K): δ 40.3; HRMS (ESI) Calcd for $C_{36}H_{40}O_3P$ $[M + H]^+$ 551.2715, found 551.2709.

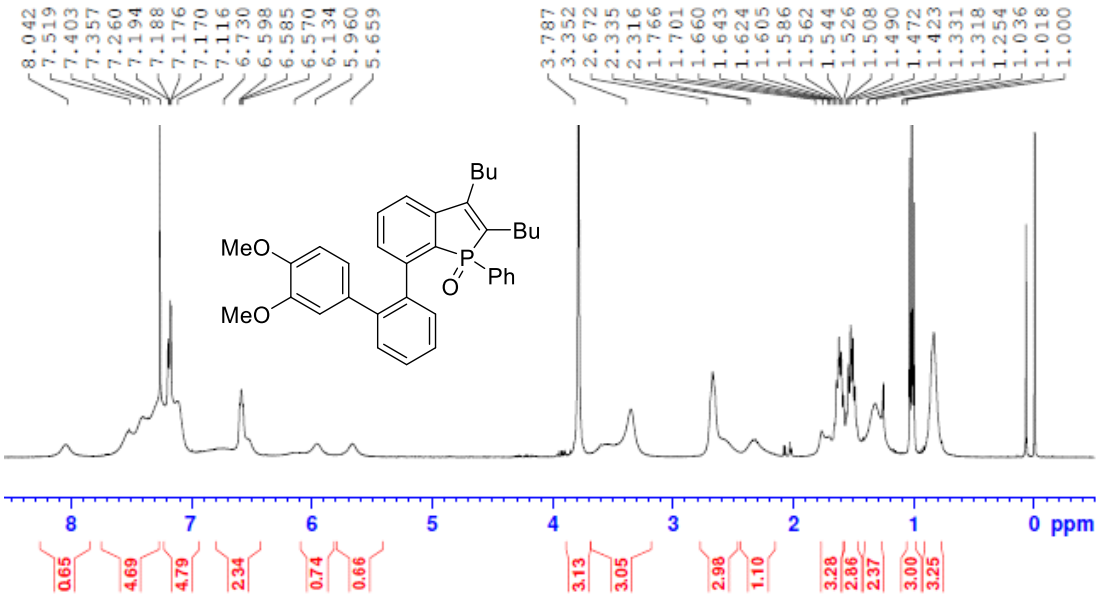

Figure 3.12. ^{1}H NMR spectra of compound **3.27a** in $CDCl_3$.

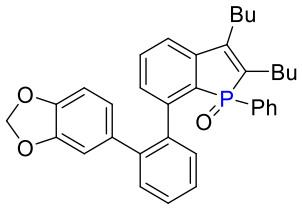

7-(2-(Benzo[*d*][1,3]dioxol-5-yl)phenyl)-2,3-dibutyl-1-phenylphosphindole 1-oxide (3.27b): The reaction was performed on 0.3 mmol scale. The title compound was afforded as colorless oil (143 mg, 89%). ^{1}H NMR (400 MHz, $CDCl_3$, 298K): δ 7.95 (bs, 1H), 7.52-7.32 (m, 4H), 7.20-7.12 (m, 5H), 6.62 (dd, J = 7.3, 2.3 Hz, 1H), 6.40 (bs, 1H), 5.82 (s, 2H), 5.64 (app. singlet, 1H), 5.56 (app. singlet, 1H), 2.67 (t, *J* = 5.5 Hz, 2H), 2.61-2.57 (m, 1H), 2.34 (app. bs,1), 1.75-1.61 (m, 3H), 1.57-1.49 (m, 3H), 1.39-1.26 (m, 2H), 1.02 (t, *J* = 7.2 Hz, 3H), 0.83 (t, *J* = 7.3 Hz, 3H); ^{13}C NMR (100 MHz, $CDCl_3$, 298K): δ 146.4 (d, J_{PC} = 83.1 Hz), 144.3 (d, J_{PC} = 8.1 Hz), 140.1, 136.5, 135.1, 131.7, 131.4 (d, J_{PC} = 101.4 Hz), 131.3, 131.2 (d, J_{PC} = 112.0 Hz), 130.9 (d, J_{PC} = 84.1 Hz), 129.7, 128.4 (d, J_{PC} = 12.1 Hz), 128.2, 126.6 (d, J_{PC} = 4.1 Hz),

122.8, 119.7 (d, J_{PC} = 10.8 Hz), 109.7, 107.4, 100.7, 31.0 (d, J_{PC} = 1.6 Hz), 30.8 (d, J_{PC} = 1.6 Hz), 26.5 (d, J_{PC} = 13.2 Hz), 26.2 (d, J_{PC} = 10.7 Hz), 23.2, 23.1, 14.0, 13.7; ^{31}P NMR (161 MHz, $CDCl_3$, 298 K): δ 39.9; HRMS (ESI) Calcd for $C_{35}H_{36}O_3P$ [M + H]$^+$ 535.2402, found 535.2399.

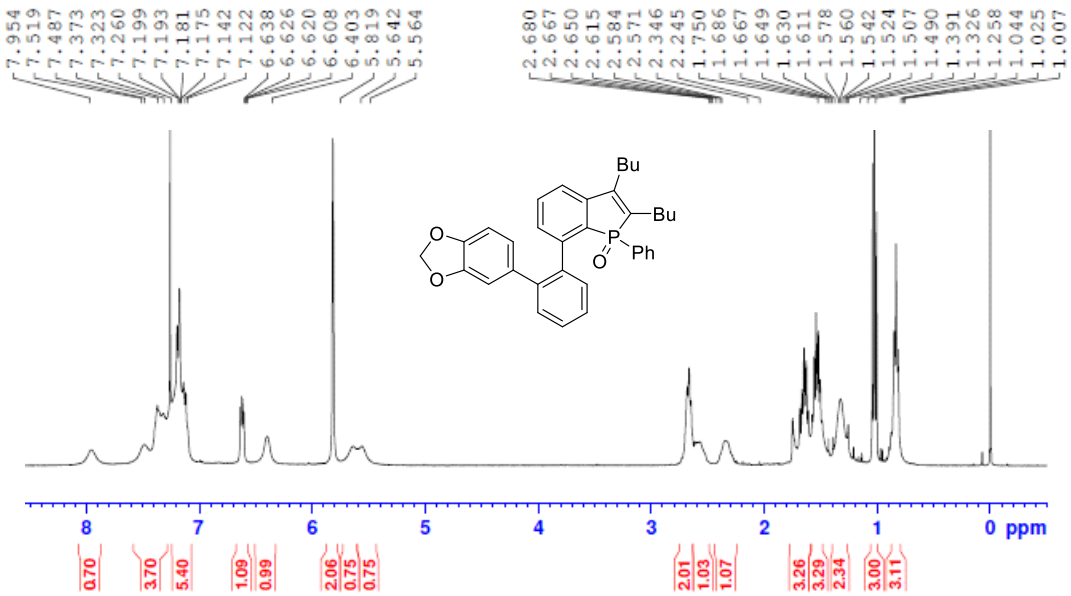

Figure 3.13. ^{1}H NMR spectra of compound **3.27b** in $CDCl_3$.

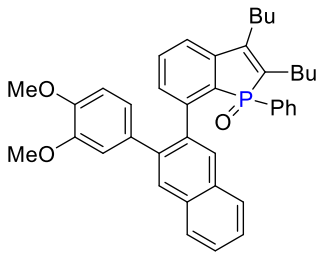

2,3-Dibutyl-7-(3-(3,4-dimethoxyphenyl)naphthalen-2-yl)-1-phenylphosphindole 1-oxide (3.27d): The reaction was performed on 0.3 mmol scale. The title compound was afforded as colorless oil (115 mg, 64%). ^{1}H NMR (400 MHz, $CDCl_3$, 298K): δ 8.6 (app. bs, 1H), 7.84-7.72 (m, 2H), 7.52-7.50 (m, 4H), 7.22-6.76 (m, 6H), 6.61 (dd, *J* = 7.4, 2.6 Hz, 2H), 6.07 (app. bs, 1H), 5.76 (app. bs, 1H), 3.83 (s, 3H), 3.50 (app.

doublet, 3H), 2.69 (app. bs, 2H), 2.56 (app. bs, 1H), 2.29 (app. bs, 1H), 1.68-1.58 (m, 4H), 1.56-1.49 (m, 2H), 1.30-1.27 (m, 2H), 1.03 (t, J = 7.2 Hz, 3H), 0.84 (app. triplet, J = 6.6 Hz, 3H); ^{13}C NMR (100 MHz, $CDCl_3$, 298K): δ 147.8 (d, J_{PC} = 30.0 Hz), 144.5 (d, J_{PC} = 2.0 Hz), 133.9, 133.1, 131.8, 128.4, 127.5, 126.7, 126.3, 121.4, 119.8 (d, J_{PC} = 11.0 Hz), 110.4, 56.0, 55.8, 31.0, 30.9, 26.6, 26.5, 23.2, 23.0, 14.1, 13.8; ^{31}P NMR (161 MHz, $CDCl_3$, 298 K): δ 41.4, 39.1; HRMS (ESI) Calcd for $C_{40}H_{42}O_3P$ [M + H]$^+$ 601.2872, found 601.2878.

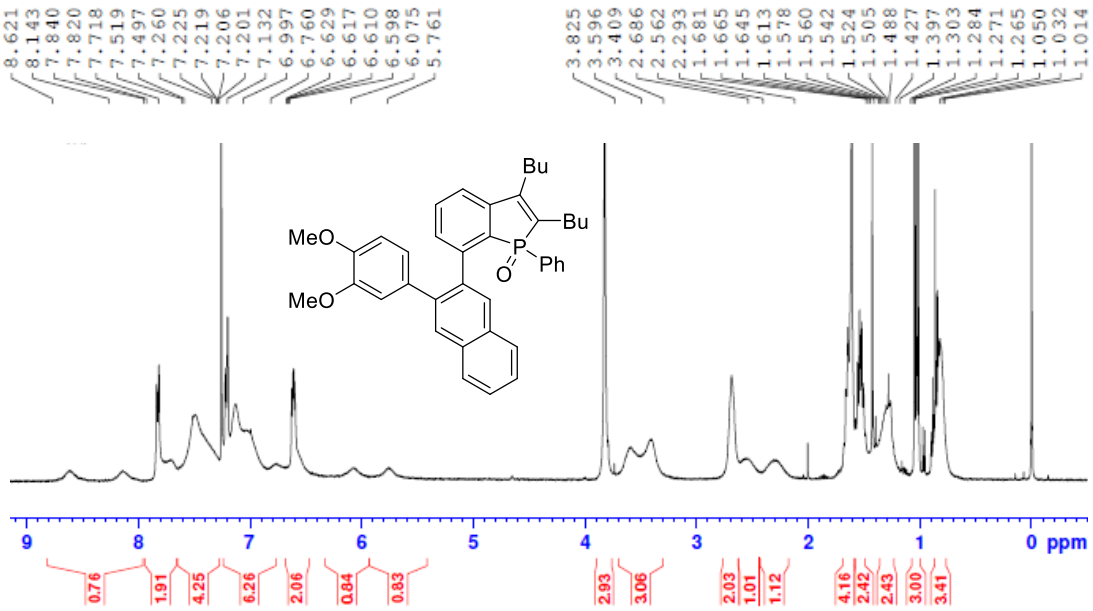

Figure 3.14. ^{1}H NMR spectra of compound **3.27d** in $CDCl_3$.

Preparation of phosphole oxide-fused triphenylenes via dehydrogenative C-C coupling

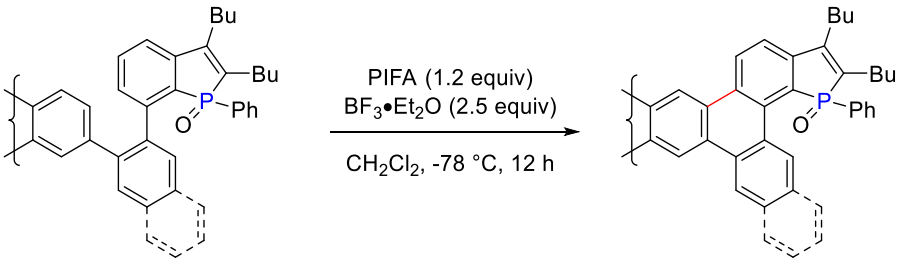

3.27a-d **3.28a-d**

Typical procedure: To a solution of **3.27a-d** (0.1 mmol) in CH_2Cl_2 (1.0 mL) was added PIFA (0.11 mmol) and BF_3•Et_2O (0.25 mmol) in a dropwise manner at -78 °C under argon. The resulting reaction mixture was kept stirring at that temperature for 12 h and then quenched with NH_4Cl. The reaction mixture was extracted with ethyl acetate (3 x 10 mL). The combined organic layers were dried over $MgSO_4$ and concentrated under reduced pressure. The crude product was purified by silica gel chromatography (eluent: ethyl acetate/hexane = 2/3) to afford the corresponding cyclized products. Unlike of the intermediates **3.27a-d**, the ^{1}H NMR spectra of the cyclized compounds **3.28a-b**, and **3.28d** showed splitting in $CDCl_3$ at room temperature. ^{1}H NMR spectra of compounds **3.28a**, **3.28b**, and **3.28d** are shown in Figures 3.15, 3.16, and 3.17 respectively.

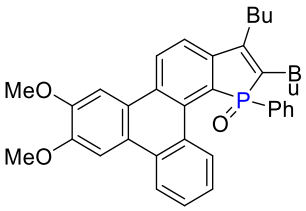

7,8-Dibutyl-2,3-dimethoxy-9-phenylphenanthro[9,10-g]phosphindole 9-oxide (3.28a): The title compound was afforded as light yellow solid (32.5 mg, 59%); m.p. 184-186 °C; ^{1}H NMR (400 MHz, $CDCl_3$, 298K): δ 9.93-9.90 (m, 1H), 8.69 (d, *J* = 8.2 Hz, 1 H), 8.30 (dd, *J* = 6.8, 2.8 Hz, 1H), 7.88 (s, 1H), 7.84 (s, 1H), 7.69 (dd, *J* = 8.5,

2.4 Hz, 1H), 7.58-7.52 (m, 4H), 7.30-7.27 (m, 1H), 7.20-7.15 (m, 2H), 4.09 (s, 3H), 4.06 (s, 3H), 2.73 (t, *J* = 7.7 Hz, 2H), 2.64-2.53 (m, 1H), 2.40-2.29 (m, 1H), 1.71-1.64 (m, 2H), 1.48-1.33 (m, 2H), 1.32-1.21 (m, 2H), 1.03 (t, *J* = 7.3 Hz, 3H), 0.80 (t, *J* = 7.2 Hz, 3H); ^{13}C NMR (100 MHz, $CDCl_3$, 298K): δ 149.6 (d, J_{PC} = 35.5 Hz), 148.8 (d, J_{PC} = 20.0 Hz), 144.4 (d, J_{PC} = 28.9 Hz), 133.9 (d, J_{PC} = 109.2 Hz), 133.4, 131.5 (d, J_{PC} = 2.8 Hz), 131.1, 131.0, 130.7 (d, J_{PC} = 8.5 Hz), 130.3, 129.95 (d, J_{PC} = 94.1 Hz), 129.94, 128.7 (d, J_{PC} = 1.4 Hz), 128.4, 128.2, 128.1, 128.0 (d, J_{PC} = 95.7 Hz), 127.98, 126.2, 124.6, 123.9, 122.0, 120.2 (d, J_{PC} = 12.7 Hz), 104.5 (d, J_{PC} = 44.6 Hz), 56.00, 55.97, 30.9, 30.8, 26.4 (d, J_{PC} = 13.7 Hz), 26.0 (d, J_{PC} = 11.7 Hz), 23.1, 22.9, 14.0, 13.7; ^{31}P NMR (161 MHz, $CDCl_3$, 298 K): δ 45.3; HRMS (ESI) Calcd for $C_{36}H_{38}O_3P$ $[M + H]^+$ 549.2559, found 549.2562.

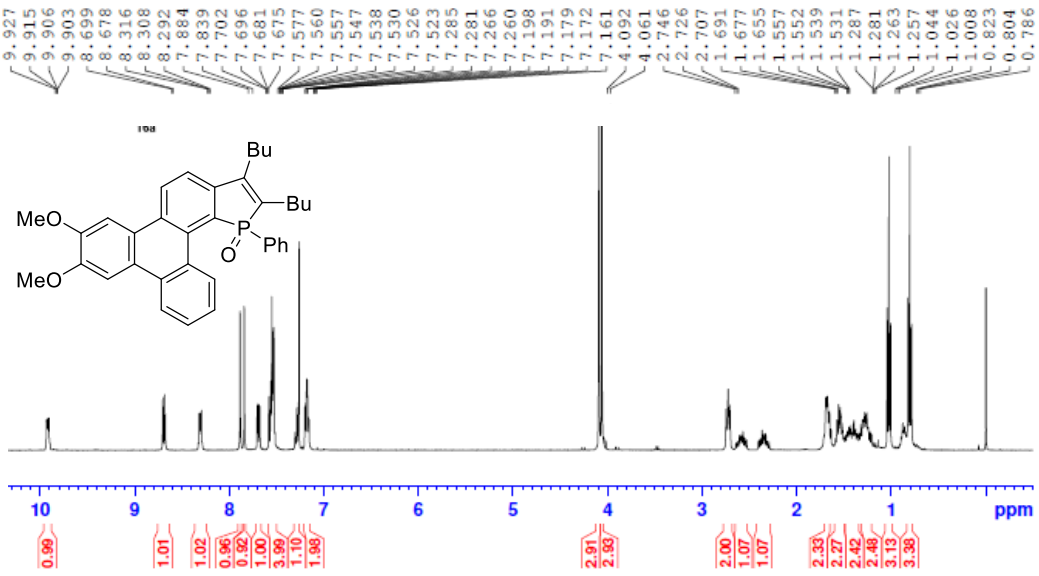

Figure 3.15. ^{1}H NMR spectra of compound **3.28a** in $CDCl_3$.

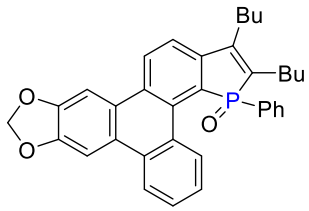

1,2-Dibutyl-3-phenylphospholo[3',2':7,8]triphenyleno[2,3-d][1,3]dioxole 3-oxide (3.28b): The title compound was afforded as light yellow solid (29.8 mg, 56%); m.p. 178-181.3 °C; ^{1}H NMR (400 MHz, $CDCl_3$, 298K): δ 9.90 (d, *J* = 8.0 Hz, 1H), 8.61 (d, *J* = 8.4 Hz, 1H), 8.23 (dd, *J* = 7.0, 2.4 Hz, 1H), 7.89 (s, 1H), 7.84 (s, 1H), 7.66 (dd, *J* = 8.5, 2.3 Hz, 1H), 7.58-7.49 (m, 4H), 7.29 (dd, *J* = 7.4, 1.2 Hz, 1H), 7.20-7.15 (m, 2H), 6.07 (s, 2H), 2.72 (t, *J* = 7.6 Hz, 2H), 2.64-2.52 (m, 1H), 2.40-2.29 (m, 1H), 1.71-1.63 (m, 2H), 1.54-1.50 (m, 2H), 1.47-1.35 (m, 2H), 1.32-1.24 (m, 2H), 1.02 (t, *J* = 7.3 Hz, 3H), 0.80 (t, *J* = 7.3 Hz, 3H); ^{13}C NMR (100 MHz, $CDCl_3$, 298K): δ 148.7 (d, J_{PC} = 19.8 Hz), 148.4 (d, J_{PC} = 23.4 Hz), 134.0 (d, J_{PC} = 102.2 Hz), 133.3 (d, J_{PC} = 7.1 Hz), 131.5 (d, J_{PC} = 3.1 Hz), 131.1, 131.0, 130.8, 130.5, 129.9 (d, J_{PC} = 94.3 Hz), 129.8, 128.6 (d, J_{PC} = 1.6 Hz), 128.4, 128.3, 128.1, 128.0 (d, J_{PC} = 95.9 Hz), 126.3, 126.2, 125.5 (d, J_{PC} = 1.5 Hz), 122.2, 120.2 (d, J_{PC} = 12.8 Hz), 102.1, 101.7 (d, J_{PC} = 23.1 Hz), 30.9 (d, J_{PC} = 1.4 Hz), 30.7 (d, J_{PC} = 2.2 Hz), 26.4 (d, J_{PC} = 13.5 Hz), 26.0 (d, J_{PC} = 11.4 Hz), 23.1, 22.9, 14.0, 13.7; ^{31}P NMR (161 MHz, $CDCl_3$, 298 K): δ 45.3; HRMS (ESI) Calcd for $C_{35}H_{34}O_3P$ $[M + H]^+$ 533.2246, found 533.2249.

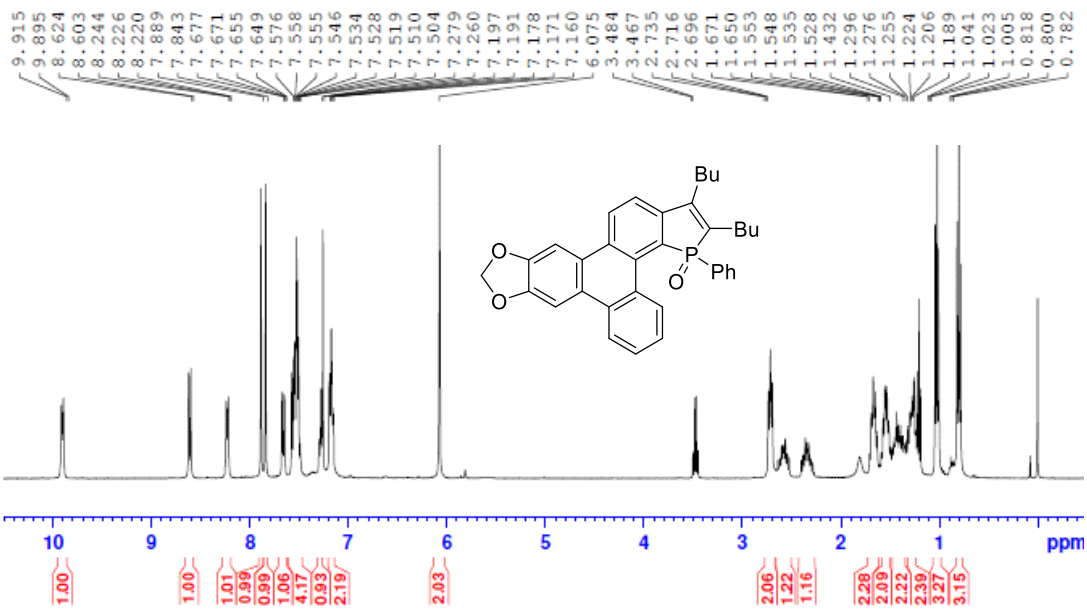

Figure 3.16. ^{1}H NMR spectra of compound **3.28b** in $CDCl_3$.

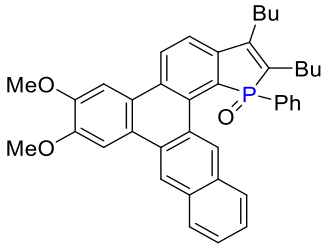

2,3-Dibutyl-7,8-dimethoxy-1-phenyltetrapheno[5,6-g]phosphindole 1-oxide (3.28d): The title compound was afforded as light yellow solid (23.9 mg, 40%); m.p. 192-194 °C; ^{1}H NMR (300 MHz, $CDCl_3$, 298K): δ 10.51 (s, 1H), 8.65 (s, 1H), 8.57 (d, *J* = 8.5 Hz, 1H), 8.29 (dd, *J* = 6.2, 3.2 Hz, 1H), 7.96-7.93 (m, 2H), 7.79 (s, 1H), 7.67-7.50 (m, 5H), 7.18 (t, *J* = 7.1 Hz, 1H), 7.11-7.07 (m, 2H), 4.10 (s, 3H), 4.07 (s, 3H), 2.73 (t, *J* = 7.4 Hz, 2H), 2.67-2.54 (m, 1H), 2.44-2.35 (m, 1H), 1.71-1-64 (m, 2H), 1.59-1.40 (m, 4H), 1.33-1.25 (m, 2H), 1.03 (t, *J* = 7.2 Hz, 3H), 0.81 (t, *J* = 7.2 Hz, 3H); ^{13}C NMR (100 MHz, $CDCl_3$, 298K): δ 149.8 (d, J_{PC} = 29.0 Hz), 149.2 (d, J_{PC} = 20.0 Hz), 144.4 (d, J_{PC} = 29.0 Hz), 134.4, 133.8 (d, J_{PC} = 96.0 Hz), 132.5, 131.7, 131.6 (d, J_{PC} = 3.0 Hz), 131.3, 131.0, 130.9, 130.7 (d, J_{PC} = 102.0 Hz), 129.7, 129.3, 129.2,

128.6, 128.5 (d, J_{PC} = 97.0 Hz), 128.4, 128.3, 127.9, 127.3, 127.2 (d, J_{PC} = 2.0 Hz), 126.8, 125.6, 124.8, 123.9 (d, J_{PC} = 2.0 Hz), 120.5 (d, J_{PC} = 12.0 Hz), 120.3, 105.1 (d, J_{PC} = 27.0 Hz), 56.2, 56.1, 31.2, 30.9 (d, J_{PC} = 2.0 Hz), 26.5 (d, J_{PC} = 14.0 Hz), 26.1 (d, J_{PC} = 12.0 Hz), 23.2, 23.0, 14.1, 13.8; ^{31}P NMR (161 MHz, $CDCl_3$, 298 K): δ 46.0; HRMS (ESI) Calcd for $C_{40}H_{40}O_3P$ $[M + H]^+$ 599.2715, found 599.2721.

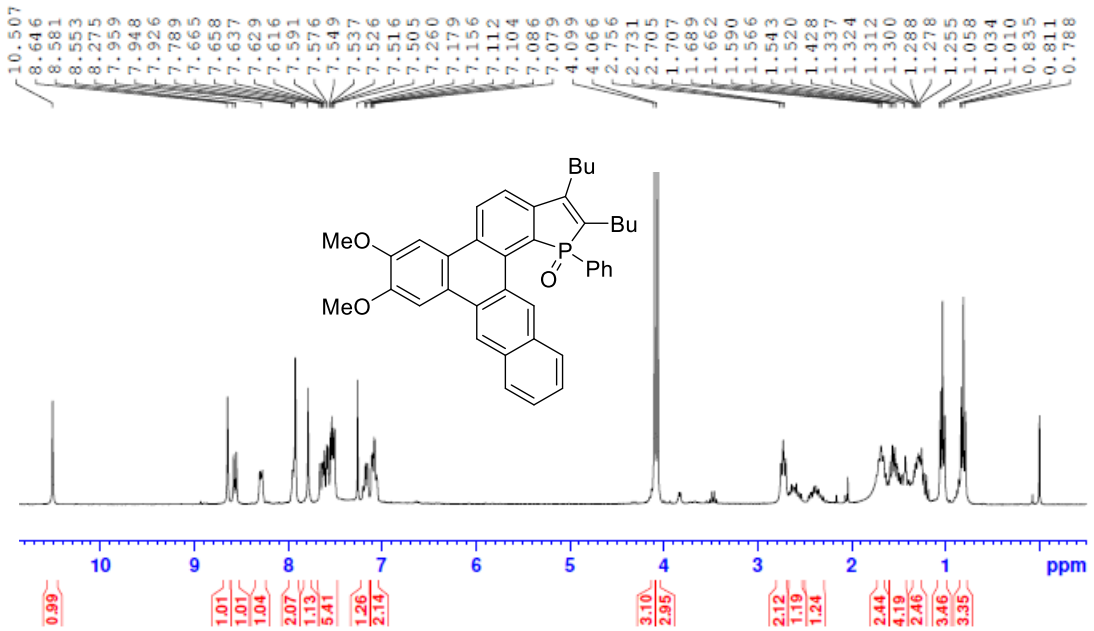

Figure 3.17. ^{1}H NMR spectra of compound **3.28d** in $CDCl_3$.

3.5 References

1. Baumgartner, T.; Réau, R. *Chem. Rev.* **2006**, *106*, 4681.

2. Hibner-Kulicka, P.; Joule, J. A.; Skalik, J.; Bałczewski, P. *RSC Adv.* **2017**, *7*, 9194.

3. Duffy, M. P.; Delaunay, W.; Bouit, P. A.; Hissler, M. *Chem. Soc. Rev.* **2016**, *45*, 5296.

4. Baumgartner, T. *Acc. Chem. Res.* **2014**, *47*, 1613.

5. Wu, B.; Yoshikai, N. *Org. Biomol. Chem.* **2016**, *14*, 5402.

6. Hobbs, M. G.; Baumgartner, T. *Eur. J. Inorg. Chem.* **2007**, *2007*, 3611.

7. Matano, Y.; Imahori, H. *Org. Biomol. Chem.* **2009**, *7*, 1258.

8. Yavari, K.; Delaunay, W.; De Rycke, N.; Reynaldo, T.; Aillard, P.; Srebro-Hooper, M.; Chang, V. Y.; Muller, G.; Tondelier, D.; Geffroy, B.; Voituriez, A.; Marinetti, A.; Hissler, M.; Crassous, J. *Chem. Eur. J.* **2019**, *25*, 5303.

9. Shameem, M. A.; Orthaber, A. *Chem. Eur. J.* **2016**, *22*, 10718.

10. Ren, Y.; Baumgartner, T. *Dalton Trans.* **2012**, *41*, 7792.

11. Tsuji, H.; Sato, K.; Sato, Y.; Nakamura, E. *J. Mat. Chem.* **2009**, *19*, 3364.

12. Tsuji, H.; Sato, K.; Sato, Y.; Nakamura, E. *Chem. Asian J.* **2010**, *5*, 1294.

13. Demmer, C. S.; Voituriez, A.; Marinetti, A. *C. R. Chem.* **2017**, *20*, 860.

14. Yamaguchi, E.; Wang, C.; Fukazawa, A.; Taki, M.; Sato, Y.; Sasaki, T.; Ueda, M.; Sasaki, N.; Higashiyama, T.; Yamaguchi, S. *Angew. Chem. Int. Ed.* **2015**, *54*, 4539.

15. Wang, C.; Taki, M.; Sato, Y.; Fukazawa, A.; Higashiyama, T.; Yamaguchi, S. *J. Am. Chem. Soc.* **2017**, *139*, 10374.

16. Pérez, D.; Guitián, E. *Chem. Soc. Rev.* **2004**, *33*, 274.

17. Zelcer, A.; Donnio, B.; Bourgogne, C.; Cukiernik, F. D.; Guillon, D. *Chem. Mat.* **2007**, *19*, 1992.

18. Chandrasekhar, S. *Liq. Crystals* **1993**, *14*, 3.

19. Watson, M. D.; Fechtenkötter, A.; Müllen, K. *Chem. Rev.* **2001**, *101*, 1267.

20. Bhalla, V.; Singh, H.; Kumar, M.; Prasad, S. K. *Langmuir* **2011**, *27*, 15275.

21. Kumar, S. *Chem. Soc. Rev.* **2006**, *35*, 83.

22. Sergeyev, S.; Pisula, W.; Geerts, Y. H. *Chem. Soc. Rev.* **2007**, *36*, 1902.

23. Boden, N.; Bushby, R. J.; Martin, P. S.; Evans, S. D.; Owens, R. W.; Smith, D. A. *Langmuir* **1999**, *15*, 3790.

24. Bengs, H.; Closs, F.; Frey, T.; Funhoff, D.; Ringsdorf, H.; Siemensmeyer, K. *Liq. Crystals* **1993**, *15*, 565.

25. Emerich, M.; Tasch, S.; Resel, R.; Leising, G.; Freudenmann, R.; Hanack, M.; Shaheen, S. E.; Jabbour, G. E.; Peyghambarian, N. *MRS Proceedings* **2011**, *598*, BB11.22.

26. Segura, J. L.; Juárez, R.; Ramos, M.; Seoane, C. *Chem. Soc. Rev.* **2015**, *44*, 6850.

27. Alam, M. A.; Motoyanagi, J.; Yamamoto, Y.; Fukushima, T.; Kim, J.; Kato, K.; Takata, M.; Saeki, A.; Seki, S.; Tagawa, S.; Aida, T. *J. Am. Chem. Soc.* **2009**, *131*, 17722.

28. Furukawa, S.; Suda, Y.; Kobayashi, J.; Kawashima, T.; Tada, T.; Fujii, S.; Kiguchi, M.; Saito, M. *J. Am. Chem. Soc.* **2017**, *139*, 5787.

29. Wu, B.; Chopra, R.; Yoshikai, N. *Org. Lett.* **2015**, *17*, 5666.

30. Berresheim, A. J.; Muller, M.; Mullen, K. *Chem. Rev.* **1999**, *99*, 1747.

31. Grzybowski, M.; Skonieczny, K.; Butenschön, H.; Gryko, D. T. *Angew. Chem. Int. Ed.* **2013**, *52*, 9900.

32. Little, M. S.; Yeates, S. G.; Alwattar, A. A.; Heard, K. W. J.; Raftery, J.; Edwards, A. C.; Parry, A. V. S.; Quayle, P. *Eur. J. Org. Chem.* **2017**, *2017*, 1694.

33. Scholl, R.; Mansfeld, J. *Ber. Deu. Chem. Ges.* **1910**, *43*, 1734.

34. Kovacic, P.; Jones, M. B. *Chem. Rev.* **1987**, *87*, 357.

35. Grätz, S.; Beyer, D.; Tkachova, V.; Hellmann, S.; Berger, R.; Feng, X.; Borchardt, L. *Chem. Commun.* **2018**, *54*, 5307.

36. Sarhan, A. A. O.; Bolm, C. *Chem. Soc. Rev.* **2009**, *38*, 2730.

37. King, B. T.; Kroulík, J.; Robertson, C. R.; Rempala, P.; Hilton, C. L.; Korinek, J. D.; Gortari, L. M. *J. Org. Chem.* **2007**, *72*, 2279.

38. Rempala, P.; Kroulík, J.; King, B. T. *J. Org. Chem.* **2006**, *71*, 5067.

39. Zhai, L.; Shukla, R.; Wadumethrige, S. H.; Rathore, R. *J. Org. Chem.* **2010**, *75*, 4748.

40. Ronlan, A.; Hammerich, O.; Parker, V. D. *J. Am. Chem. Soc.* **1973**, *95*, 7132.

41. Ronlan, A.; Parker, V. D. *J. Org. Chem.* **1974**, *39*, 1014.

42. Rathore, R.; Kochi, J. K. *J. Org. Chem.* **1995**, *60*, 7479.

43. Szűcs, R.; Riobé, F.; Escande, A.; Joly, D.; Bouit, P.-A.; Nyulászi, L.; Hissler, M. *Pure Appl. Chem.* **2017**, *89*, 341.

44. Delaunay, W.; Szűcs, R.; Pascal, S.; Mocanu, A.; Bouit, P. A.; Nyulászi, L.; Hissler, M. *Dalton Trans.* **2016**, *45*, 1896.

45. Wu, B.; Santra, M.; Yoshikai, N. *Angew. Chem. Int. Ed.* **2014**, *53*, 7543.

46. Yoshikai, N.; Santra, M.; Wu, B. *Organometallics* **2017**, *36*, 2637.

47. Tan, B.-H.; Dong, J.; Yoshikai, N. *Angew. Chem. Int. Ed.* **2012**, *51*, 9610.

48. Tan, B.-H.; Yoshikai, N. *Org. Lett.* **2014**, *16*, 3392.

49. Yan, J.; Yoshikai, N. *ACS Catal.* **2016**, *6*, 3738.

50. Rahman, M. S.; Yoshikai, N. *Org. Lett.* **2019**, *21*, 3232.

51. Fukazawa, A.; Osaki, H.; Yamaguchi, S. *Asian J. Org. Chem.* **2014**, *3*, 122.

Chapter 4. Palladium-Catalyzed Annulation of 1-Halo-8-arylnaphthalenes and Alkynes Leading to Heptagon-Embedded Aromatic Systems

4.1. Introduction

Polycyclic aromatic hydrocarbons (PAHs) are ubiquitous structural motifs of functional molecules that have numerous applications in optical and electronic devices.[1-5] PAHs such as carbon nanotubes, fullerenes, and graphene have straight tubular, hollow spherical/ellipsoidal, and flat sheet-type structures, respectively, and comprised of sp^2 carbon atoms. These nanocarbons hold important place in material science due to their inherent intriguing chemical, thermal, mechanical and electrical properties. When a seven-membered ring, heptagon with all sp^2 carbon atoms is embedded, these nanocarbons can be significantly deformed from their original structures to retain the C(sp^2)–C(sp^2) distance and thus, influenced the physicochemical and electrical properties.[6-9] In this context, PAHs containing heptagon have attracted much attention because of their unique non-planar, curved structures that could lead to intriguing optoelectronic properties.[7, 9-15] Representative examples of functional non-planar heptagon-embedded PAHs include carbon nanotube **4.1**, warped nanographene **4.2**, and saddle-shaped **4.3** (Figure 4.1).[7, 9, 12, 16-17]

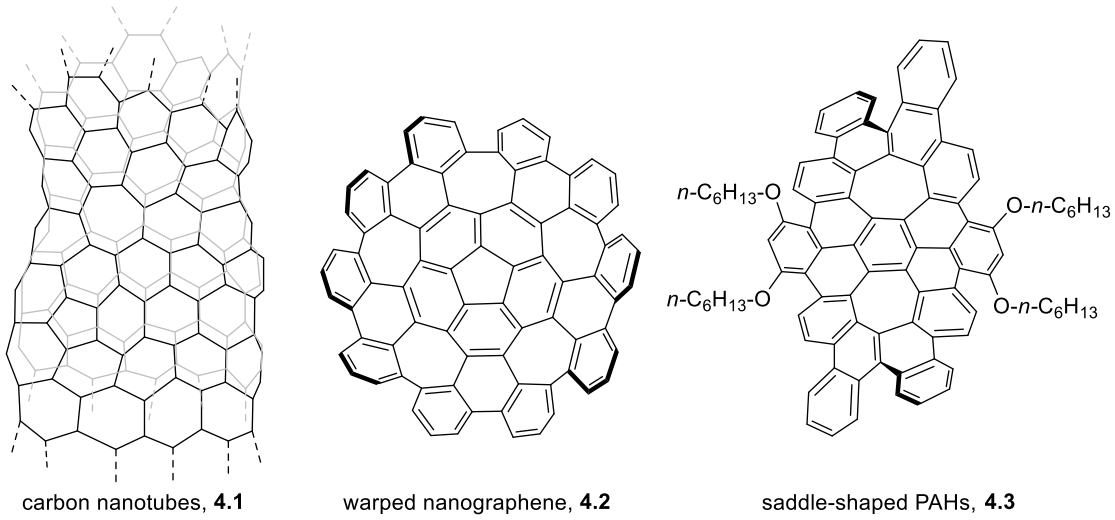

Figure 4.1. Representative heptagon-embedded non-planar PAHs

4.1.1 Synthesis of Hexagonal PAHs via Annulation

The development of efficient methods for the synthesis of new PAHs from easily available starting materials is among important subjects in synthetic organic chemistry. In this context, extension of the π-conjugation of existing aromatic systems through an annulation process is an attractive strategy. In fact, a series of transition metal-catalyzed annulation reactions between aromatic compounds and alkynes have been developed for the synthesis of acene- and phenacene-type PAH derivatives. In this section, two type of annulation reactions are discussed: (1) transition metal-catalyzed [2 + 2 + 2] annulation between monofunctionalized (or even unfunctionalized) aromatic substrates and alkynes, (2) transition metal-catalyzed [4 + 2] annulation reactions between 2-functionalized biaryls or dibenzoheteroles and alkynes.

4.1.1.1 Synthesis of PAHs via [2 + 2 + 2] Annulation

The [2 + 2 + 2] annulation between an aromatic compound and two molecules alkynes allows for the straightforward construction of naphthalene-type molecules. Such reactions are particularly attractive when the starting aromatic compounds are readily available monofunctionalized (or even unfunctionalized) derivatives, and the annulation process involves the activation of the *ortho* C–H bond. A variety of monofunctionalized arenes such as haloarenes,[18-21] benzoic acids,[22-24] benzyl alcohols,[25] arylboronic acids,[26-27] aroyl chlorides,[28] arylmetal reagents[29-30] have been demonstrated to participate in annulation reactions with alkynes (Scheme 4.1). Heck,[18] Miura,[19] and Sarkar[20] independently reported the annulation reactions of *ortho*-haloarenes and alkynes by using palladium catalysis. Miura and Satoh achieved annulation of benzoic acids[22] or arylboronic acids[26] and alkynes in the presence of rhodium or iridium catalysts. Nakamura[30] and Yoshikai[29] independently utilized iron catalysis to achieve annulation employing aryl Grignard reagents and arylindium reagents, respectively, under oxidative conditions.

Scheme 4.1. Transition metal-catalyzed [2 + 2 + 2] annulation between *ortho*-functionalized arenes and alkynes

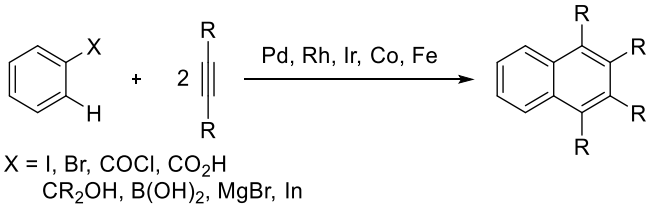

The mechanism of the above [2 + 2 + 2] annulation reactions would depend on the arene substrate and the transition metal catalyst. As an illustrative example, a plausible catalytic cycle for the palladium-catalyzed annulation of aryl halide and

alkyne is shown in Scheme 4.2.[19, 29] The oxidative addition of the aryl halide to Pd(0) is followed by migratory insertion of the alkyne to give an intermediate **4.8**. The intermediate **4.8** would undergo insertion of the second alkyne molecule (pathway a) and subsequent intramolecular palladation of the aryl ring to give a seven-membered palladacycle **4.10**. Alternatively, the intermediate **4.8** could also undergo intramolecular *ortho* C-H activation to give a five-membered palladacycle **4.9** (pathway b), followed by insertion of the second alkyne molecule and thus, affording the intermediated **4.10**. Finally, C–C reductive elimination produces the cyclized product **4.11** and regenerates Pd(0).

Scheme 4.2. Possible catalytic cycle for Pd-catalyzed [2 + 2 + 2] annulation

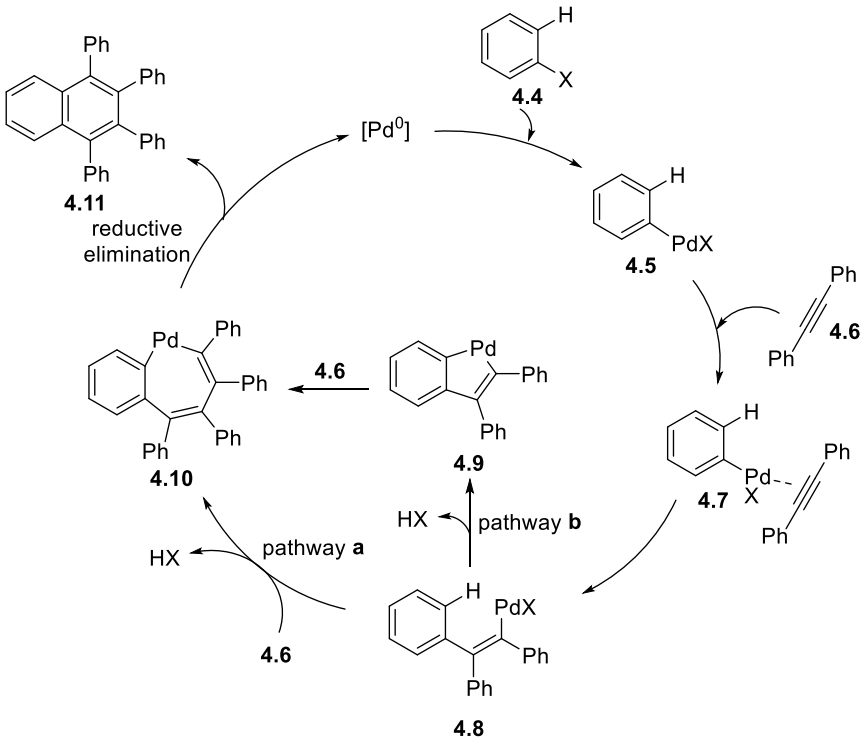

Cramer *et al.* reported an elegant method to construct homologated acenes via rhodium(III)-catalyzed oxidative [2 + 2 + 2] annulation of simple arenes and alkynes

involving double C–H activation (Scheme 4.3).[31] The notable feature about this method is that the unfunctionalized arenes without any directing group can be utilized.

Scheme 4.3. Rhodium-catalyzed synthesis of acenes through C-H functionalization/annulation

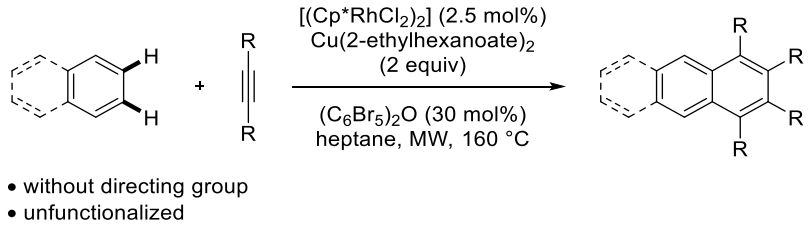

- without directing group
- unfunctionalized

A proposed mechanism of the above annulation is shown in Scheme 4.4. Firstly, naphthalene **4.12** would undergo non-chelation-assisted metalation with the rhodium(III) catalyst to produce an arylrhodium species **4.13**, which upon migratory insertion of one molecule of the alkyne **4.14** to give an intermediate **4.16**. The intermediate **4.16** would undergo an intramolecular C–H bond activation to give rhodacycle **4.17** or **4.18**. The rhodacycle **4.18** should be favored over **4.17** due to the less steric clash. Incorporation of another molecule of alkyne would produce seven-membered rhodacycle **4.19** or **4.20**. Lastly, reductive elimination would afford the cyclized product **4.21** and a rhodium(I) species, the latter being reoxidized to rhodium(III) by the copper(II) oxidant.

Scheme 4.4. Proposed reaction pathway for Rh-catalyzed C-H activation/annulation

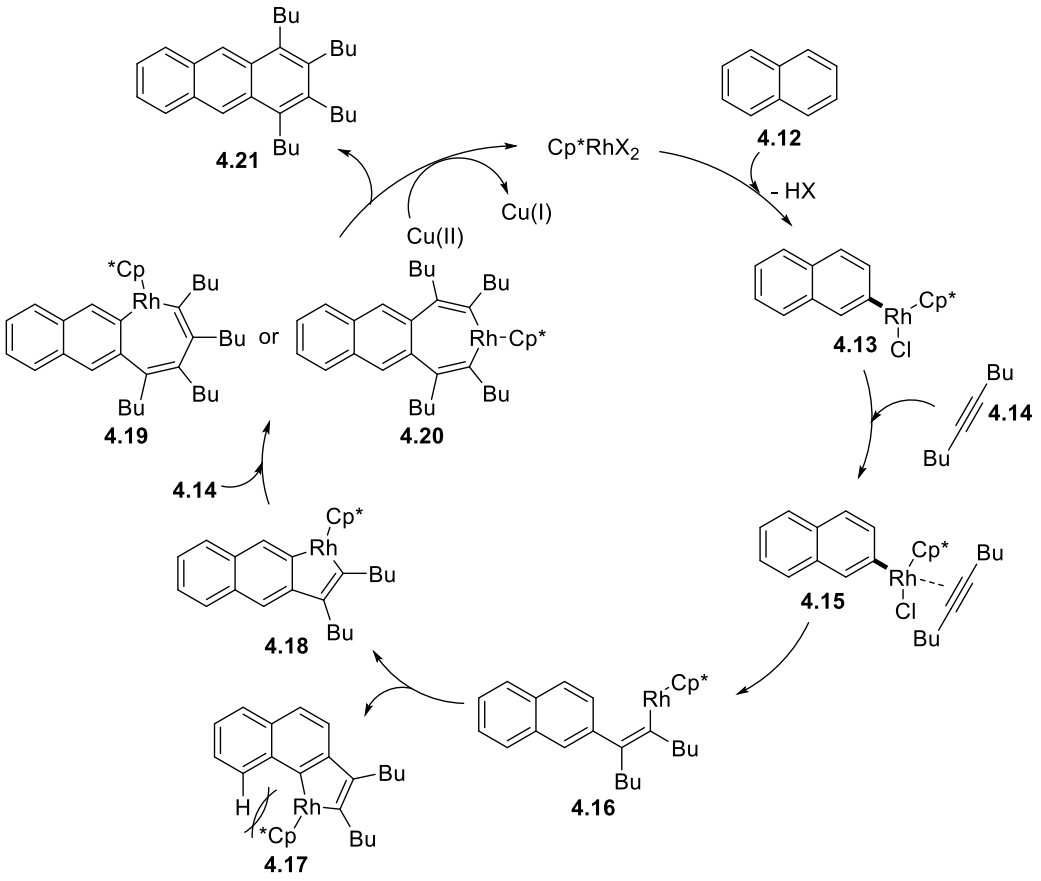

4.1.1.2 Synthesis of PAHs via [4 + 2] Annulation

In comparison to the [2 + 2 + 2] annulation, the [4 + 2] annulation reactions between a biaryl derivative and an alkyne enable the construction of phenanthrene-type hexagonal polyaromatic hydrocarbons (Scheme 4.5).[18, 32-36] 2-Functionalized biaryls are frequently used as the starting materials for this type of annulation, which involves the C–H activation of the 2'-position of the unfunctionalized aryl group. Some of the representative examples of such reactions are discussed below.

Scheme 4.5. Synthesis of phenanthrene derivatives via transition metal-catalyzed [4 + 2] annulation

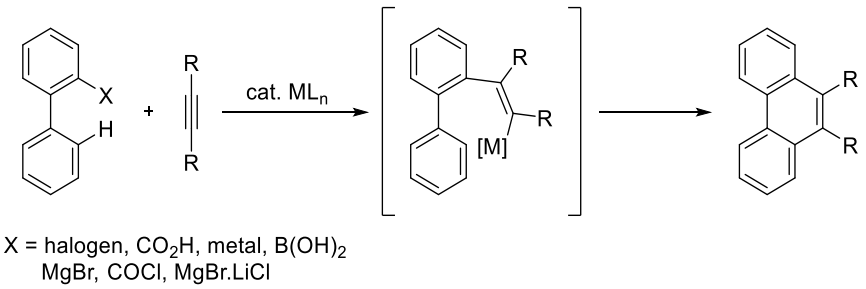

In 1987, Heck and coworkers reported an isolated example of [4 + 2] annulation of 2-iodobiphenyl and diphenylacetylene promoted by $Pd(OAc)_2$-PPh_3 as a catalyst and Et_3N as a base in CH_3NO_2 at 100 °C, affording the corresponding phenanthrene derivative (Scheme 4.6a).[18] Later, in 1997, Larock *et al.* extended the substrate scope of Heck's phenanthrene synthesis by improving the reaction conditions including the salt additive and the solvent (Scheme 4.6b).[32]

Scheme 4.6. Palladium-catalyzed synthesis of phenanthrene scaffolds

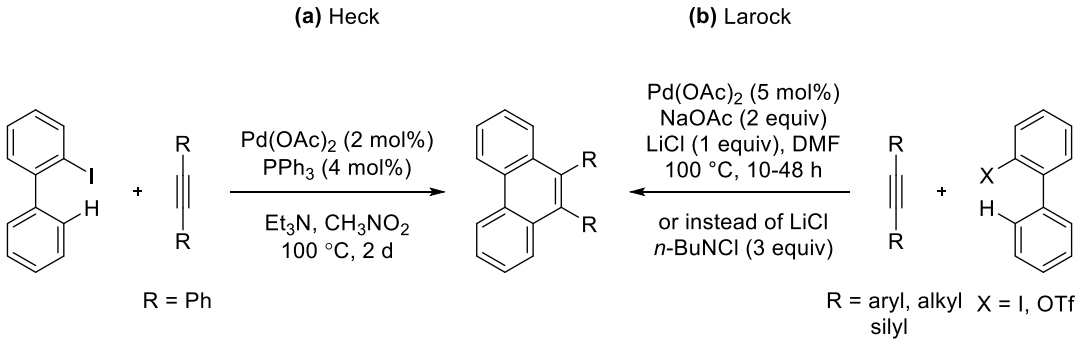

Wang and Glorius used 2-phenylbenzoic acids as substrates for palladium-catalyzed decarboxylative [4 + 2] annulation with alkynes through successive C-H and C-C bond cleavage.[33] Nakamura and coworkers described a modular synthesis of phenanthrene derivatives from biaryl- or 2-alkenyphenyl Grignard reagents and alkynes in the presence of an iron-4,4'-di-*tert*-butylbipyridine catalyst and 1,2-

dichloroisobutane oxidant (Scheme 4.7).[34] The reaction tolerated a variety of functional groups such as bromide, chloride, trimethylsilyl, and so on.

Scheme 4.7. Iron-catalyzed [4 + 2] annulation between alkyne and biaryl Grignard reagent leading to phenanthrenes

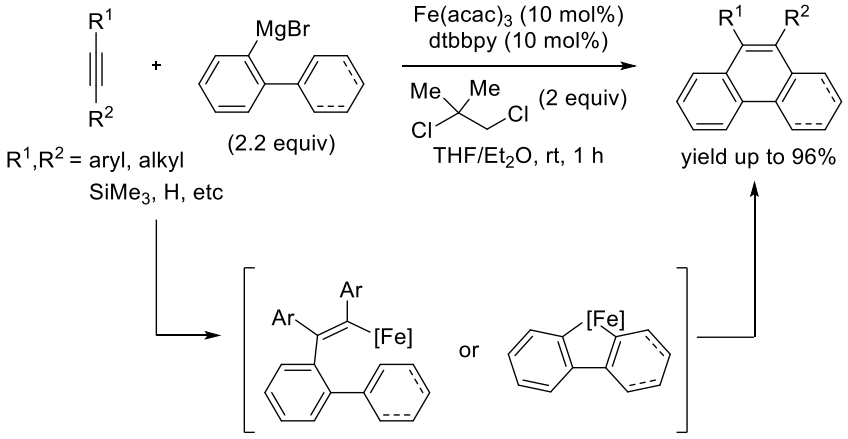

Recently, Yoshikai group also reported the synthesis of phenanthrene derivatives from 2-biarylmagnesium bromides and related Grignard reagents with internal alkyne under chromium catalysis (Scheme 4.8).[37] Unlike Nakamura's iron-catalyzed phenanthrene synthesis, where excess (2.2 equiv) Grignard reagent was used in combination with 1,2-dichloroisobutane as the oxidant, the chromium-catalyzed reaction employed excess alkyne, which also acted as a hydrogen acceptor. Based on deuterium labeling experiments, the reaction was proposed to involve a five-membered metallacycle, its alkyne insertion, and reductive elimination to give the phenanthrene product along with the 1,2,3-triarylnaphthalene as a side product.

Scheme 4.8. Chromium-catalyzed synthesis of phenanthrene derivatives

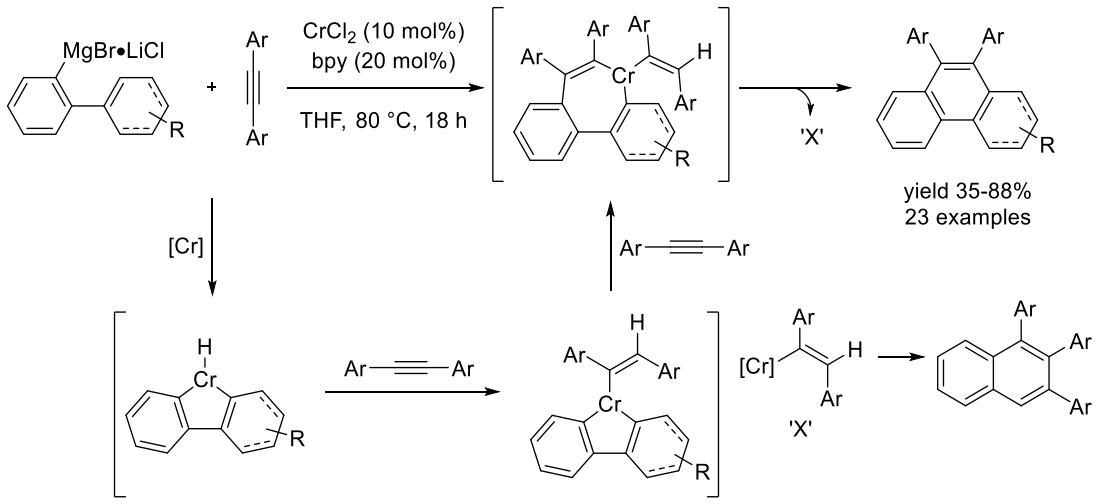

Besides 2-functionalized biaryls, heteroatom-bridged biaryls have also proved to serve as versatile substrates for the [4 + 2] annulation. Itami and coworkers reported the annulation of dibenzosiloles or dibenzogermoles with alkynes by using a cationic palladium(II)/*o*-chloranil catalytic system (Scheme 4.9a).[38] In another report, they utilized 9-chloro-9-borafluorene instead of dibenzosiloles or germoles as reaction partners in [4 + 2] annulation with alkynes (Scheme 4.9b).[39] In both of these reports, the reactions are highly efficient to construct condensed PAHs in a single step and furthermore, tolerate various sensitive functional groups. Prior to these reports, Takahashi and co-workers reported the annulative reaction of 2,2'-dibromo-1,1'-biphenyl and alkynes under chromium catalysis.[40] In addition, Wen *et al.* described [4 + 2] annulation reaction of diaryliodonium salts with alkynes by using palladium catalysis.[41]

Scheme 4.9. Synthesis of phenanthrene derivatives via [4 + 2] annulation

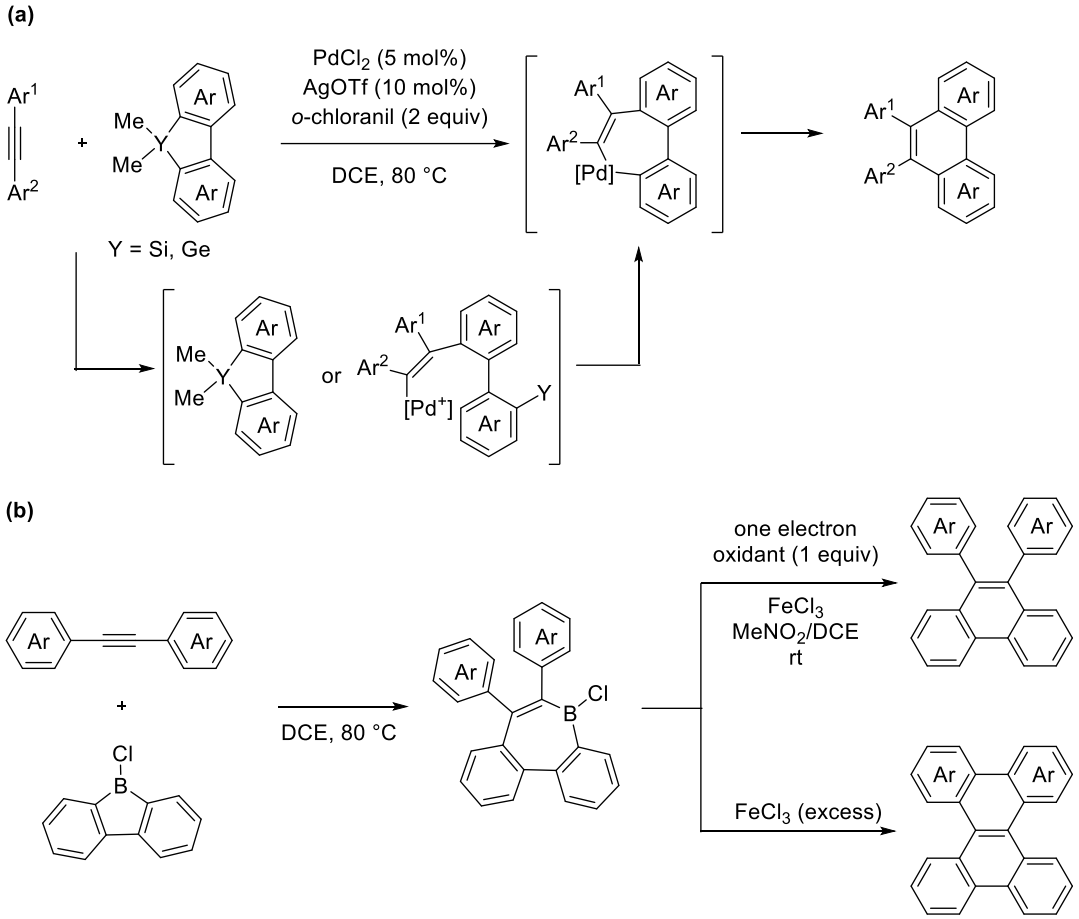

4.1.2 Synthesis of Heptagon-Embedded PAHs

The direct construction of heptagon-embedded PAHs is very rare and often required multiple steps and prefunctionalized starting materials. In this section, representative examples of synthetic studies on heptagon-containing PAHs are discussed. In the 1970's, Muller and Craig independently reported the first multi-step synthesis of heptagon-embedded aromatic systems (Scheme 4.10).[42] The synthesis started with the coupling reaction of 1-bromo-8-napthoate **4.22** and iodobenzene, followed by reduction and bromination with PBr_3, affording compound **4.23**. The conversion of **4.23** to the heptagon product **4.27** required several steps, where the key ring closure was achieved by the intramolecular Friedel–Crafts acylation.

Scheme 4.10. Synthesis of benzo[4,5]cyclohepta[1,2,3-*de*]naphthalene

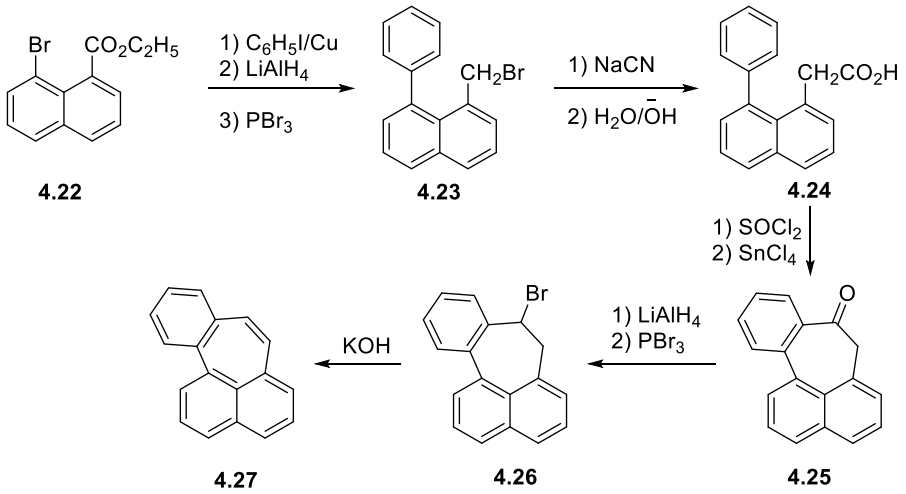

4.22 **4.23** **4.24** **4.25** **4.26** **4.27**

In 1987, Murata and co-workers described the synthesis and properties of cyclohepta[*a*]phenalene (Scheme 4.11).[43] The key step of the synthesis was the benzene ring expansion by rhodium-catalyzed intramolecular ketocarbene reaction.

Scheme 4.11. Synthesis and properties of cyclohepta[*a*]phenalene

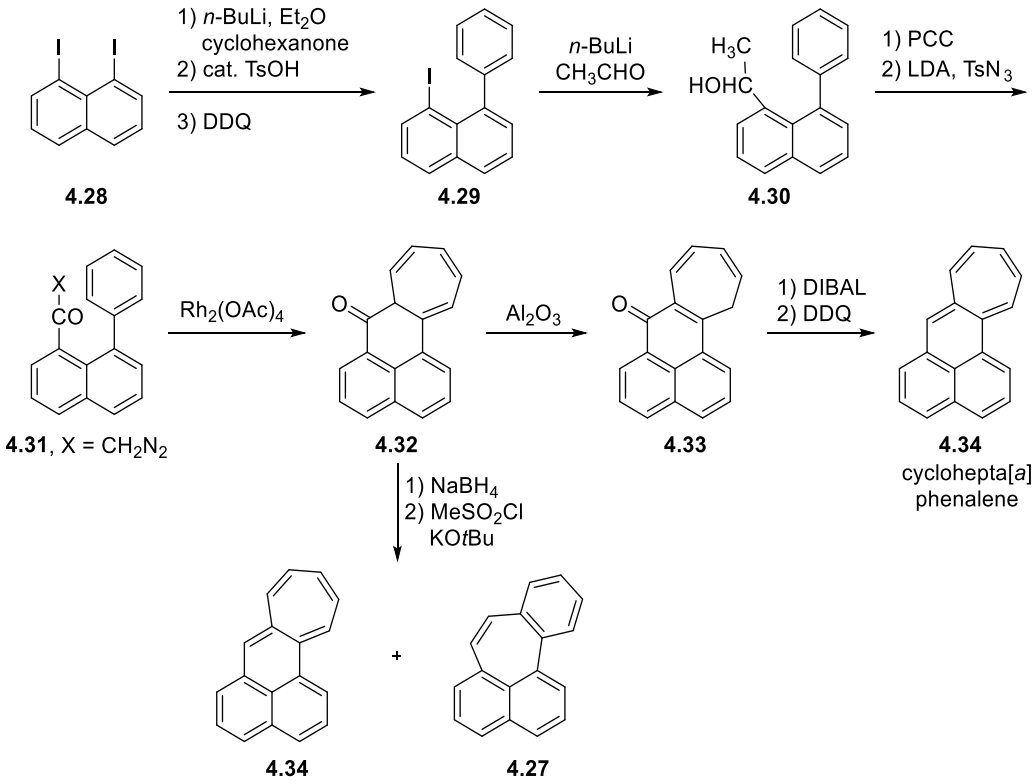

Gevorgyan *et al*. developed a palladium-catalyzed intermolecular annulation reaction of 3-iodobenzylindole derivatives with alkynes leading to the generation of heptagon-embedded polycyclic systems (Scheme 4.12).[44] Notable feature of this reaction was the impact of the base on the product selectivity between seven- and five-membered ring systems. The use of triethylamine led to the exclusive formation of the seven-membered ring, while cesium acetate favored the five-membered ring. Note that the heptagon moiety of the product is not purely sp^2 carbon-based but contains one sp^3 carbon center.

Scheme 4.12. Synthesis of heptagon containing polyaromatic compounds

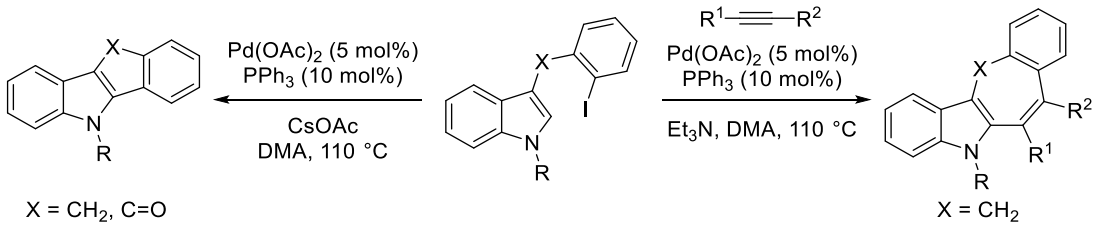

Itami and coworkers designed several elegant synthetic routes to access novel warped nanographene containing heptagon scaffolds (Scheme 4.13). The synthetic route, which is consisting of two steps, firstly involves C-H activation of corannulene **4.35** followed by C-C coupling with arylboroxin in the presence of $Pd(OAc)_2$ and *o*-chloranil. Dehydrogenative cyclization of **4.36** and **4.37** by using Scholl reaction conditions, appended grossly warped nanographene **4.38** and **4.39** in 50% and 62% yield respectively.[9] They disclosed the unique properties of heptagon containing nanographenes such as, strong intermolecular π-π interaction in solid-phase, rigid and chiral in solid state but racemized upon dissolved in solution, warped geometry enhanced solubility and green florescent.[9, 11-13]

Scheme 4.13. Synthesis of heptagon-embedded warped graphene

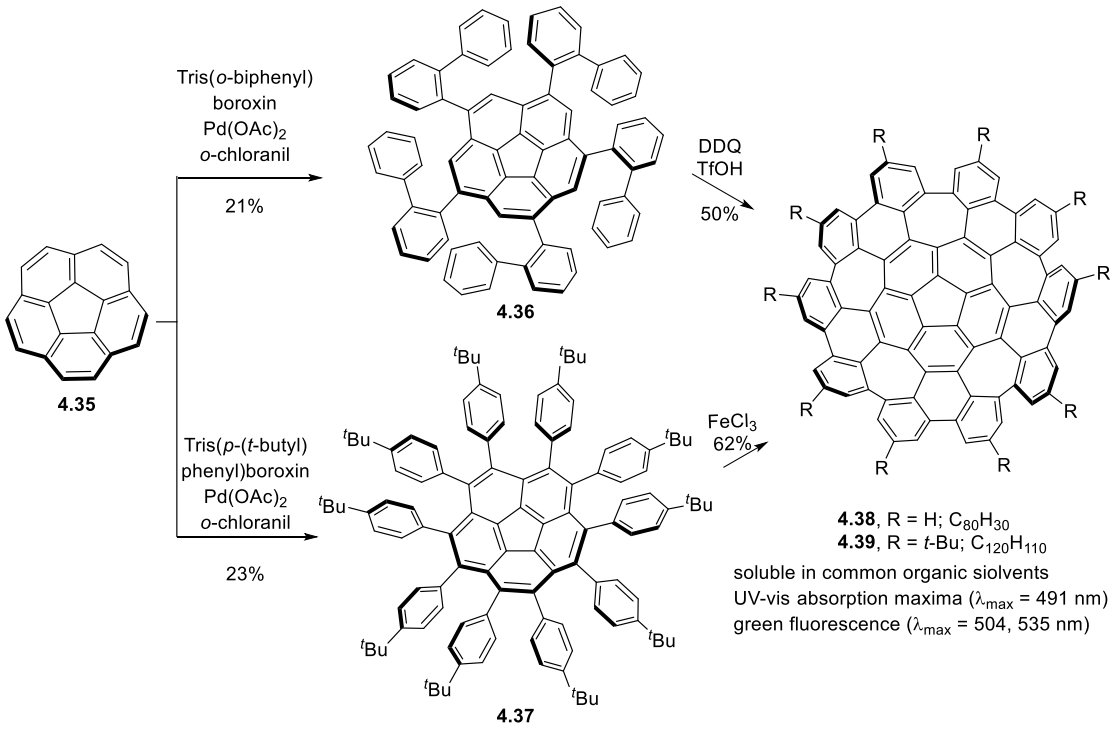

Miao's groups designed various synthetic routes to access saddle-shaped, warped, heptagon-embedded large polyaromatic hydrocarbons that showed unique optoelectronic properties.[7, 14, 45-46] They also disclosed about the nonplanarity, bond distance, and semiconductor properties of saddle-shaped PAHs. Synthesis of one of the representative saddle-shape heptagon containing PAHs is described below (Scheme 4.14).[7]

Scheme 4.14. Synthesis of heptagon-embedded saddle-shape PAHs

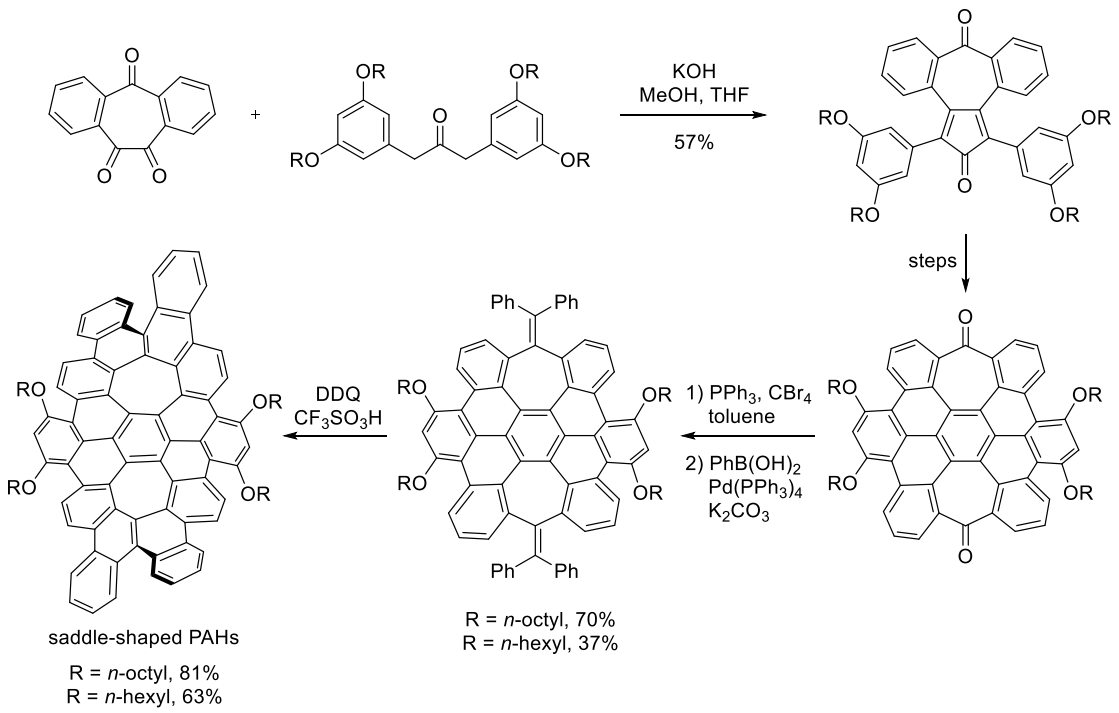

4.1.3 Perspective of Thesis Chapter 4

Recently, Lin, Kwong, and coworkers described the synthesis of heptagon-embedded aromatic compounds via three-component annulation reaction of aryl/heteroaryl iodide, 8-bromo-1-naphthoic acid, and norbornadiene by using Pd/PCy_3 catalytic system (Scheme 4.15).[47] The naphthalene and benzene rings are linked by a *cis*-ethenyl (C_2H_2) bridge which came from norbornadiene. However, the substrate scope is narrow and only several derivatives were reported.

Scheme 4.15. Synthesis of heptagon-embedded PAHs via Pd-catalyzed three-component annulation reaction

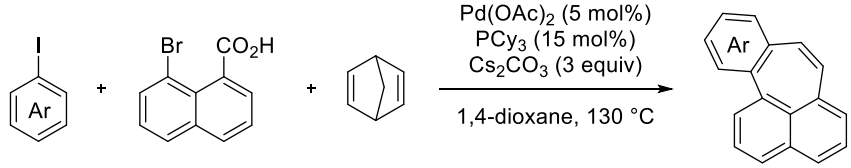

Apart from this report, direct access of heptagon-embedded aromatic compounds with all sp^2 carbon center via annulative approach, is remain elusive. Moreover, the unique physico-chemical properties of heptagon-embedded PAHs as demonstrated by Itami and Miao, we envisioned that employing different functionality around heptagons, might influence its optoelectronic properties and thus, leads to new organic materials. In this work, we developed a palladium-catalyzed annulation reaction between 1-halo-8-aryl-naphthalene and diphenylacetylene to afford heptagon containing polycyclic aromatic systems (Scheme 4.16).[48] Notable feature of the reaction is the broad substrate scope and variety of aryl groups on the 7- and 8-positions of the benzo[4,5]cyclohepta[1,2,3-*de*]naphthalenes and two-fold annulated heptagon containing PAHs.

Scheme 4.16. Pd-Catalyzed synthesis of heptagon-embedded PAHs

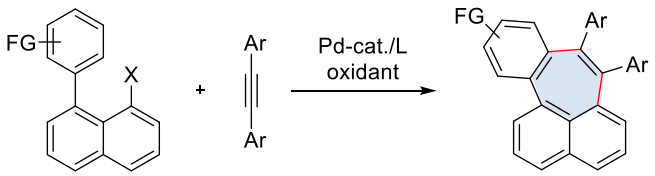

4.2 Results and Discussion

The present study started with the screening of reaction conditions for the annulation of 1-bromo-8-phenylnaphthylene, **4.40a** and diphenylacetylene, **4.41a** (Table 4.1). The initial optimization reaction was performed in the presence of $Pd(OAc)_2$ (10 mol%) and Ag_2CO_3 (1 equiv) in dichloroethane at 80 °C, after 18 h, afforded the desired heptagon product **4.42aa** in a low yield of 18% (Table 1, entry 1). When 30 mol% of triphenylphosphine was used as ligand, the yield of **4.42aa** was

decreased to 8% while generating a trace amount of fluoranthene **4.43** (entry 2).[49-52] The employment of less electron donating triphenylarsine promoted full conversion of **4.40a** and improved the yield of desired product **4.42aa** to 59% along with increased yield (20%) of fluoranthene **4.43** (entry 3). Note that, at the reaction time of 1.5 h, the yields of **4.42aa** and **4.43** were 29% and 21% respectively. This indicates that the formation of **4.43** stopped at an early stage of the reaction. On the other hand, moderate electron-deficient triarylphosphines, such as $P(4\text{-}ClC_6H_4)_3$, $P(3\text{-}ClC_6H_4)_3$ and $P(4\text{-}FC_6H_4)_3$, were found to accelerate the annulation and subsequent afford **4.42aa** in up to 78% yield, whereas suppressing the formation of fluoranthene (entries 4-6). Note that the annulation reaction reached to full conversion at 1.5 h in comparable yield with that of at 18 h (entry 4). The use of more electron-deficient triarylphosphine ligands such as $P(4\text{-}CF_3C_6H_4)_3$ and $P(C_6F_5)_3$ proved to be sluggish (entries 7 and 8) for the annulation reaction. The annulation was completely inhibited with electron-rich $P(4\text{-}MeOC_6H_4)_3$ (entry 9). Other monophosphines, such as tri(furyl)phosphine and SPhos proved to be ineffective for the annulation (entries 10 and 11). The employment of AgOAc instead of Ag_2CO_3 produced **4.42aa** in a slightly lower yield but comparable (entry 12), whereas in the absence of Ag_2CO_3, the reaction became sluggish (entry 13).

Table 4.1. Screening of reaction conditions.[a]

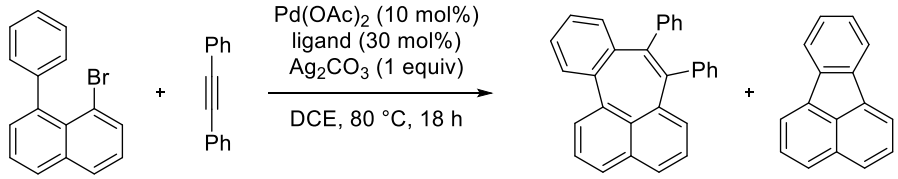

4.40a **4.41a** **4.42aa** **4.43**

Entry	Ligand	Conv of **4.40a** [%][b]	**4.42aa** [%][b]	**4.43** [%][b]
1	None	45	18	0
2	PPh_3	58	8	3
3	$AsPh_3$	100 (60)	59 (29)	20 (21)
4	$P(4\text{-}ClC_6H_4)_3$	100 (75)	78 (75)	3 (4)
5	$P(3\text{-}ClC_6H_4)_3$	100	77	3
6	$P(4\text{-}FC_6H_4)_3$	100	65	0
7	$P(4\text{-}CF_3C_6H_4)_3$	55	37	4
8	$P(C_6F_{54})_3$	29	15	0
9	$P(4\text{-}MeOC_6H_4)_3$	20	0	1
10	$P(2\text{-furyl})_3$	85	38	2
11	SPhos	83	10	3
12[c]	$P(4\text{-}ClC_6H_4)_3$	100	72	4
13[d]	$P(4\text{-}ClC_6H_4)_3$	40	30	0

[a] The reaction was performed using 0.1 mmol of 1-bromo-8-arylnaphthalene (**4.40a**) and 0.2 mmol of diphenylacetylene (**4.41a**). [b] Determined by GC using *n*-tridecane as an internal standard. The conversion and yield in the parentheses were determined at the reaction time of 1.5 h. [c] The reaction was performed in the presence of AgOAc instead of Ag_2CO_3. [d] The reaction was performed in the absence of Ag_2CO_3.

After established the optimal reaction conditions, firstly, we explored the substrate scope of various diarylacetylenes (Scheme 4.17). Diphenylacetylenes bearing electron-donating group such as methoxy, methyl, and trimethylsilyl groups at *para*-positions participated in the reaction to afford corresponding products (**4.42ab-4.42ad)** in moderate to good yield. Likewise, diphenylacetylenes bearing electron-withdrawing groups at *para*-position such as halogen, trifluoromethyl groups could also underwent reaction with **4.41a** to afford corresponding products (**4.42ae-4.42ag**) in moderate

yields. Di(3,4-dimethoxyphenyl)acetylene also participated in the reaction and afford **4.42ah** in 57% on 0.6 mmol scale. Di(2-methoxyphenyl)acetylene and di(3-methylphenyl)acetylene smoothly underwent in the reaction to afford **4.42ai** and **4.42aj** in 77% and 67% yields respectively. However, diphenylacetylene bearing 1-naphthyl reacted sluggishly in less than 5% GC yield and this is presumably because of steric crowd. Di(2-thienyl)acetylene was also susceptible to the present annulation, and thus affording **4.42ak** in 70% yield. Unfortunately, other type of internal alkynes such 5-decyne, diethylacetylenedicarboxylate, and 1-phenyl-1-butyne failed to participate in the annulation with **4.40a** under the present reaction conditions.

Scheme 4.17. Heptagons synthesized from different diphenylacetylenes and 1-halo-8-arylnaphthalene.[a]

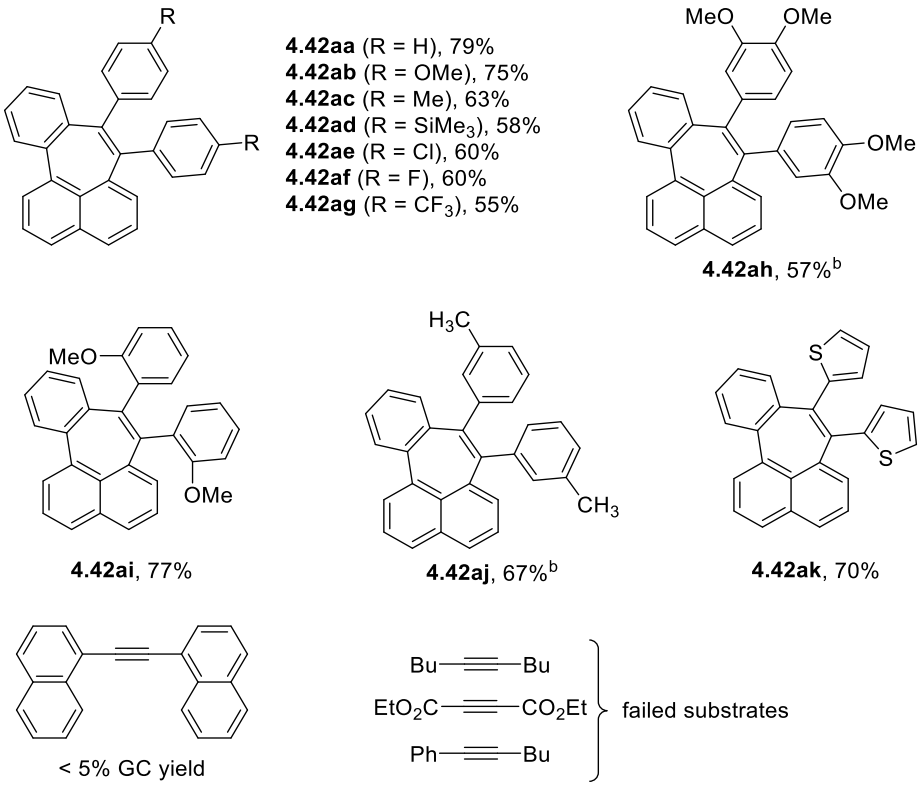

[a] The reaction was performed using 0.1 mmol of **4.40a** and 0.2 mmol of **4.40a-4.40k.** The yields are isolated and based on **4.40a**. [b] The reaction was performed on 0.6 mmol scale.

Next, we tested variety of 1-halo-8-arylnaphthalenes for the annulation reaction with **4.41a** (Scheme 4.18). The substrate 1-iodo-8-(4-methoxyphenyl)naphthalene (**4.40b**) efficiently underwent the annulation to afford **4.42ba** in 66% yield. The **4.42ba** was crystallized in EtOAc and its nonplanar structure was unambiguously confirmed by single crystal X-ray analysis. The naphthalene substrates bearing electron withdrawn group such as Cl, CF_3, CN, and COMe at *para*-position of phenyl moiety, underwent annulation without any difficulty and thus, affording products **4.42ca-4.42fa** in moderate to good yields. Notably, the substrate bearing a *meta*-tolyl group (**1g**) smoothly underwent annulation on the less hindered aryl C-H bond and affords **4.42ga** as a single regioisomer in 76% yield. The *ortho*-tolyl group (**4.40h**) also demonstrate its utility in the annulation and affords **4.42ha**, albeit in low yield and this could be due to the steric class between the methyl group and the naphthyl ring. By contrast, the substrate bearing 2-naphthyl group (**4.40i**) generated mixture of two annulated regioisomers **4.42ia** and **4.42ia'** in 74% yield with low regioselectivity, which could be attributed to the difficulty in controlling the regioselective C-H palladation of naphthalene.[53] The annulation at the less hindered naphthyl moiety was more favored (**4.42ia**: **4.42ia'** = 1.4:1). The present reaction conditions tolerated the substrate bearing 4-pyridyl group (**4.40j**), affords **4.42ja** albeit with low yield.

Scheme 4.18. Synthesis of heptagons from diphenylacetylene and different 1-halo-8-arylnaphthalene.[a]

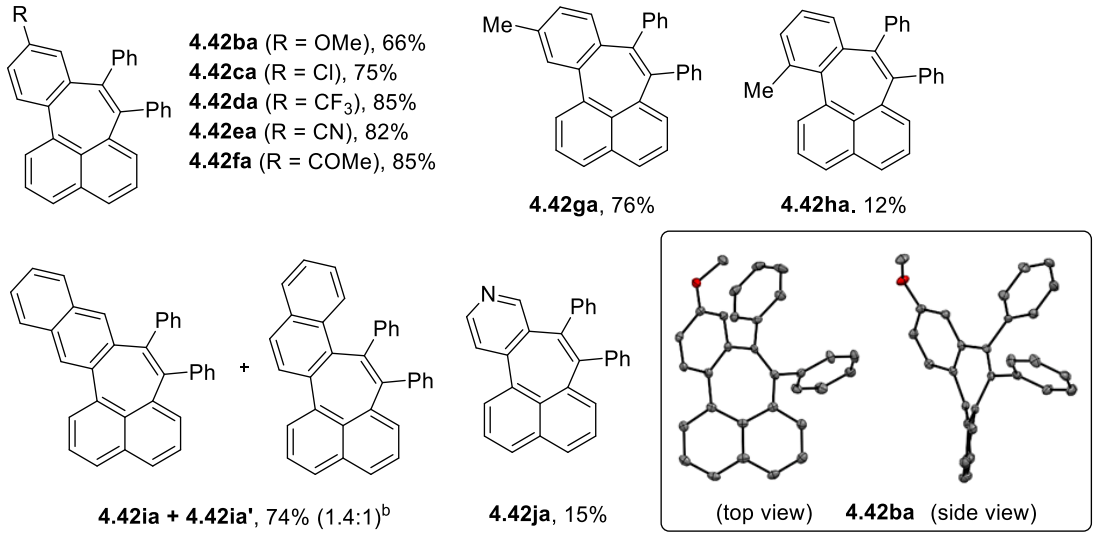

[a] The reaction was performed using 0.1 mmol of **4.40b-4.40j** and 0.2 mmol of **4.41a.** The yields are isolated and based on **4.41a**. [b] The ratio was determined by ^{1}H NMR.

The present catalytic system also proved to be effective for two-fold annulation between teraryl substrate **5** bearing two 1-bromonaphthyl moieties and diphenylacetylene **4.41**, which afforded the double heptagon product **4.45** in respective yield of 47% (Scheme 4.19a). The compound **4.45** was recrystallized from CH_2Cl_2 and the structure was unambiguously confirmed by X-ray analysis (Figure 4.2). From the X-ray analysis, it is revealed that the **4.45** is highly non-planar and *Ci*-symmetric and moreover, there is lack of π-π stacking in the crystal packing (Figure 4.3). However, we could not detect two-fold annulated product in the reaction between 1,5-dibromo-9,10-diarylanthracene **4.46** and diphenylacetylene **4.41a**. The reaction generated multiple products and among which only **4.47** was isolated in 10% yield (Scheme 4.19b). The structure was unambiguously established by single crystal X-ray analysis (Figure 4.2). In substrate **4.46**, one of the reaction sites expectedly participated in the

annulation with one molecule of diphenylacetylene **4.41a** to form heptagon, while the other site reacted with two molecules of diphenylacetylene to generate a peculiar bridge polycyclic moiety through cleavage of the C^1-C^{9a} bond of the anthracene **4.46** (Scheme 4.19b).

Scheme 4.19. Attempts on two-fold annulation

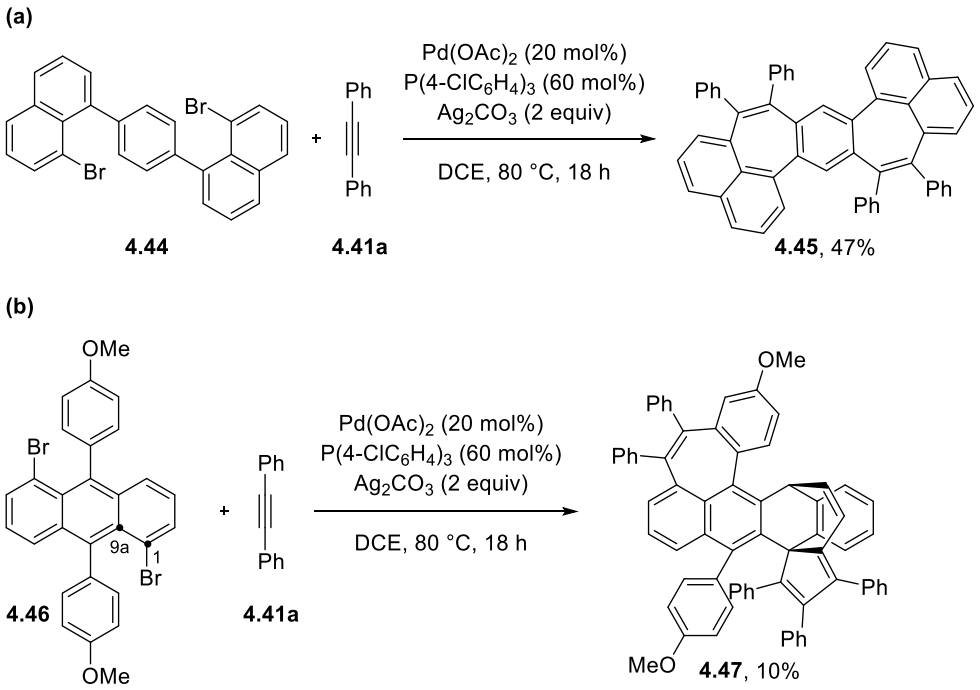

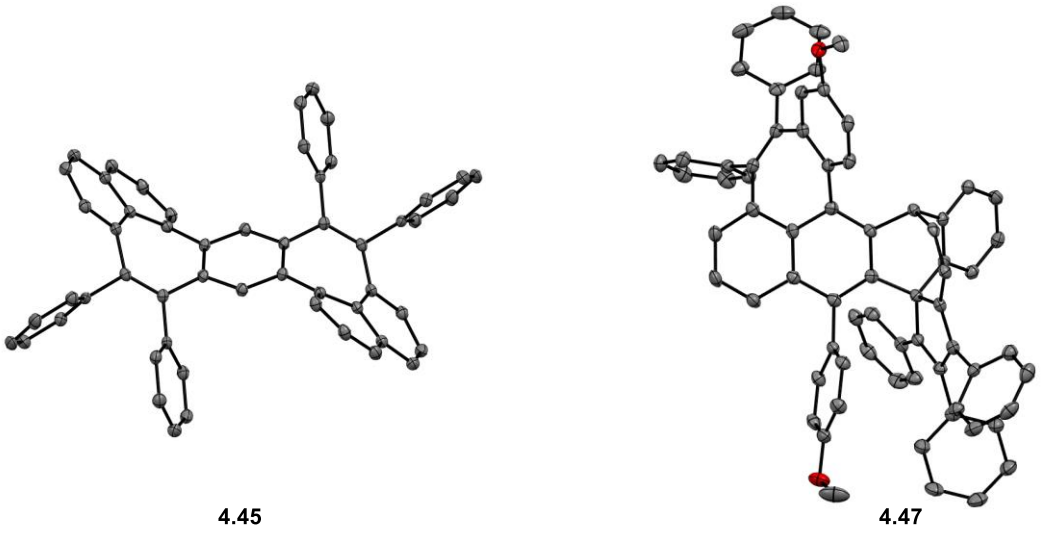

Figure 4.2. ORTEP diagram of compound **4.45** and **4.47**. Thermal ellipsoids are drawn at 50% probability.

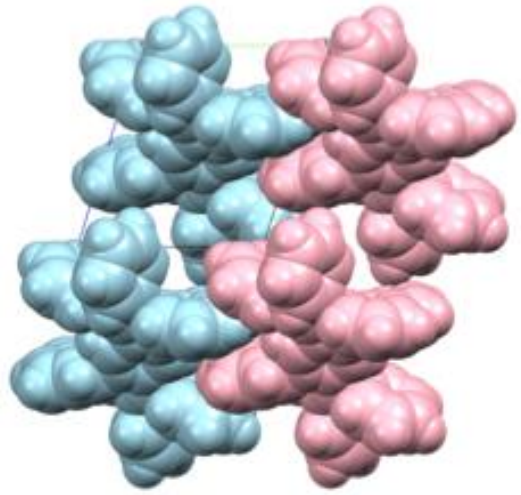

Figure 4.3. Packing structure of **4.45** as viewed along an axis.

Next, we subjected the heptagon products **4.42aa** and **4.42ab** to dehydrogenative C-C coupling between the aryl substituents or between the aryl substituents and heptagonal core by using DDQ/methanesulfonic acid, which is among the typical Scholl reaction conditions.[54] In contrast, we could not observe the desired dehydrogenative C-C coupling between the aryl substituents or between the aryl substituents and heptagonal core. Instead, oxidative fragmentation and ring contraction of the heptagonal core took place to afford 4*H*-benzo[*de*]anthracen-4-one derivatives **4.48a** and **4.48b** (Scheme 4.20) in modest yields. The oxidation of **4.42aa** and **4.42ab** requires the presence of water. The source of water might from methanesulfonic acid. Previously, Campana[15] and Harvey[55] independently reported the oxidation of allylic carbon by DDQ/methansulfonic acid. The compound **4.48b** was recrystallized from CH_2Cl_2 and structure was confirmed by X-ray analysis.

Scheme 4.20. Dehydrogenative cyclization leading to an extended conjugated system

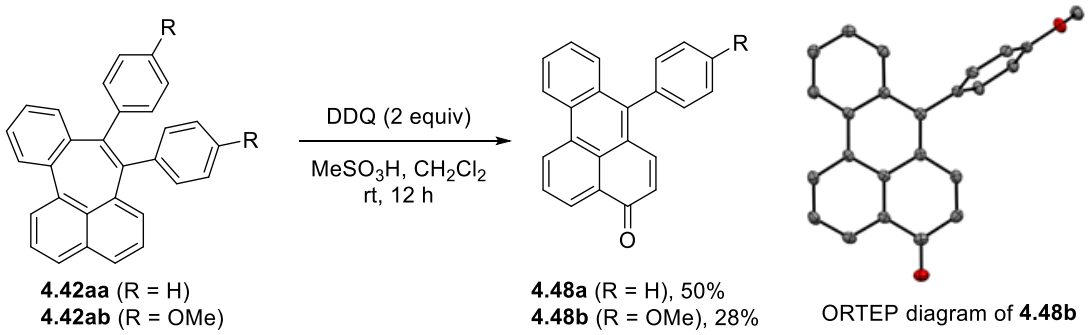

4.42aa (R = H)
4.42ab (R = OMe)

4.48a (R = H), 50%
4.48b (R = OMe), 28%

ORTEP diagram of **4.48b**

UV-vis absorption spectra of selected mono-heptagon derivatives in CH_2Cl_2, showed the longest the wavelength maximum (λ_{max}) around 350-360 nm. From the absorption behavior, it is concluded that there is moderate impact of peripheral substituents on λ_{max} (Figure 4.4 and 4.5). Note that, none of the heptagon moieties showed visible fluorescence in dilute solution and this could be due to nonradiative decay of the excited state through facile rotation of the aryl-aryl bonds. In contrast, bis-heptagon compound **4.45** showed wavelength maximum (λ_{max}) of 380, 320, and 284 nm and moderate fluorescence at 558 nm, with quantum yield 0.38 (reference with quinine sulfate) (Figures 4.6). However, all the heptagon compounds in the solid state were distinctively emissive with λ_{max} of 489, 496, and 508 nm for **4.42ab**, **4.42fa**, and **4.45**, respectively (Figure 4.7). As all the mono-heptagon compounds showed weak emission in solution state, thus, we studied aggregation-induced emission (AIE)[56] behavior one of the representative compounds **4.42ab** using THF/water mixture samples (Figure 4.8). As the percentage of water increases in the THF/water mixture samples, the fluorescence behavior of **4.42ab** also increases. This fluorescence phenomenon presumably ascribed to the non-planar geometry that prevents π-π stacking as well as the restricted rotation of aryl-aryl bonds in the aggregated state.

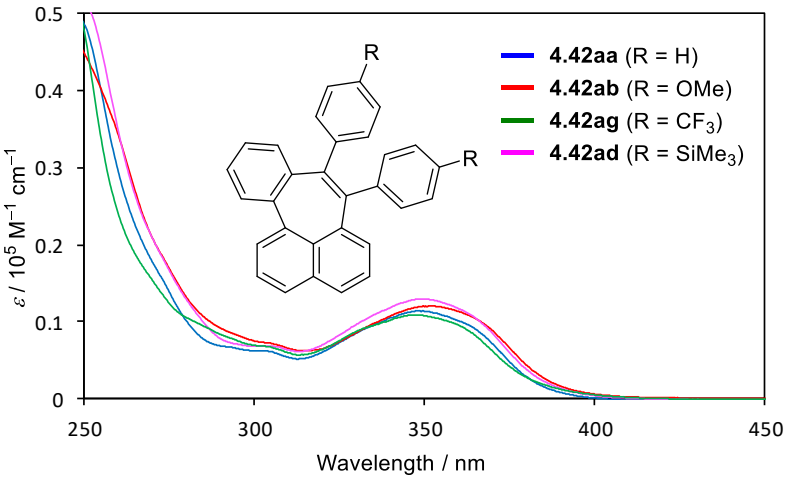

Figure 4.4. Absorption spectra of **4.42aa**, **4.42ab**, **4.42ag**, and **4ah** in CH_2Cl_2 (1 x 10^{-5} M).

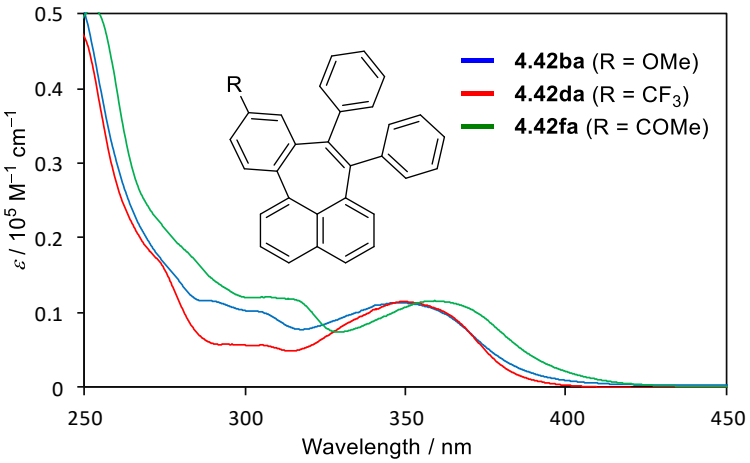

Figure 4.5. Absorption spectra of **4.42ba**, **4.42da**, and **4.42fa** in CH_2Cl_2 (1 x 10^{-5} M).

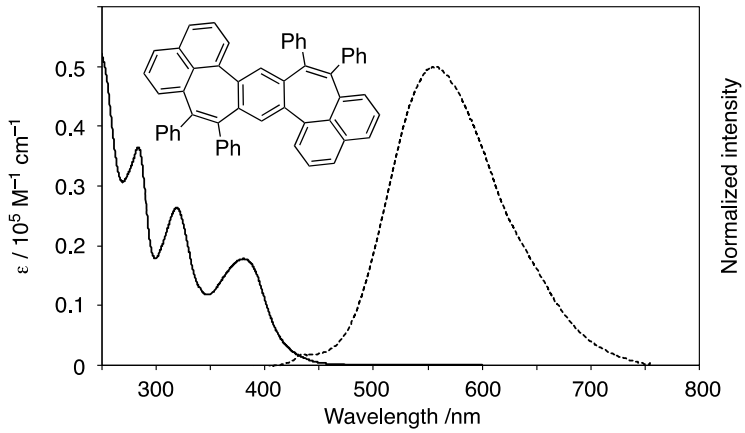

Figure 4.6. Absorption (solid) and fluorescence (dashed) spectra of **4.45** in CH_2Cl_2 (1 × 10^{-5} M).

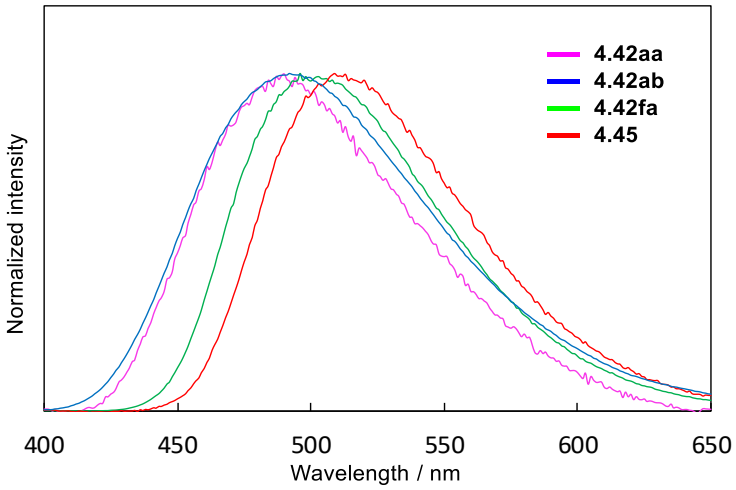

Figure 4.7. Fluorescence spectra of **4.42aa**, **4.42ab**, **4.42fa**, and **4.45** in the film state.

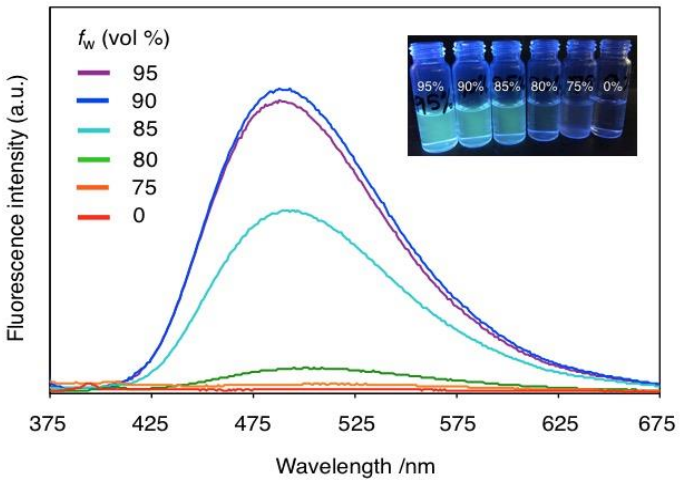

Figure 4.8. Fluorescence spectra of **4.42ab** in THF/water mixtures with different water fractions (f_w). Inset: fluorescence photograph under 365 nm UV irradiation.

Next, we proposed reaction pathways of the present annulation reaction between 1-halo-8-arylnaphthalene and diarylacetylene are shown in Scheme 4.21. The first step is the oxidative addition of the C-Br of **4.40a** to Pd^0 and subsequent halide abstraction by Ag_2CO_3, leads to a naphthylpalladium species **A** (X = carbonate). Insertion of alkyne **4.41a** into **A** followed by intramolecular C-H palladation of the alkenylpalladium species **B**, presumably via the concerted metalation-deprotonation mechanism, would generate an eight-membered palladacycle **C**. Lastly, reductive elimination of intermediate **C** would produce the heptagon product **3** and regenerate the Pd^0. On the other hand, the species **A** could also undergo intramolecular C-H palladation to generate a six-membered palladacycle **D**, which upon reductive elimination to give fluoranthene **4.43**. Intermediate **D** could also undergo alkyne insertion into either of the Pd-C bonds, leading to **C** or its isomer.

Scheme 4.21. Proposed reaction mechanism

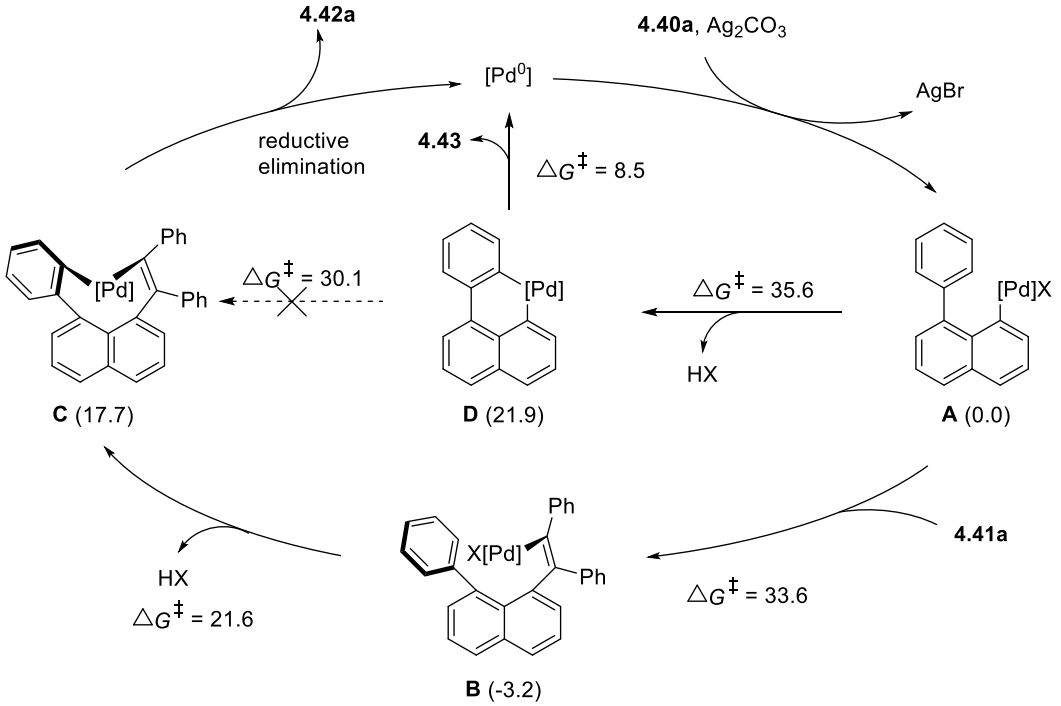

Relative energies (in parentheses) and activation energies (kcal mol^{-1}) were calculated for a model system with [Pd] = $PdP(4\text{-}ClC_6H_4)_3$ and X = OAc.

To get insight of the feasibility of the key steps in the catalytic cycle, we performed DFT calculation (PCM(DCE)-M06L/def2-TZVP//B3LYP(D3)/631LAN) starting from a model 8-phenylnaphthylpalladium complex **A** bearing $P(4\text{-}ClC_6H_4)_3$ and acetate ligand (Figure 4.9 and Figure 4.10). Insertion of diphenylacetylene into **A** required an activation energy ($\Delta G^{\ddagger}$) of 33.6 kcal mol^{-1} (**TS1**), which is slightly lower than that of intramolecular C-H palladation of **A** ($\Delta G^{\ddagger}$ = 35.6 kcal mol^{-1}) (**TS4**). The alkyne insertion was exergonic by 3.2 kcal mol^{-1} (**CP3**). The activation energy of C-H palladation of **B** ($\Delta G^{\ddagger}$ = 21.6 kcal mol^{-1}) (**TS2**) and reductive elimination of **C** ($\Delta G^{\ddagger}$ = 1.7 kcal mol^{-1}) (**CP4**) occurred with low barriers. The formation of **D** was endergonic by 21.9 kcal mol^{-1} (**CP7**). In contrast, reductive elimination of **D** was feasible ($\Delta G^{\ddagger}$ = 8.5 kcal mol^{-1}) (**TS5**), alkyne insertion into **D** required an exceedingly higher barrier ($\Delta G^{\ddagger}$ = 30.1 kcal mol^{-1}) (**TS6**). Thus, **D** is unlikely to be responsible

for the product **4.42a**, and the selectivity between **4.42a** and **4.43** would be determined by the competition between alkyne insertion and C-H palladation pathways of **A**.

Summary of Reaction Pathways, Energy Diagrams and Representative Structures

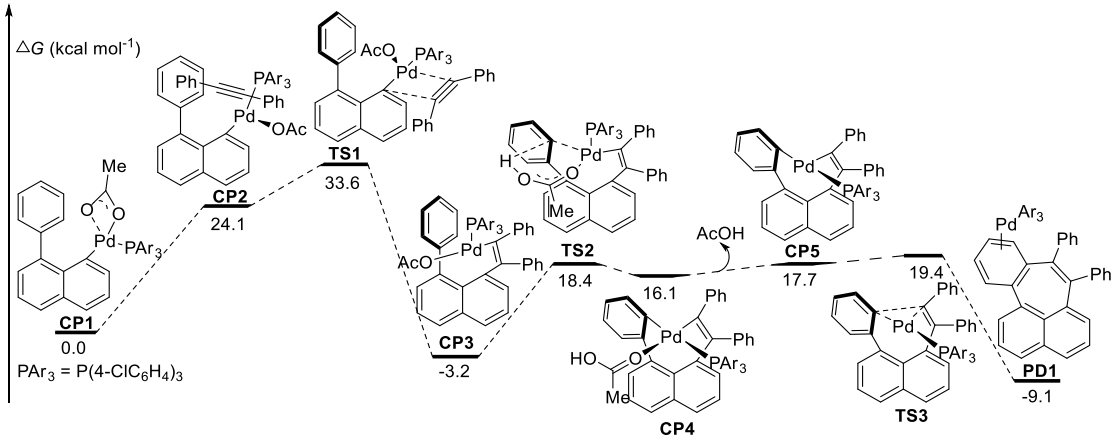

Figure 4.9. Free energy diagram for the annulation of 8-phenylnaphth-1-ylpalladium species with diphenylacetylene (PCM(DCE)-M06L/def2-TZVP//B3LYP(D3)/631LAN).

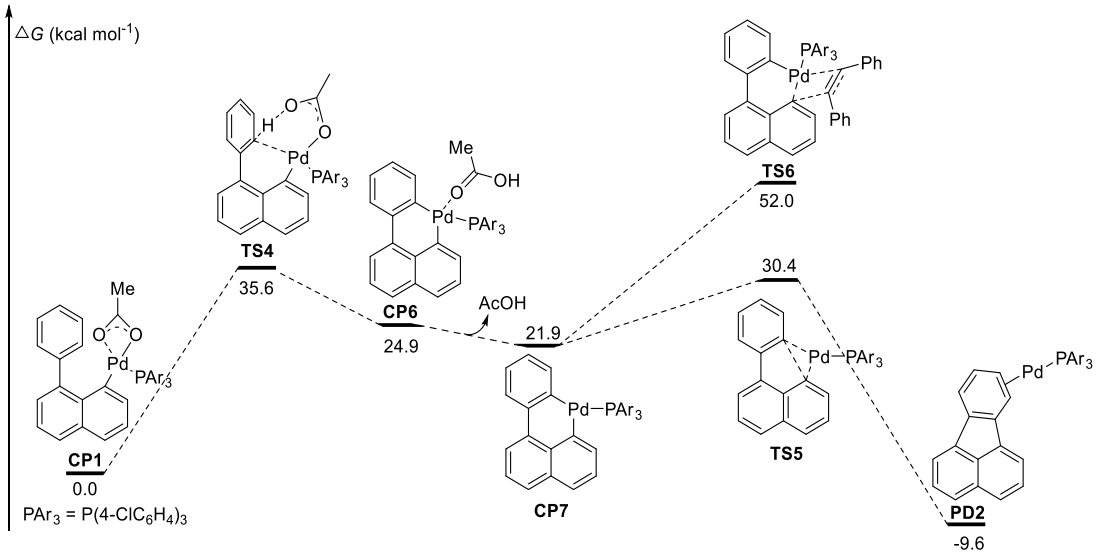

Figure 4.10. Free energy diagram for the conversion of 8-phenylnaphth-1-ylpalladium species to fluoranthene (PCM(DCE)-M06L/def2-TZVP//B3LYP(D3)/631LAN).

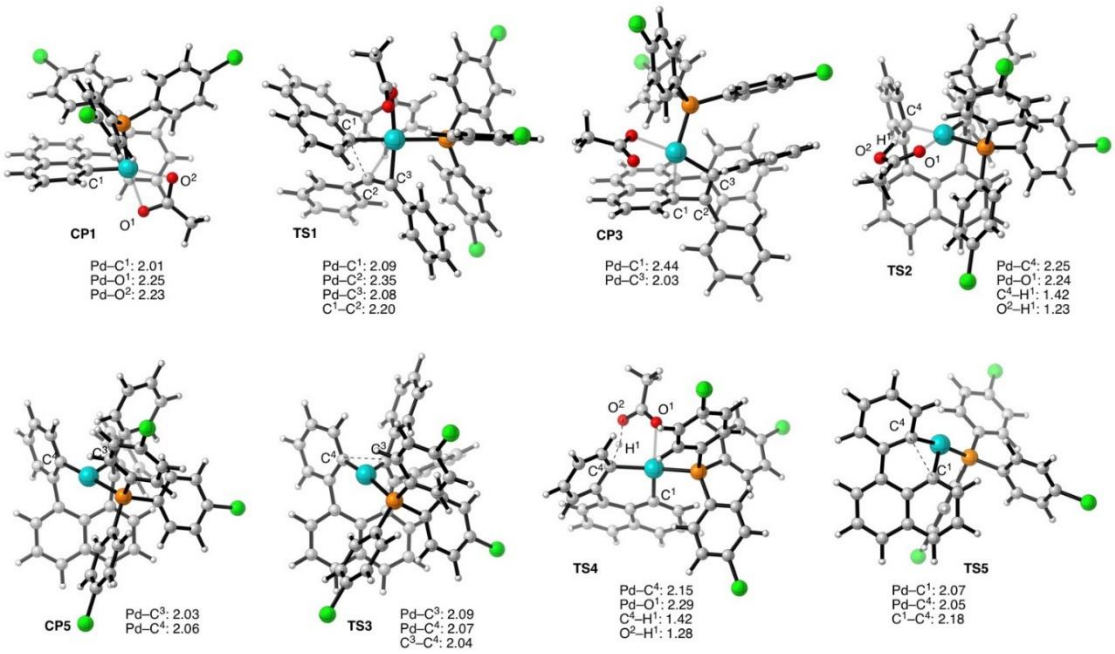

Figure 4.11. Structures of representative intermediates and transition states (color code: turquoise, Pd; orange, P; green, Cl; red, O; grey, C; white, H). Bond lengths are given in Å.

In reference with this implication, the reaction of pentadeuterated substrate [D_5]-**4.40a** and **4.41a** using $AsPh_3$ or P(4-ClC_6H_4)$_3$ resulted in markedly diminished yield of **4.43** (Scheme 4.22), compared with the reaction of parent **4.40a** (Table 4.1, entries 3 and 4).

Scheme 4.22. Annulation of pentadeuterated substrate [D_5]-**4.40a** with **4.41a**.

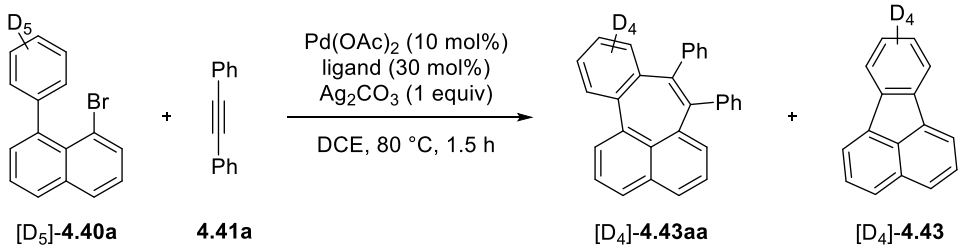

[D_5]-**4.40a** **4.41a** [D_4]-**4.43aa** [D_4]-**4.43**

ligand = $AsPh_3$	41%	6%
ligand = $P(4\text{-}ClC_6H_4)_3$	81%	0%

4.3 Conclusion

In summary, we have developed a versatile palladium-catalyzed [5 + 2] annulation reaction between 1-halo-arynaphthalenes and diarylacetylenes with moderate to good yield. The reaction represents a rare example of direct access of heptagons from simple readily available aromatic precursors, enabling facile preparation of polyaromatic hydrocarbons with warped geometries. The present protocol also provides an opportunity to access novel two-fold heptagon scaffolds. The distinctly emissive behavior of the heptagons in solid state might lead to the development of new materials for optoelectronic devices.

4.4 Experimental Section

Materials and Methods

General. All reactions dealing with air- or moisture-sensitive compound were performed by standard Schlenk techniques in oven-dried reaction vessels under nitrogen atmosphere. Analytical thin-layer chromatography (TLC) was performed on Merck 60 F254 silica gel plates. Flash column chromatography was performed using 40-63 μm silica gel (Si 60, Merck). Preparative HPLC was performed on a Japan

Analytical Industry LC-9110NEXT system equipped with GPC columns JAIGEL-1H and JAIGEL-2H and a UV detector using chloroform as an eluent. ^{1}H and ^{13}C nuclear magnetic resonance (NMR) spectra were recorded on JEOL ECA-400 (400 MHz) or Bruker AV-400 (400 MHz) or Bruker AV-500 (500 MHz) NMR spectrometers. ^{1}H and ^{13}C NMR spectra are reported in parts per million (ppm) downfield from an internal standard, tetramethylsilane (0 ppm) and $CHCl_3$ (77.0 ppm), respectively. Gas chromatographic (GC) analysis was performed on a Shimadzu GC-2010 system equipped with an FID detector and a capillary column, DB-5 (Agilent J&W, 0.25 mm i.d. x 30 m, 0.25 μm film thickness). High-resolution mass spectra (HRMS) were obtained with a Q-Tof Premier LC HR mass spectrometer. Melting points were determined using a capillary melting point apparatus and are uncorrected. UV-vis and fluorescence spectra were recorded on Shimadzu UV-1800 spectrophotometer and Shimadzu RF-5301PC spectrofluorophotometer, respectively.

Materials. Unless otherwise noted, commercial reagents were purchased from Aldrich, Alfa Aesar, TCI and other commercial suppliers and were used as received. 1,2-Dichloroethane (DCE) was distilled over calcium hydride. 1-Halo-8-arylnaphthalenes (**4.40a**–**4.40j**) were synthesized according to the literature procedure by Suzuki–Miyaura coupling between 1,8-dihalonaphthalene and arylboronic acid (Figure 4.12).[57] The ^{1}H and ^{13}C NMR spectra of known 1-halo-8-arylnaphthalenes showed good agreement with the literature data.[58-59] Diarylalkynes except **4.41a** were prepared according to the literature procedure,[60] and their ^{1}H and ^{13}C NMR spectra showed good agreement with the literature data.[60-64]

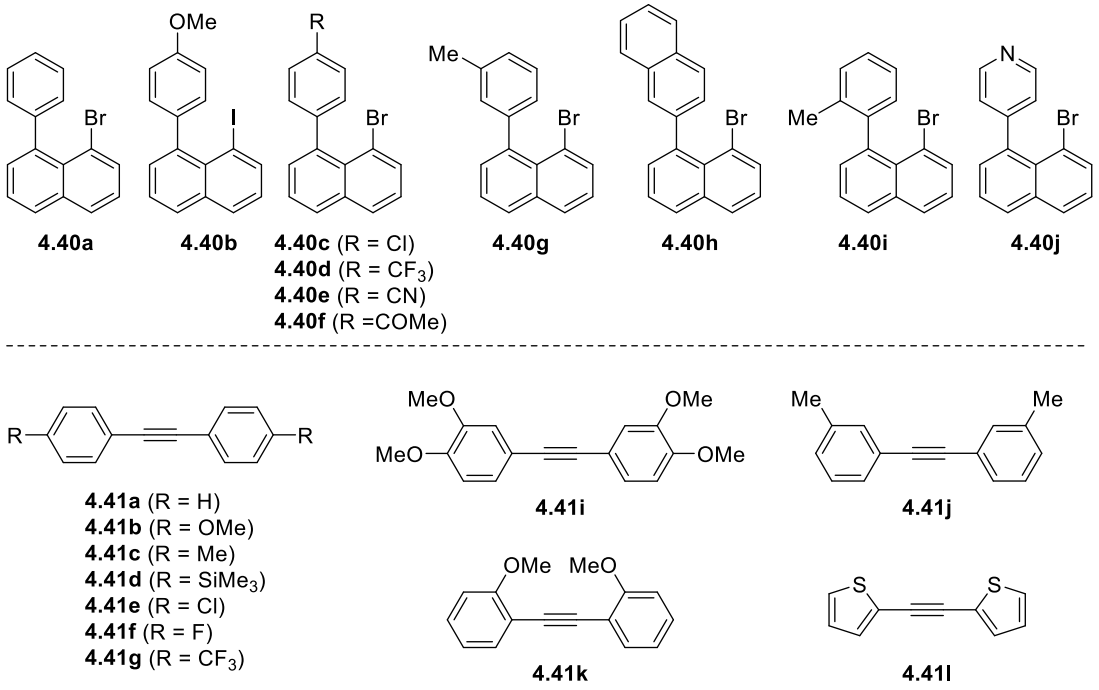

Figure 4.12. 1-Halo-8-arylnaphthalenes and diarylalkynes used in this study.

The characterization data for new 1-halo-8-arylnaphthalenes, and the synthesis and characterization of **5** and **7** are described below.

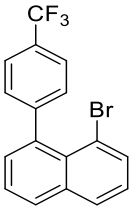

1-Bromo-8-(4-(trifluoromethyl)phenyl)naphthalene (4.40d): The reaction was performed on 1.7 mmol scale. White solid (331 mg, 55%, eluent: hexane/EtOAc = 58/2); m.p. 87-89 °C; ^{1}H NMR (400 MHz, $CDCl_3$): δ 7.93-7.90 (m, 2H), 7.80 (dd, *J* = 7.4, 1.2 Hz, 1H), 7.65 (d, *J* = 8.0 Hz, 2H), 7.52 (dd, *J* = 7.1, 1.0 Hz, 1H), 7.46 (d, *J* = 7.9 Hz, 2H), 7.40 (dd, *J* = 7.1, 1.4 Hz, 1H), 7.32 (dd, *J* = 8.0, 0.4 Hz, 1H); ^{13}C NMR (100 MHz, $CDCl_3$) δ 146.7, 138.9, 136.1, 134.0, 131.2, 130.4, 129.6, 129.4 (d, *J* = 2.0

Hz), 129.1 (q, J_{CF} = 32.1 Hz), 129.0, 126.4, 125.3, 124.4 (q, J = 7.4, 3.7 Hz), 120.5 (q, J_{CF} = 270.3 Hz), 119.8; HRMS (ESI) Calcd for $C_{17}H_{11}BrF_3$ $[M + H]^+$ 350.9996, found 350.9957..

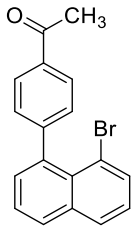

1-(4-(8-Bromonaphthalen-1-yl)phenyl)ethan-1-one (4.40f): The reaction was performed on 1.5 mmol scale. White solid (262 mg, 49%, eluent: hexane/EtOAc = 97/3); m.p. 123-125 °C; ^{1}H NMR (300 MHz, $CDCl_3$): δ 8.00 (d, J = 8.1 Hz, 2H), 7.91 (d, J = 8.2 Hz, 2H), 7.79 (app. t, J = 6.6 Hz, 1H), 7.52 (app. t, J = 7.4 Hz, 1H), 7.46-7.43 (m, 2H), 7.41 (dd, J = 7.1, 1.2 Hz, 1H), 7.32 (app. t, J = 7.9 Hz, 1H), 2.68 (s, 3H); ^{13}C NMR (100 MHz, $CDCl_3$) δ 198.0, 148.1, 139.3, 136.1, 135.8, 133.9, 131.0, 130.4, 129.46, 129.40, 129.0, 127.5, 126.3, 125.3, 119.9, 26.7; HRMS (ESI) Calcd for $C_{18}H_{14}BrO$ $[M + H]^+$ 325.0228, found 325.0222.

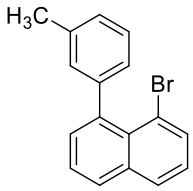

1-Bromo-8-(*m*-tolyl)naphthalene (4.40g): The reaction was performed on 1.7 mmol scale. Colorless oil (216 mg, 43%, eluent: hexane/EtOAc = 49/1); ^{1}H NMR (300 MHz, $CDCl_3$): δ 7.94-7.91 (m, 2H), 7.83 (d, J = 7.4 Hz, 1H), 7.57-7.47 (m, 2H), 7.35 (d, J = 7.7 Hz, 1H), 7.31 (d, J = 1.2 Hz, 1H), 7.23-7.18 (m, 3H), 2.45 (s, 3H); ^{13}C NMR (100 MHz, $CDCl_3$) δ 142.6, 140.5, 136.8, 136.0, 133.7, 131.06, 131.02, 129.6, 128.82,

128.68, 127.6, 127.28, 127.27, 125.9, 125.2, 120.2, 21.4; HRMS (ESI) Calcd for $C_{17}H_{14}Br$ $[M + H]^+$ 297.0279, found 297.0290.

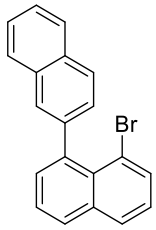

8-Bromo-1,2'-binaphthalene (4.40h): The reaction was performed on 2.0 mmol scale. Light yellow oil (398 mg, 60%, eluent: hexane/EtOAc = 49/1); ^{1}H NMR (300 MHz, $CDCl_3$): δ 7.93-7.78 (m, 7H), 7.57-7.48 (m, 5H), 7.32 (app. t, *J* = 7.9 Hz, 1H); ^{13}C NMR (100 MHz, $CDCl_3$) δ 140.7, 140.4, 136.2, 133.8, 133.0, 132.5, 131.6, 129.8, 129.2, 129.02, 128.97, 128.4, 128.1, 127.8, 126.6, 126.17, 126.16, 125.9, 125.4, 120.3; HRMS (ESI) Calcd for $C_{20}H_{14}Br$ $[M + H]^+$ 333.0279, found 333.0277.

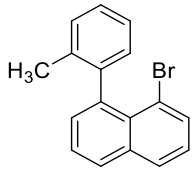

1-Bromo-8-(*o*-tolyl)naphthalene (4.40i): The reaction was performed on 1.5 mmol scale. Colorless oil (216 mg, 48%, eluent: hexane/EtOAc = 49/1); ^{1}H NMR (400 MHz, $CDCl_3$): δ 7.92 (d, *J* = 8.4 Hz, 2H), 7.81 (dd, *J* = 7.2, 1.2 Hz, 1H), 7.55 (app. t, *J* = 7.2 Hz, 1H), 7.39 (dd, *J* = 7.0, 1.2 Hz, 1H), 7.36-7.31 (m, 2H), 7.29-7.28 (m, 1H), 7.24-7.21 (m, 2H), 2.01 (s, 3H); ^{13}C NMR (100 MHz, $CDCl_3$) δ 142.5, 139.6, 137.3, 135.9, 133.6, 130.6, 130.3, 129.7, 129.16, 129.14, 128.96, 127.4, 125.9, 125.6, 125.0, 120.0, 20.5; HRMS (ESI) Calcd for $C_{17}H_{14}Br$ $[M + H]^+$ 297.0279, found 297.0282.

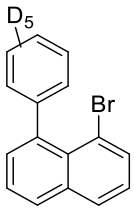

1-Bromo-8-(phenyl-*d*5)naphthalene ([D5]- 4.40a): The reaction was performed on 2.0 mmol scale. Colorless oil (292 mg, 51%, eluent: hexane/EtOAc = 49/1); ^{1}H NMR (300 MHz, $CDCl_3$): δ 7.91-7.87 (m, 2H), 7.79 (dd, *J* = 7.4, 1.2 Hz, 1H), 7.52 (app. t, *J* = 7.1 Hz, 1H), 7.47 (dd, *J* = 7.1, 1.5 Hz, 1H), 7.30 (app. t, *J* = 7.9 Hz, 1H); ^{13}C NMR (100 MHz, $CDCl_3$) δ 142.7, 140.4, 136.2, 135.5, 133.8, 131.25, 130.16, 129.84, 129.69, 128.9, 127.3, 126.5, 126.1, 125.4, 120.2; HRMS (ESI) Calcd for $C_{16}H_7D_5Br$ $[M + H]^+$ 288.0431, found 288.0436.

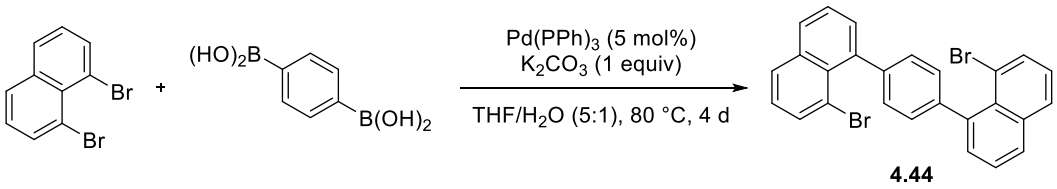

1,4-Bis(8-bromonaphthalen-1-yl)benzene (4.44): In a 100 mL three-necked flask, 1,8-dibromonaphthalene (500 mg, 1.50 mmol), 1,4-phenylenediboronic acid (124 mg, 0.75 mmol), and $Pd(PPh_3)_4$ (86.7 mg, 0.075 mmol) were dissolved in a mixture of degassed THF (30 mL) and aqueous K_2CO_3 (1.50 mmol in 6 mL of water). The mixture was stirred at 80 °C for 4 days. The reaction mixture was extracted three times with Et_2O, and the combined organic fractions were washed three times with water and dried over $MgSO_4$. The solvent was removed under reduced pressure. The crude product was purified by silica gel column chromatography (eluent: hexane/CH_2Cl_2 =

20/1) to afford **4.44** as a white solid (153 mg, 42%). m.p. 180.3–184.9 °C; ^{1}H NMR (400 MHz, $CDCl_3$): δ 7.95–7.87 (m, 4H), 7.82 (t, *J* = 7.4 Hz, 2H), 7.65–7.45 (m, 4H), 7.44–7.40 (m, 2H), 7.38–7.28 (m, 4H); ^{13}C NMR (100 MHz, $CDCl_3$) δ 142.2, 141.9, 140.6, 136.3, 133.9, 131.8, 129.3, 129.0, 128.9, 126.2, 125.5, 120.8, 120.4; HRMS (ESI) Calcd for $C_{26}H_{17}Br_2$ $[M + H]^+$ 486.9697, found 486.9686.

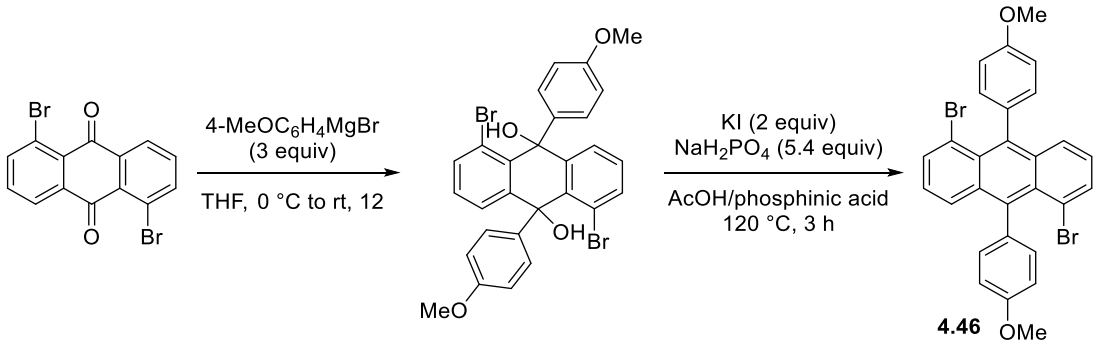

1,5-Dibromo-9,10-bis(4-methoxyphenyl)anthracene (4.46): The compound **4.46** was synthesized according to the literature procedure.[65] To a stirred solution of 1,8-dibromoanthraquinone (220 mg, 0.60 mmol) in anhydrous THF (3 mL), 4-methoxyphenylmagnesium bromide (1.11 M in THF, 1.62 mL, 1.80 mmol) was added dropwise at 0 °C. The reaction mixture was allowed to warm to room temperature and stirred for 12 h. The reaction was quenched with water at 0 °C and extracted with EtOAc (3 × 50 mL). The combined organic layers were washed with brine, dried over $MgSO_4$ and concentrated under reduced pressure. Silica gel column chromatography (eluent: EtOAc/hexane = 1:4) of the crude product afforded 1,5-dibromo-9,10-bis(4-methoxyphenyl)-9,10-dihydroanthracene-9,10-diol as an off-white solid (134 mg, 39%). ^{1}H NMR (400 MHz, $CDCl_3$) δ 8.06 (dd, *J* = 8.2, 0.9 Hz, 2H), 7.48 (dd, *J* = 7.7, 0.8 Hz, 2H) 7.24-7.20 (m, 6H), 6.76-6.74 (m, 4H), 4.49 (s, 2H), 3.76 (s, 6H); ^{13}C NMR (100 MHz, $CDCl_3$) δ 158.6, 143.3, 139.1, 135.0, 134.5, 129.6, 128.4, 127.7,

122.0, 113.4, 74.9, 55.2; HRMS (ESI) Calcd for $C_{28}H_{23}Br_2O_4$ $[M + H]^+$ 580.9963, found 580.9966.

In a 10 mL round bottom flask, 1,5-dibromo-9,10-bis(4-methoxyphenyl)-9,10-dihydroanthracene-9,10-diol (175 mg, 0.30 mmol) was dissolved in 2.0 mL of glacial acetic acid, followed by KI (100 mg, 0.60 mmol) and monosodium phosphate (172 mg, 1.62 mmol) then refluxed at 120 °C for 2 h. At this temperature, 50% phosphoric acid (0.6 mL) was added and kept refluxing for another 1 h. The reaction mixture was allowed to cool to room temperature and quenched with saturated NH_4Cl. The resulting reaction mixture was extracted with EtOAc (3 × 30 mL). The combined organic layers were dried over $MgSO_4$, filtered, and concentrated under reduced pressure. The crude product was purified by silica gel column chromatography (eluent: EtOAc/hexane = 1:49) to affords the desired product **4.46** as a yellow solid (66.7 mg, 41%); ^{1}H NMR (400 MHz, $CDCl_3$): δ 7.78-7.73 (m, 4H), 7.29-7.27 (m, 4H), 7.09-7.05 (m, 6H), 3.95 (s, 6H); ^{13}C NMR (100 MHz, $CDCl_3$) δ 159.7, 137.6, 134.0, 133.9, 133.7, 132.1, 128.2, 128.0, 125.0, 120.1, 113.4, 55.5; HRMS (ESI) Calcd for $C_{28}H_{21}Br_2O_2$ $[M + H]^+$ 546.9908, found 546.9918.

Pd-Catalyzed Annulation of 1-Halo-8-arylnaphthalenes and Alkynes

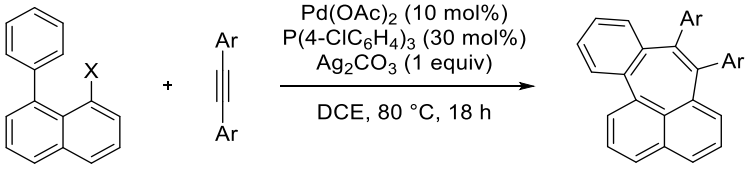

Typical procedure: Ag_2CO_3 (27.5 mg, 0.10 mmol) was placed in a 10 mL Schlenk tube, which was then dried at 150 °C under vacuum for 3 h. Upon cooling, 1-bromo-8-

arylnaphtalene (0.20 M solution in DCE prepared in a separated Schlenk tube, 0.50 mL, 0.10 mmol), diarylacetylene (0.20 mmol), $Pd(OAc)_2$ (2.2 mg, 0.010 mmol), and $P(4\text{-}ClC_6H_4)_3$ (11.0 mg, 0.030 mmol) were added to the Schlenk tube under N_2 atmosphere. The Schlenk tube was sealed, and the resulting mixture was stirred at 80 °C for 18 h. The reaction mixture was cooled to room temperature, and then concentrated under reduced pressure. The organic residue was dissolved in CH_2Cl_2 and subjected to column chromatography on silica gel (eluent: hexane/CH_2Cl_2 or hexane/EtOAc) to afford the desired product.

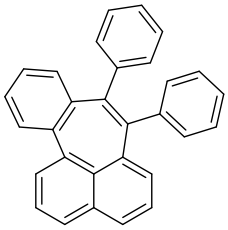

7,8-Diphenylbenzo[4,5]cyclohepta[1,2,3-*de*]naphthalene (4.42aa): Light yellow solid (30.0 mg, 79%, eluent: hexane/CH_2Cl_2 = 40/1); m.p. 210.7–212.6 °C; ^{1}H NMR (400 MHz, $CDCl_3$): δ 7.75-7.73 (m, 2H), 7.64–7.52 (m, 1H), 7.36–6.91 (m, 17H); ^{13}C NMR (100 MHz, $CDCl_3$) δ 145.1, 144.3, 143.4, 141.1, 140.3, 140.2, 139.1, 138.3, 136.5, 133.8, 133.3, 131.4, 130.8, 130.4, 128.8, 127.6, 127.47, 127.45, 127.3, 126.9, 126.8, 126.0, 125.85, 125.77, 124.9 (one of the aromatic ^{13}C peaks originates from overlapped signals); HRMS (ESI) Calcd for $C_{30}H_{21}$ $[M + H]^+$ 381.1643, found 381.1637.

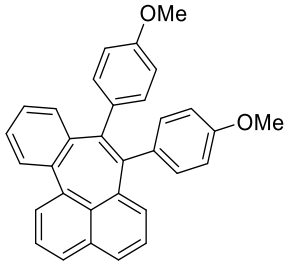

7,8-Bis(4-methoxyphenyl)benzo[4,5]cyclohepta[1,2,3-*de*]naphthalene (4.42ab): Light yellow solid (33.0 mg, 75%, eluent: hexane/EtOAc = 30/1); m.p. 201.5–205.2 °C; ^{1}H NMR (400 MHz, $CDCl_3$): δ 7.76–7.67 (m, 2H), 7.58–7.50 (m, 2H), 7.33–7.24 (m, 1H), 7.22–7.03 (m, 7H), 6.83-6.81 (m, 2H), 6.73–6.64 (m, 2H), 6.64–6.57 (m, 2H), 3.72 (s, 3H), 3.70 (s, 3H); ^{13}C NMR (100 MHz, $CDCl_3$) δ 157.4, 157.3, 144.1, 141.0, 140.2, 140.1, 139.6, 138.4, 138.1, 137.1, 136.2, 133.6, 133.2, 131.8, 131.4, 130.9, 128.6, 127.4, 126.8, 126.6, 125.9, 124.9, 112.9, 112.7, 55.02, 55.00 (two of the aromatic ^{13}C peaks originate from overlapped signals); HRMS (ESI) Calcd for $C_{32}H_{25}O_2$ $[M + H]^+$ 441.1855, found 441.1847.

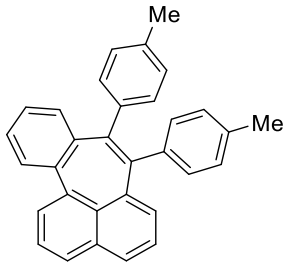

7,8-Di-*p*-tolylbenzo[4,5]cyclohepta[1,2,3-*de*]naphthalene (4.42ac): brown solid (25.7 mg, 63%, eluent: hexane/CH_2Cl_2 = 40/1); m.p. 205.8–208.4 °C; ^{1}H NMR (400 MHz, $CDCl_3$): δ 7.73-7.71 (m, 2H), 7.60–7.50 (m, 2H), 7.31–7.22 (m, 1H), 7.21–7.02 (m, 7H), 6.93-6.91 (m, 2H), 6.87-6.85 (m, 2H), 6.81-6.79 (m, 2H), 2.22 (s, 3H), 2.19 (s, 3H); ^{13}C NMR (100 MHz, $CDCl_3$) δ 144.1, 142.4, 141.0, 140.6, 140.20, 140.17, 139.5, 138.4, 136.9, 135.1, 135.0, 133.6, 133.2, 131.3, 130.9, 130.6, 130.2, 128.6,

128.1, 128.0, 127.34, 127.33, 126.8, 126.6, 125.8, 124.9, 21.12, 21.11; HRMS (ESI) Calcd for $C_{32}H_{25}$ $[M + H]^+$ 409.1956, found 409.1951.

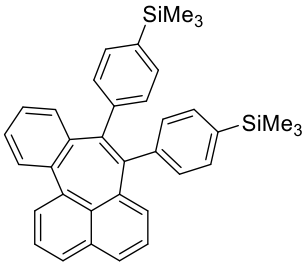

(Benzo[4,5]cyclohepta[1,2,3-*de*]naphthalene-7,8-diylbis(4,1-phenylene))bis(trimethylsilane) (4.42ad): Light yellow solid (30.4 mg, 58%, eluent: hexane/CH_2Cl_2 = 50/1); m.p. 206.8–210.4 °C; ^{1}H NMR (400 MHz, $CDCl_3$): δ 7.74-7.72 (m, 2H), 7.61–7.51 (m, 2H), 7.34–7.25 (m, 1H), 7.24–7.13 (m, 8H), 7.10-7.08 (m, 3H), 6.88-6.86 (m, 2H), 0.15 (s, 9H), 0.14 (s, 9H); ^{13}C NMR (100 MHz, $CDCl_3$) δ 145.5, 144.6, 143.8, 141.2, 140.6, 140.2, 139.1, 138.6, 137.40, 137.37, 136.5, 133.9, 133.5, 132.4, 132.2, 131.5, 130.9, 130.2, 129.8, 128.9, 127.8, 127.6, 127.0, 126.9, 126.1, 125.1, -1.1 (6C); HRMS (ESI) Calcd for $C_{36}H_{37}Si_2$ $[M + H]^+$ 525.2434, found 525.2435.

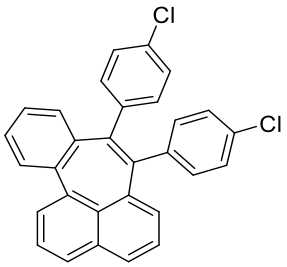

7,8-Bis(4-chlorophenyl)benzo[4,5]cyclohepta[1,2,3-*de*]naphthalene (4.42ae): brown solid (23.7 mg, 53%, eluent: hexane/CH_2Cl_2 = 40/1); m.p. 203.2–207.4 °C; ^{1}H NMR (400 MHz, $CDCl_3$): δ 7.81–7.67 (m, 2H), 7.63–7.51 (m, 2H), 7.33-7.30 (m, 1H), 7.23–6.93 (m, 11H), 6.85-6.83 (m, 2H); ^{13}C NMR (100 MHz, $CDCl_3$) δ 143.5, 143.3,

141.5, 141.2, 140.1, 139.6, 138.4, 138.0, 135.9, 133.9, 133.3, 132.1, 132.0, 131.9, 131.6, 131.4, 130.7, 129.1, 128.0, 127.8, 127.6, 127.2, 127.0, 126.1, 124.9 (one of the aromatic ^{13}C peaks originates from overlapped signals); HRMS (ESI) Calcd for $C_{30}H_{19}Cl_2$ $[M + H]^+$ 449.0864, found 449.0852.

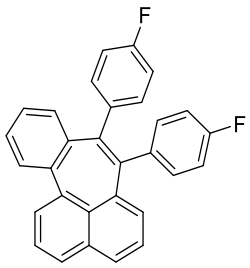

7,8-Bis(4-fluorophenyl)benzo[4,5]cyclohepta[1,2,3-*de*]naphthalene (4.42af): Light yellow solid (24.9 mg, 60%, eluent: hexane/CH_2Cl_2 = 40/1); m.p. 212.8–215.3 °C; ^1H NMR (400 MHz, $CDCl_3$): δ 7.80–7.69 (m, 2H), 7.63–7.52 (m, 2H), 7.33-7.31 (m, 1H), 7.22–7.00 (m, 7H), 6.92–6.73 (m, 6H); ^{13}C NMR (101 MHz, $CDCl_3$) δ 161.0 (d, $^1J_{CF}$ = 246.5 Hz), 160.9 (d, $^1J_{CF}$ = 246.3 Hz), 143.8, 141.1, 141.0 (d, $^4J_{CF}$ = 3.6 Hz), 140.1, 139.9, 139.2 (d, $^4J_{CF}$ = 3.7 Hz), 138.7, 138.1, 136.2, 133.9, 133.3, 132.2 (d, $^3J_{CF}$ = 7.9 Hz), 131.8 (d, $^3J_{CF}$ = 8.0 Hz), 131.4, 130.7, 129.0, 127.7, 127.5, 127.0, 126.9, 126.0, 124.9, 114.6 (d, $^2J_{CF}$ = 21.3 Hz), 114.5 (d, $^2J_{CF}$ = 21.4 Hz); ^{19}F NMR (282 MHz, $CDCl_3$) δ -116.19, -116.23; HRMS (ESI) Calcd for $C_{30}H_{19}F_2$ $[M + H]^+$ 417.1455, found 417.1467.

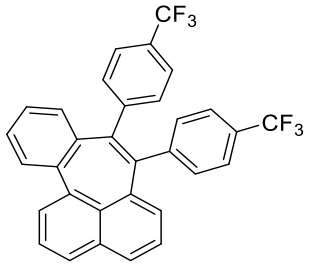

7,8-Bis(4-(trifluoromethyl)phenyl)benzo[4,5]cyclohepta[1,2,3-*de*]naphthalene (4.42ag): yellow solid (28.4 mg, 55%, eluent: hexane/CH_2Cl_2 = 30/1); m.p. 220.5–223.7 °C; ^{1}H NMR (400 MHz, $CDCl_3$): δ 7.77-7.75 (m, 2H), 7.66–7.55 (m, 2H), 7.41-7.39 (m, 2H), 7.36–7.31 (m, 3H), 7.31–7.24 (m, 2H), 7.23–7.14 (m, 2H), 7.14–7.10 (m, 1H), 7.05-7.03 (m, 2H), 7.01–6.95 (m, 2H); ^{13}C NMR (100 MHz, $CDCl_3$) δ 148.1, 146.4, 143.6, 141.3, 140.1, 139.6, 137.89, 137.86, 135.3, 134.0, 133.4, 131.5, 131.0, 130.60, 130.58, 129.4, 128.5 (q, $^2J_{CF}$ = 32.5 Hz), 128.4 (q, $^2J_{CF}$ = 32.6 Hz), 128.1, 127.7, 127.5, 127.1, 126.2, 125.0, 124.8 (q, $^3J_{CF}$ = 3.8 Hz), 124.6 (q, $^3J_{CF}$ = 3.7 Hz), 124.00 (q, $^1J_{CF}$ = 273.1 Hz), 123.97 (q, $^1J_{CF}$ = 273.0 Hz); ^{19}F NMR (373 MHz, $CDCl_3$) δ -62.5; HRMS (ESI) Calcd for $C_{32}H_{19}F_6$ $[M + H]^+$ 517.1391, found 517.1369.

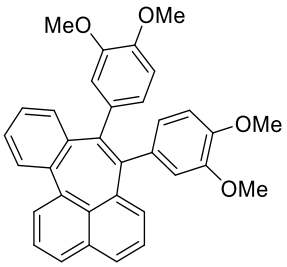

7,8-Bis(3,4-dimethoxyphenyl)benzo[4,5]cyclohepta[1,2,3-*de*]naphthalene (4.42ai): The reaction was performed on a 0.6 mmol scale. Yellow solid (167 mg, 57%, eluent: hexane/EtOAc = 2:1); m.p. 140-142 °C; ^{1}H NMR (400 MHz, $CDCl_3$): δ 7.74-7.71 (m, 2H), 7.58-7.54 (m, 2H), 7.31-7.27 (m, 1H), 7.20-7.17 (m, 2H), 7.16-7.15 (m, 2H), 7.08 (d, *J* = 7.8 Hz, 1H), 6.73 (dd, *J* = 8.2, 1.8 Hz, 1H), 6.68-6.61 (m, 3H), 6.54 (d, *J* = 8.0 Hz, 1H), 6.41 (s, 1H), 3.80 (s, 3H), 3.78 (s, 3H), 3.72 (s, 3H), 3.65 (s, 3H); ^{13}C NMR (100 MHz, $CDCl_3$) δ 148.1, 147.8, 147.0, 144.1, 140.9, 140.3, 140.1, 139.4, 138.1, 136.6, 136.3, 133.7, 133.3, 131.2, 130.7, 128.8, 127.5, 126.86, 126.82, 125.9, 125.0, 123.3, 123.0, 114.6, 114.1, 110.2, 110.1, 55.86, 55.84, 55.64; HRMS (ESI) Calcd for $C_{34}H_{28}O_4$ $[M + H]^+$ 501.2066, found 501.2066.

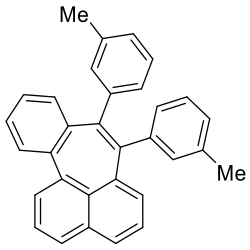

7,8-Di-*m*-tolylbenzo[4,5]cyclohepta[1,2,3-*de*]naphthalene (4.42aj): Yellow solid (27.5 mg, 67%, eulent: hexane/EtOAc = 50/1); m.p. 180-182 °C; ^{1}H NMR (400 MHz, $CDCl_3$): δ 7.73 (d, *J* = 7.6 Hz, 2H), 7.58-7.54 (m, 2H), 7.30-7.27 (m, 1H), 7.20-7.11 (m, 4H), 7.08 (d, *J* = 7.9 Hz, 1H), 7.01-6.91 (m, 4H), 6.83-6.70 (m, 4H), 2.19 (s, 3H), 2.15 (s, 3H); ^{13}C NMR (100 MHz, $CDCl_3$) δ 145.0, 144.3, 143.2, 141.0, 140.3, 140.1, 139.3, 138.38, 138.37, 136.67, 136.58, 136.55, 133.7, 133.3, 131.6, 131.3, 131.2, 130.8, 128.7, 127.9, 127.5, 127.4, 127.1, 126.9, 126.8, 126.7, 126.43, 126.36, 125.9, 124.9, 21.26, 21.24; HRMS (ESI) Calcd for $C_{32}H_{24}$ $[M + H]^+$ 409.1956, found 409.1956.

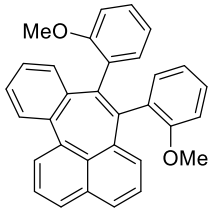

7,8-Bis(2-methoxyphenyl)benzo[4,5]cyclohepta[1,2,3-*de*]naphthalene (4.42ak): Light yellow solid (33.9 mg, 77%, eluent: hexane/EtOAc = 40/1); m.p. 195.6–199.5 °C; ^{1}H NMR (400 MHz, $CDCl_3$): δ 7.76–7.66 (m, 2H), 7.58–7.49 (m, 2H), 7.33–7.19 (m, 2H), 7.18–7.03 (m, 6H), 7.01–6.94 (m, 2H), 6.77–6.64 (m, 2H), 6.62–6.56 (m, 2H), 3.71 (s, 3H), 3.58 (s, 3H); ^{13}C NMR (100 MHz, $CDCl_3$) δ 156.0, 155.9, 141.2, 140.9, 140.1, 138.6, 138.5, 137.1, 136.3, 135.5, 133.7, 133.3, 133.1, 130.0, 129.71, 129.68, 129.4, 128.6, 128.0, 127.7, 127.4, 127.2, 126.9, 126.4, 125.7, 125.0, 119.6,

119.5, 110.3, 55.2, 55.1 (one of the aromatic ^{13}C peaks originates from overlapped signals); HRMS (ESI) Calcd for $C_{32}H_{25}O_2$ $[M + H]^+$ 441.1855, found 441.1868.

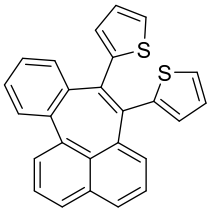

2,2'-(Benzo[4,5]cyclohepta[1,2,3-*de*]naphthalene-7,8-diyl)dithiophene (4.42al): Light yellow oil (27.4 mg, 70%, eluent: hexane/CH_2Cl_2 = 30/1); ^1H NMR (400 MHz, $CDCl_3$): δ 7.75-7.71 (m, 2H), 7.59 (dd, *J* = 7.7, 1.2 Hz, 1H), 7.57–7.52 (m, 1H), 7.38–7.30 (m, 2H), 7.28–7.15 (m, 4H), 7.12 (dd, *J* = 5.0, 1.2 Hz, 1H), 7.02 (dd, *J* = 7.8, 1.0 Hz, 1H), 6.97–6.88 (m, 3H), 6.83 (dd, *J* = 5.2, 3.6 Hz, 1H); ^{13}C NMR (100 MHz, $CDCl_3$) δ 145.8, 144.9, 141.2, 139.7, 138.9, 138.0, 137.5, 136.6, 136.2, 133.5, 133.2, 131.7, 131.4, 130.2, 129.9, 129.3, 127.60, 127.58, 127.2, 126.7, 126.4, 126.12, 126.10, 126.0, 125.8, 125.1; HRMS (ESI) Calcd for $C_{26}H_{17}S_2$ $[M + H]^+$ 393.0772, found 393.0781.

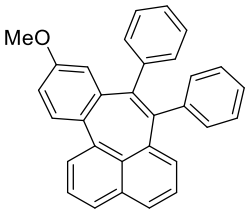

10-Methoxy-7,8-diphenylbenzo[4,5]cyclohepta[1,2,3-*de*]naphthalene (4.42ba): Light yellow solid (27.1 mg, 66%, eluent: hexane/EtOAc = 30/1); m.p. 229.9–230.7 °C; ^1H NMR (400 MHz, $CDCl_3$): δ 7.74–7.63 (m, 2H), 7.60–7.50 (m, 2H), 7.22–6.96 (m, 11H), 6.95–6.90 (m, 2H), 6.87 (dd, *J* = 8.7, 2.8 Hz, 1H), 6.68 (d, *J* = 2.8 Hz, 1H), 3.66 (s, 3H); ^{13}C NMR (101 MHz, $CDCl_3$) δ 158.5, 145.2, 144.5, 143.2, 140.2, 140.0,

139.7, 138.2, 136.4, 135.3, 134.0, 133.4, 131.4, 130.7, 130.4, 127.4, 127.3, 126.90, 126.86, 126.8, 125.94, 125.89, 125.7, 124.8, 116.2, 114.5, 55.1; HRMS (ESI) Calcd for $C_{31}H_{23}O$ $[M + H]^+$ 411.1749, found 411.1738. Recrystallization from EtOAc afforded single crystals of **4.42ba** suitable for X-ray diffraction analysis, which unambiguously confirmed its molecular structure (Scheme 4.18).

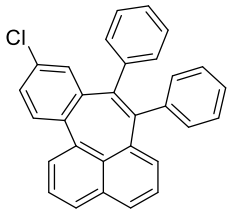

10-Chloro-7,8-diphenylbenzo[4,5]cyclohepta[1,2,3-*de*]naphthalene (4.42ca): Light yellow solid (26.1 mg, 63%, eluent: hexane/CH_2Cl_2 = 30/1); m.p. 210.3–214.5 °C; ^{1}H NMR (400 MHz, $CDCl_3$): δ 7.73 (d, *J* = 8.0 Hz, 1H), 7.67 (d, *J* = 7.1 Hz, 1H), 7.61–7.51 (m, 2H), 7.28–7.20 (m, 1H), 7.21–6.95 (m, 12H), 6.88 (d, *J* = 6.4 Hz, 2H); ^{13}C NMR (100 MHz, $CDCl_3$) δ 145.6, 145.0, 142.6, 140.8, 140.1, 139.7, 139.2, 137.3, 136.3, 135.3, 133.4, 133.3, 131.8, 130.8, 130.4, 130.3, 128.8, 127.8, 127.7, 127.63, 127.60, 127.1, 126.3, 126.1, 126.0, 125.2; HRMS (ESI) Calcd for $C_{30}H_{20}Cl$ $[M + H]^+$ 415.1254, found 415.1247.

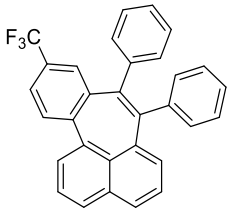

7,8-Diphenyl-10-(trifluoromethyl)benzo[4,5]cyclohepta[1,2,3-*de*]naphthalene (4.42da): White solid (39.3 mg, 85%, eluent: hexane/EtOAc = 48/2); m.p. 220-222 °C; ^{1}H NMR (300 MHz, $CDCl_3$) δ 7.78 (d, *J* = 8.0 Hz, 1H), 7.73 (d, *J* = 7.1 Hz, 1H),

7.61-7.56 (m, 2H), 7.51-7.48 (d, *J* = 8.7 Hz, 1H), 7.37 (s, 1H), 7.22-7.06 (m, 7H), 7.03-6.99 (m, 4H), 6.90 (d, *J* = 6.9 Hz, 2H); ^{13}C NMR (100 MHz, $CDCl_3$) δ 145.8, 144.8, 144.5, 142.4, 140.2, 139.8, 139.2, 137.0, 136.1, 134.3, 133.3, 131.9, 130.7, 130.2, 129.1 (q, J_{CF} = 32.2 Hz), 128.3, 128.2, 127.6, 127.5, 127.5, 127.5, 127.1, 126.3, 126.0, 125.4, 125.2, 125.0 (q, J_{CF} = 7.0, 3.5 Hz), 120.0 (q, J_{CF} = 270.3 Hz; HRMS (ESI) Calcd for $C_{31}H_{20}F_3$ $[M + H]^+$ 449.1517, found 449.1526.

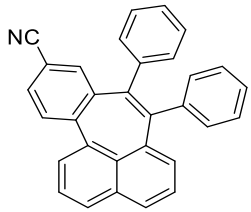

7,8-Diphenylbenzo[4,5]cyclohepta[1,2,3-*de*]naphthalene-10-carbonitrile (4.42ea): Colorless solid (33.1 mg, 82%, eluent: hexane/EtOAc = 9/1), m.p. 189-192 °C; ^{1}H NMR (400 MHz, $CDCl_3$): δ 7.80 (d, *J* = 7.9 Hz, 1H), 7.71 (d, *J* = 7.1 Hz, 1H), 7.59 (app. t, *J* = 7.8 Hz, 2H), 7.52 (dd, *J* = 8.2, 1.4 Hz, 1H), 7.39 (d, *J* = 1.2 Hz, 1H), 7.21 (app. t, *J* = 7.4 Hz, 1H), 7.14-7.11 (m, 6H), 7.09-7.04 (m, 3H), 7.01 (app. t, *J* = 7.0 Hz, 1H), 6.89 (d, *J* = 6.8 Hz, 2H); ^{13}C NMR (100 MHz, $CDCl_3$) δ 146.4, 145.7, 144.6, 142.1, 140.5, 140.2, 138.5, 136.6, 135.9, 134.5, 133.4, 132.1, 131.3, 130.6, 130.0, 128.8, 128.6, 127.8, 127.6, 127.3, 126.5, 126.13, 126.08, 125.3, 119.0, 110.7; HRMS (ESI) Calcd for $C_{31}H_{20}N$ $[M + H]^+$ 406.1596, found 406.1572.

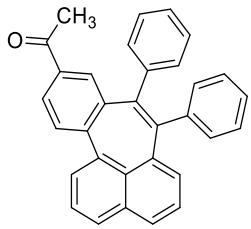

1-(7,8-Diphenylbenzo[4,5]cyclohepta[1,2,3-*de*]naphthalen-10-yl)ethan-1-one (4.42fa): White solid (39 mg, 85%, eluent: hexane/EtOAc = 48/2); m.p. 189-192 °C; ^{1}H NMR (400 MHz, $CDCl_3$): δ 7.83 (dd, *J* = 8.3, 1.9 Hz, 1H), 7.79-7.76 (m, 2H), 7.71 (d, *J* = 1.9 Hz, 1H), 7.61-7.57 (m, 2H), 7.21-7.08 (m, 8H), 7.08-6.97 (m, 3H), 6.92-6.90 (m, 2H), 2.39 (s, 3H); ^{13}C NMR (100 MHz, $CDCl_3$) δ 197.6, 145.7, 145.2, 144.9, 142.8, 140.1, 139.6, 139.4, 137.2, 136.3, 135.3, 134.2, 133.4, 131.8, 131.3, 130.7, 130.3, 128.4, 128.3, 127.8, 127.6, 127.1, 126.2, 125.98, 125.97, 125.2, 26.4; HRMS (ESI) Calcd for $C_{32}H_{23}O$ $[M + H]^+$ 423.1749, found 423.1754.

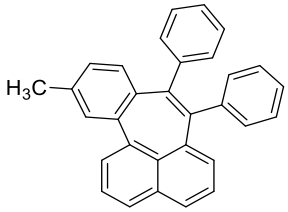

11-Methyl-7,8-diphenylbenzo[4,5]cyclohepta[1,2,3-*de*]naphthalene (4.42ga): Colorless solid (76%, eluent: hexane/EtOAc = 49/1); m.p. 119-122 °C; ^{1}H NMR (400 MHz, $CDCl_3$): δ 7.72 (dd, *J* = 7.0, 1.4 Hz, 2H), 7.55 (app. t, *J* = 7.2 Hz, 2H), 7.17-7.13 (m, 3H), 7.11-7.07 (m, 3H), 7.06-7.00 (m, 3H), 6.98-7.92 (m, 6H); ^{13}C NMR (100 MHz, $CDCl_3$) δ 145.2, 143.53, 143.48, 140.9, 140.3, 140.0, 138.6, 138.4, 136.5, 136.4, 134.3, 133.3, 131.2, 130.9, 130.8, 130.5, 127.7, 127.4, 127.3, 126.7, 125.9, 125.8, 125.7, 124.9, 21.1; HRMS (ESI) Calcd for $C_{31}H_{23}$ $[M + H]^+$ 395.1800, found 395.1808.

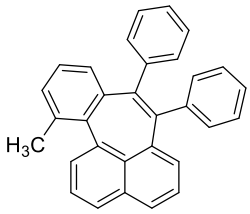

12-Methyl-7,8-diphenylbenzo[4,5]cyclohepta[1,2,3-*de*]naphthalene (4.42ha): Off-white solid (4.8 mg, 12%, eluent: hexane/EtOAc = 50/1); m.p. 159-160 °C; ^{1}H NMR (400 MHz, $CDCl_3$): δ 7.73 (dd, *J* = 7.1, 0.9 Hz, 1H), 7.59-7.51 (m, 2H), 7.45 (dd, *J* = 7.0, 1.0 Hz, 1H), 7.21-7.14 (m, 4H), 7.11-6.95 (m, 10H), 6.83 (d, *J* = 6.7 Hz, 1H), 1.95 (s, 3H); ^{13}C NMR (75 MHz, $CDCl_3$) δ 144.9, 144.2, 143.3, 141.0, 140.4, 140.2, 139.5, 137.8, 136.2, 134.3, 132.8, 131.43, 131.40, 131.1, 130.9, 130.3, 127.9, 127.5, 127.2, 126.9, 126.7, 126.1, 125.8, 125.7, 124.9, 124.2, 22.8; HRMS (ESI) Calcd for $C_{31}H_{23}$ $[M + H]^+$ 395.1800, found 395.1814.

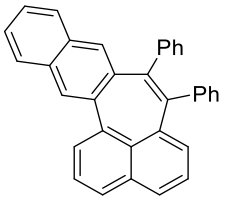

3ia

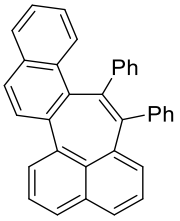

3ia'

7,8-Diphenylcyclohepta[1,2-b:3,4,5-d'e']dinaphthalene (3ia) and 7,8diphenylcyclohepta[1,2-a:3,4,5-d'e']dinaphthalene (4.42ia'): Silica gel chromatography (eluent: hexane/CH_2Cl_2 = 95/5 to 93/7) afforded a mixture of **4.42ia** and **4.42ia'** as light yellow solid (31.7 mg, 74% overall yield), whose ratio was determined to be 1.4:1 by ^{1}H NMR analysis. Partial separation of these isomers was performed using preparative TLC (eluent: hexane/CH_2Cl_2/Et_2O = 94.5/5/0.5), which afforded samples of **4.42ia** (6.1 mg) and **4.42ia'** (7.0 mg), each containing a small amount of the other regioisomer. **4.42ia:** ^{1}H NMR (400 MHz, $CDCl_3$): δ 7.91 (dd, *J* = 7.0, 1.1 Hz, 1H), 7.81 (dd, *J* = 8.1, 1.1 Hz, 1H), 7.77 (dd, *J* = 7.4, 1.5 Hz, 1H), 7.65-7.60 (m, 3H), 7.56 (s, 1H), 7.55 (s, 1H), 7.40-7.33 (m, 2H), 7.25-7.23 (m, 2H), 7.21-7.13 (m, 4H), 7.09-7.03 (m, 3H), 7.01-6.91 (m, 3H); ^{13}C NMR (100 MHz, $CDCl_3$) δ 145.4, 144.1, 143.6, 140.2, 139.8, 138.8, 138.3, 137.5, 136.2, 133.8, 133.13, 133.07,

132.1, 131.9, 130.9, 130.41, 130.32, 128.3, 127.9, 127.6, 127.44, 127.35, 127.1, 126.2, 126.0, 125.9, 125.7, 125.0; HRMS (ESI) Calcd for $C_{34}H_{23}$ $[M + H]^+$ 431.1800, found 431.1820.

4.42ia': ^{1}H NMR (400 MHz, $CDCl_3$): δ 8.12-8.06 (m, 2H), 7.78 (d, *J* = 8.8 Hz, 1H), 7.71-7.68 (m, 2H), 7.61 (d, *J* = 7.2 Hz, 1H), 7.53 (dd, *J* = 8.0, 0.8 Hz, 1H), 7.34-7.30 (m, 2H), 7.25-7.14 (m, 6H), 7.06-7.03 (m, 3H), 6.91-6.89 (m, 2H); ^{13}C NMR (100 MHz, $CDCl_3$), δ 145.9, 144.7, 143.9, 140.8, 140.3, 138.0, 137.9, 136.9, 135.5, 133.0, 132.8, 132.3, 131.9, 131.07, 131.04, 130.9, 130.2, 130.1, 128.7, 127.94, 127.88, 127.85, 127.6, 127.3, 127.1, 126.8, 126.7, 126.3, 126.2, 125.8, 125.64, 125.59, 125.45, 125.1

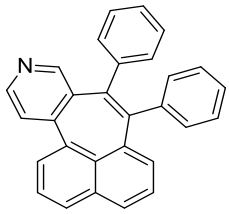

7,8-Diphenylnaphtho[1',8':3,4,5]cyclohepta[1,2-*c*]pyridine (4.42ja): Light yellow solid (5.6 mg, 15%, eluent: hexane/EtOAc = 2/1); m.p. 229-232 °C; ^{1}H NMR (400 MHz, $CDCl_3$) δ 8.43 (d, *J* = 5.3 Hz, 1H), 8.29 (s, 1H), 7.82-7.77 (m, 2H), 7.61-7.58 (m, 2H), 7.21 (d, *J* = 7.5 Hz, 1H), 7.18-7.10 (m, 5H), 7.08-7.04 (m, 3H), 7.02-6.97 (m, 2H), 6.93-6.91 (m, 2H); ^{13}C NMR (100 MHz, $CDCl_3$) δ 152.2, 149.0, 148.2, 146.5, 144.6, 141.9, 140.1, 138.2, 136.2, 135.7, 134.7, 133.7, 132.2, 130.7, 130.2, 129.2, 128.1, 127.63, 127.58, 127.2, 126.5, 126.3, 126.1, 125.3; HRMS (ESI) Calcd for $C_{29}H_{20}N$ $[M + H]^+$ 282.1596, found 382.1590.

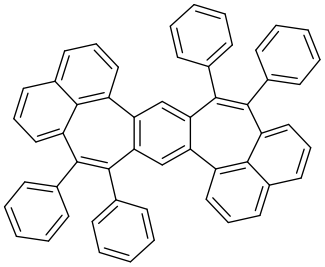

Compound 4.45: Ag_2CO_3 (27.5 mg, 0.10 mmol) was placed in a 10 mL Schlenk tube, which was then dried at 150 °C in vacuum for 3 h. Upon cooling, 1,4-bis(8-bromonaphthalen-1-yl)benzene (**5**) (0.20 M solution in DCE, 0.50 mL, 0.10 mmol), diphenylacetylene (71.6 mg, 0.40 mmol), $Pd(OAc)_2$ (4.4 mg, 0.020 mmol), and $P(4\text{-}ClC_6H_4)_3$ (22.0 mg, 0.06 mmol) were added to the Schlenk tube under N_2 atmosphere. The Schlenk tube was sealed, and the resulting mixture was stirred at 80 °C for 18 h. The resulting mixture was cooled to room temperature and concentrated under reduced pressure. The organic residue was dissolved in CH_2Cl_2 and subjected to silica gel column chromatography (eluent: hexane/CH_2Cl_2 = 10/1) to afford **4.45** as a light yellow solid (32.1 mg, 47%). m.p. > 300 °C (decomposed); ^{1}H NMR (400 MHz, $CDCl_3/CS_2$): δ 7.63 (d, *J* = 8.1 Hz, 2H), 7.51 (d, *J* = 7.5 Hz, 2H), 7.36 (t, *J* = 7.7 Hz, 2H), 7.24 (d, *J* = 7.2 Hz, 2H), 7.18–7.08 (m, 10H), 7.08–7.00 (m, 8H), 6.99–6.95 (m, 2H), 6.88 (d, *J* = 7.4 Hz, 4H), 6.79 (s, 2H); ^{13}C NMR (100 MHz, $CDCl_3/CS_2$) δ 145.2, 144.5, 143.0, 140.0, 139.6, 139.5, 137.8, 136.8, 136.5, 133.4, 131.7, 130.7, 130.4, 128.6, 127.64, 127.56, 127.4, 127.3, 126.9, 126.02, 125.96, 125.8, 125.0; HRMS (ESI) Calcd for $C_{54}H_{35}$ $[M + H]^+$ 683.2739, found 683.2745. Recrystallization from chloroform afforded single crystals of **4.45** (with $CHCl_3$ molecules) suitable for X-ray diffraction analysis, which unambiguously confirmed its molecular structure (Figure 4.2).

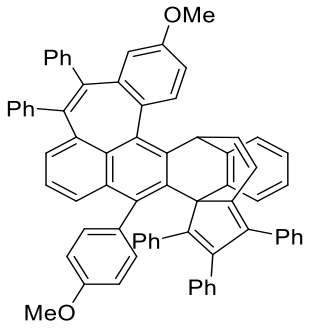

Compound 4.47: Ag_2CO_3 (55 mg, 0.20 mmol) was placed in a 10 mL oven-dried Schlenk tube, dried under vacuum at 150 °C for 3 h, and then cooled down to room temperature under N_2. Thereafter, 1,5-dibromo-9,10-bis(4-methoxyphenyl)anthracene, **7** (55 mg, 0.10 mmol), 1,2-dichloroethane (0.5 mL), diphenylacetylene (71 mg, 0.40 mmol), $Pd(OAc)_2$ (4.5 mg, 0.20 mmol) and $P(4\text{-}ClC_6H_4)_3$ (22 mg, 0.60 mmol) were added sequentially. The resulting mixture was stirred at 80 °C for 18 h. The reaction mixture was concentrated under reduced pressure, and the residue was extracted with EtOAc (3 x 10 mL). The combined organic extracts were dried over $MgSO_4$, concentrated under reduced pressure, and purified by silica gel column chromatography (eluent: hexane/EtOAc = 9/1) to afford the compound **4.47** as brown solid (9.5 mg, 10%, eluent: hexane/EtOAc = 9/1); m.p. 170-172 °C; ^{1}H NMR (400 MHz, $CDCl_3$): δ 7.52 (s, 1H), 7.31 (aap. t, *J* = 7.2 Hz, 4H), 7.23-7.13 (m, 11H), 7.11-7.08 (m, 3H), 7.06-6.99 (m, 6H), 6.97-6.85 (m, 11H), 6.81 (dd, *J* = 8.4, 2.6 Hz, 1H), 6.72 (d, *J* = 7.5 Hz, 2H), 6.49-6.32 (m, 4H), 5.90 (dd, *J* = 8.3, 2.1 Hz, 1H), 5.19 (d, *J* = 7.9 Hz, 1H), 3.83 (s, 3H), 3.75 (s, 3H); ^{13}C NMR (100 MHz, $CDCl_3$) δ 158.4, 158.1, 157.68, 157.64, 157.57, 142.2, 141.67, 141.58, 141.4, 141.0, 140.70, 140.65, 140.2, 140.0, 139.5, 138.9, 138.1, 137.6, 136.9, 136.5, 136.4, 135.6, 135.2, 134.5, 133.8, 132.9, 131.6, 131.0, 130.8, 130.6, 130.23, 130.20, 130.15, 130.10, 129.7, 129.3, 129.1, 128.8, 128.7, 128.5, 128.4, 128.3, 128.11, 128.05, 127.75, 127.67, 127.60, 127.53, 126.84, 126.73, 126.66, 126.58, 125.8, 125.5, 115.6, 115.4, 113.28, 113.22, 113.1,

112.5, 86.65, 86.58, 74.1, 73.7, 65.8, 55.2, 55.1; HRMS (ESI) Calcd for $C_{70}H_{50}O_2$ [M + H]$^+$ 923.3889, found 923.3895.

Recrystallization from dichloromethane afforded single crystals of **4.47** suitable for X-ray diffraction analysis, which unambiguously confirmed its molecular structure (Figure 4.2).

Oxidative Fragmentation of Heptagon Products

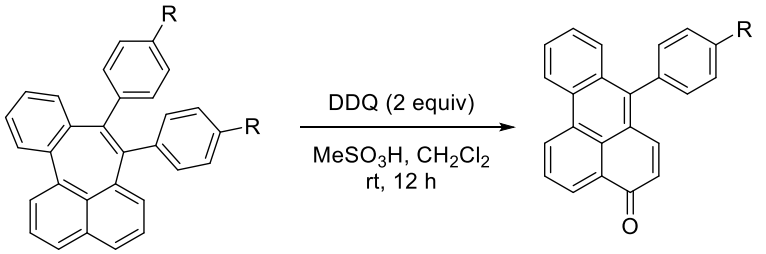

4.42aa (R = H)
4.42ab (R = OMe)

4.48a (R = H), 50%
4.48b (R = OMe), 28%

7-Phenyl-4*H*-benzo[*de*]anthracen-4-one (4.48a): An oven-dried 25 mL Schlenk tube was charged with **4.42aa** (38 mg, 0.10 mmol), CH_2Cl_2 (9 mL), and 2,3-dichloro-5,6-dicyano-1,4-benzoquinone (45 mg, 0.20 mmol). The Schlenk tube was placed in an ice bath, and then methanesulfonic acid (1.0 mL) was added dropwise. The reaction mixture was kept stirring at 0 °C for 30 min and then allowed to stir at room temperature for 12 h. The reaction was quenched by the reaction of aqueous NH_4Cl and extracted with CH_2Cl_2 (3 x 10 mL). The combined organic layer was washed with brine, dried over $MgSO_4$, and concentrated under reduced pressure. The crude material was purified by silica gel column chromatography to afford the title compound as a yellow solid (16.3 mg, 50%, eluent: hexane/EtOAc = 9/1); m.p. 178-180 °C; ^{1}H NMR (400 MHz, $CDCl_3$): δ 9.04 (dd, *J* = 8.2, 0.9 Hz, 1H), 8.79 (d, *J* = 8.3, Hz, 1H), 8.70

(dd, *J* = 7.5, 1.1 Hz, 1H), 7.94 (app. t, *J* = 8.0 Hz, 1H), 7.78-7.73 (m, 1H), 7.62-7.51 (m, 6H), 7.41-7.39 (m, 2H), 6.64 (d, *J* = 10.1 Hz, 1H); ^{13}C NMR (100 MHz, $CDCl_3$) δ 185.6, 145.1, 144.4, 143.3, 141.1, 140.3, 140.2, 139.4, 138.2, 136.8, 136.7, 133.8, 133.4, 131.7, 131.4, 131.3, 130.9, 128.8, 128.0, 127.6, 127.5, 127.2, 127.0, 126.9, 126.7, 126.53, 126.45, 126.0, 125.0; HRMS (ESI) Calcd for $C_{23}H_{15}O$ $[M + H]^+$ 307.1123, found 307.1128.

7-(4-Methoxyphenyl)-4*H*-benzo[*de*]anthracen-4-one (4.48b): Yellow solid (9.4 mg, 28%, eluent: hexane/EtOAc = 5/1); m.p. 160-163 °C; ^{1}H NMR (400 MHz, $CDCl_3$): δ 9.02 (dd, *J* = 8.2, 0.9 Hz, 1H), 8.78 (d, *J* = 8.3 Hz, 1H), 8.70 (dd, *J* = 7.5, 1.1 Hz, 1H), 7.92 (t, *J* = 7.8 Hz, 1H), 7.77-7.73 (m, 1H), 7.68 (dd, *J* = 8.3, 0.9 Hz, 1H), 7.63 (d, *J* = 10.1 Hz, 1H), 7.56-7.52 (m, 1H), 7.34-7.30 (m, 2H), 7.13-7.10 (m, 2H), 6.65 (d, *J* = 10.1 Hz, 1H), 3.95 (s, 3H); ^{13}C NMR (100 MHz, $CDCl_3$) δ 185.7, 159.7, 145.4, 140.8, 132.2, 131.9, 131.6, 130.1, 129.6, 129.2, 129.0, 128.8, 128.4, 128.1, 127.4, 127.26, 127.17, 124.4, 122.9, 113.9, 55.4; HRMS (ESI) Calcd for $C_{24}H_{17}O_2$ $[M + H]^+$ 337.1229, found 337.1233.

Recrystallization from CH_2Cl_2 afforded single crystals of **4.48b** (with CH_2Cl_2 molecules) suitable for X-ray diffraction analysis, which unambiguously confirmed its molecular structure (Scheme 4.20). The possible reaction pathway for the oxidative fragmentation is discussed below.

Scheme 4.23. Possible pathway for the oxidative fragmentation.

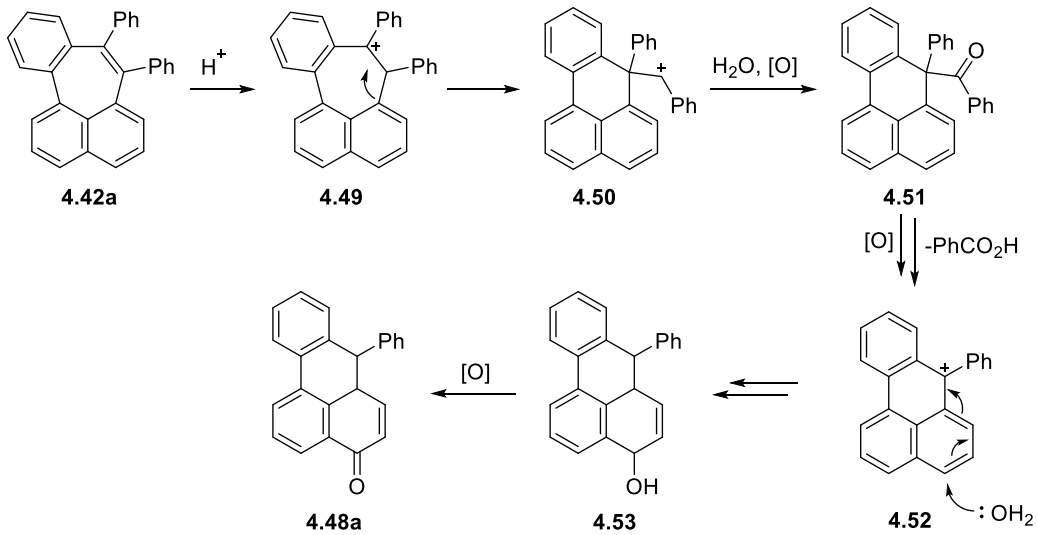

Deuterium-Labeling Experiments

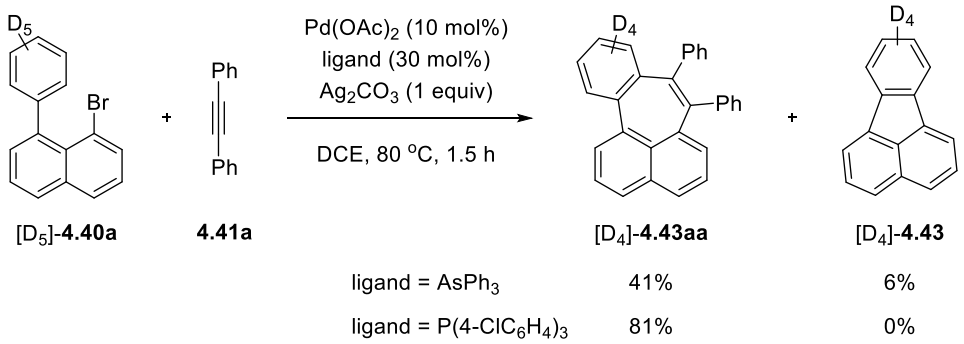

The reaction of [D_5]-**4.40a** and **4.41a** was set up according to the standard procedure using $AsPh_3$ or P(4-ClC_6H_4)$_3$ as the ligand. The reaction was quenched at 1.5 h, and the crude reaction mixture was analyzed by GC using *n*-tridecane as an internal standard to determine the yields of [D_4]-**4.42aa** and [D_4]-**4.43**. For the reaction using P(4-ClC_6H_4), the product [D_4]-**4.42aa** was isolated by silica gel chromatography to demonstrate that no extra deuterium atom was lost during the reaction.

Characterization data for [D_4]-**4.42aa:** Yellow solid (28 mg, 73%, eluent: hexane/EtOAc = 50/1); m.p. 215-217 °C; ^{1}H NMR (400 MHz, $CDCl_3$): δ 7.73 (d, *J* =

7.6 Hz, 2H), 7.58-7.54 (m, 2H), 7.18-7.14 (m, 3H), 7.12-7.09 (m, 3H), 7.07-6.95 (m, 4H), 6.92 (d, *J* = 6.8 Hz, 2H), ^{13}C NMR (100 MHz, $CDCl_3$) δ 145.2, 144.3, 143.4, 141.0, 140.3, 140.2, 139.0, 138.3, 136.5, 133.3, 131.4, 130.8, 130.4, 127.6, 127.44, 127.43, 127.3, 126.8, 125.94, 125.83, 125.75, 124.9.

DFT Calculations

All the density functional theory (DFT) calculations were performed using Gaussian 09.[66] Geometry optimizations were performed with the B3LYP functional[67-69] augmented with the D3 version of Grimme's empirical dispersion correction[70] using the LANL2DZ effective core potential[71] for palladium and the 6-31G(d) basis set for all other atoms. This set of basis sets is referred to as 631LAN. The B3LYP/631LAN calculations provided the energies (E1) of the intermediates and transition states. Harmonic frequency calculations were performed for each stationary point to ensure that it has no imaginary frequency (for ground state) or only one imaginary frequency (for transition state) and to obtain free energy correction values (Gcorr). Single-point energy calculations were performed with the M06L functional[72] and the def2TZVP basis set[73-74] for all atoms, using the IEFPCM solvation model for dichloroethane.[75] The thus-obtained energy (E2) was corrected by Gcorr, and the resulting value was used to discuss relative free energies. The optimized structures were visualized using CYLview.[76]

4.5 References

1. Wu, J.; Pisula, W.; Müllen, K. *Chem. Rev.* **2007**, *107*, 718.

2. Anthony, J. E. *Angew. Chem. Int. Ed.* **2008**, *47*, 452.

3. Anthony, J. E. *Angew. Chem. Int. Ed.* **2008**, *120*, 460.

4. Narita, A.; Feng, X.; Müllen, K. *Chem. Rec.* **2015**, *15*, 295.

5. Segawa, Y.; Ito, H.; Itami, K. *Nat. Rev. Mat.* **2016**, *1*, 15002.

6. Rieger, R.; Müllen, K. *J. Phys. Org. Chem.* **2010**, *23*, 315.

7. Cheung, K. Y.; Xu, X.; Miao, Q. *J. Am. Chem. Soc.* **2015**, *137*, 3910.

8. Kapko, V.; Drabold, D. A.; Thorpe, M. F. *Phys. Status Solidi B* **2010**, *247*, 1197.

9. Kawasumi, K.; Zhang, Q.; Segawa, Y.; Scott, L. T.; Itami, K. *Nat. Chem.* **2013**, *5*, 739.

10. Tan, Y.-Z.; Chen, R.-T.; Liao, Z.-J.; Li, J.; Zhu, F.; Lu, X.; Xie, S.-Y.; Li, J.; Huang, R.-B.; Zheng, L.-S. *Nat. Commun.* **2011**, *2*, 420.

11. Lin, H.-A.; Kato, K.; Segawa, Y.; Scott, L. T.; Itami, K. *Chem. Sci.* **2019**, *10*, 2326.

12. Kato, K.; Segawa, Y.; Scott, L. T.; Itami, K. *Chem. Asian J.* **2015**, *10*, 1635.

13. Kawai, K.; Kato, K.; Peng, L.; Segawa, Y.; Scott, L. T.; Itami, K. *Org. Lett.* **2018**, *20*, 1932.

14. Gu, X.; Li, H.; Shan, B.; Liu, Z.; Miao, Q. *Org. Lett.* **2017**, *19*, 2246.

15. Márquez, I. R.; Fuentes, N.; Cruz, C. M.; Puente-Muñoz, V.; Sotorrios, L.; Marcos, M. L.; Choquesillo-Lazarte, D.; Biel, B.; Crovetto, L.; Gómez-Bengoa, E.; González, M. T.; Martin, R.; Cuerva, J. M.; Campaña, A. G. *Chem. Sci.* **2017**, *8*, 1068.

16. Scott, L. T.; Jackson, E. A.; Zhang, Q.; Steinberg, B. D.; Bancu, M.; Li, B. *J. Am. Chem. Soc.* **2012**, *134*, 107.

17. Baldridge, K. K.; Siegel, J. S. Theor. *Chem. Acc.* **1997**, *97*, 67.

18. Wu, G.; Rheingold, A. L.; Geib, S. J.; Heck, R. F. *Organometallics* **1987**, *6*, 1941.

19. Kawasaki, S.; Satoh, T.; Miura, M.; Nomura, M. *J. Org. Chem.* **2003**, *68*, 6836.

20. Bej, A.; Chakraborty, A.; Sarkar, A. *RSC Adv.* **2013**, *3*, 15812.

21. Komeyama, K.; Kashihara, T.; Takaki, K. *Tet. Lett.* **2013**, *54*, 5659.

22. Ueura, K.; Satoh, T.; Miura, M. *J. Org. Chem.* **2007**, *72*, 5362.

23. Yamashita, M.; Hirano, K.; Satoh, T.; Miura, M. *Org. Lett.* **2009**, *11*, 2337.

24. Yamashita, M.; Horiguchi, H.; Hirano, K.; Satoh, T.; Miura, M. *J. Org. Chem.* **2009**, *74*, 7481.

25. Uto, T.; Shimizu, M.; Ueura, K.; Tsurugi, H.; Satoh, T.; Miura, M. *J. Org. Chem.* **2008**, *73*, 298.

26. Fukutani, T.; Hirano, K.; Satoh, T.; Miura, M. *J. Org. Chem.* **2011**, *76*, 2867.

27. Fukutani, T.; Hirano, K.; Satoh, T.; Miura, M. *Org. Lett.* **2009**, *11*, 5198.

28. Yasukawa, T.; Satoh, T.; Miura, M.; Nomura, M. *J. Am. Chem. Soc.* **2002**, *124*, 12680.

29. Adak, L.; Yoshikai, N. *Tetrahedron* **2012**, *68*, 5167.

30. Ilies, L.; Matsumoto, A.; Kobayashi, M.; Yoshikai, N.; Nakamura, E. *Synlett* **2012**, *23*, 2381.

31. Pham, M. V.; Cramer, N. *Angew. Chem. Int. Ed.* **2014**, *53*, 3484.

32. Larock, R. C.; Doty, M. J.; Tian, Q.; Zenner, J. M. *J. Org. Chem.* **1997**, *62*, 7536.

33. Wang, C.; Rakshit, S.; Glorius, F. *J. Am. Chem. Soc.* **2010**, *132*, 14006.

34. Matsumoto, A.; Ilies, L.; Nakamura, E. *J. Am. Chem. Soc.* **2011**, *133*, 6557.

35. Nagata, T.; Hirano, K.; Satoh, T.; Miura, M. *J. Org. Chem.* **2014**, *79*, 8960.

36. Nagata, T.; Satoh, T.; Nishii, Y.; Miura, M. *Synlett* **2016**, *27*, 1707.

37. Yan, J.; Yoshikai, N. *Org. Lett.* **2017**, *19*, 6630.

38. Ozaki, K.; Murai, K.; Matsuoka, W.; Kawasumi, K.; Ito, H.; Itami, K. *Angew. Chem. Int. Ed.* **2017**, *56*, 1361.

39. Shoji, Y.; Tanaka, N.; Muranaka, S.; Shigeno, N.; Sugiyama, H.; Takenouchi, K.; Hajjaj, F.; Fukushima, T. *Nat. Commun.* **2016**, *7*, 12704.

40. Kanno, K.-i.; Liu, Y.; Iesato, A.; Nakajima, K.; Takahashi, T. *Org. Lett.* **2005**, *7*, 5453.

41. Wu, Y.; Wu, F.; Zhu, D.; Luo, B.; Wang, H.; Hu, Y.; Wen, S.; Huang, P. *Org. Biomol. Chem.* **2015**, *13*, 10386.

42. Craig, J. T.; Tan, K. W.; Woolhouse, A. D. *Tet. Lett.* **1971**, *12*, 3209.

43. Sugihara, Y.; Yamamoto, H.; Mizoue, K.; Murata, I. *Angew. Chem. Int. Ed.* **1987**, *26*, 1247.

44. Chernyak, N.; Tilly, D.; Li, Z.; Gevorgyan, V. *Chem. Commun.* **2010**, *46*, 150.

45. Pun, S. H.; Chan, C. K.; Luo, J.; Liu, Z.; Miao, Q. *Angew. Chem. Int. Ed.* **2018**, *57*, 1581.

46. Pun, S. H.; Chan, C. K.; Luo, J.; Liu, Z.; Miao, Q. *Angew. Chem. Int. Ed.* **2018**, *130*, 1597.

47. Fu, W. C.; Wang, Z.; Chan, W. T. K.; Lin, Z.; Kwong, F. Y. *Angew. Chem. Int. Ed.* **2017**, *56*, 7166.

48. Yan, J.; Rahman, M. S.; Yoshikai, N. *Chem. Eur. J.* **2019**, *25*, 9395.

49. Smet, M.; Van Dijk, J.; Dehaen, W. *Synlett* **1999**, *1999*, 495.

50. Bheemireddy, S. R.; Ubaldo, P. C.; Finke, A. D.; Wang, L.; Plunkett, K. N. *J. Mat. Chem. C* **2016**, *4*, 3963.

51. Rice, J. E.; Cai, Z. W. *J. Org. Chem.* **1993**, *58*, 1415.

52. Yamaguchi, M.; Higuchi, M.; Tazawa, K.; Manabe, K. *J. Org. Chem.* **2016**, *81*, 3967.

53. Neufeldt, S. R.; Sanford, M. S. *Acc. Chem. Res.* **2012**, *45*, 936.

54. Grzybowski, M.; Skonieczny, K.; Butenschön, H.; Gryko, D. T. *Angew. Chem. Int. Ed.* **2013**, *52*, 9900.

55. Lee, H.; Harvey, R. G. *J. Org. Chem.* **1983**, *48*, 749.

56. Mei, J.; Leung, N. L. C.; Kwok, R. T. K.; Lam, J. W. Y.; Tang, B. Z. *Chem. Rev.* **2015**, *115*, 11718.

57. Romero-Nieto, C.; López-Andarias, A.; Egler-Lucas, C.; Gebert, F.; Neus, J.-P.; Pilgram, O. *Angew. Chem. Int. Ed.* **2015**, *54*, 15872.

58. Moorthy, J. N.; Mandal, S.; Parida, K. N. *Org. Lett.* **2012**, *14*, 2438.

59. Cha, S. J.; Han, N. S.; Song, J. K.; Park, S.-R.; Jeon, Y. M.; Suh, M. C. *Dyes Pigments* **2015**, *120*, 200.

60. Mio, M. J.; Kopel, L. C.; Braun, J. B.; Gadzikwa, T. L.; Hull, K. L.; Brisbois, R. G.; Markworth, C. J.; Grieco, P. A. *Org. Lett.* **2002**, *4*, 3199.

61. Brown, A. E.; Eichler, B. E. *Tet. Lett.* **2011**, *52*, 1960.

62. Melzig, L.; Metzger, A.; Knochel, P. *Chem. Eur. J.* **2011**, *17*, 2948.

63. Verma, A. K.; Joshi, M.; Singh, V. P. *Org. Lett.* **2011**, *13*, 1630.

64. Jia, X.; Petrone, D. A.; Lautens, M. *Angew. Chem. Int. Ed.* **2012**, *51*, 9870.

65. Vilà, N.; Zhong, Y.-W.; Henderson, J. C.; Abruña, H. D. *Inorg. Chem.* **2010**, *49*, 796.

66. M. J. Frisch, G. W. Trucks, H. B. Schlegel, G. E. Scuseria, M. A. Robb, J. R. Cheeseman, G. Scalmani, V. Barone, G. A. Petersson, H. Nakatsuji, X. Li, M. Caricato, A. Marenich, J. Bloino, B. G. Janesko, R. Gomperts, B. Mennucci, H. P. Hratchian, J. V. Ortiz, A. F. Izmaylov, J. L. Sonnenberg, D. Williams-

Young, F. Ding, F. Lipparini, F. Egidi, J. Goings, B. Peng, A. Petrone, T. Henderson, D. Ranasinghe, V. G. Zakrzewski, J. Gao, N. Rega, G. Zheng, W. Liang, M. Hada, M. Ehara, K. Toyota, R. Fukuda, J. Hasegawa, M. Ishida, T. Nakajima, Y. Honda, O. Kitao, H. Nakai, T. Vreven, K. Throssell, J. A. Montgomery, Jr., J. E. Peralta, F. Ogliaro, M. Bearpark, J. J. Heyd, E. Brothers, K. N. Kudin, V. N. Staroverov, T. Keith, R. Kobayashi, J. Normand, K. Raghavachari, A. Rendell, J. C. Burant, S. S. Iyengar, J. Tomasi, M. Cossi, J. M. Millam, M. Klene, C. Adamo, R. Cammi, J. W. Ochterski, R. L. Martin, K. Morokuma, O. Farkas, J. B. Foresman, and D. J. Fox, Gaussian, Inc., Wallingford CT, **2016**.

67. Becke, A. D. *J. Chem. Phys.* **1993**, *98*, 5648.
68. Lee, C.; Yang, W.; Parr, R. G. *Phys. Rev. B* **1988**, *37*, 785.
69. Vosko, S. H.; Wilk, L.; Nusair, M. *Can. J. Phys.* **1980**, *58*, 1200.
70. Grimme, S.; Antony, J.; Ehrlich, S.; Krieg, H. *J. Chem. Phys.* **2010**, *132*, 154104.
71. Hay, P. J.; Wadt, W. R. *J. Chem. Phys.* **1985**, *82*, 270.
72. Zhao, Y.; Truhlar, D. G. *Theor. Chem. Acc.* **2008**, *120*, 215.
73. Schäfer, A.; Huber, C.; Ahlrichs, R. *J. Chem. Phys.* **1994**, *100*, 5829.
74. Weigend, F.; Ahlrichs, R. *Phys. Chem. Chem. Phys.* **2005**, *7*, 3297.
75. Tomasi, J.; Mennucci, B.; Cammi, R. *Chem. Rev.* **2005**, *105*, 2999.
76. Legault, C. Y. CYLview, 1.0b; Université de Sherbrooke, **2009**; http://www.cylview.org.

Chapter 5 Conclusion

During the past four years of my Ph.D. studies, I worked on the synthesis and properties of novel (hetero)aromatic polycyclic systems. My Ph.D. thesis comprised of two parts. Part I of the thesis described the synthesis and properties of phosphole-embedded polycyclic aromatic systems. Based on our previous reports on the synthesis of benzo[*b*]phosphole oxides derivatives by using cobalt-Xantphos catalysis system, the presence of *meta*-alkoxy group on benzene, showed secondary directing effect on 1,4-cobalt migratory step and as a result, a major regioisomer was formed in close proximity to alkoxy group. Therefore, I have realised the 7-hydroxybenzo[*b*]phosphole oxide can be achieved in one pot by using the cobalt-Xantphos catalysis system and then utilised as a synthetic handle to construct phosphahelicenes bearing an inner-rim phosphorus center and novel P-embedded polycyclic aromatic π-systems. Moreover, phosphole-embedded polycyclic aromatic compounds showed unique physico-chemical properties and our interest to further functionalized the cobalt-catalysed synthesis of benzo[*b*]phosphole oxides series, has motivated me to synthesize new phosphole-embedded polycyclic aromatic systems (Scheme 5.1). The important synthetic precursor, 7-hydroxybenzo[*b*]phosphole oxide, was prepared from 3-(methoxymethyl)phenylzinc reagent, 5-decyne, and chlorodiphenylphosphine in a regioselective manner through 1,4-cobalt migration as a key step.

Scheme 5.1. Synthesis of phosphole-embedded polycyclic aromatic compounds

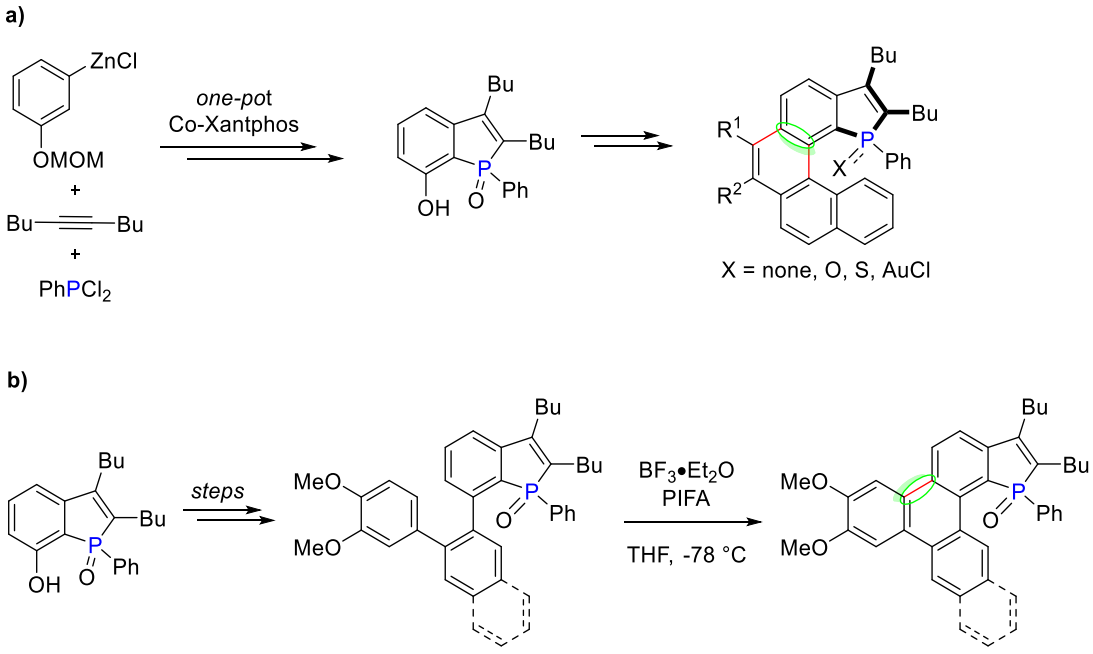

In Chapter 2, I have developed a concise strategy to synthesize phospha[5]helicene derivatives bearing an inner-rim phosphorus center (Scheme 5.1a). The thus-synthesized phospha[5]helicenes are structurally distinct from previously reported phosphahelicenes with respect to the position of the phosphorus atom and the helical axis. Based on ^{1}H NMR studies and single crystal X-ray analysis, the presence of phosphorus center significant impact the diastereomeric ratio as well as facile equilibration between the diastereomers through helix inversion, which was also supported by DFT calculations. The thus-synthesized phospha[5]helicene derivatives showed blue luminescent color.

In Chapter 3, I have demonstrated the synthesis and optical properties of phosphole oxide-fused triphenylene derivatives (Scheme 5.1b). As was in the case of synthesis of phospha[5]helicenes, 7-hydroxybenzo[*b*]phosphole oxide utilized as a key synthetic scaffold to construct phosphorus containing polycyclic aromatic π-systems.

The synthesis features a dehydrogenative C-C coupling promoted by Lewis acid (Scholl reaction conditions) at elevated temperature. The final products showed strong emission and solvatochromism behavior depending on the polarity of the solvents. The single crystal X-ray analysis revealed planar structure of phosphole oxide-fused triphenylenes.

In Thesis Part II, Chapter 4, I have developed a palladium-catalyzed annulation reaction between internal alkynes and 1-halo-8-arylnaphthalenes leading to heptagon-embedded aromatic systems with all *sp*2 carbon center (Scheme 5.2). The annulative reaction facilitated by a catalytic system comprised of $Pd(OAc)_2$, moderated electron-deficient triarylphosphine $P(4\text{-}ClC_6H_4)_3$ and Ag_2CO_3. The notable feature of the methodology is the direct access of heptagon-embedded aromatic systems with broad substrate scope. The thus-synthesized compounds showed weak emission in solution and in contrast, showed strong fluorescent in solid state.

Scheme 5.2. Pd-Catalyzed synthesis of heptagon-embedded aromatic systems

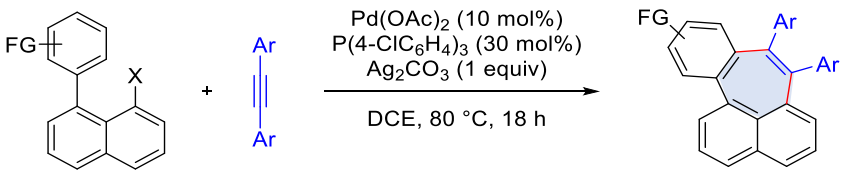

Overall, this thesis research has led to significant advancement in the synthesis of novel phosphole and heptagon containing polycyclic aromatic compounds of extended π-conjugation. Several phospha[5]helicenes bearing an inner-rim phosphorus center and phosphole-fused triphenylenes derivatives have been constructed from 7-

hydroxybenzo[*b*]phosphole oxide. On the other hand, I have demonstrated a direct access of heptagon-embedded PAHs can be achieved by using palladium catalysis. Note that, the thus-synthesized (hetero)aromatic polycyclic aromatic compounds demonstrated strong luminescent behavior in solution as well as in solid state. Therefore, the synthesized novel (hetero)aromatic polycyclic compounds can be utilized as organic light emitting diode, organic field-effect transistor, and biological fluorescent probe materials. Future work would be focused on the synthesis and properties of more stable, rigid, phospha[6]helicenes bearing an inner-rim phosphorus center. Furthermore, expansion of substrate scope of heptagon-embedded PAHs via palladium-catalyzed [5 + 2] annulation reaction between alkynes and substituted 1-halo-8-arylnaphthalenes.